Symmetry restoration and configuration mixing calculations with Gogny functionals: Nuclear structure and double beta decay

Tomás R. Rodríguez

EMMI Workshop: From Ultracold Fermi Gases to Neutron-Rich Many-Body Systems: Universal Aspects and Modern Approaches to Density Functional Theory

March 2013

Bundesministerium für Bildung und Forschung

HIC for FAIR
Helmholtz International Center

NAVI
Nuclear Astrophysics Virtual Institute

TECHNISCHE UNIVERSITÄT DARMSTADT

Outline

1. Introduction

2. Theoretical framework

3. Applications

4. Some formal aspects

5. Summary and outlook

Astronomical observations

Low energy QCD

Astronomical observations

Phenomenological nuclear interactions

Unitary Transformations (SRG,UCOM, ...)

Chiral Effective Field Theory

Low energy QCD

Astronomical observations

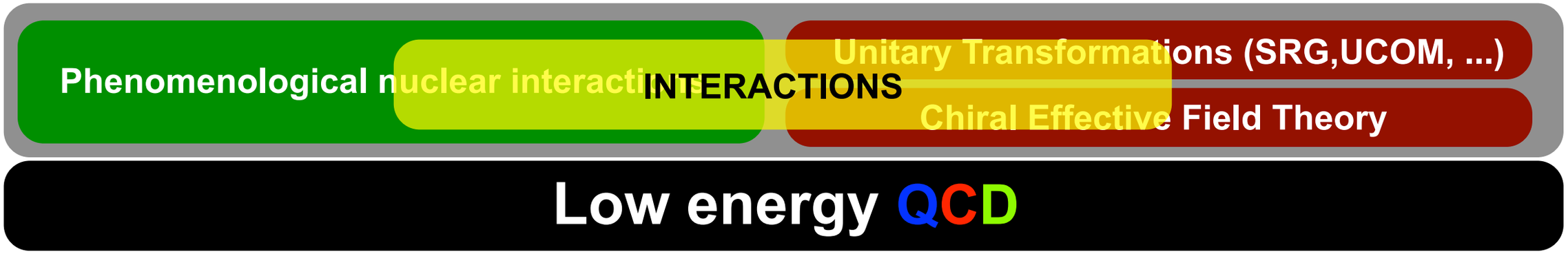

Astronomical observations

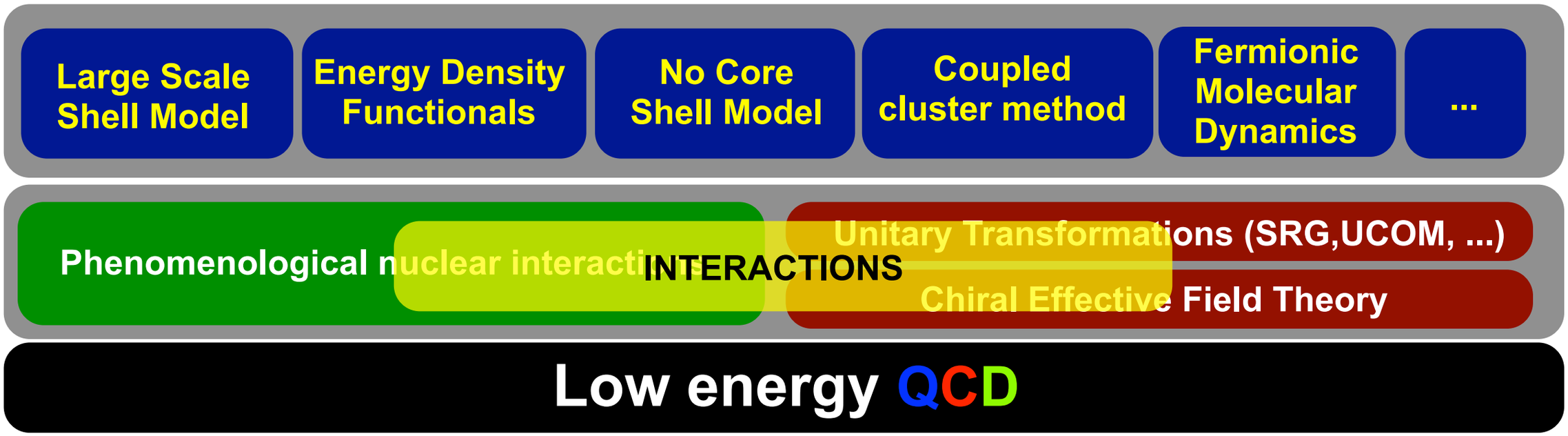

Astronomical observations

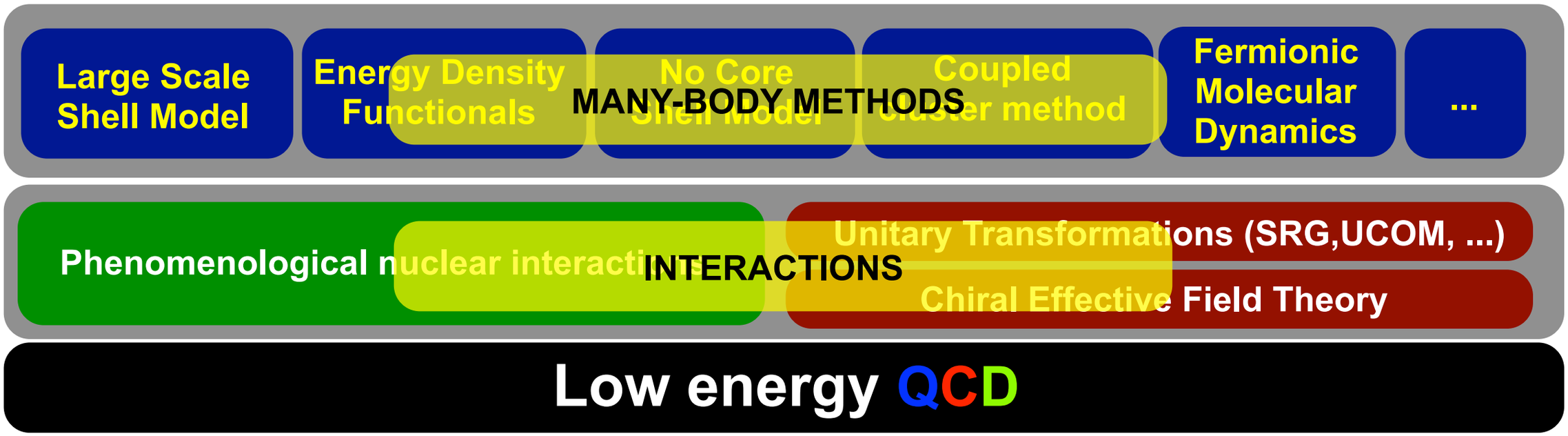

Astronomical observations

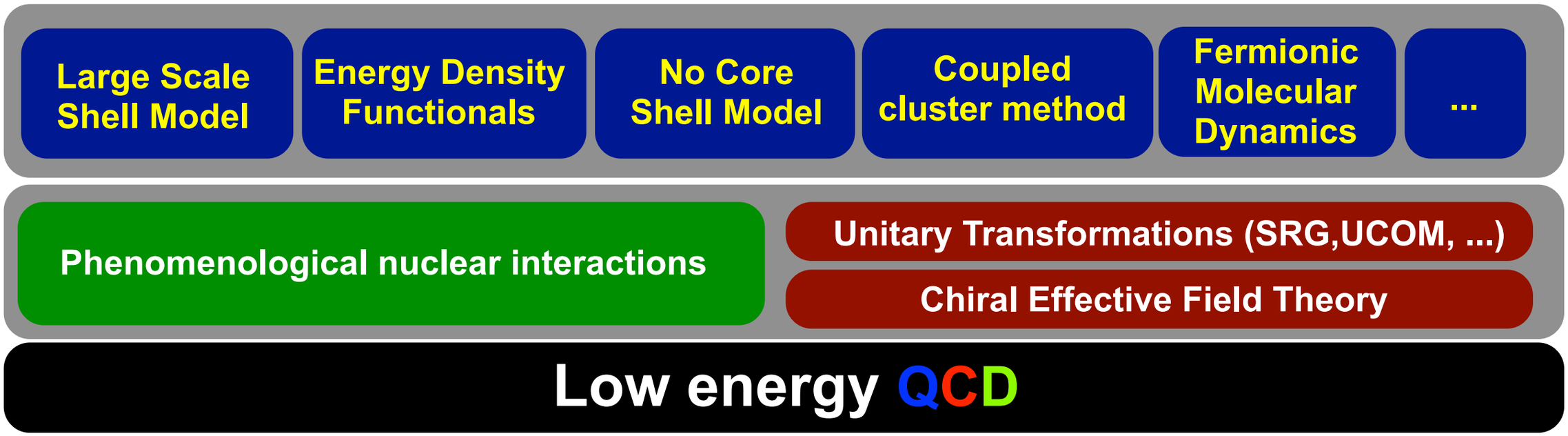

Astronomical observations

Nuclear structure and reactions observables

- Experiments
- Theoretical calculations

Large Scale Shell Model | Energy Density Functionals | No Core Shell Model | Coupled cluster method | Fermionic Molecular Dynamics | ...

Phenomenological nuclear interactions

Unitary Transformations (SRG,UCOM, ...)

Chiral Effective Field Theory

Low energy QCD

Astronomical observations

Astrophysical simulations

Stellar nucleosynthesis

Stellar explosions

Nuclear structure and reactions observables

- Experiments
- Theoretical calculations

Large Scale Shell Model

Energy Density Functionals

No Core Shell Model

Coupled cluster method

Fermionic Molecular Dynamics

...

Phenomenological nuclear interactions

Unitary Transformations (SRG,UCOM, ...)

Chiral Effective Field Theory

Low energy QCD

Astronomical observations

Astrophysical simulations

Stellar nucleosynthesis

Stellar explosions

Nuclear structure and reactions observables

- Experiments
- Theoretical calculations

Large Scale Shell Model

Energy Density Functionals

No Core Shell Model

Coupled cluster method

Fermionic Molecular Dynamics

...

Phenomenological nuclear interactions

Unitary Transformations (SRG,UCOM, ...)

Chiral Effective Field Theory

Low energy QCD

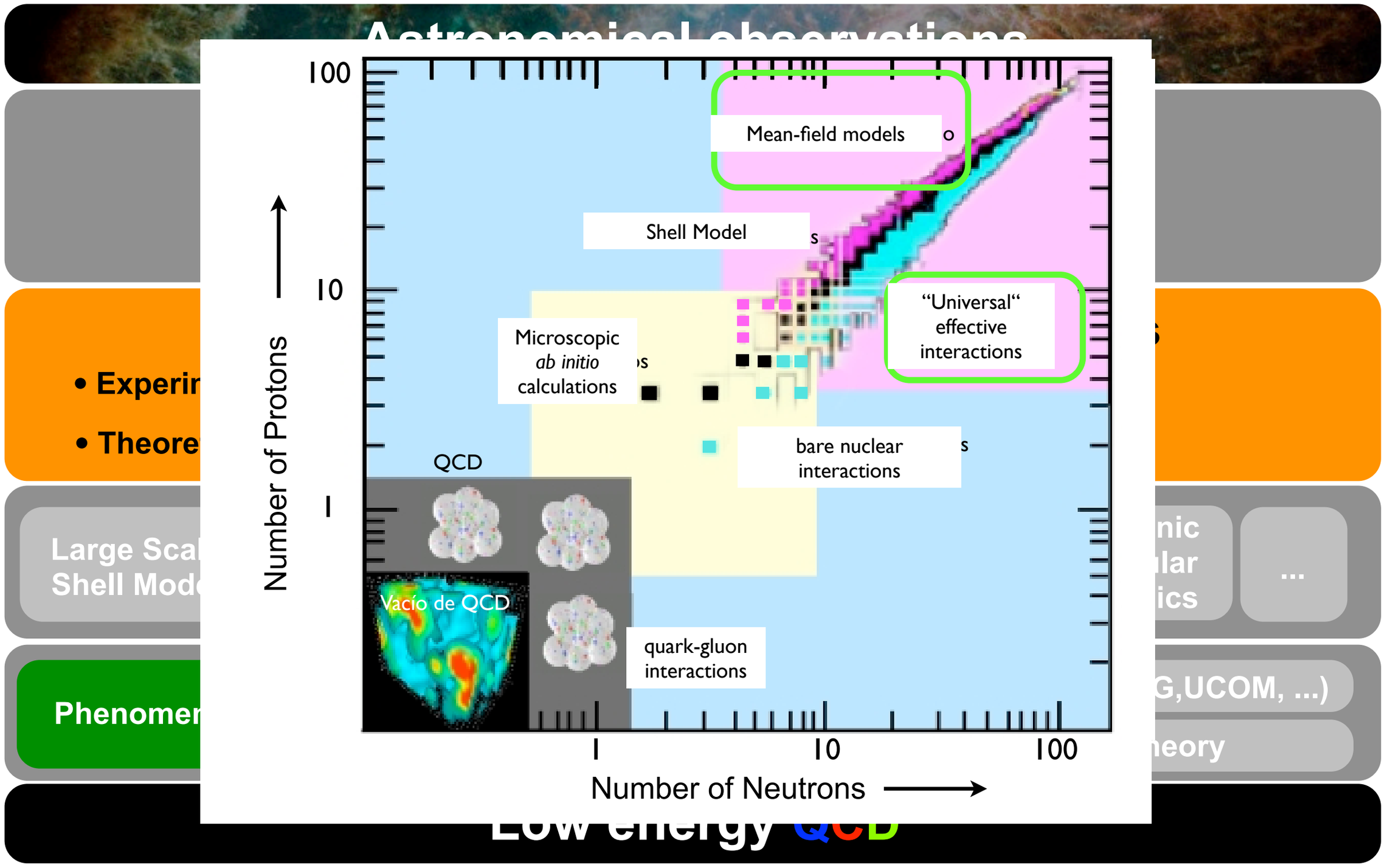
Mean-field models
Shell Model
"Universal" effective interactions
Microscopic ab initio calculations
bare nuclear interactions
QCD
Vacío de QCD
quark-gluon interactions
Number of Protons
Number of Neutrons
1
10
100
• Experir
• Theore
Large Scal
Shell Mod
Phenomer
...
G,UCOM, ...)
heory

Theoretical framework

- Initial intrinsic states: PN-VAP (M. Anguiano et al., Nucl. Phys. A 683, 227 (2001))

$$E^{N,Z}[\Phi] = \frac{\langle\Phi|\hat{H}_{2b}\hat{P}^N\hat{P}^Z|\Phi\rangle}{\langle\Phi|\hat{P}^N\hat{P}^Z|\Phi\rangle} + \varepsilon_{DD}^{N,Z}(\Phi) - \lambda_{q_{20}}\langle\Phi|\hat{Q}_{20}|\Phi\rangle - \lambda_{q_{22}}\langle\Phi|\hat{Q}_{22}|\Phi\rangle$$

- Intermediate Particle Number and Angular Momentum Projected states

$$|IMK;NZ;\beta\gamma\rangle = \frac{2I+1}{8\pi^2}\int \mathcal{D}^{I*}_{MK}(\Omega)\hat{R}(\Omega)\hat{P}^N\hat{P}^Z|\Phi(\beta,\gamma)\rangle d\Omega$$

- Final GCM states $|IM;NZ\sigma\rangle = \sum_{K\beta\gamma} f^{I;NZ,\sigma}_{K\beta\gamma}|IMK;NZ;\beta\gamma\rangle$

$$\sum_{K'\beta'\gamma'}\left(\mathcal{H}^{I;NZ}_{K\beta\gamma K'\beta'\gamma'} - E^{I;NZ;\sigma}\mathcal{N}^{I;NZ}_{K\beta\gamma K'\beta'\gamma'}\right) f^{I;NZ;\sigma}_{K'\beta'\gamma'} = 0$$

$$\begin{aligned}
\mathcal{N}^{I;NZ}_{K\beta\gamma K'\beta'\gamma'} &\equiv \langle IMK;NZ;\beta\gamma|IMK';NZ;\beta'\gamma'\rangle \\
\mathcal{H}^{I;NZ}_{K\beta\gamma K'\beta'\gamma'} &\equiv \langle IMK;NZ;\beta\gamma|\hat{H}_{2b}|IMK';NZ;\beta'\gamma'\rangle + \varepsilon^{IKK';NZ}_{DD}[\Phi(\beta,\gamma),\Phi'(\beta',\gamma')]
\end{aligned}$$

Theoretical framework

- Initial intrinsic states: PN-VAP (M. Anguiano et al., Nucl. Phys. A 683, 227 (2001))

$$E^{N,Z}[\Phi] = \langle\Phi|\hat{H}\ldots\hat{P}^N\hat{P}^Z|\Phi\rangle$$

- Intermedia ... es

$$|IMK;$$

- Final GCM

$$\sum_{K'\beta'\gamma'}\left(\mathcal{H}^{I;NZ}_{K\beta\gamma\ldots}\right.$$

Recent 3D AMP implementations

Skyrme: M. Bender, P.-H. Heenen, Phys. Rev. C 78, 024309 (2008)
- Particle number and angular momentum restoration of intrinsic LN states.

Relativistic: J.M. Yao et al., Phys. Rev. C 81, 04431 (2010)
- Angular momentum restoration of intrinsic HFB states.

Gogny: T.R.R., J.L. Egido, Phys. Rev C 81, 064323 (2010)
- Particle number and angular momentum restoration of PN-VAP states.

$$\mathcal{H}^{I;NZ}_{K\beta\gamma K'\beta'\gamma'} \equiv \langle IMK;NZ;\beta\gamma|\hat{H}_{2b}|IMK';NZ;\beta'\gamma'\rangle + \varepsilon^{IKK';NZ}_{DD}\left[\Phi(\beta,\gamma),\Phi'(\beta',\gamma')\right]$$

Theoretical framework

- Initial intrinsic states: PN-VAP (M. Anguiano et al., Nucl. Phys. A 683, 227 (2001))

$$E^{N,Z}[\Phi] = \frac{\langle\Phi|\hat{H}_{2b}\hat{P}^N\hat{P}^Z|\Phi\rangle}{\langle\Phi|\hat{P}^N\hat{P}^Z|\Phi\rangle} + \varepsilon_{DD}^{N,Z}(\Phi) - \lambda_{q_{20}}\langle\Phi|\hat{Q}_{20}|\Phi\rangle - \lambda_{q_{22}}\langle\Phi|\hat{Q}_{22}|\Phi\rangle$$

- Intermediate Particle Number and Angular Momentum Projected states

$$|IMK;NZ;\beta\gamma\rangle = \frac{2I+1}{8\pi^2}\int \mathcal{D}^{I*}_{MK}(\Omega)\hat{R}(\Omega)\hat{P}^N\hat{P}^Z|\Phi(\beta,\gamma)\rangle d\Omega$$

- Final GCM states $|IM;NZ\sigma\rangle = \sum_{K\beta\gamma} f^{I;NZ,\sigma}_{K\beta\gamma}|IMK;NZ;\beta\gamma\rangle$

$$\sum_{K'\beta'\gamma'}\left(\mathcal{H}^{I;NZ}_{K\beta\gamma K'\beta'\gamma'} - E^{I;NZ;\sigma}\mathcal{N}^{I;NZ}_{K\beta\gamma K'\beta'\gamma'}\right) f^{I;NZ;\sigma}_{K'\beta'\gamma'} = 0$$

$$\begin{aligned}
\mathcal{N}^{I;NZ}_{K\beta\gamma K'\beta'\gamma'} &\equiv \langle IMK;NZ;\beta\gamma|IMK';NZ;\beta'\gamma'\rangle \\
\mathcal{H}^{I;NZ}_{K\beta\gamma K'\beta'\gamma'} &\equiv \langle IMK;NZ;\beta\gamma|\hat{H}_{2b}|IMK';NZ;\beta'\gamma'\rangle + \varepsilon^{IKK';NZ}_{DD}[\Phi(\beta,\gamma),\Phi'(\beta',\gamma')]
\end{aligned}$$

Theoretical framework

TECHNISCHE UNIVERSITÄT DARMSTADT

- Initial intrinsic states: PN-VAP (M. Anguiano et al., Nucl. Phys. A 683, 227 (2001))

$$E^{N,Z}[\Phi] = \frac{\langle\Phi|\hat{H}_{2b}\cancel{\hat{P}^N\hat{P}^Z}|\Phi\rangle}{\langle\Phi|\cancel{\hat{P}^N\hat{P}^Z}|\Phi\rangle} + \varepsilon_{DD}^{N,Z}(\Phi) - \lambda_{q_{20}}\langle\Phi|\hat{Q}_{20}|\Phi\rangle - \lambda_{q_{22}}\langle\Phi|\hat{Q}_{22}|\Phi\rangle$$

- Intermediate Particle Number and Angular Momentum Projected states

$$|IMK;NZ;\beta\gamma\rangle = \frac{2I+1}{8\pi^2}\int \mathcal{D}^{I*}_{MK}(\Omega)\hat{R}(\Omega)\hat{P}^N\hat{P}^Z|\Phi(\beta,\gamma)\rangle d\Omega$$

- Final GCM states $|IM;NZ\sigma\rangle = \sum_{K\beta\gamma} f^{I;NZ,\sigma}_{K\beta\gamma}|IMK;NZ;\beta\gamma\rangle$

$$\sum_{K'\beta'\gamma'}\left(\mathcal{H}^{I;NZ}_{K\beta\gamma K'\beta'\gamma'} - E^{I;NZ;\sigma}\mathcal{N}^{I;NZ}_{K\beta\gamma K'\beta'\gamma'}\right) f^{I;NZ;\sigma}_{K'\beta'\gamma'} = 0$$

$$\begin{aligned}
\mathcal{N}^{I;NZ}_{K\beta\gamma K'\beta'\gamma'} &\equiv \langle IMK;NZ;\beta\gamma|IMK';NZ;\beta'\gamma'\rangle \\
\mathcal{H}^{I;NZ}_{K\beta\gamma K'\beta'\gamma'} &\equiv \langle IMK;NZ;\beta\gamma|\hat{H}_{2b}|IMK';NZ;\beta'\gamma'\rangle + \varepsilon^{IKK';NZ}_{DD}\left[\Phi(\beta,\gamma),\Phi'(\beta',\gamma')\right]
\end{aligned}$$

Theoretical framework

- Initial intrinsic states: PN-VAP (M. Anguiano et al., Nucl. Phys. A 683, 227 (2001))

$$E^{N,Z}[\Phi] = \frac{\langle\Phi|\hat{H}_{2b}\hat{P}^N\hat{P}^Z|\Phi\rangle}{\langle\Phi|\hat{P}^N\hat{P}^Z|\Phi\rangle} + \varepsilon_{DD}^{N,Z}(\Phi) - \lambda_{q_{20}}\langle\Phi|\hat{Q}_{20}|\Phi\rangle - \lambda_{q_{22}}\langle\Phi|\hat{Q}_{22}|\Phi\rangle$$

- Intermediate Particle Number and Angular Momentum Projected states

$$|IMK;NZ;\beta\gamma\rangle = \frac{2I+1}{8\pi^2}\int \mathcal{D}^{I*}_{MK}(\Omega)\hat{R}(\Omega)\hat{P}^N\hat{P}^Z|\Phi(\beta,\gamma)\rangle d\Omega$$

- Final GCM states $|IM;NZ\sigma\rangle = \sum_{K\beta\gamma} f^{I;NZ,\sigma}_{K\beta\gamma}|IMK;NZ;\beta\gamma\rangle$

$$\sum_{K'\beta'\gamma'}\left(\mathcal{H}^{I;NZ}_{K\beta\gamma K'\beta'\gamma'} - E^{I;NZ;\sigma}\mathcal{N}^{I;NZ}_{K\beta\gamma K'\beta'\gamma'}\right) f^{I;NZ;\sigma}_{K'\beta'\gamma'} = 0$$

$$\begin{aligned}
\mathcal{N}^{I;NZ}_{K\beta\gamma K'\beta'\gamma'} &\equiv \langle IMK;NZ;\beta\gamma|IMK';NZ;\beta'\gamma'\rangle \\
\mathcal{H}^{I;NZ}_{K\beta\gamma K'\beta'\gamma'} &\equiv \langle IMK;NZ;\beta\gamma|\hat{H}_{2b}|IMK';NZ;\beta'\gamma'\rangle + \varepsilon^{IKK';NZ}_{DD}[\Phi(\beta,\gamma),\Phi'(\beta',\gamma')]
\end{aligned}$$

Theoretical framework

- Initial intrinsic states: PN-VAP (M. Anguiano et al., Nucl. Phys. A 683, 227 (2001))

$$E^{N,Z}[\Phi] = \frac{\langle\Phi|\hat{H}_{2b}\hat{P}^N\hat{P}^Z|\Phi\rangle}{\langle\Phi|\hat{P}^N\hat{P}^Z|\Phi\rangle} + \varepsilon_{DD}^{N,Z}(\Phi) - \lambda_{q_{20}}\langle\Phi|\hat{Q}_{20}|\Phi\rangle - \lambda_{q_{22}}\langle\Phi|\hat{Q}_{22}|\Phi\rangle$$

- Intermediate Particle Number and Angular Momentum Projected states

$$|IMK;NZ;\beta\gamma\rangle = \frac{2I+1}{8\pi^2}\int \mathcal{D}^{I*}_{MK}(\Omega)\hat{R}(\Omega)\cancel{\hat{P}^N\hat{P}^Z}|\Phi(\beta,\gamma)\rangle d\Omega$$

- Final GCM states $|IM;NZ\sigma\rangle = \sum_{K\beta\gamma} f^{I;NZ,\sigma}_{K\beta\gamma}|IMK;NZ;\beta\gamma\rangle$

$$\sum_{K'\beta'\gamma'}\left(\mathcal{H}^{I;NZ}_{K\beta\gamma K'\beta'\gamma'} - E^{I;NZ;\sigma}\mathcal{N}^{I;NZ}_{K\beta\gamma K'\beta'\gamma'}\right) f^{I;NZ;\sigma}_{K'\beta'\gamma'} = 0$$

$$\begin{aligned}
\mathcal{N}^{I;NZ}_{K\beta\gamma K'\beta'\gamma'} &\equiv \langle IMK;NZ;\beta\gamma|IMK';NZ;\beta'\gamma'\rangle \\
\mathcal{H}^{I;NZ}_{K\beta\gamma K'\beta'\gamma'} &\equiv \langle IMK;NZ;\beta\gamma|\hat{H}_{2b}|IMK';NZ;\beta'\gamma'\rangle + \varepsilon^{IKK';NZ}_{DD}\left[\Phi(\beta,\gamma),\Phi'(\beta',\gamma')\right]
\end{aligned}$$

Theoretical framework

- Initial intrinsic states: PN-VAP (M. Anguiano et al., Nucl. Phys. A 683, 227 (2001))

$$E^{N,Z}[\Phi] = \frac{\langle\Phi|\hat{H}_{2b}\hat{P}^N\hat{P}^Z|\Phi\rangle}{\langle\Phi|\hat{P}^N\hat{P}^Z|\Phi\rangle} + \varepsilon_{DD}^{N,Z}(\Phi) - \lambda_{q_{20}}\langle\Phi|\hat{Q}_{20}|\Phi\rangle - \lambda_{q_{22}}\langle\Phi|\hat{Q}_{22}|\Phi\rangle$$

- Intermediate Particle Number and Angular Momentum Projected states

$$|IMK;NZ;\beta\gamma\rangle = \frac{2I+1}{8\pi^2}\int \mathcal{D}^{I*}_{MK}(\Omega)\hat{R}(\Omega)\hat{P}^N\hat{P}^Z|\Phi(\beta,\gamma)\rangle d\Omega$$

- Final GCM states $|IM;NZ\sigma\rangle = \sum_{K\beta\gamma} f^{I;NZ,\sigma}_{K\beta\gamma}|IMK;NZ;\beta\gamma\rangle$

$$\sum_{K'\beta'\gamma'}\left(\mathcal{H}^{I;NZ}_{K\beta\gamma K'\beta'\gamma'} - E^{I;NZ;\sigma}\mathcal{N}^{I;NZ}_{K\beta\gamma K'\beta'\gamma'}\right) f^{I;NZ;\sigma}_{K'\beta'\gamma'} = 0$$

$$\begin{aligned}
\mathcal{N}^{I;NZ}_{K\beta\gamma K'\beta'\gamma'} &\equiv \langle IMK;NZ;\beta\gamma|IMK';NZ;\beta'\gamma'\rangle \\
\mathcal{H}^{I;NZ}_{K\beta\gamma K'\beta'\gamma'} &\equiv \langle IMK;NZ;\beta\gamma|\hat{H}_{2b}|IMK';NZ;\beta'\gamma'\rangle + \varepsilon^{IKK';NZ}_{DD}[\Phi(\beta,\gamma),\Phi'(\beta',\gamma')]
\end{aligned}$$

Theoretical framework

Effective nucleon-nucleon interaction: Gogny force (D1S/D1M)

$$V(1,2) = \sum_{i=1}^{2} e^{-(\vec{r}_1-\vec{r}_2)^2/\mu_i^2} \left(W_i + B_i P^\sigma - H_i P^\tau - M_i P^\sigma P^\tau\right)$$

$$+iW_0(\sigma_1+\sigma_2)\vec{k}\times\delta(\vec{r}_1-\vec{r}_2)\vec{k} + V_{\mathrm{Coulomb}}(\vec{r}_1,\vec{r}_2)$$

$$+t_3(1+x_0P^\sigma)\delta(\vec{r}_1-\vec{r}_2)\rho^\alpha\left((\vec{r}_1+\vec{r}_2)/2\right)$$

Theoretical framework

Effective nucleon-nucleon interaction: Gogny force (D1S/D1M)

$$V(1,2) = \sum_{i=1}^{2} e^{-(\vec{r}_1-\vec{r}_2)^2/\mu_i^2} \left(W_i + B_i P^\sigma - H_i P^\tau - M_i P^\sigma P^\tau\right)$$
$$+iW_0(\sigma_1+\sigma_2)\vec{k}\times\delta(\vec{r}_1-\vec{r}_2)\vec{k} + V_{\mathrm{Coulomb}}(\vec{r}_1,\vec{r}_2)$$

2-body potential

$$+t_3(1+x_0P^\sigma)\delta(\vec{r}_1-\vec{r}_2)\rho^\alpha\left((\vec{r}_1+\vec{r}_2)/2\right)$$

Theoretical framework

TECHNISCHE UNIVERSITÄT DARMSTADT

Effective nucleon-nucleon interaction: Gogny force (D1S/D1M)

$$V(1,2) = \sum_{i=1}^{2} e^{-(\vec{r}_1-\vec{r}_2)^2/\mu_i^2} \left(W_i + B_i P^\sigma - H_i P^\tau - M_i P^\sigma P^\tau\right)$$
$$+iW_0(\sigma_1+\sigma_2)\vec{k}\times\delta(\vec{r}_1-\vec{r}_2)\vec{k} + V_{\mathrm{Coulomb}}(\vec{r}_1,\vec{r}_2)$$

2-body potential

$$+t_3(1+x_0P^\sigma)\delta(\vec{r}_1-\vec{r}_2)\rho^\alpha\left((\vec{r}_1+\vec{r}_2)/2\right)$$

Density dependent term

Theoretical framework

TECHNISCHE UNIVERSITÄT DARMSTADT

- Effective nucleon-nucleon interaction: Gogny force (D1S/D1M)

$$V(1,2) = \sum_{i=1}^{2} e^{-(\vec{r}_1-\vec{r}_2)^2/\mu_i^2}\left(W_i + B_i P^\sigma - H_i P^\tau - M_i P^\sigma P^\tau\right)$$
$$+iW_0(\sigma_1+\sigma_2)\vec{k}\times\delta(\vec{r}_1-\vec{r}_2)\vec{k} + V_{\rm Coulomb}(\vec{r}_1,\vec{r}_2)$$

2-body potential

$$+t_3(1+x_0P^\sigma)\delta(\vec{r}_1-\vec{r}_2)\rho^\alpha\left((\vec{r}_1+\vec{r}_2)/2\right)$$

Density dependent term

- Prescriptions:

$$\varepsilon_{DD}^{N,Z}(\Phi)$$

$$\rho_H^{NZ}(\vec{r}) \equiv \frac{\langle\Phi|\hat{\rho}(\vec{r})P^N P^Z|\Phi\rangle}{\langle\Phi|P^N P^Z|\Phi\rangle}$$

$$\varepsilon_{DD}^{IKK';NZ}\left[\Phi(\beta,\gamma),\Phi'(\beta',\gamma')\right]$$

$$\rho_H^{NZ}(\Omega,\vec{r}) \equiv \frac{\langle\Phi|\hat{\rho}(\vec{r})\hat{R}(\Omega)P^N P^Z|\Phi'\rangle}{\langle\Phi|\hat{R}(\Omega)P^N P^Z|\Phi'\rangle}$$

Particle number projection

Example: ^{24}Mg

$$\delta E^{N,Z}\left[\bar{\Phi}(\beta,\gamma)\right]\Big|_{\bar{\Phi}=\Phi} = 0$$

$$E^{N,Z}[\Phi] = \frac{\langle\Phi|\hat{H}_{2b}\hat{P}^N\hat{P}^Z|\Phi\rangle}{\langle\Phi|\hat{P}^N\hat{P}^Z|\Phi\rangle} + \varepsilon^{N,Z}_{DD}(\Phi) - \lambda_{q_{20}}\langle\Phi|\hat{Q}_{20}|\Phi\rangle - \lambda_{q_{22}}\langle\Phi|\hat{Q}_{22}|\Phi\rangle$$

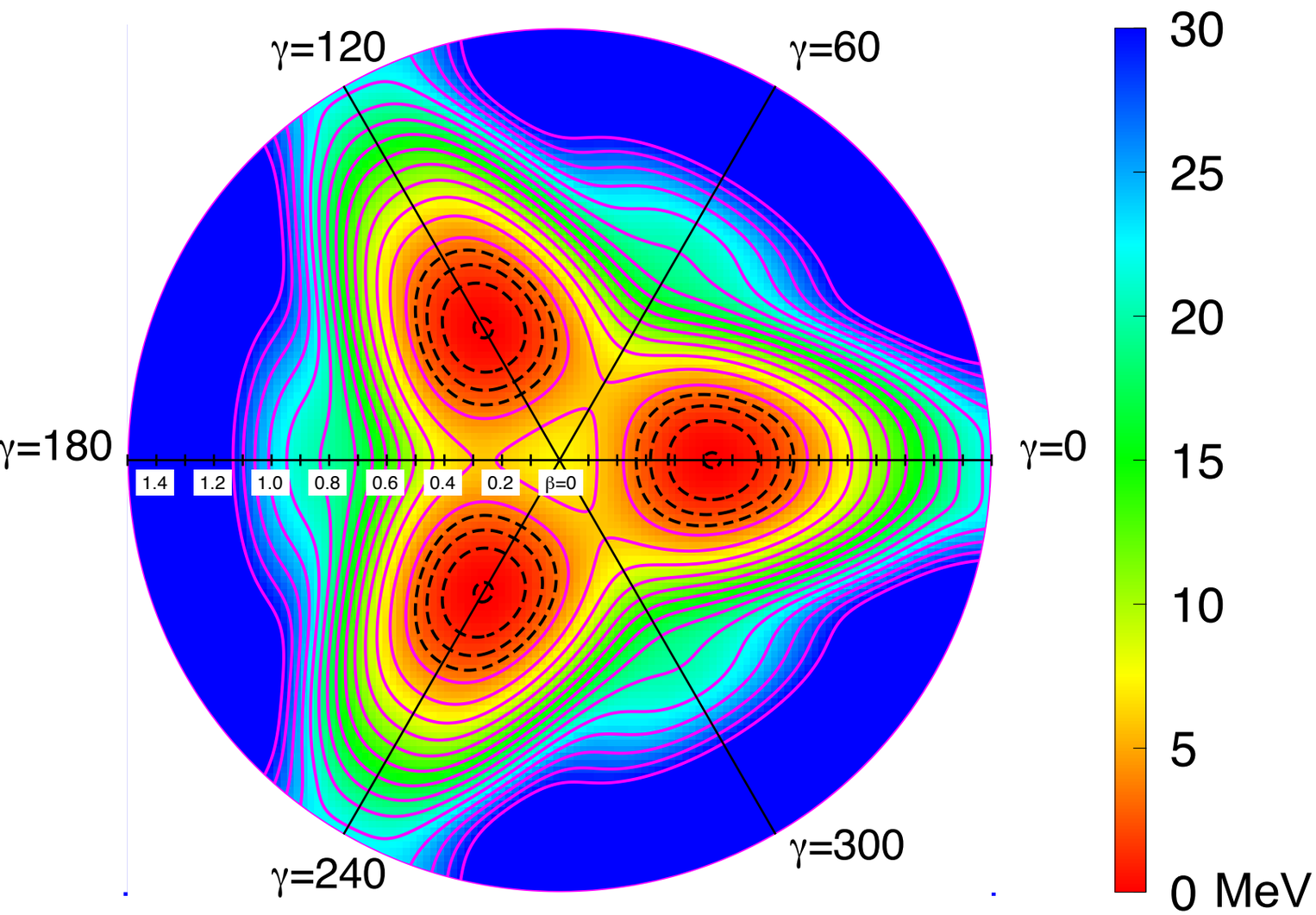

- Symmetry corresponding to the different orientation of the axes
- All configurations are included between γ∈[0º,60º]

T. R. R., J. L. Egido, PRC 81, 064323 (2010)

Particle number projection

Example: ^{24}Mg

$$\delta E^{N,Z}\left[\bar{\Phi}(\beta,\gamma)\right]\Big|_{\bar{\Phi}=\Phi} = 0$$

$$E^{N,Z}[\Phi] = \frac{\langle\Phi|\hat{H}_{2b}\hat{P}^N\hat{P}^Z|\Phi\rangle}{\langle\Phi|\hat{P}^N\hat{P}^Z|\Phi\rangle} + \varepsilon^{N,Z}_{DD}(\Phi) - \lambda_{q_{20}}\langle\Phi|\hat{Q}_{20}|\Phi\rangle - \lambda_{q_{22}}\langle\Phi|\hat{Q}_{22}|\Phi\rangle$$

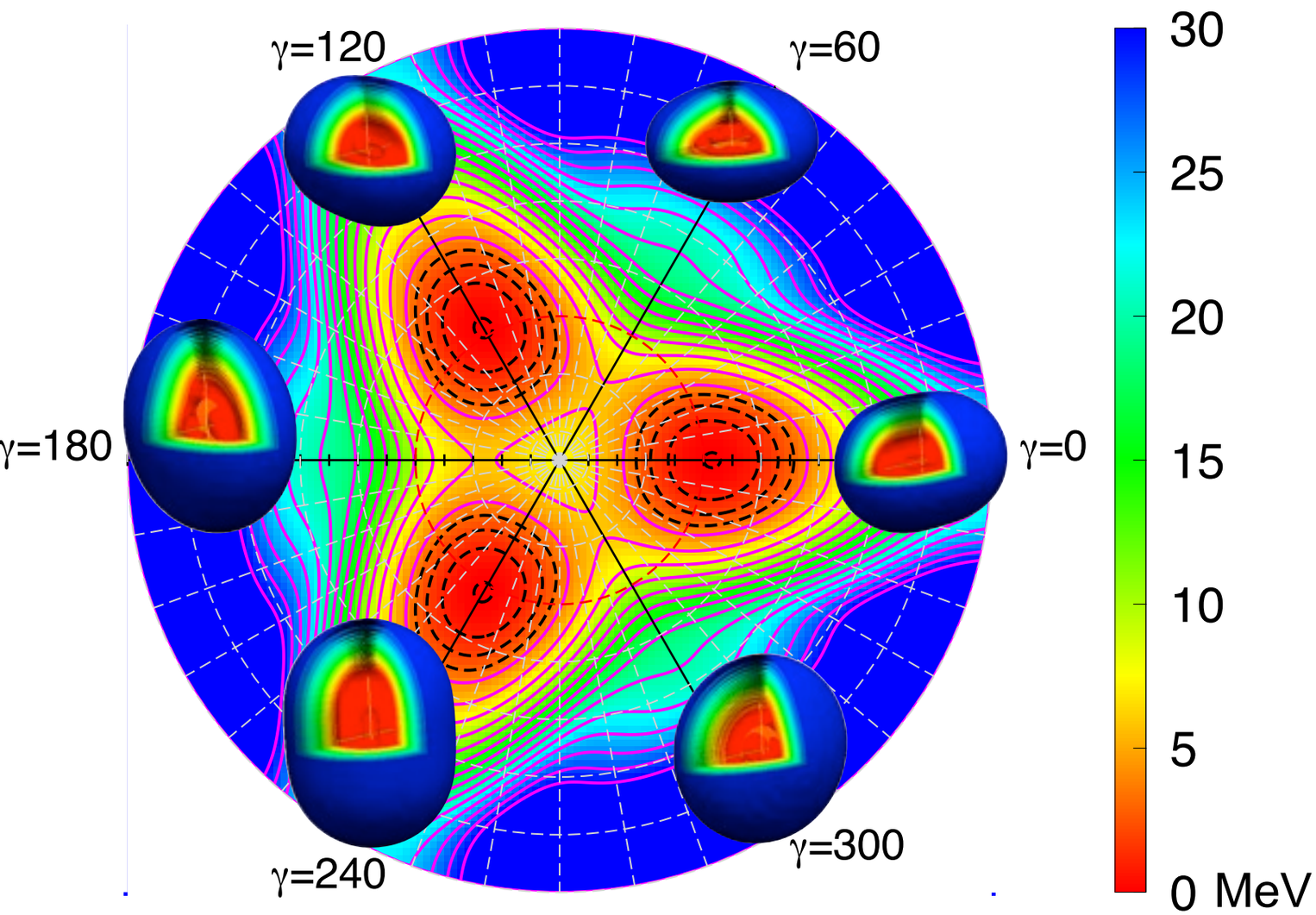

- Symmetry corresponding to the different orientation of the axes
- All configurations are included between γ∈[0º,60º]

T. R. R., J. L. Egido, PRC 81, 064323 (2010)

Particle number projection

Example: ^{24}Mg

$$\delta E^{N,Z}\left[\bar{\Phi}(\beta,\gamma)\right]\Big|_{\bar{\Phi}=\Phi} = 0$$

$$E^{N,Z}[\Phi] = \frac{\langle\Phi|\hat{H}_{2b}\hat{P}^N\hat{P}^Z|\Phi\rangle}{\langle\Phi|\hat{P}^N\hat{P}^Z|\Phi\rangle} + \varepsilon^{N,Z}_{DD}(\Phi) - \lambda_{q_{20}}\langle\Phi|\hat{Q}_{20}|\Phi\rangle - \lambda_{q_{22}}\langle\Phi|\hat{Q}_{22}|\Phi\rangle$$

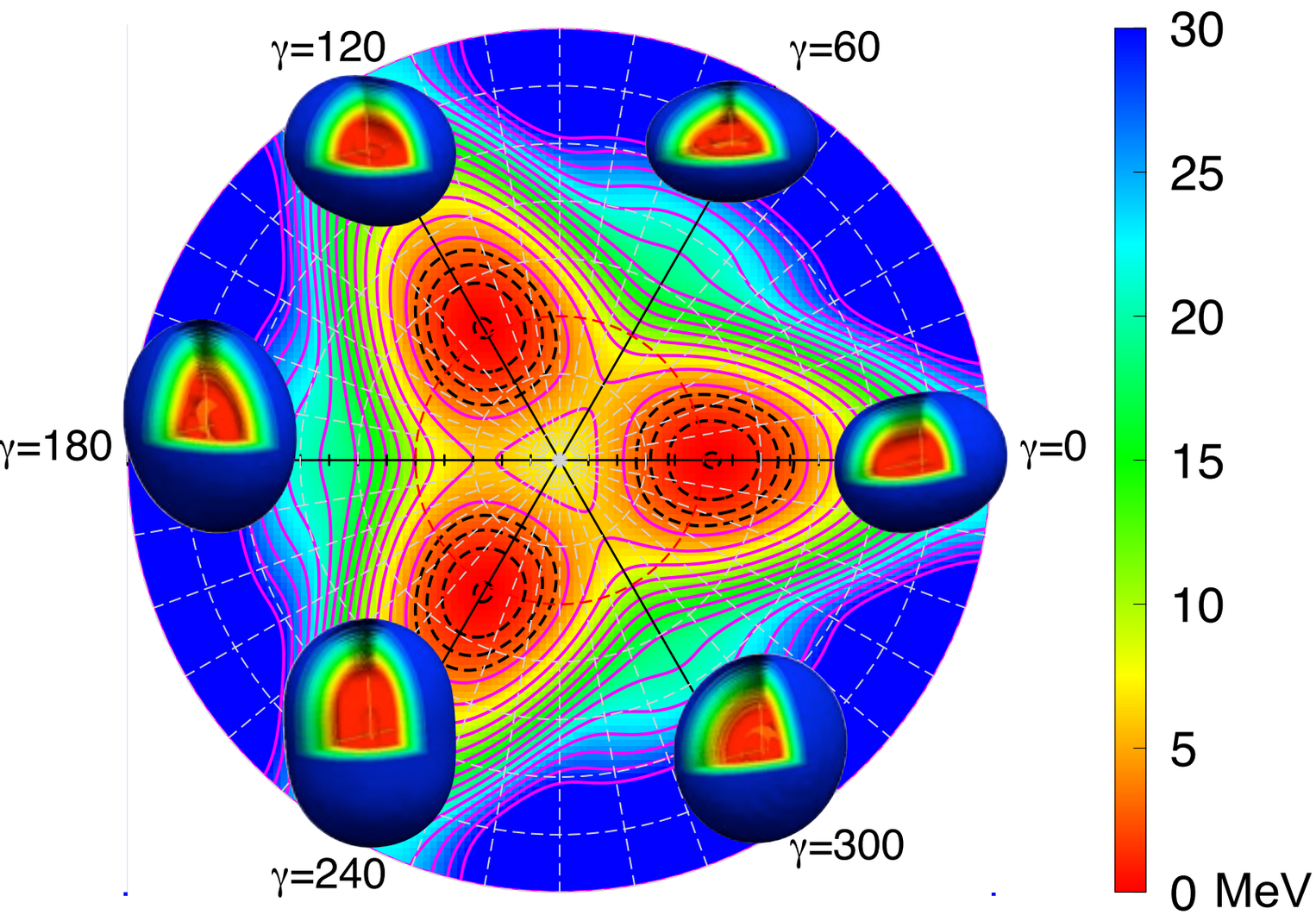

- Symmetry corresponding to the different orientation of the axes
- All configurations are included between γ∈[0º,60º]

T. R. R., J. L. Egido, PRC 81, 064323 (2010)

Particle number and angular momentum projection

Example: ^{24}Mg

$$|IMK;NZ;\beta\gamma\rangle = \frac{2I+1}{8\pi^2}\int \mathcal{D}^{I*}_{MK}(\Omega)\hat{R}(\Omega)\hat{P}^N\hat{P}^Z|\Phi(\beta,\gamma)\rangle d\Omega$$

Convergence in Euler angles I

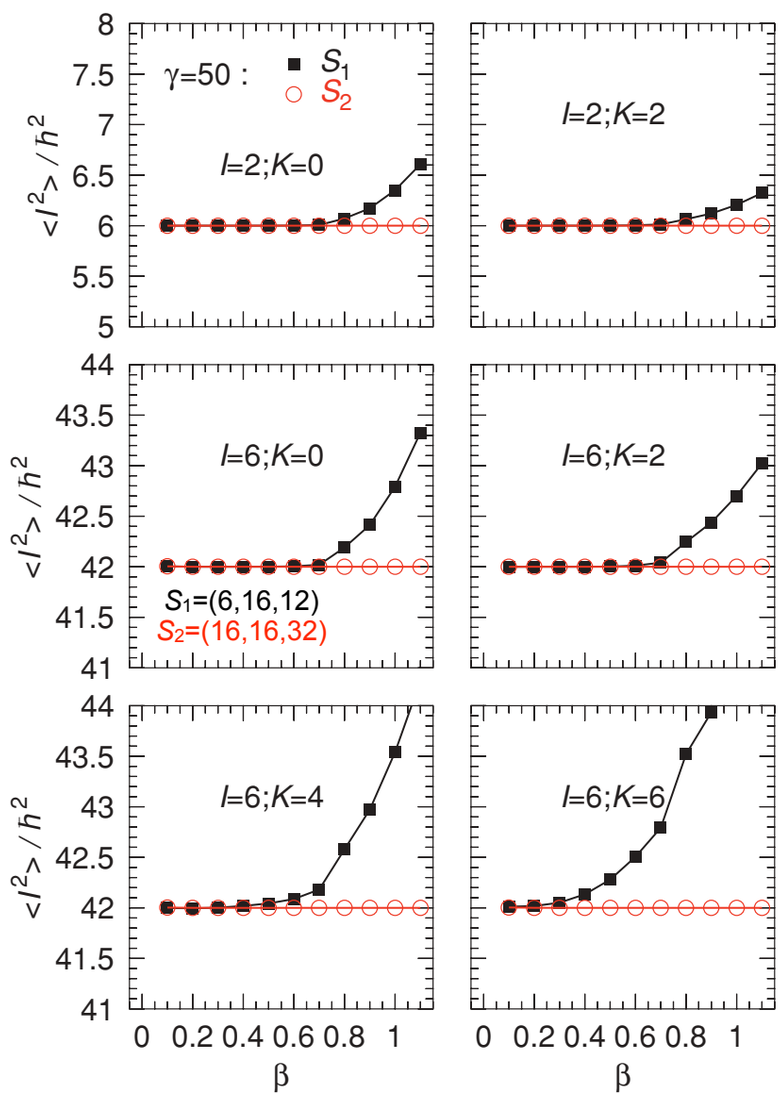

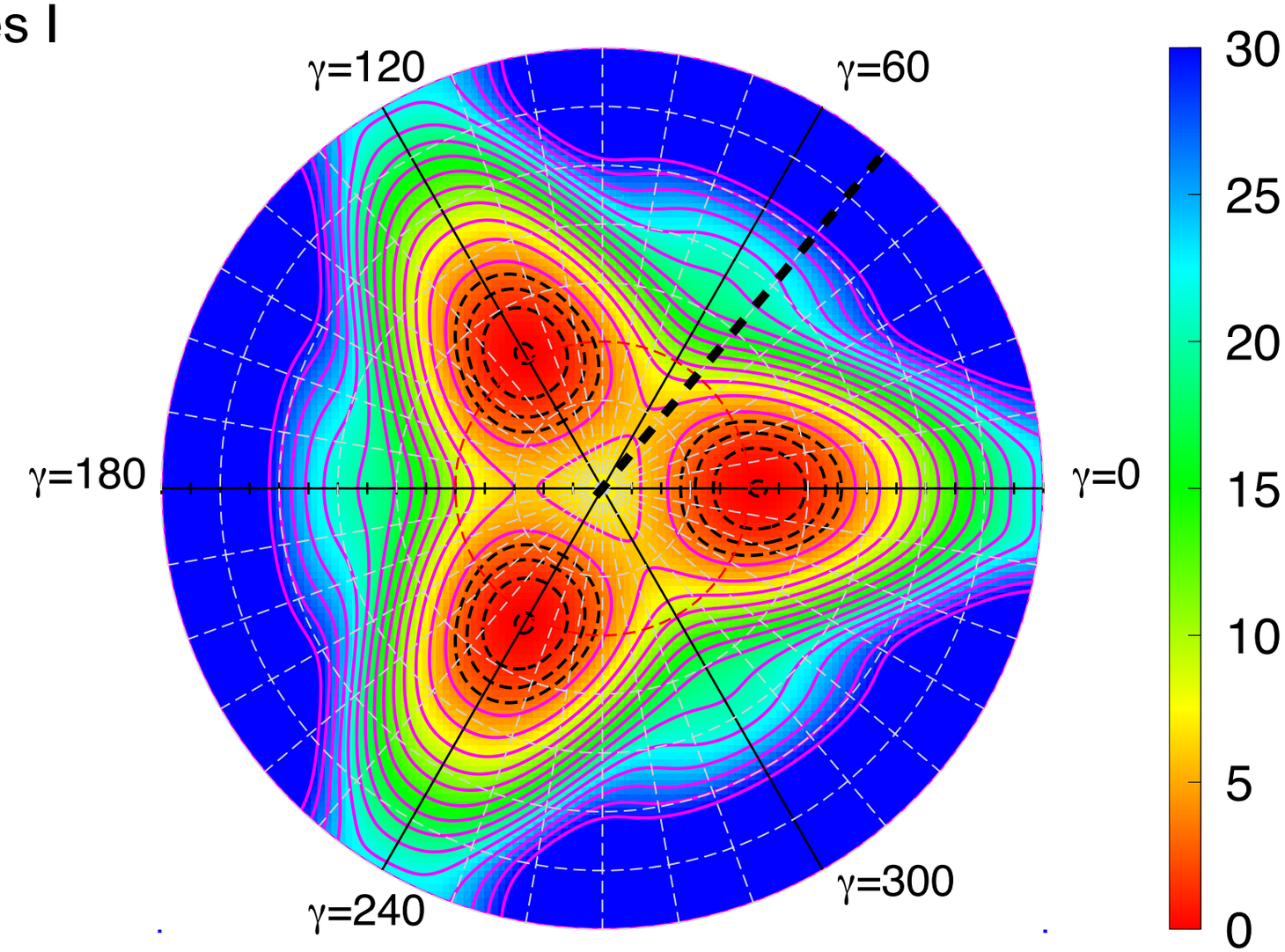

T. R. R., J. L. Egido, PRC 81, 064323 (2010)

Particle number and angular momentum projection

TECHNISCHE UNIVERSITÄT DARMSTADT

Example: ^{24}Mg

$$|IMK;NZ;\beta\gamma\rangle = \frac{2I+1}{8\pi^2}\int \mathcal{D}^{I*}_{MK}(\Omega)\hat{R}(\Omega)\hat{P}^N\hat{P}^Z|\Phi(\beta,\gamma)\rangle d\Omega$$

Convergence in Euler angles II

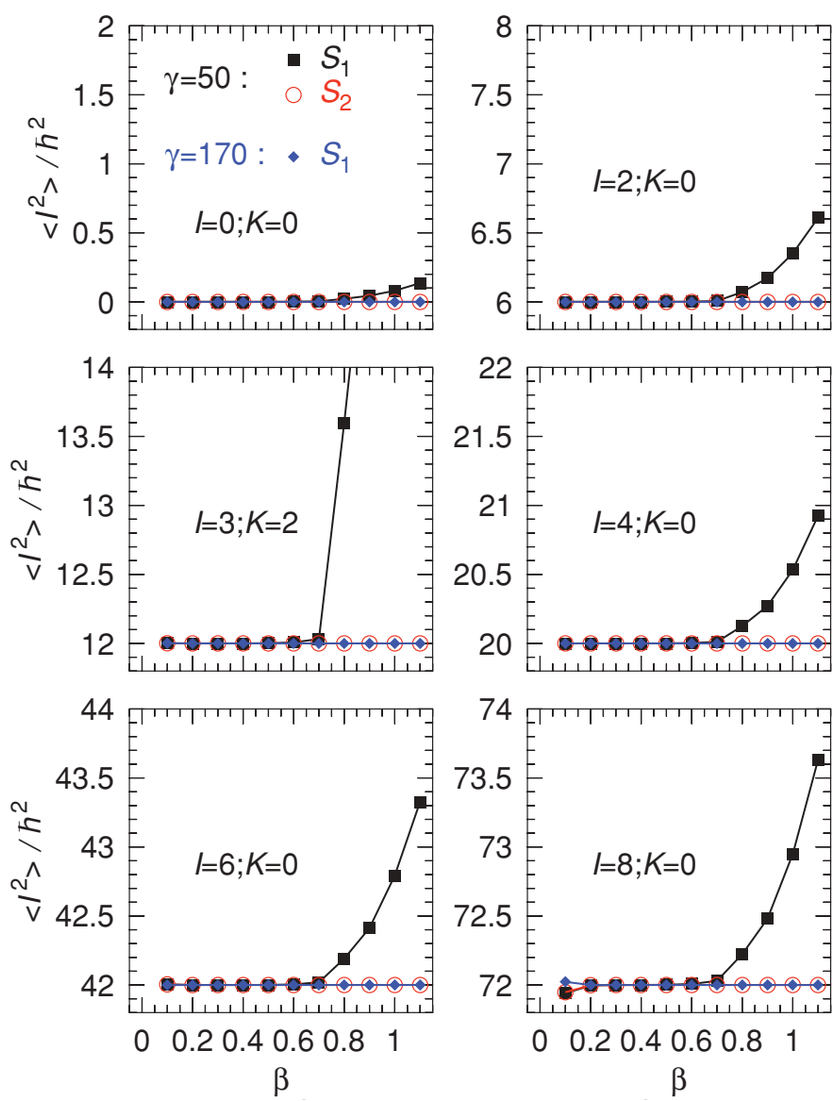

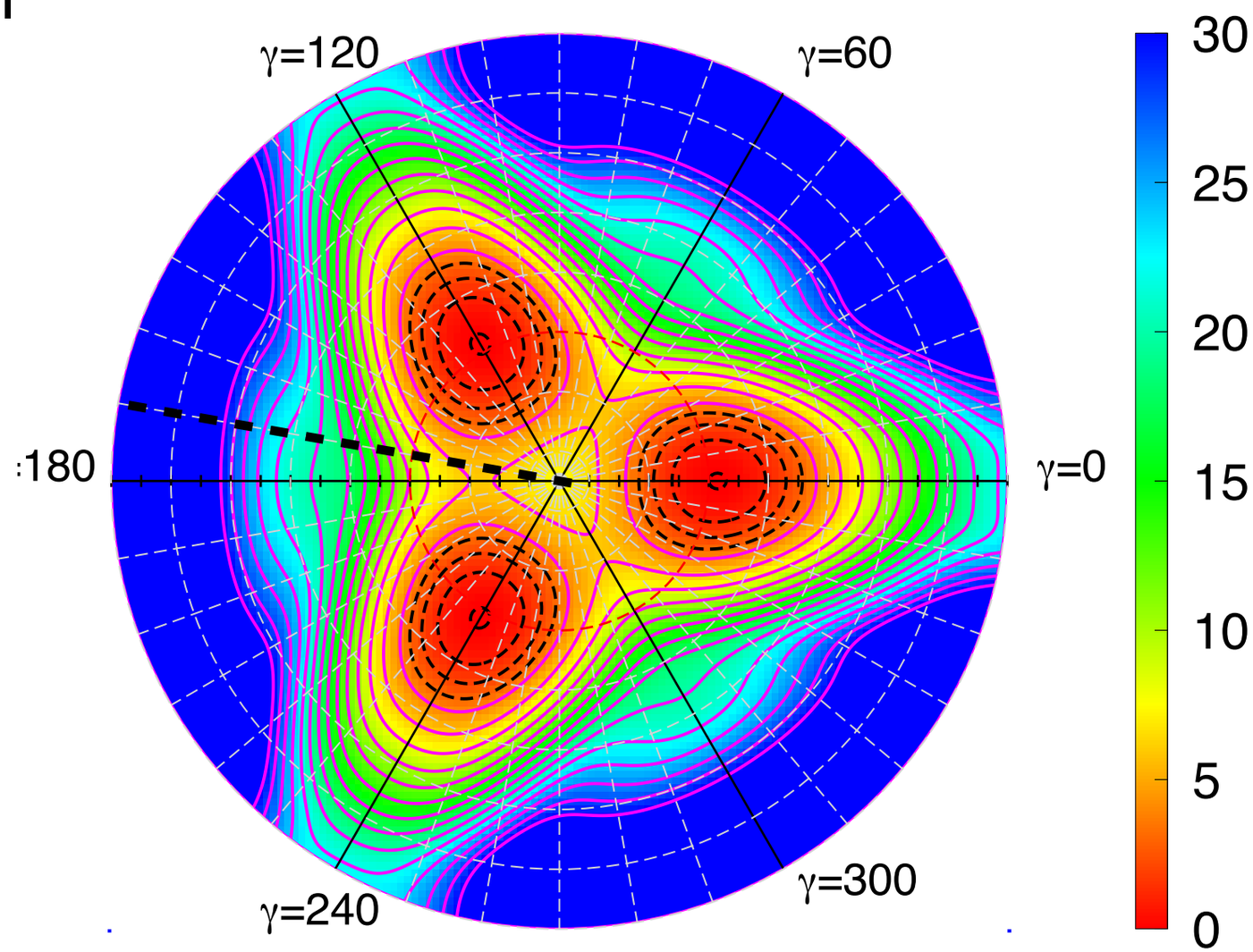

T. R. R., J. L. Egido, PRC 81, 064323 (2010)

Particle number and angular momentum projection

TECHNISCHE UNIVERSITÄT DARMSTADT

Example: ^{24}Mg

$$|IMK;NZ;\beta\gamma\rangle = \frac{2I+1}{8\pi^2}\int \mathcal{D}^{I*}_{MK}(\Omega)\hat{R}(\Omega)\hat{P}^N\hat{P}^Z|\Phi(\beta,\gamma)\rangle d\Omega$$

$$|IM;NZ;\beta\gamma\rangle = \sum_K g_K^{IM;NZ;\beta\gamma}|IMK;NZ;\beta\gamma\rangle$$

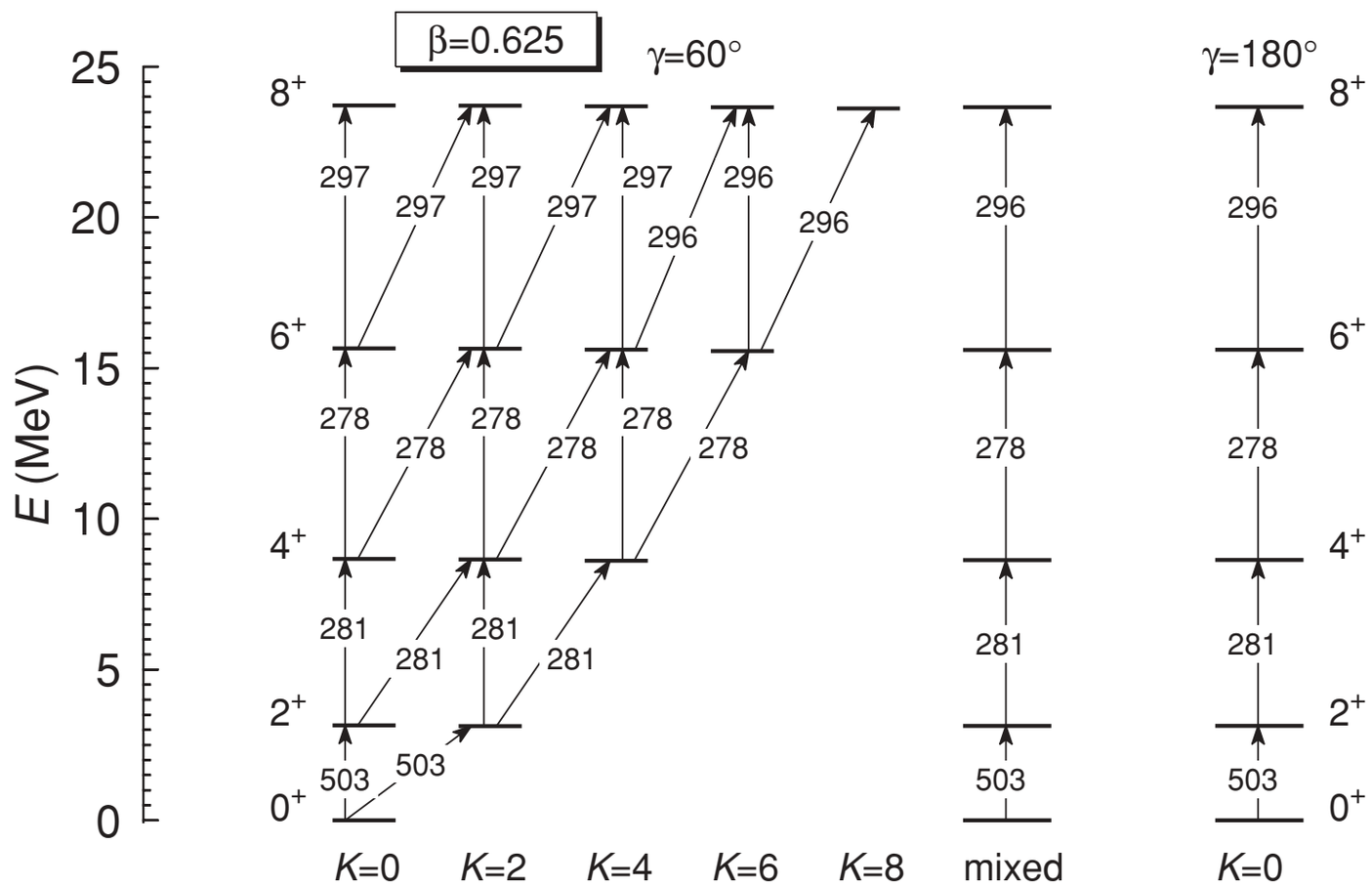

K-mixing and consistency I

T. R. R., J. L. Egido, PRC 81, 064323 (2010)

Particle number and angular momentum projection

TECHNISCHE UNIVERSITÄT DARMSTADT

Example: ^{24}Mg

$$|IMK;NZ;\beta\gamma\rangle = \frac{2I+1}{8\pi^2}\int \mathcal{D}^{I*}_{MK}(\Omega)\hat{R}(\Omega)\hat{P}^N\hat{P}^Z|\Phi(\beta,\gamma)\rangle d\Omega$$

$$|IM;NZ;\beta\gamma\rangle = \sum_K g_K^{IM;NZ;\beta\gamma}|IMK;NZ;\beta\gamma\rangle$$

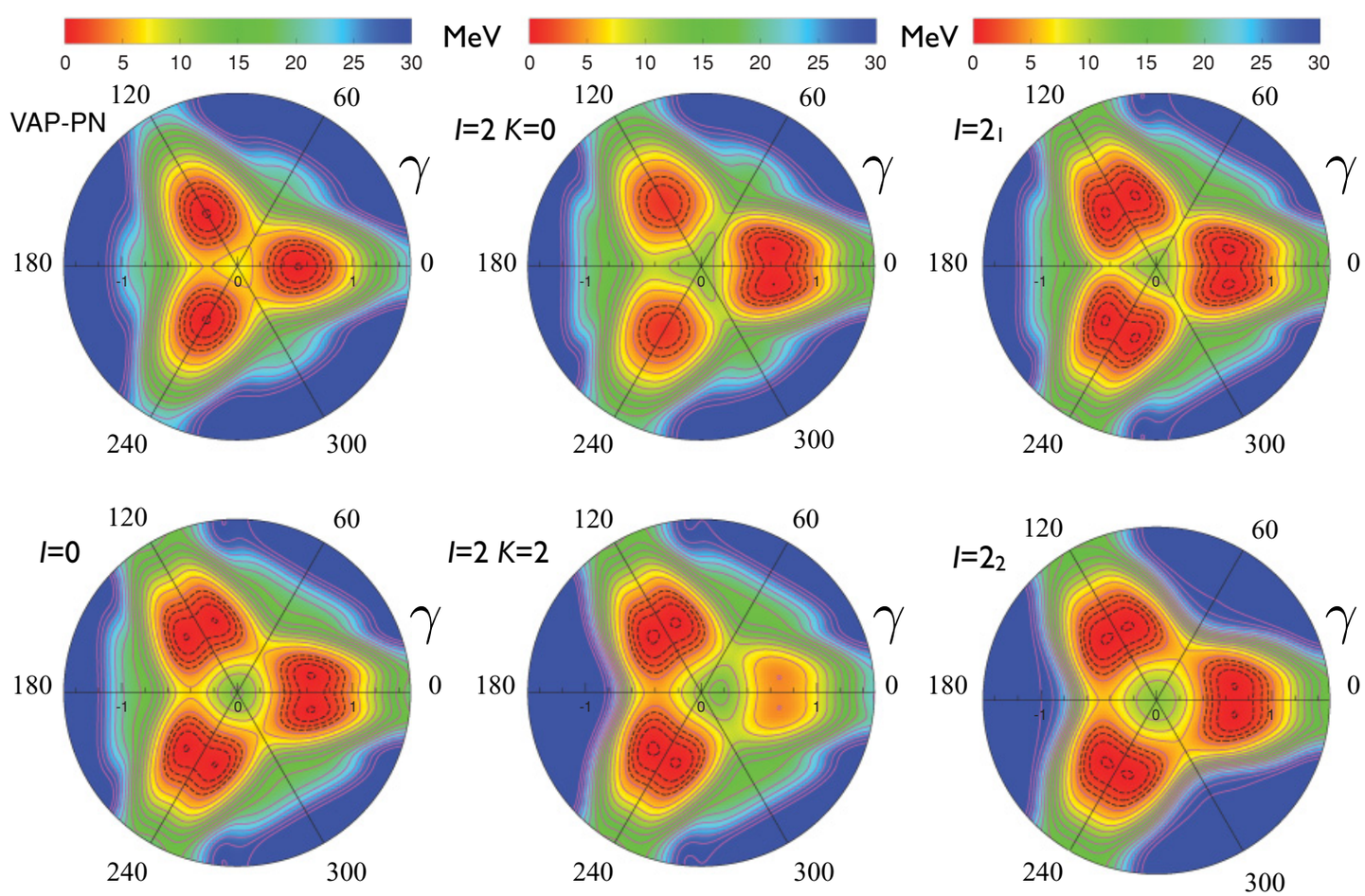

K-mixing and consistency II

PES without *K*-mixing depend on the orientation of the reference frame!

Particle number and angular momentum projection

Example: ^{24}Mg

$$|IMK;NZ;\beta\gamma\rangle = \frac{2I+1}{8\pi^2}\int \mathcal{D}^{I*}_{MK}(\Omega)\hat{R}(\Omega)\hat{P}^N\hat{P}^Z|\Phi(\beta,\gamma)\rangle d\Omega$$

$$|IM;NZ;\beta\gamma\rangle = \sum_K g_K^{IM;NZ;\beta\gamma}|IMK;NZ;\beta\gamma\rangle$$

- Minimum displaced to triaxial shapes.
- Projection onto odd *I* angular momentum
- Softening of PES with increasing *I*.
- Difference between triaxial minimum and axial saddle point of ~ 0.7 MeV (0^+)

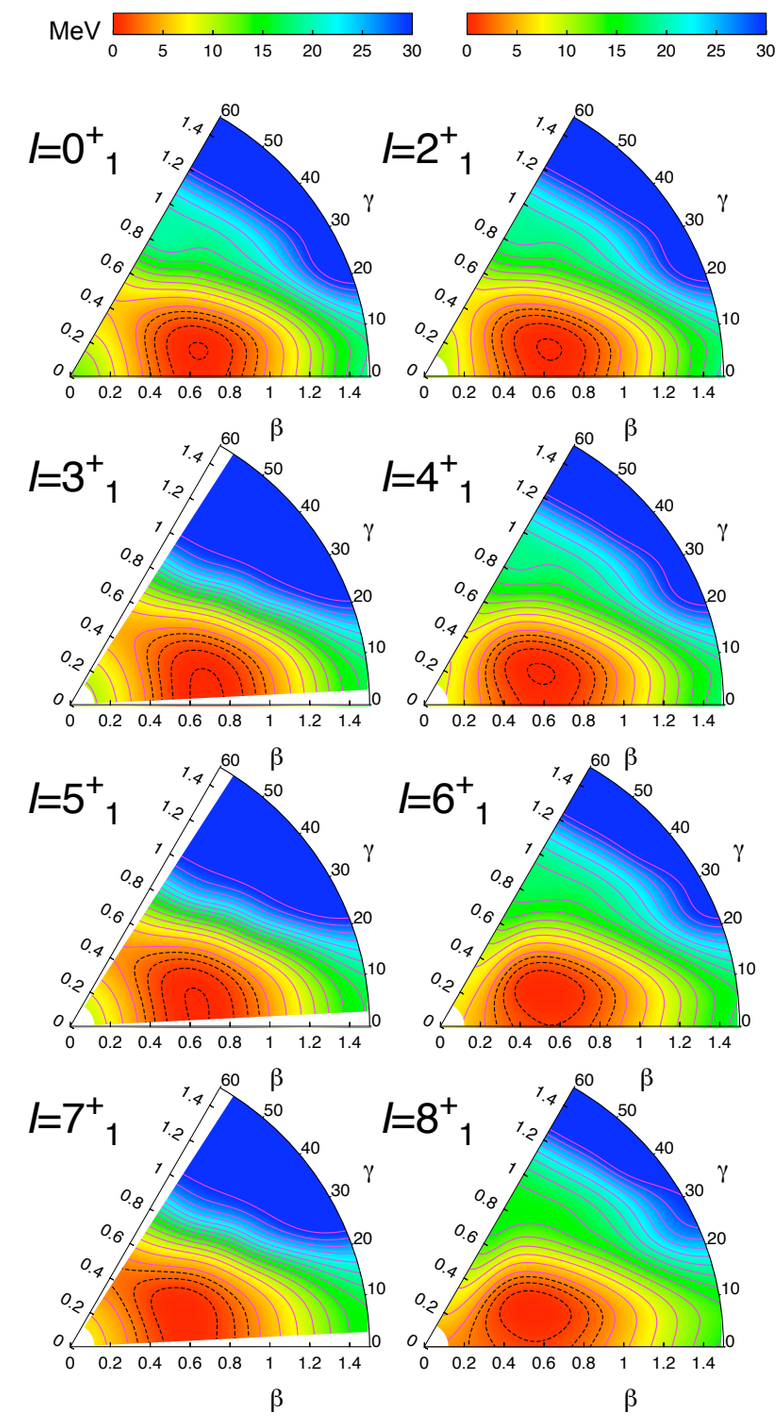

Example: ^{24}Mg

Selection of the mesh. Resolution.

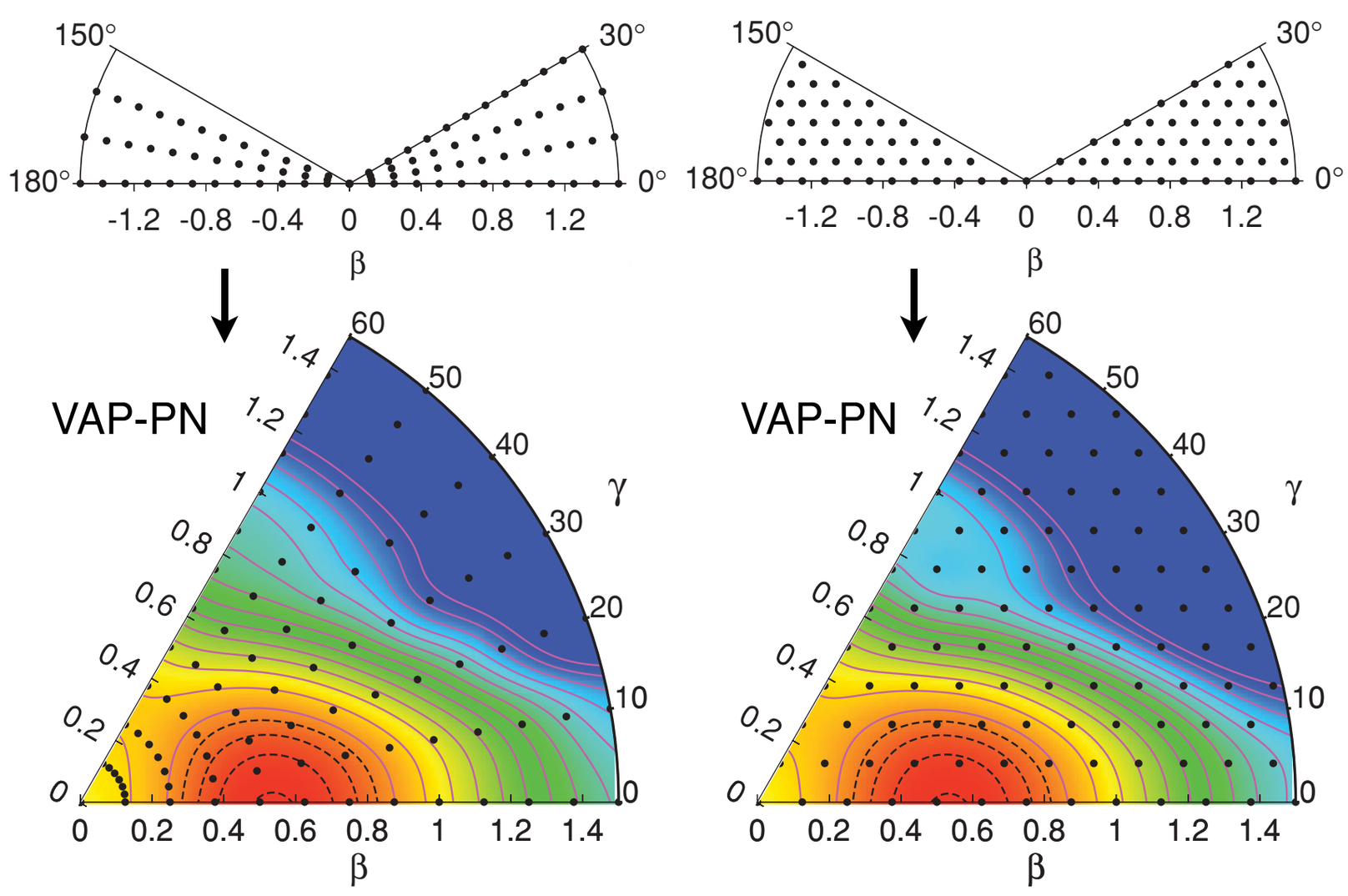

Example: ^{24}Mg

Selection of the mesh. Resolution.

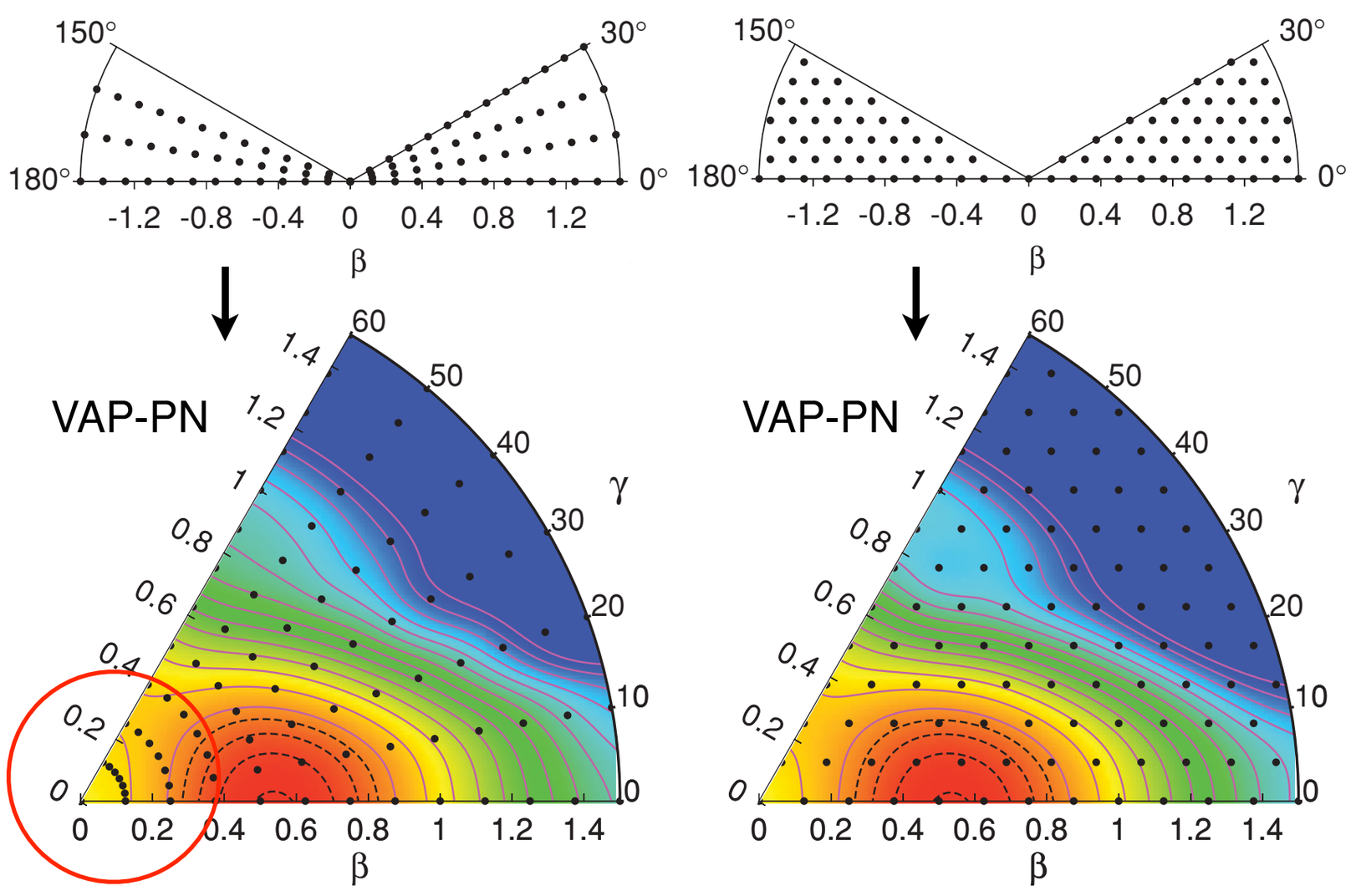

Example: ^{24}Mg

Selection of the mesh. Resolution.

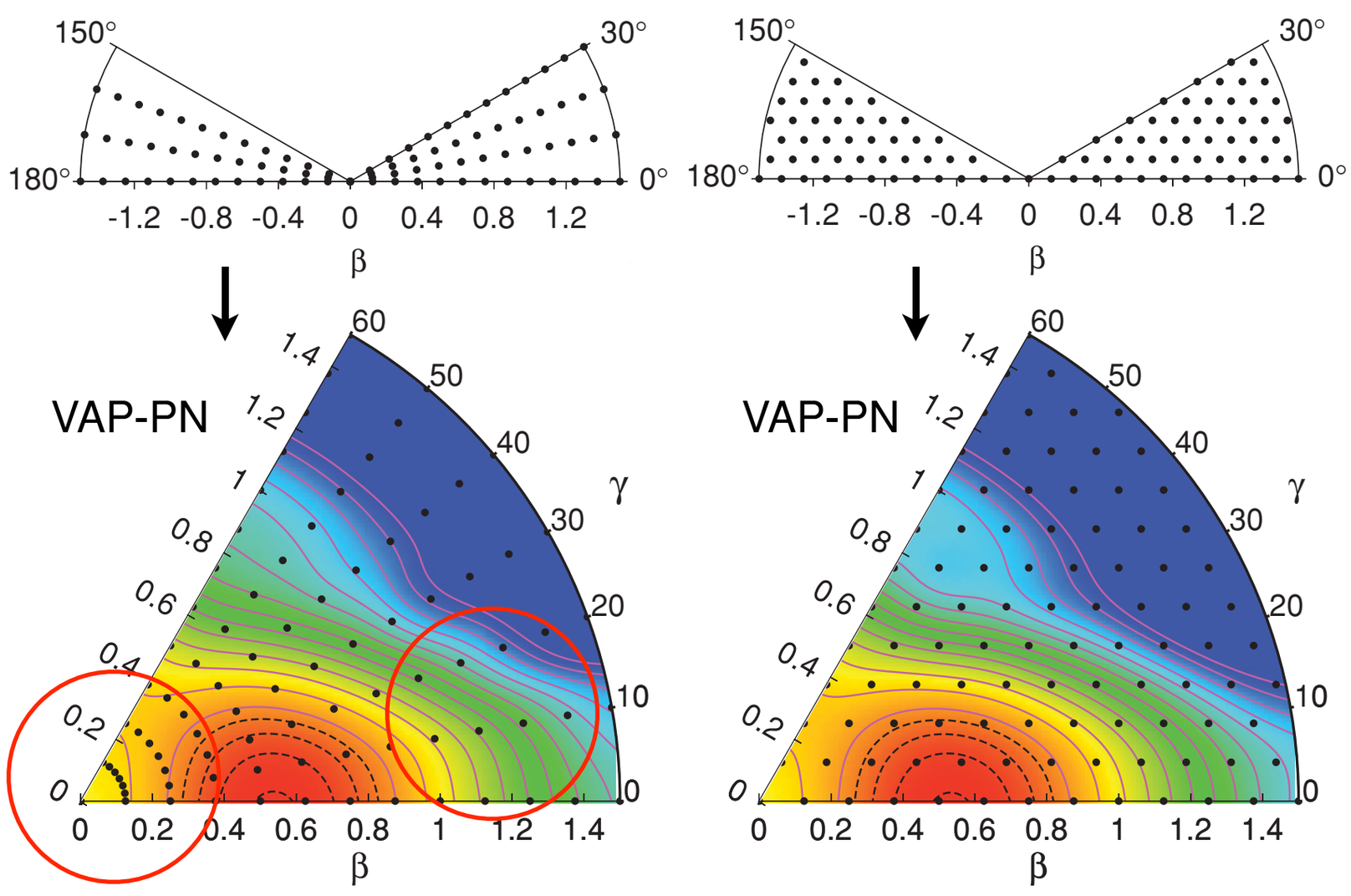

Example: ^{24}Mg

Selection of the mesh. Resolution.

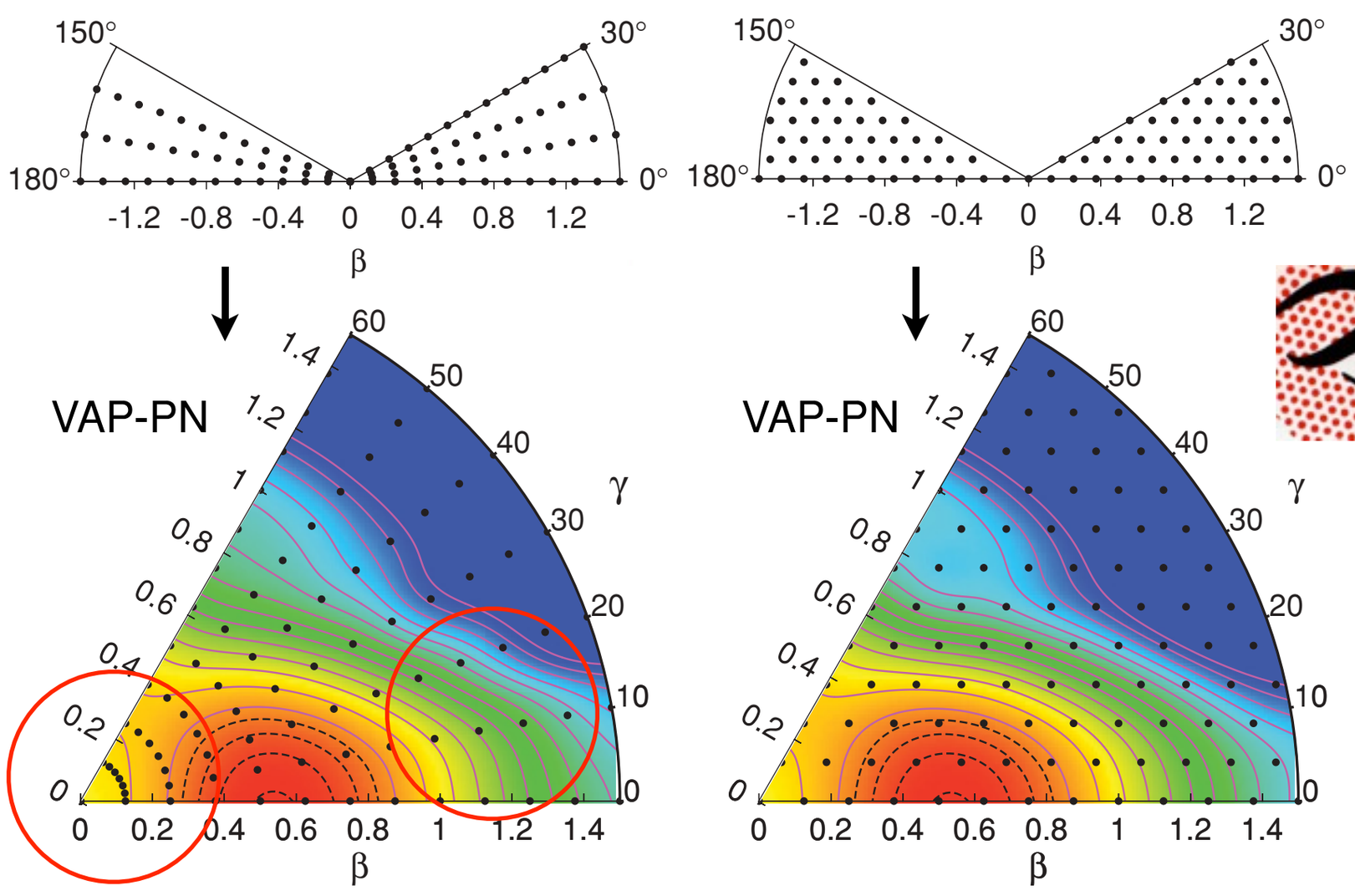

Configuration (shape and *K*) mixing

TECHNISCHE UNIVERSITÄT DARMSTADT

Example: ^{24}Mg

Configuration mixing within the framework of the **Generator Coordinate Method (GCM)**.
***K* and deformation mixing**

$$|IM;NZ\sigma\rangle = \sum_{K\beta\gamma} f^{I;NZ,\sigma}_{K\beta\gamma} |IMK;NZ;\beta\gamma\rangle$$

$$\sum_{K'\beta'\gamma'} \left(\mathcal{H}^{I;NZ}_{K\beta\gamma K'\beta'\gamma'} - E^{I;NZ;\sigma} \mathcal{N}^{I;NZ}_{K\beta\gamma K'\beta'\gamma'} \right) f^{I;NZ;\sigma}_{K'\beta'\gamma'} = 0$$

Convergence of the GCM states

- Plateau condition as a function of natural states.

- Orthogonalization requirements.

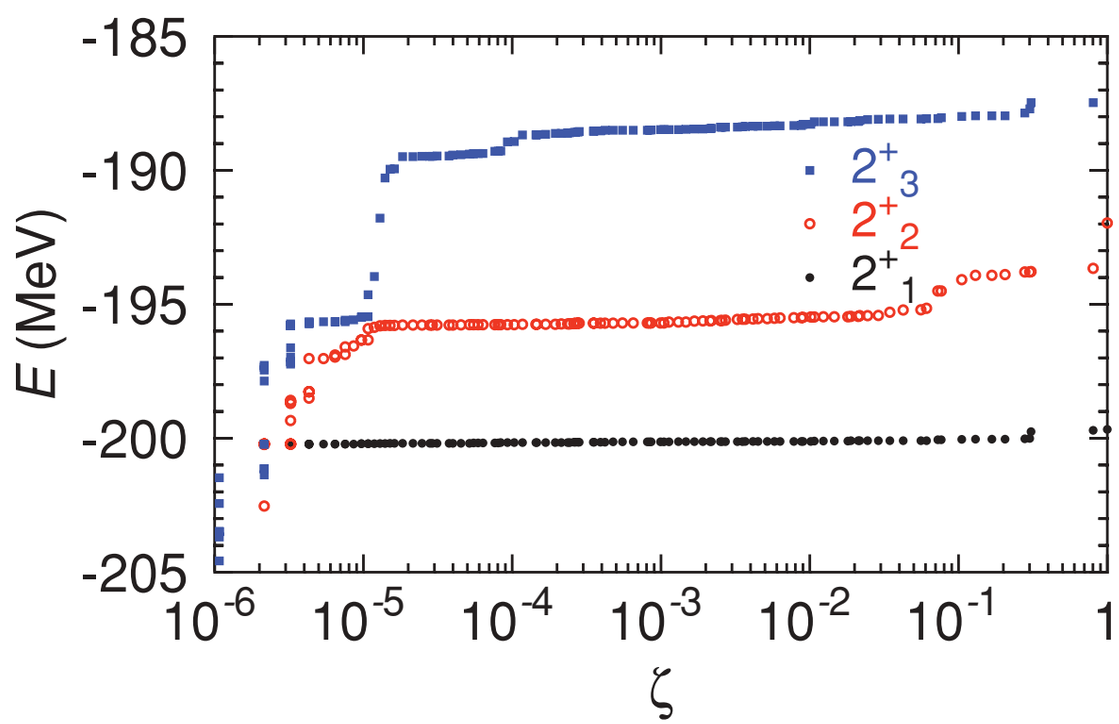

Configuration (shape and *K*) mixing

TECHNISCHE UNIVERSITÄT DARMSTADT

Example: ^{24}Mg

Configuration mixing within the framework of the **Generator Coordinate Method (GCM)**. ***K* and deformation mixing**

$$|IM;NZ\sigma\rangle = \sum_{K\beta\gamma} f^{I;NZ,\sigma}_{K\beta\gamma} |IMK;NZ;\beta\gamma\rangle$$

$$\sum_{K'\beta'\gamma'} \left(\mathcal{H}^{I;NZ}_{K\beta\gamma K'\beta'\gamma'} - E^{I;NZ;\sigma} \mathcal{N}^{I;NZ}_{K\beta\gamma K'\beta'\gamma'} \right) f^{I;NZ;\sigma}_{K'\beta'\gamma'} = 0$$

- Axial ground state rotational band
- Second band associated to a gamma band
- Third band with shape mixing

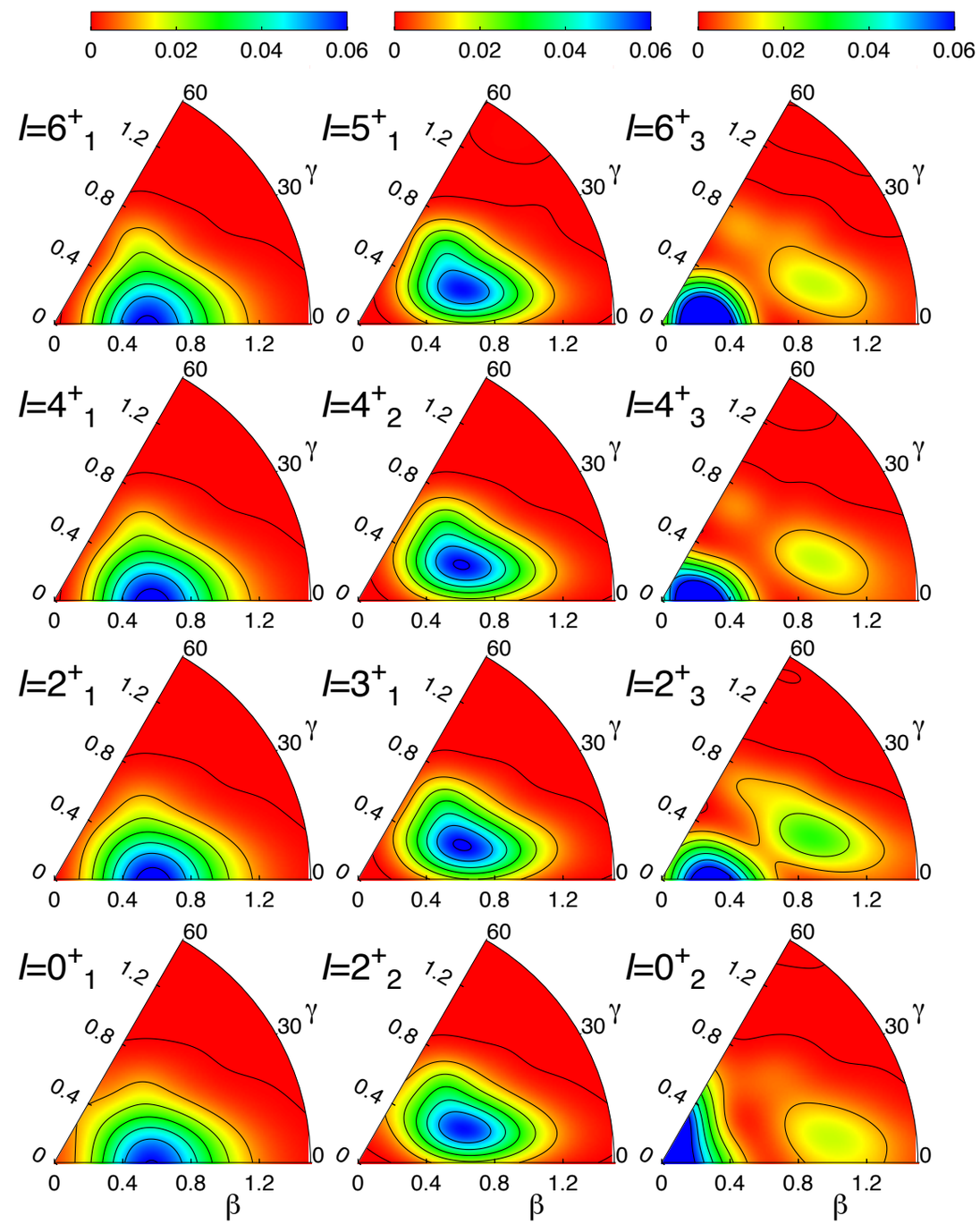

Example: ^{24}Mg

T. R. R., J. L. Egido, PRC 81, 064323 (2010)

Configuration mixing within the framework of the **Generator Coordinate Method (GCM)**.
***K* and deformation mixing**

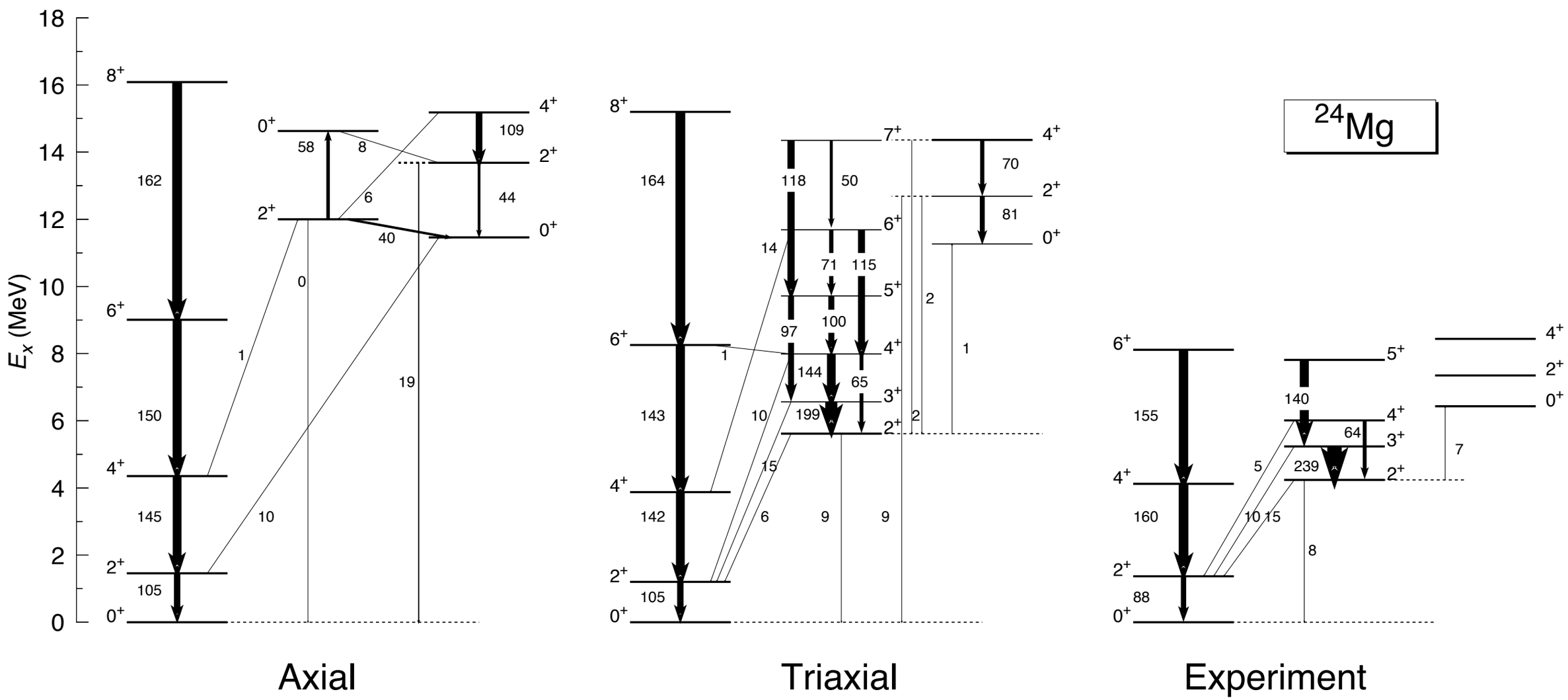

Configuration (shape) mixing

TECHNISCHE UNIVERSITÄT DARMSTADT

Example: ^{24}Mg

T. R. R., J. L. Egido, PRC 81, 064323 (2010)

Configuration mixing within the framework of the **Generator Coordinate Method (GCM)**.
***K* and deformation mixing**

^{24}Mg is a bad choice to see triaxial effects!!

Particle number projection

Example: ^{80}Zr

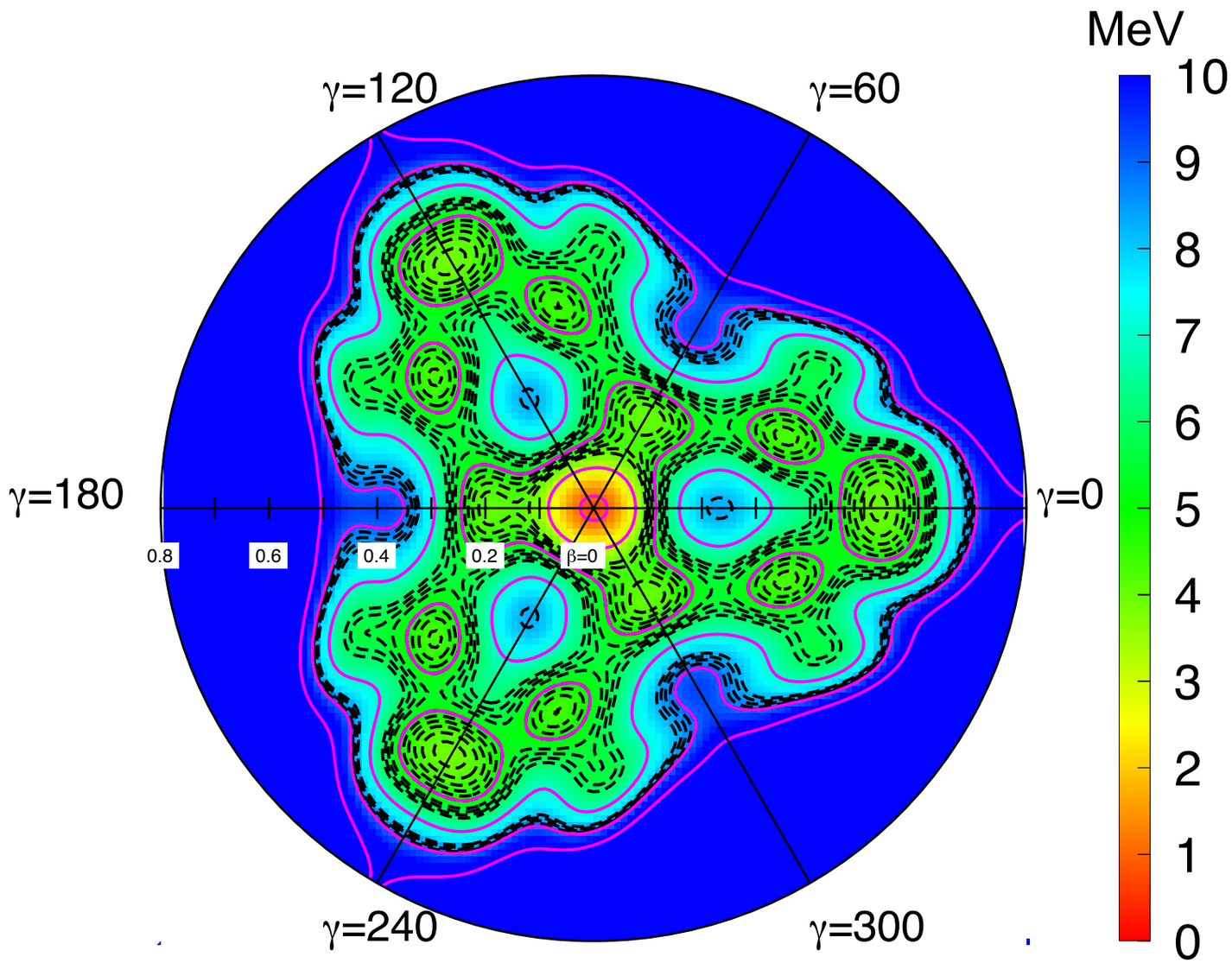

- Symmetry corresponding to the different orientation of the axes
- All configurations are included between γ∈[0º,60º]

T. R. R., J. L. Egido, Phys. Lett. B 705, 255 (2011)

Particle number projection

Example: ^{80}Zr

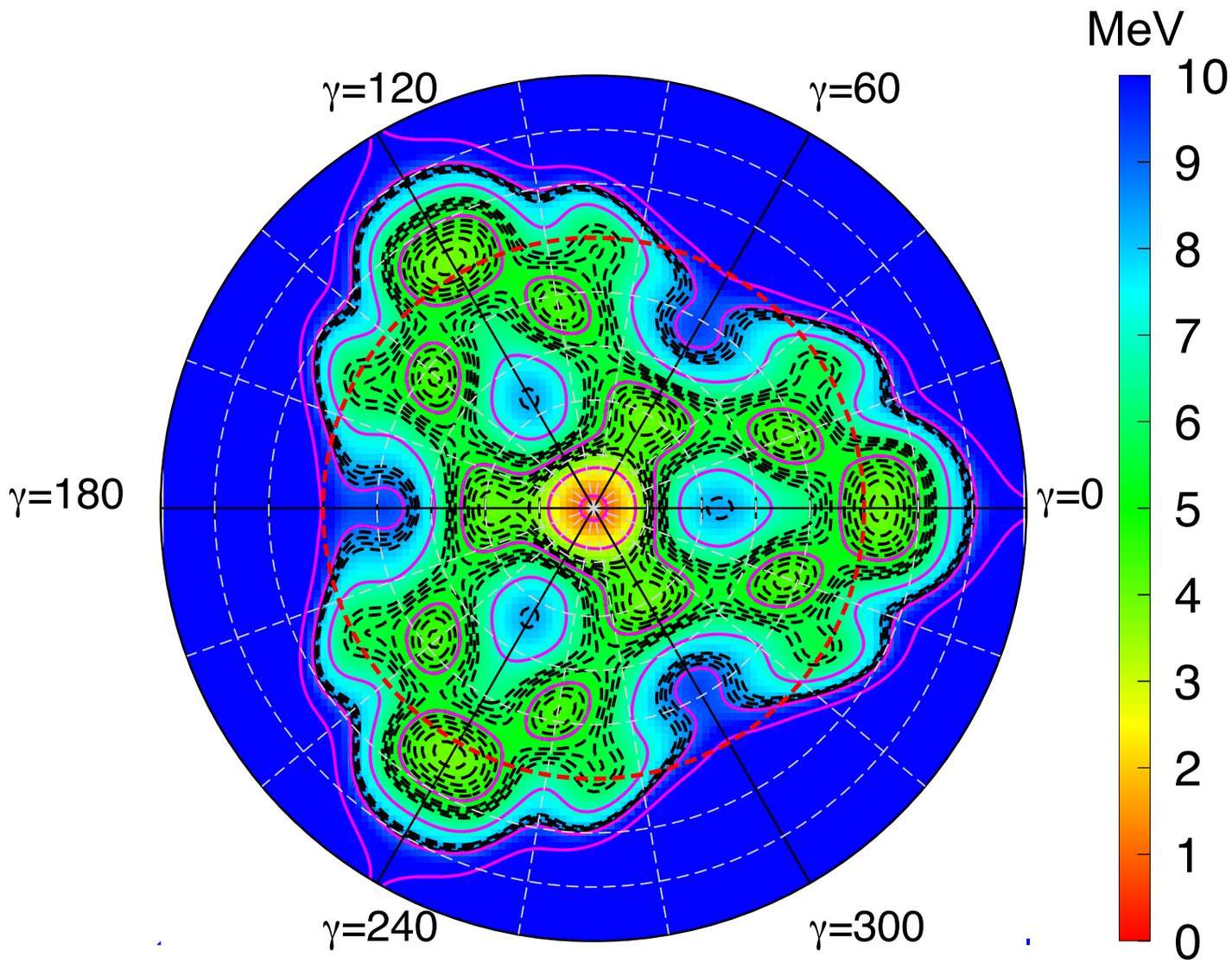

- Symmetry corresponding to the different orientation of the axes
- All configurations are included between $\gamma \in [0^o, 60^o]$

T. R. R., J. L. Egido, Phys. Lett. B 705, 255 (2011)

Particle number projection

Example: ^{80}Zr

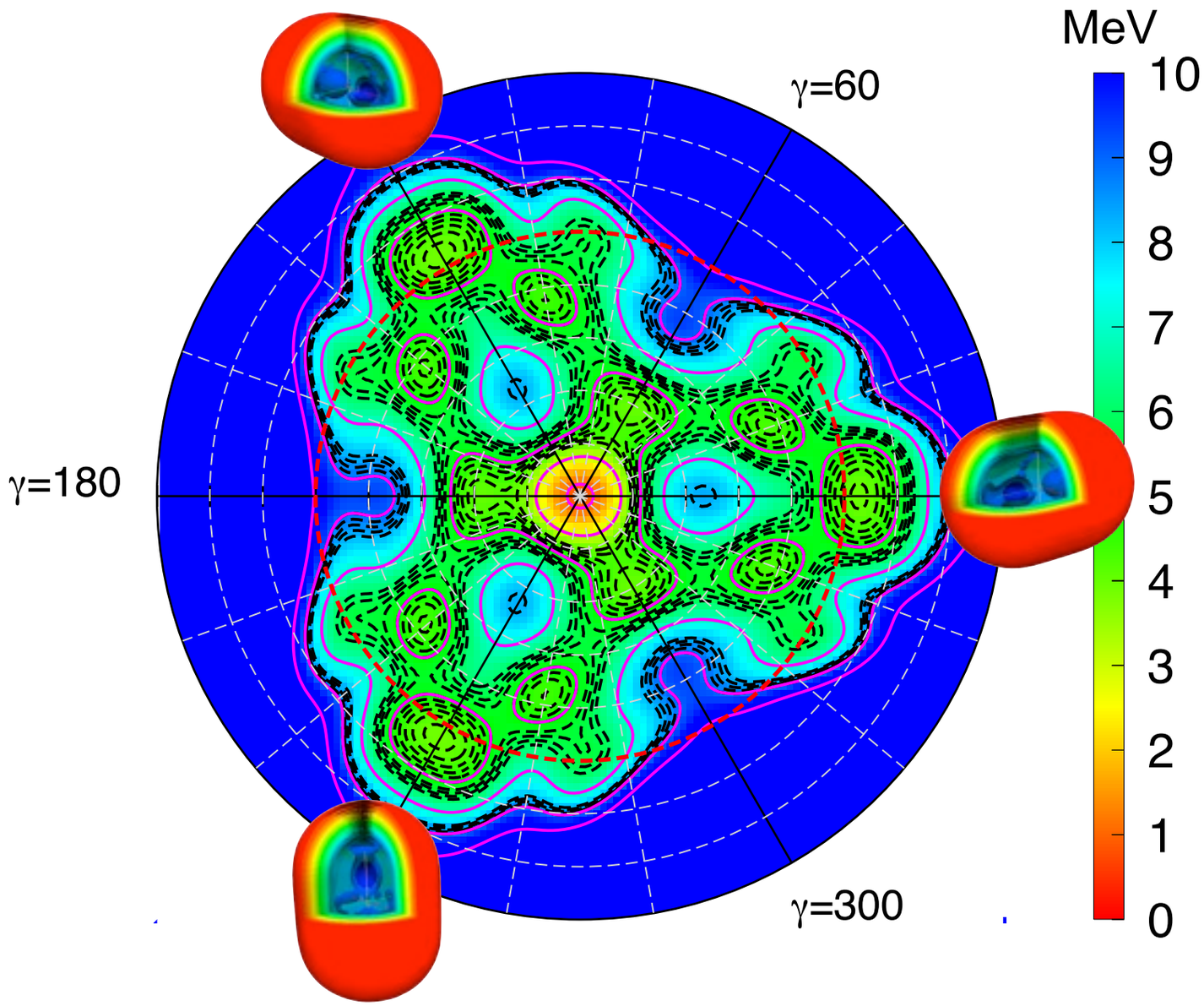

- Symmetry corresponding to the different orientation of the axes
- All configurations are included between γ∈[0º,60º]

T. R. R., J. L. Egido, Phys. Lett. B 705, 255 (2011)

Particle number projection

Example: ^{80}Zr

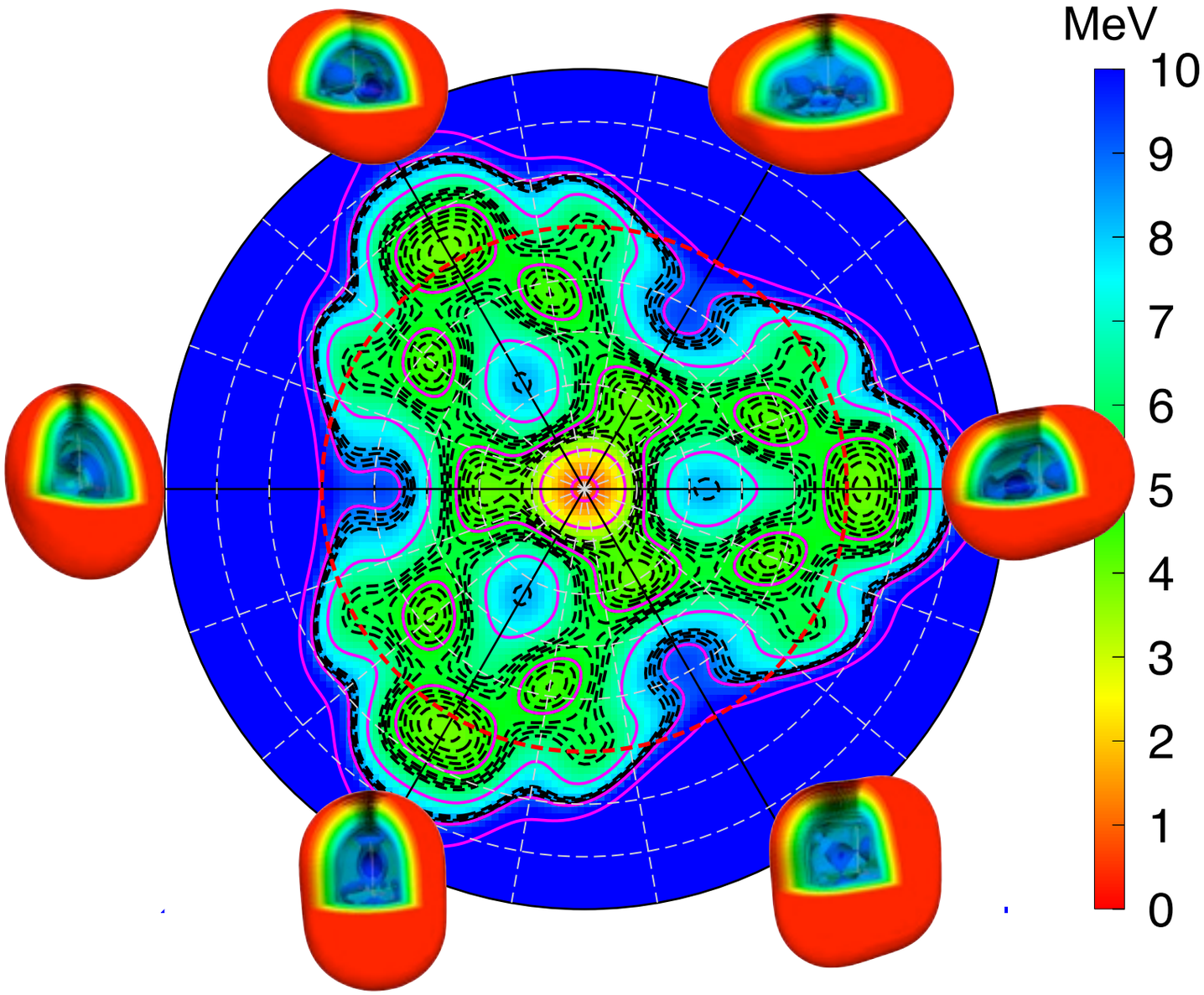

- Symmetry corresponding to the different orientation of the axes
- All configurations are included between $\gamma \in [0^o, 60^o]$

T. R. R., J. L. Egido, Phys. Lett. B 705, 255 (2011)

Particle number projection

Example: ^{80}Zr

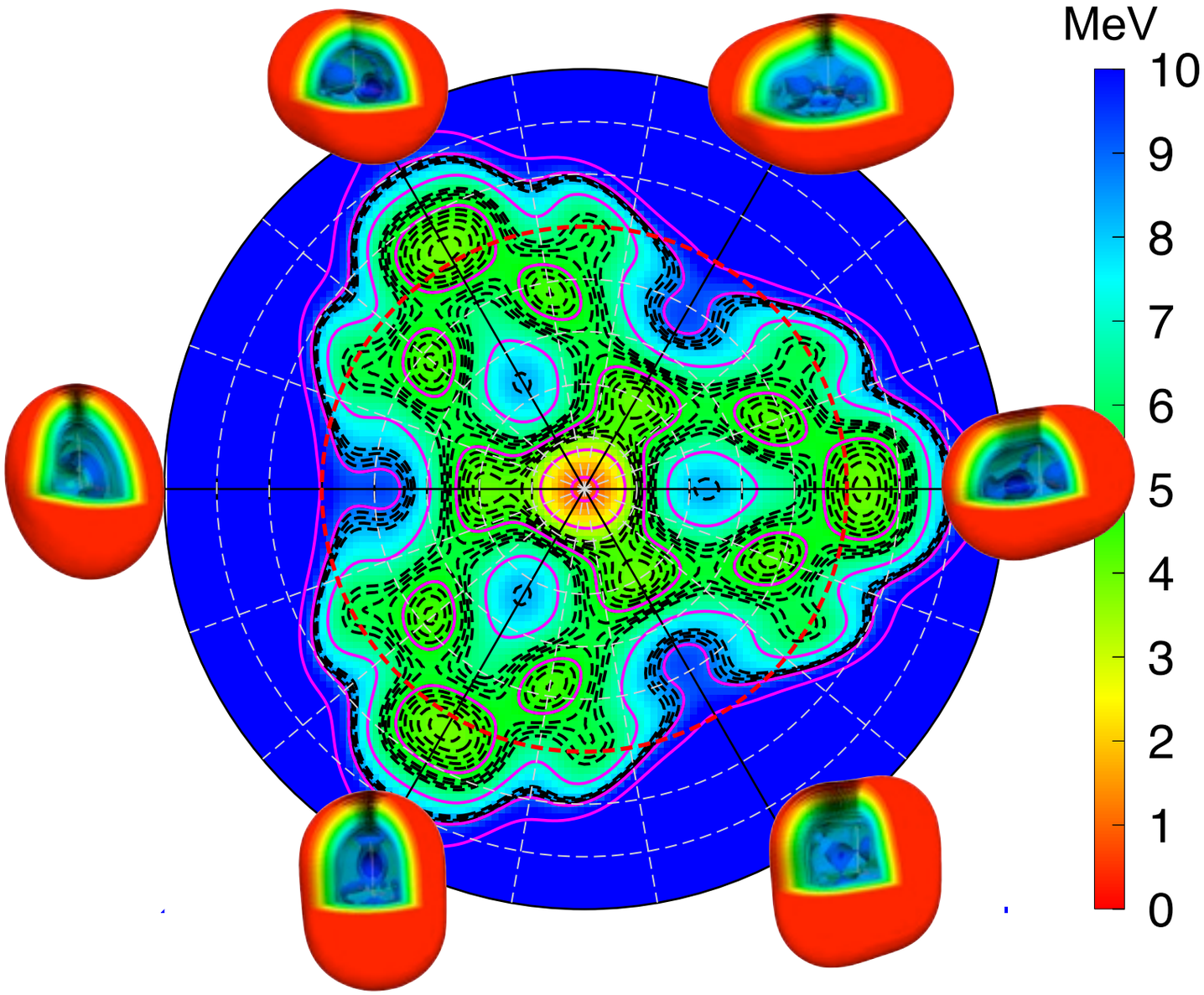

- Symmetry corresponding to the different orientation of the axes
- All configurations are included between $\gamma \in [0^o, 60^o]$

T. R. R., J. L. Egido, Phys. Lett. B 705, 255 (2011)

Example: ^{80}Zr

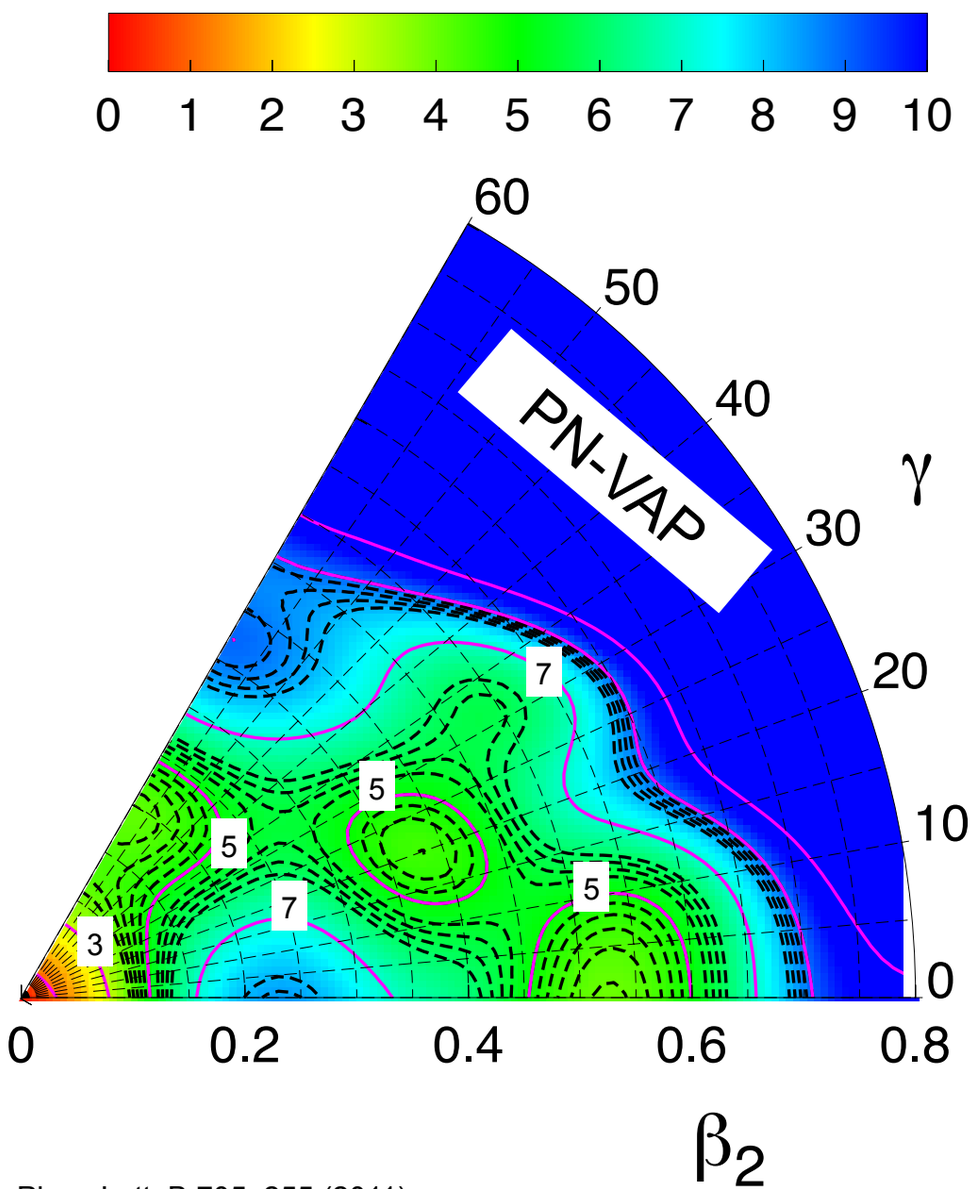

- Up to five minima in the potential energy surface.
- Absolute minimum corresponds to spherical configuration (*N*=40 spherical gap)
- Other minima related to the filling in and out of $g_{9/2}$, $p_{1/2}$, $f_{5/2}$ and $d_{5/2}$ orbits.

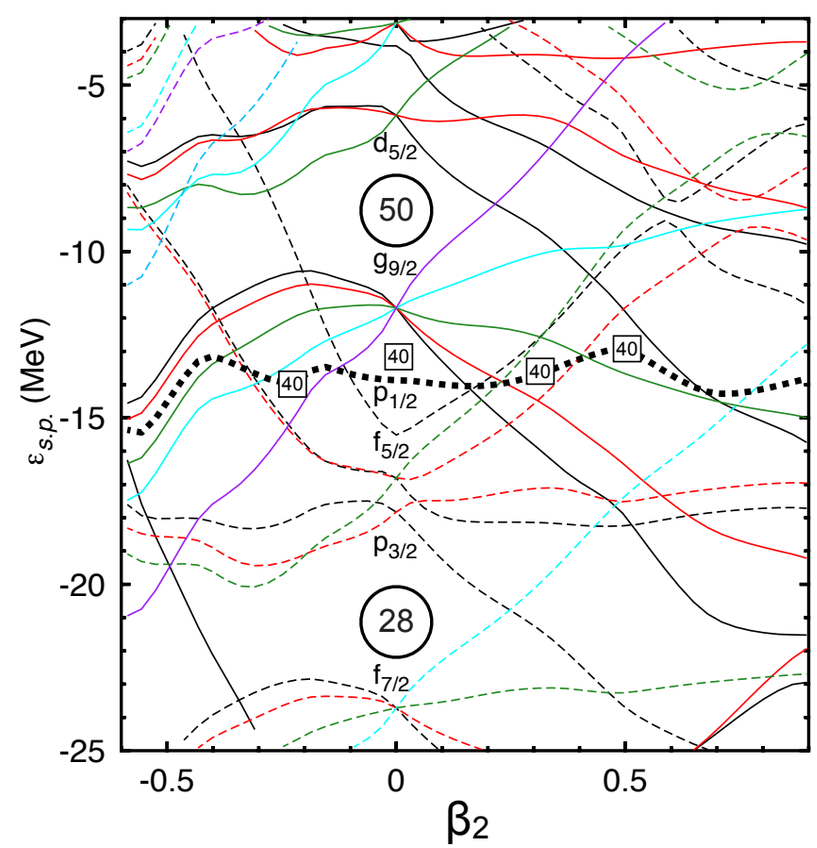

T. R. R., J. L. Egido, Phys. Lett. B 705, 255 (2011)

Particle number and angular momentum projection

TECHNISCHE UNIVERSITÄT DARMSTADT

Example: ^{80}Zr

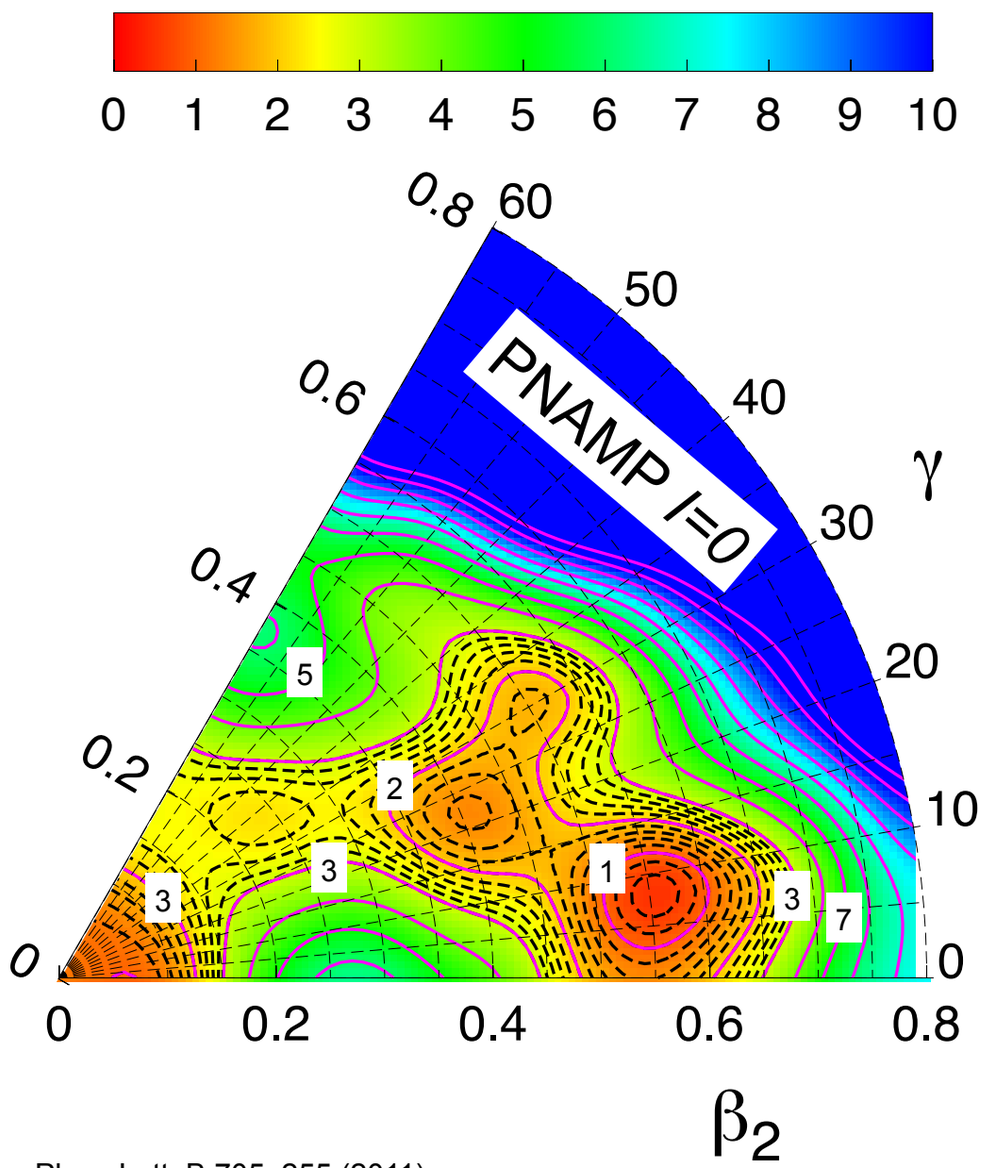

- Five minima are closer in energy whenever the rotational invariance is restored.
- Absolute minima corresponds to deformed configuration β~0.55
- Barriers between the minima are less than 1 MeV. Mixing?

T. R. R., J. L. Egido, Phys. Lett. B 705, 255 (2011)

Example: ^{80}Zr

Relevance of angular momentum projection

(Similar feature as in ^{32}Mg, see R. Rodriguez-Guzmán et al., Nucl. Phys. A 709, 201 (2002))

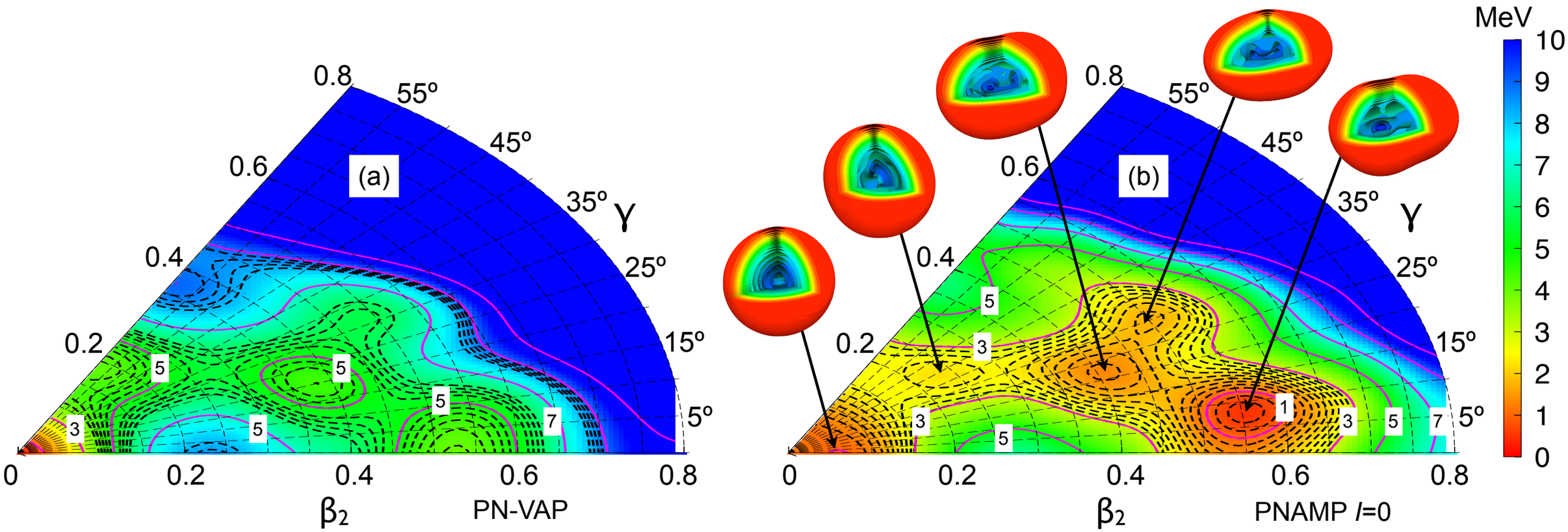

T. R. R., J. L. Egido, Phys. Lett. B 705, 255 (2011)

Configuration (shape) mixing

TECHNISCHE UNIVERSITÄT DARMSTADT

Example: ^{80}Zr

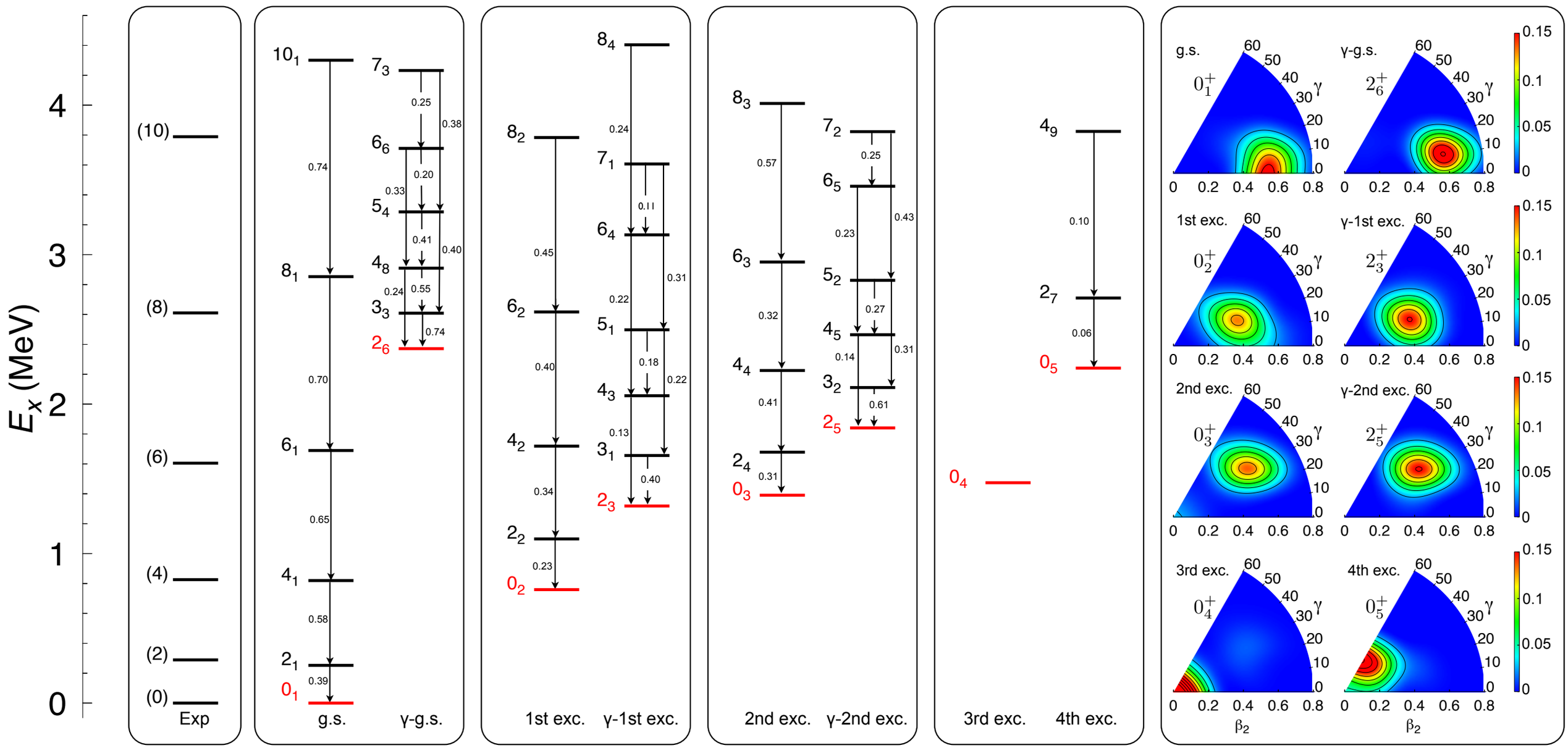

T. R. R., J. L. Egido, Phys. Lett. B 705, 255 (2011)

Configuration (shape) mixing

TECHNISCHE UNIVERSITÄT DARMSTADT

Example: ^{80}Zr

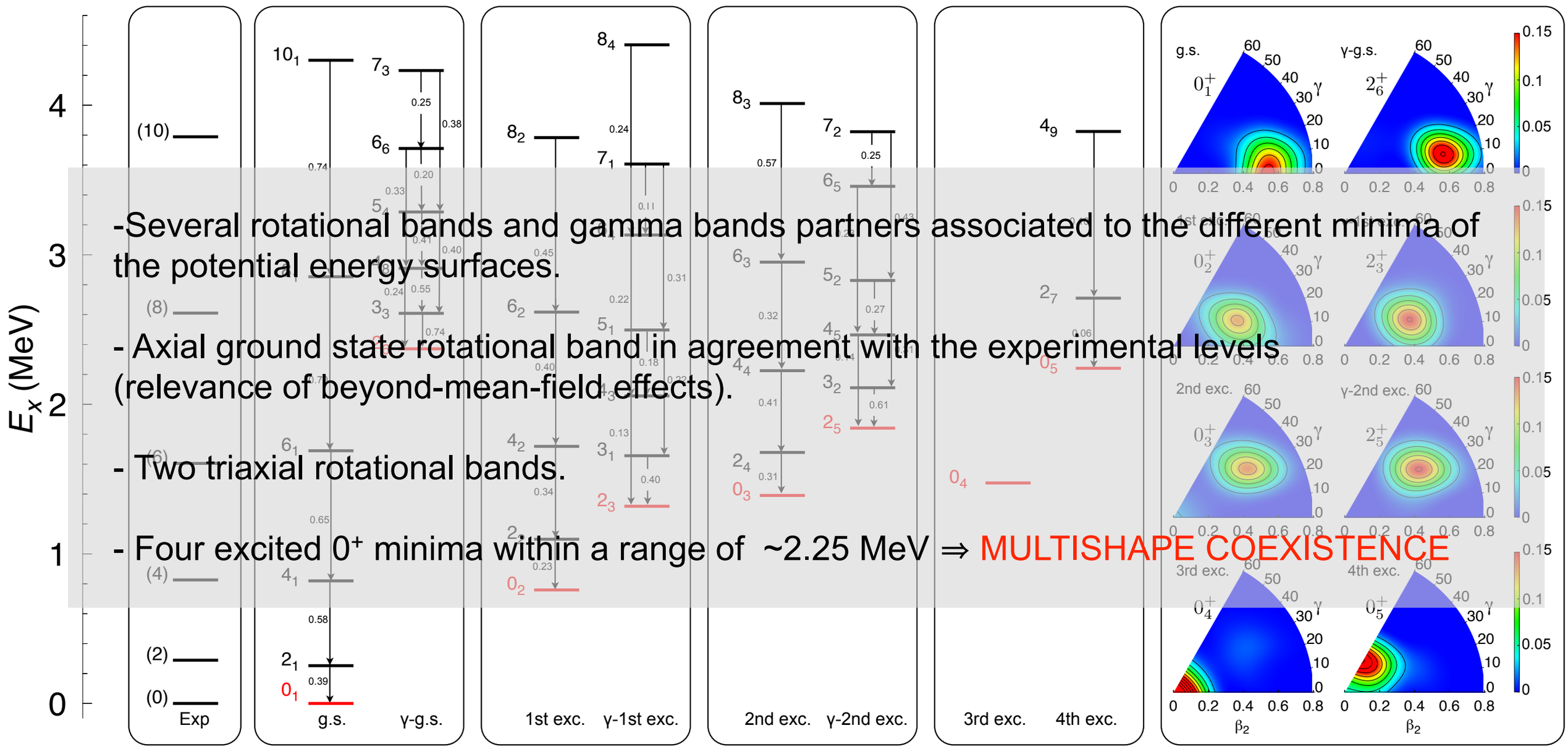

-Several rotational bands and gamma bands partners associated to the different minima of the potential energy surfaces.

- Axial ground state rotational band in agreement with the experimental levels (relevance of beyond-mean-field effects).

- Two triaxial rotational bands.

- Four excited 0^+ minima within a range of ~2.25 MeV ⇒ MULTISHAPE COEXISTENCE

T. R. R., J. L. Egido, Phys. Lett. B 705, 255 (2011)

Applications

• Nuclear structure applications

✓ Appearance of new shell closures in neutron rich Calcium isotopes: N=32, N=34?

✓ Degradation of N=28 shell closure.

✓ Shell quenching in N=82 for Cadmium isotopes? Key relevance in r-process nucleosynthesis (waiting points)

✓ Shape (phase) transitions in Nd/Sm/Gd isotopes.

• Neutrinoless double beta decay

• Comments on formal aspects

✓ Convergence of the results.

✓ ‘Contaminations’.

N=32 and/or *N*=34 in Ca, Ti and Cr isotopes.

The tendency of the **experimental data** for the excitation energies $E(2^+)$ and transition probabilities $B(E2,0^+\rightarrow 2^+)$ shows the presence of sub-shell closures.

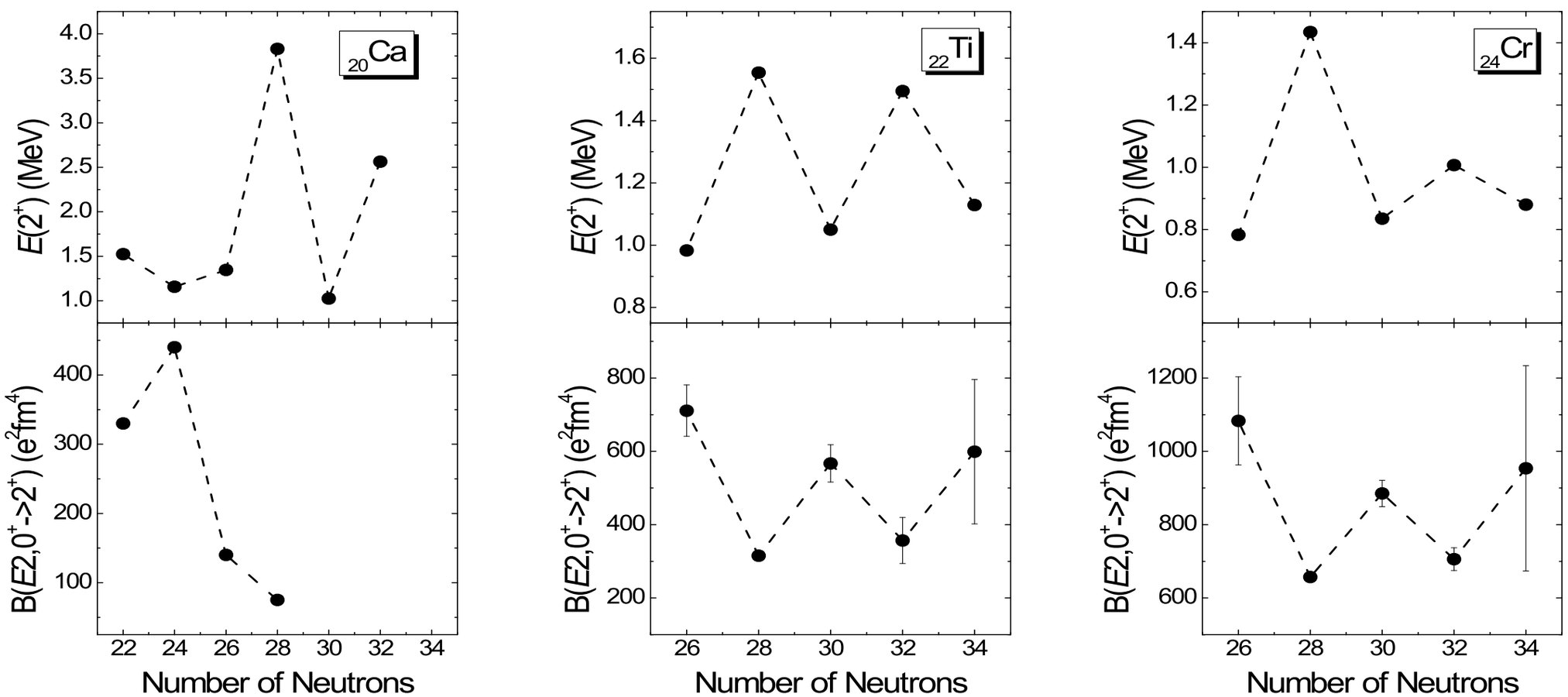

Schielke *et al* (PL B571, 29(2003)) Dinca *et al* (PR C71,041302(2005)) Bürger *et al* (PL B662, 29(2005))

N=32 and/or *N*=34 in Ca, Ti and Cr isotopes.

The tendency of the **experimental data** for the excitation energies $E(2^+)$ and transition probabilities $B(E2,0^+\rightarrow 2^+)$ shows the presence of sub-shell closures.

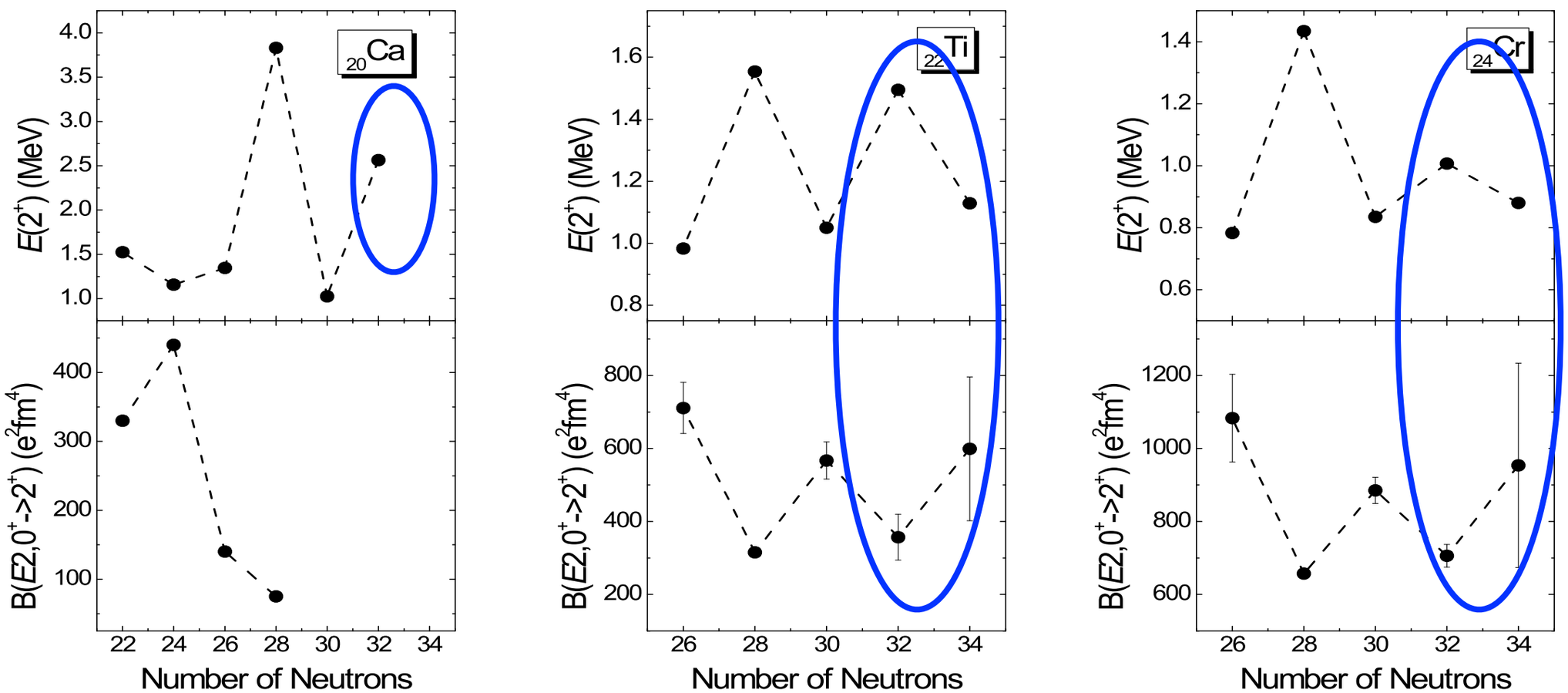

Schielke *et al* (PL B571, 29(2003)) Dinca *et al* (PR C71,041302(2005)) Bürger *et al* (PL B662, 29(2005))

N=32 and/or *N*=34 in Ca, Ti and Cr isotopes.

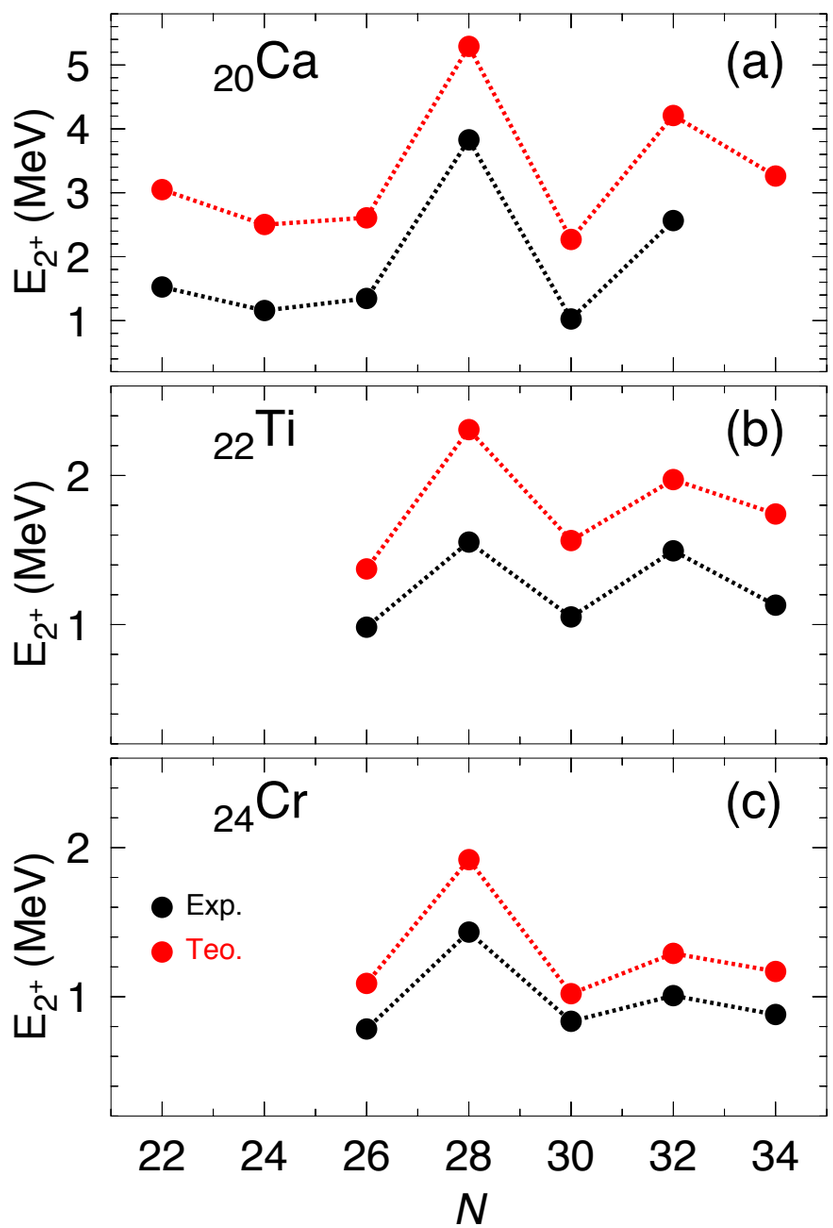

✓ AXIAL calculations

✓ Excellent qualitative agreement for the excitation energies $E(2^+)$.

✓ *N*=32 is a good sub-shell closure while *N*=34 is not. **EXPERIMENTALLY CONFIRMED 2012!!**

T.R.R and J.L. Egido, Phys. Rev. Lett. 99, 06201 (2007)

Shell closures

N=32 and/or *N*=34 in Ca, Ti and Cr isotopes.

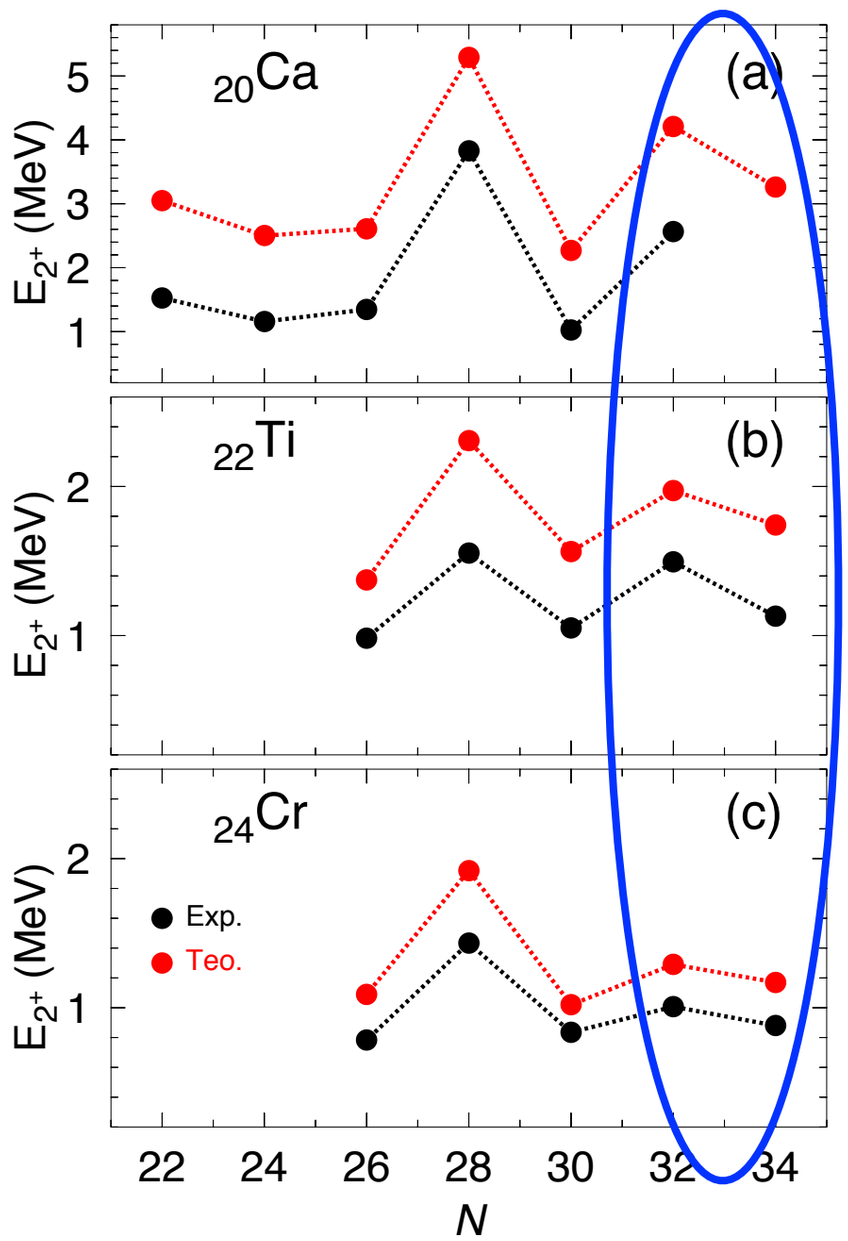

✓ AXIAL calculations

✓ Excellent qualitative agreement for the excitation energies $E(2^+)$.

✓ *N*=32 is a good sub-shell closure while *N*=34 is not. **EXPERIMENTALLY CONFIRMED 2012!!**

T.R.R and J.L. Egido, Phys. Rev. Lett. 99, 06201 (2007)

Triaxial calculations ^{44}S (N=28)

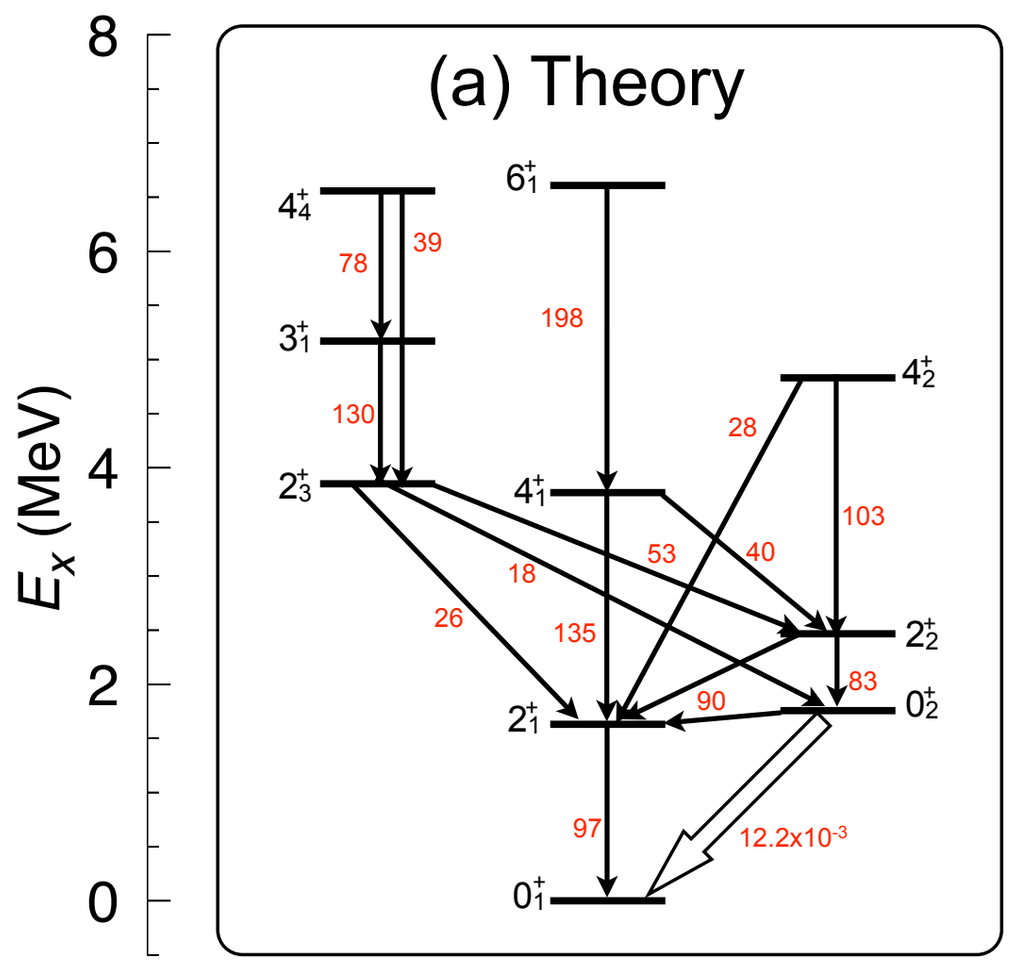

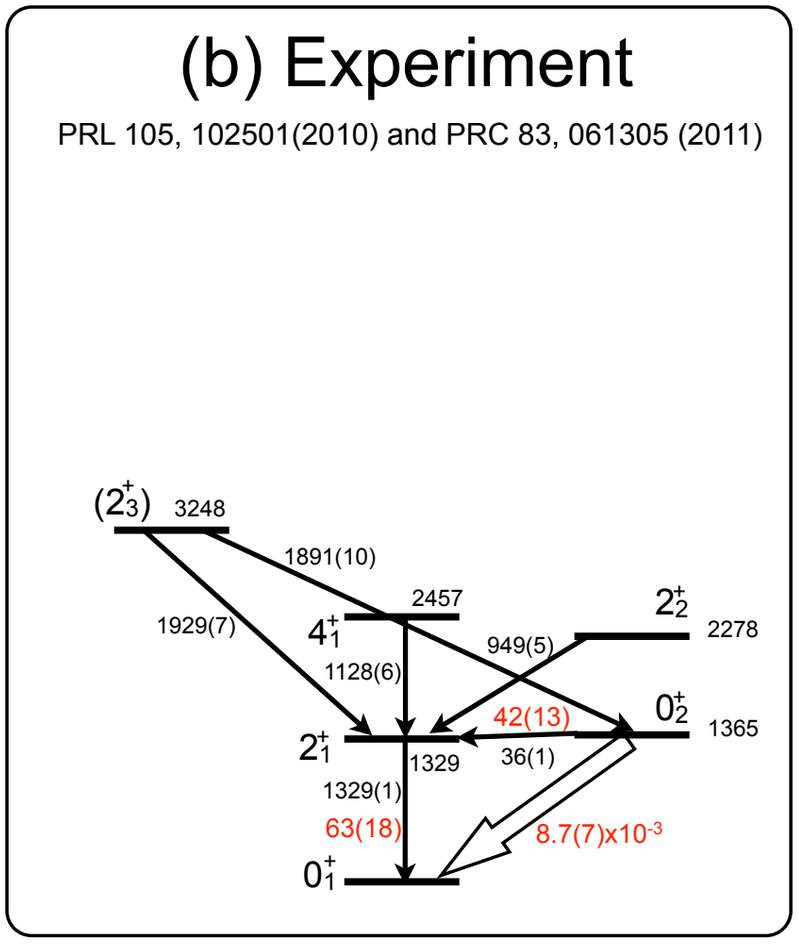

T.R.R and J.L. Egido, PRC 84, R051307 (2011)

✓ Very good qualitative description of the observed levels and reduced transition probabilities.

✓ Degradation of N=28 shell closure.

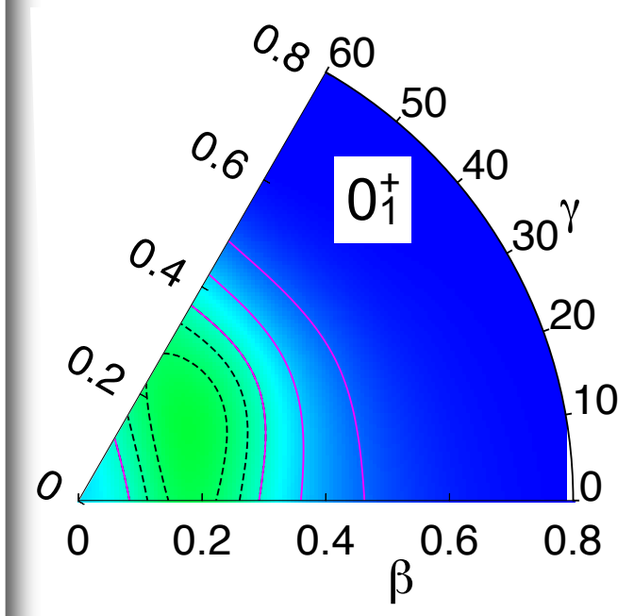

Systematics of the *E*(2) and *B*(E2) in Cadmium isotopes

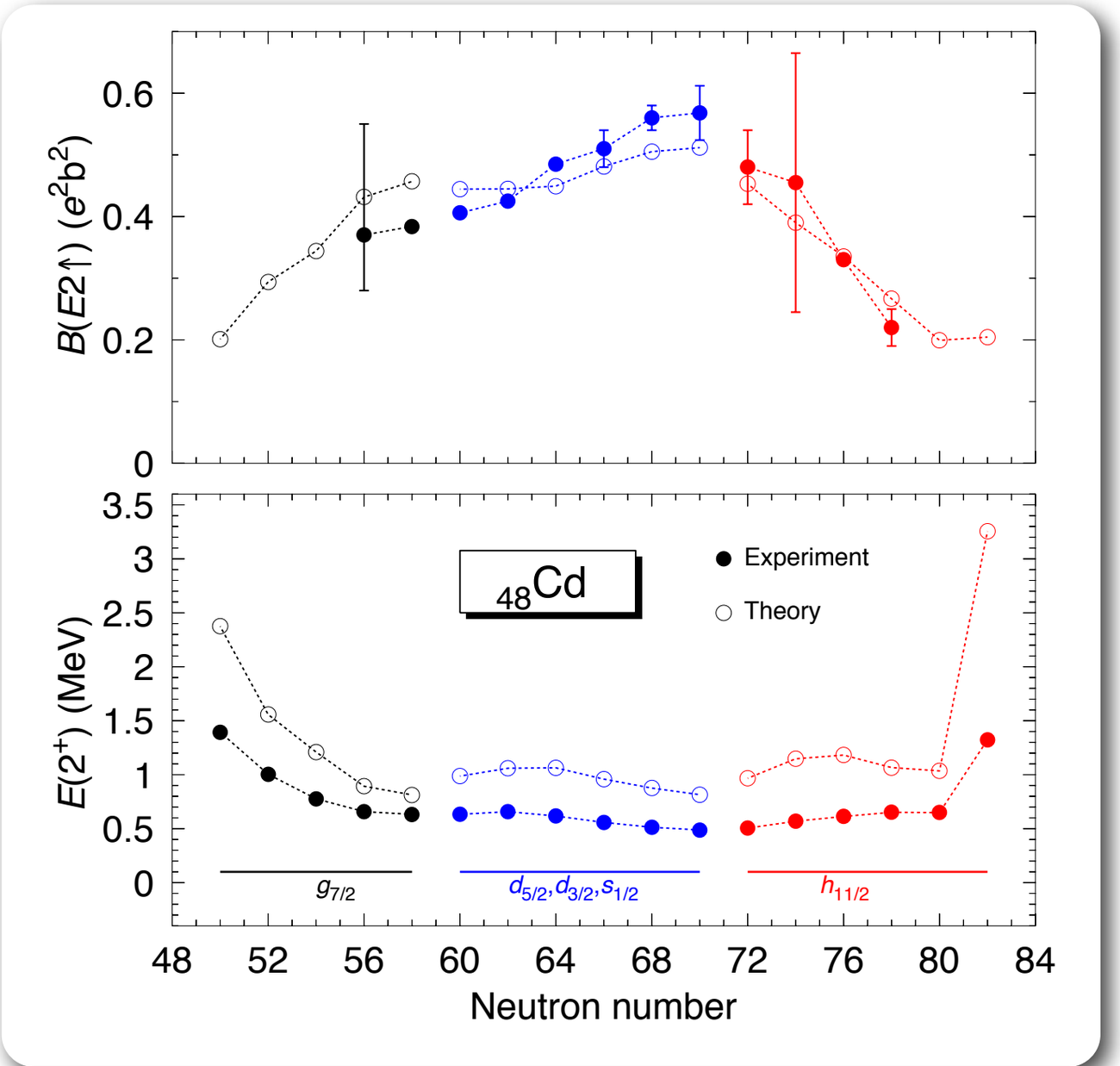

✓ AXIAL calculations

✓ Good qualitative agreement for the $E(2^+)$ excitation energies and B(E2) transition probabilities from shell to shell

✓ N=50-58 parabolic behavior (filling $g_{7/2}$ shell)

✓ N=60-70 flat behavior (filling $d_{5/2}$, $d_{3/2}$, $s_{1/2}$ shells)

✓ Anomalous behavior of $E(2^+)$ for ^{128}Cd has been is well reproduced

T.R.R, J.L. Egido, A. Jungclaus, Phys. Lett. B 668, 410 (2008)

Systematics of the *E*(2) and *B*(E2) in Cadmium isotopes

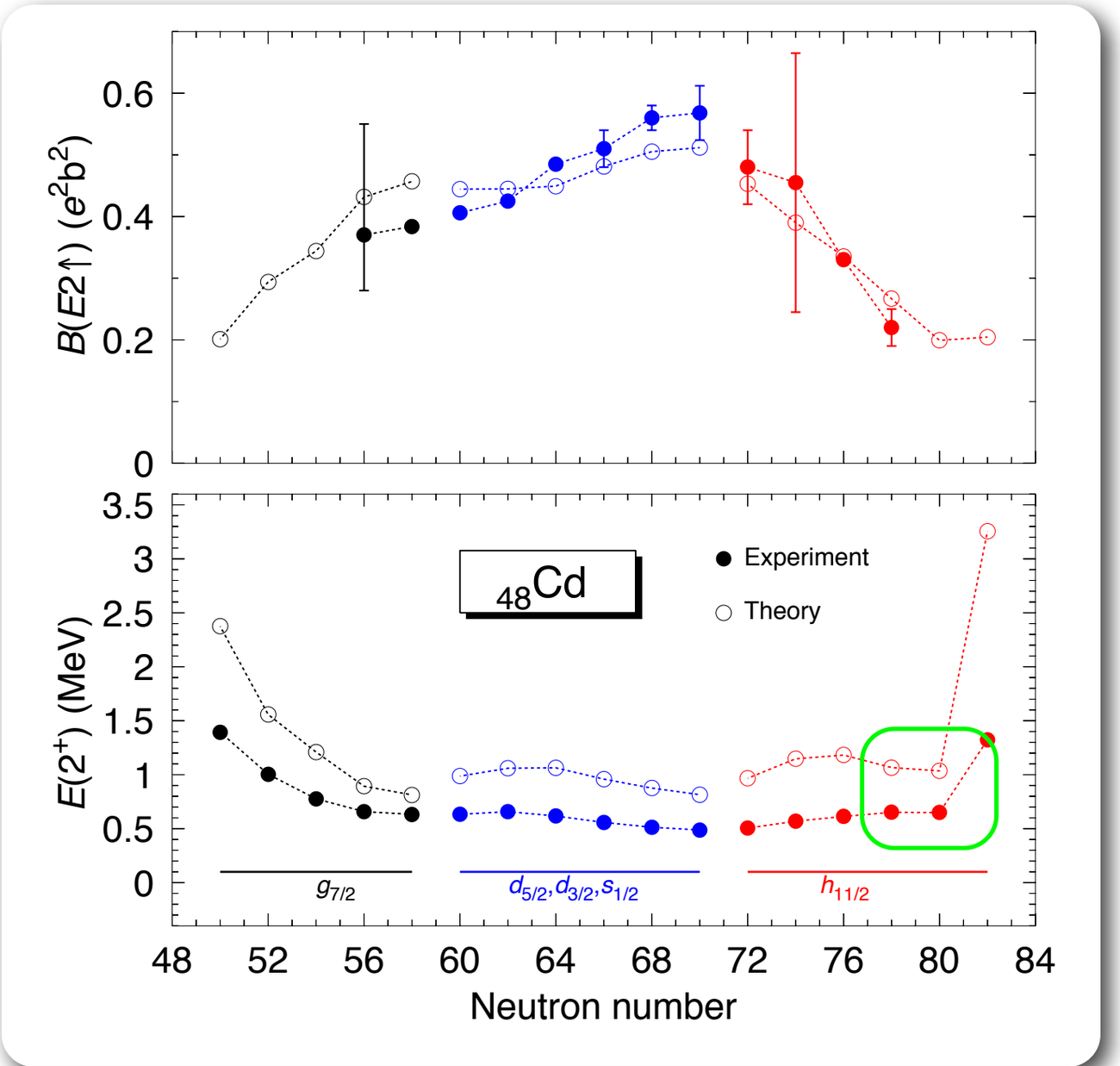

✓ AXIAL calculations

✓ Good qualitative agreement for the $E(2^+)$ excitation energies and B(E2) transition probabilities from shell to shell

✓ N=50-58 parabolic behavior (filling $g_{7/2}$ shell)

✓ N=60-70 flat behavior (filling $d_{5/2}$, $d_{3/2}$, $s_{1/2}$ shells)

✓ Anomalous behavior of $E(2^+)$ for ^{128}Cd has been is well reproduced

T.R.R, J.L. Egido, A. Jungclaus, Phys. Lett. B 668, 410 (2008)

Shape transitions in Nd isotopes

TECHNISCHE UNIVERSITÄT DARMSTADT

T.R.R. and J.L. Egido Phys.Lett. B 663, 49 (2008)

84		86		88		90		92		94		96
Nd144 2.29E+15 y 0+ α 23.80	Nd145 7/2- 8.30	Nd146 0+ 17.19	Nd147 10.98 d 5/2- β-	Nd148 0+ 5.76	Nd149 1.728 h 5/2- β-	Nd150 1.1E19 y 0+ β- 5.64	Nd151 12.44 m 3/2+ β-	Nd152 11.4 m 0+ β-	Nd153 31.6 s (3/2)- β-	Nd154 25.9 s 0+ β-	Nd155 8.9 s β-	Nd156 5.47 s 0+ β-

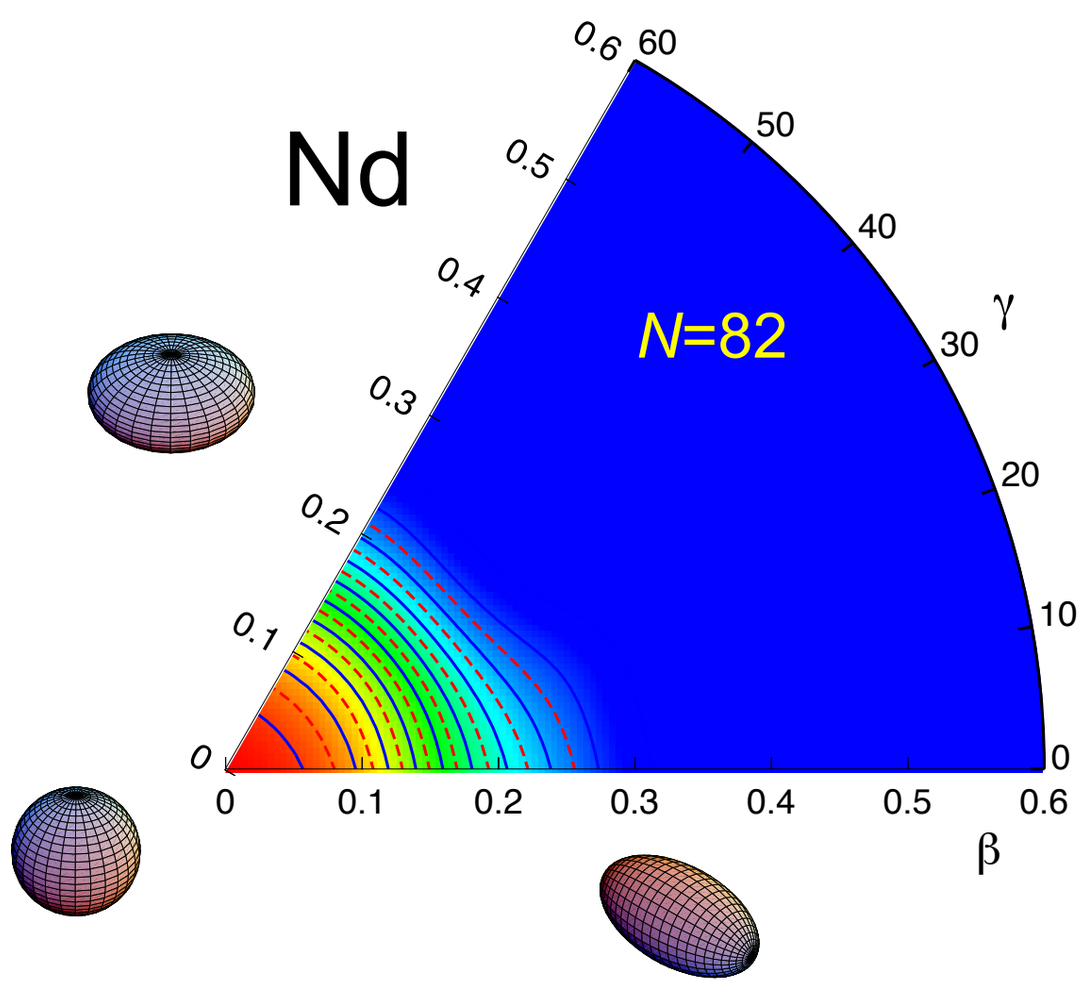

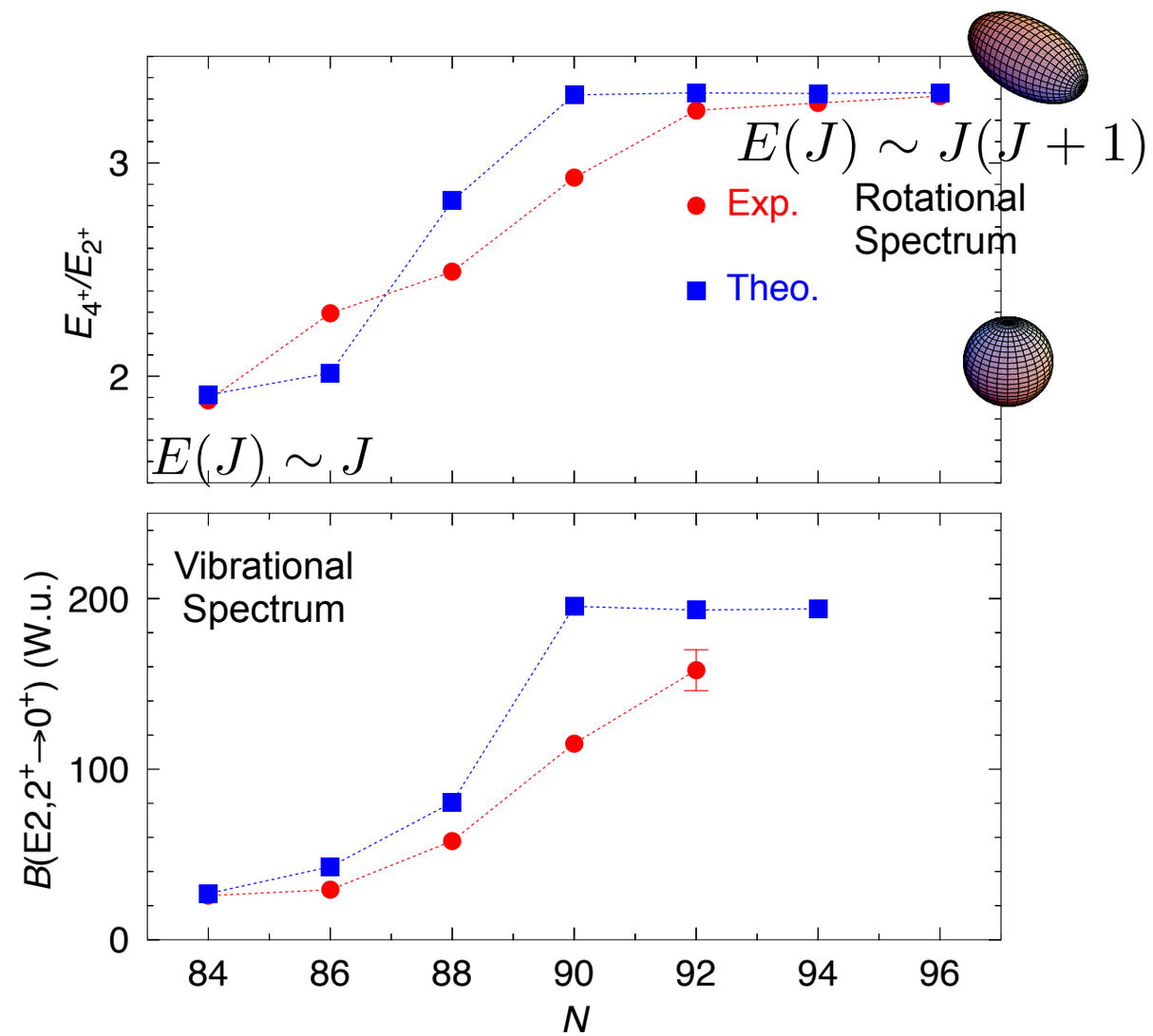

Shape transitions in Nd isotopes

TECHNISCHE UNIVERSITÄT DARMSTADT

T.R.R. and J.L. Egido Phys.Lett. B 663, 49 (2008)

84		86		88		90		92		94		96
Nd144 2.29E+15 y 0+ α 23.80	Nd145 7/2- 8.30	Nd146 0+ 17.19	Nd147 10.98 d 5/2- β-	Nd148 0+ 5.76	Nd149 1.728 h 5/2- β-	Nd150 1.1E19 y 0+ β- 5.64	Nd151 12.44 m 3/2+ β-	Nd152 11.4 m 0+ β-	Nd153 31.6 s (3/2)- β-	Nd154 25.9 s 0+ β-	Nd155 8.9 s β-	Nd156 5.47 s 0+ β-

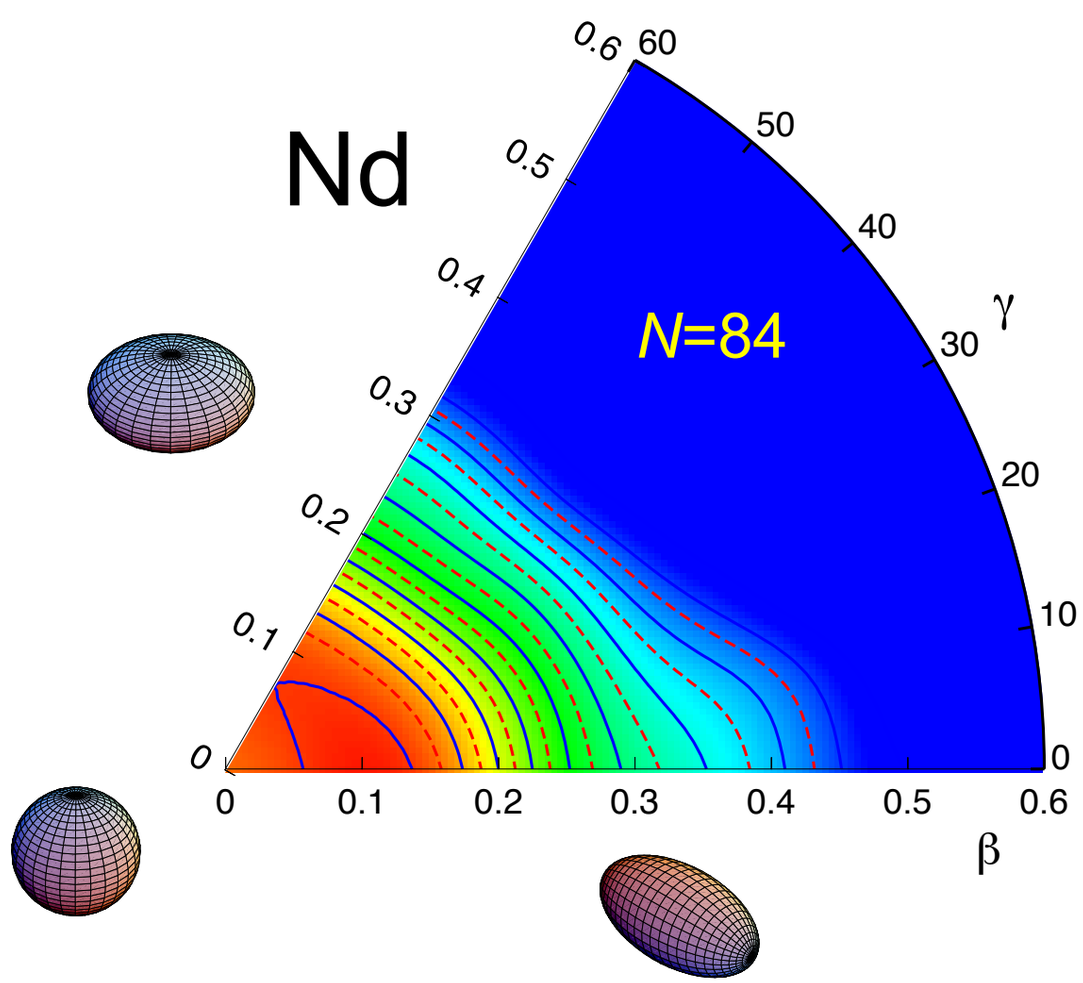

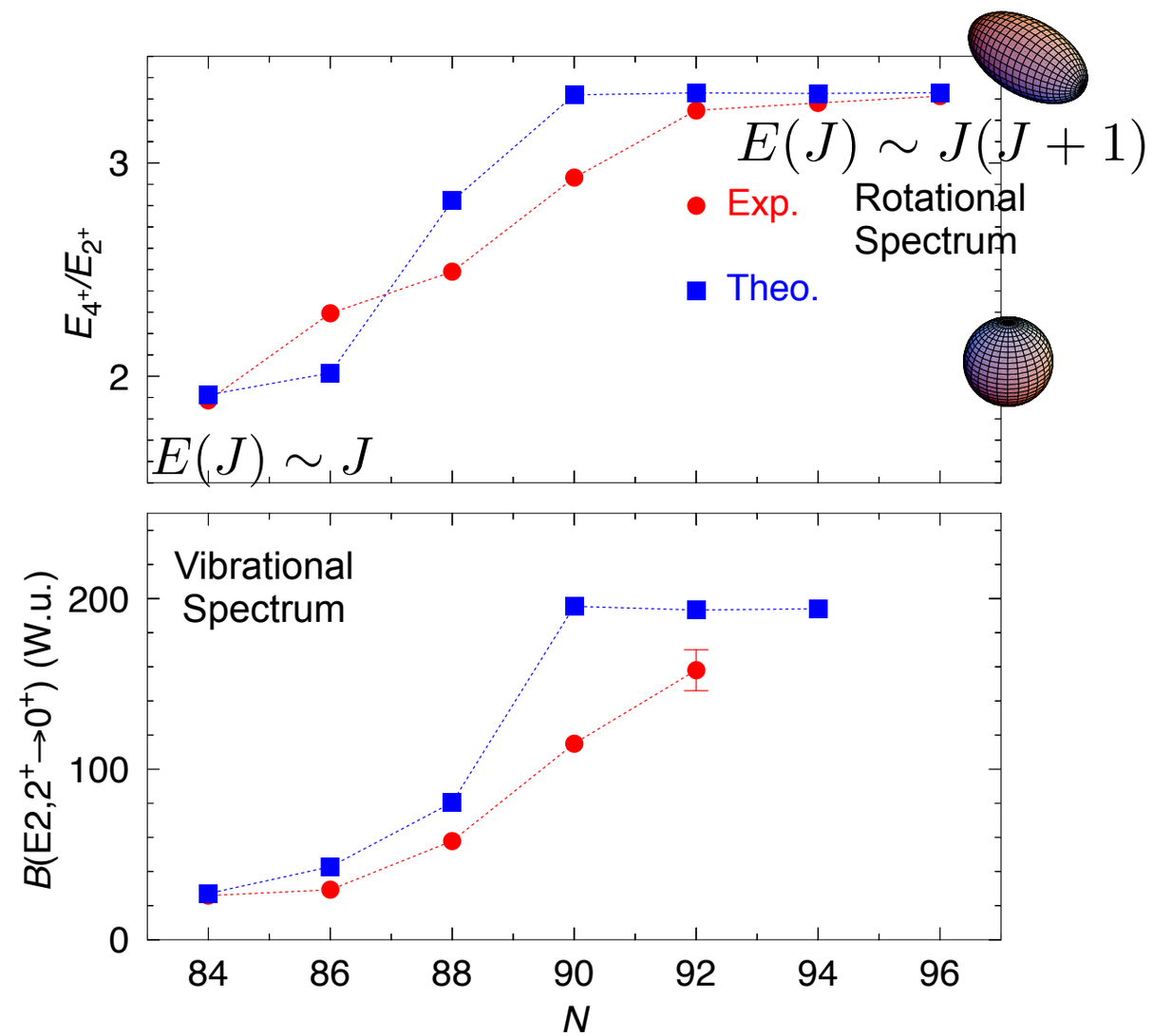

Shape transitions in Nd isotopes

T.R.R. and J.L. Egido Phys.Lett. B 663, 49 (2008)

84		86		88		90		92		94		96
Nd144	Nd145	Nd146	Nd147	Nd148	Nd149	Nd150	Nd151	Nd152	Nd153	Nd154	Nd155	Nd156
2.29E+15 y			10.98 d		1.728 h	1.1E19 y	12.44 m	11.4 m	31.6 s	25.9 s	8.9 s	5.47 s
0+	7/2-	0+	5/2-	0+	5/2-	0+	3/2+	0+	(3/2)-	0+		0+
α 23.80	8.30	17.19	β-	5.76	β-	β- 5.64	β-	β-	β-	β-	β-	β-

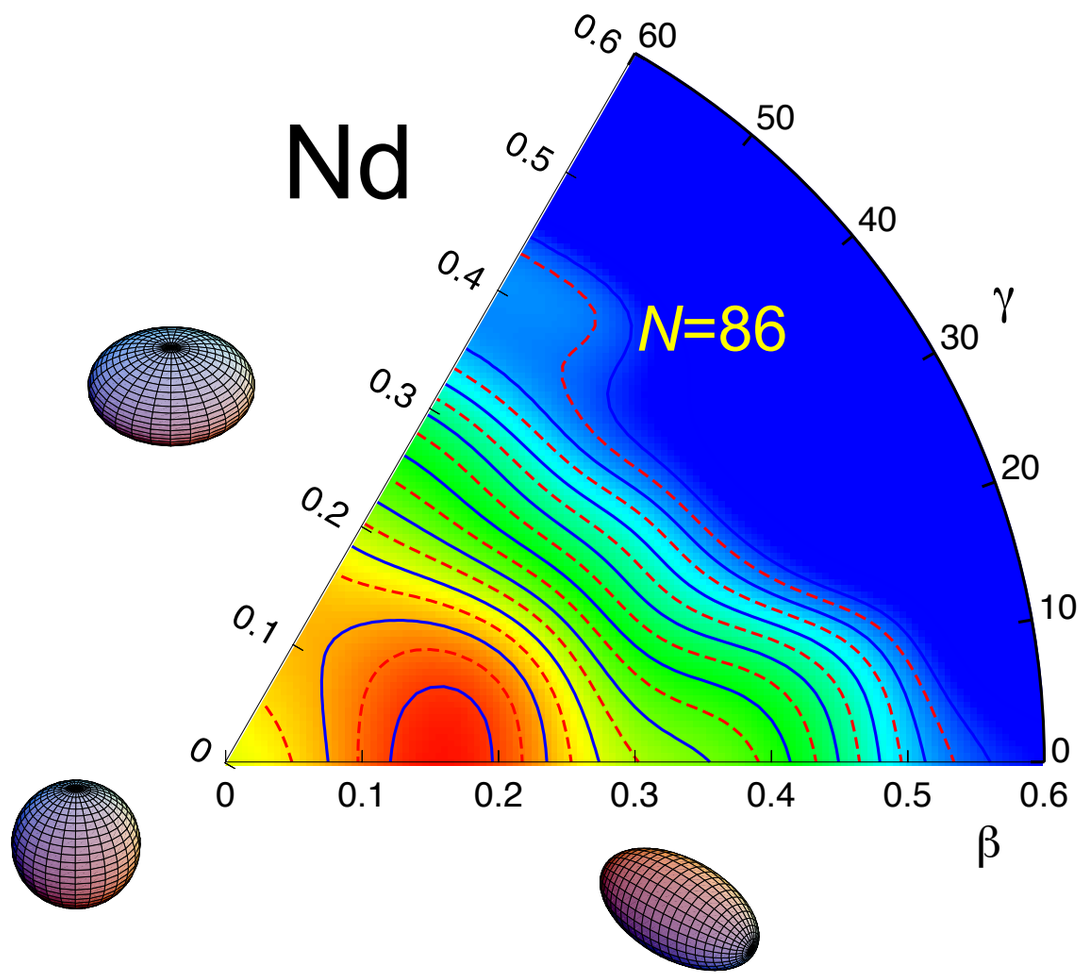

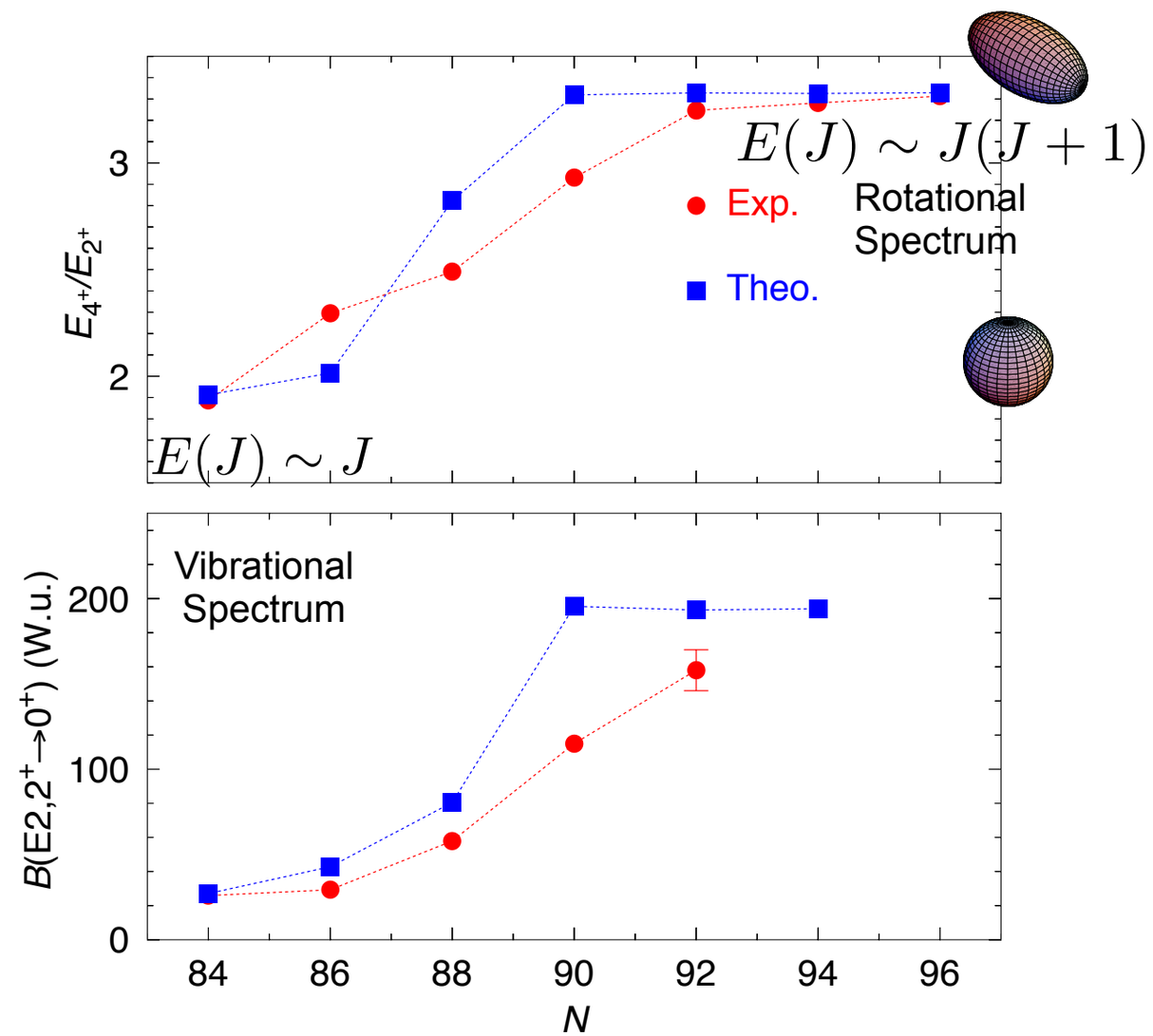

Shape transitions in Nd isotopes

T.R.R. and J.L. Egido Phys.Lett. B 663, 49 (2008)

84		86		88		90		92		94		96
Nd144	Nd145	Nd146	Nd147	Nd148	Nd149	Nd150	Nd151	Nd152	Nd153	Nd154	Nd155	Nd156
2.29E+15 y			10.98 d		1.728 h	1.1E19 y	12.44 m	11.4 m	31.6 s	25.9 s	8.9 s	5.47 s
0+	7/2-	0+	5/2-	0+	5/2-	0+	3/2+	0+	(3/2)-	0+		0+
α 23.80	8.30	17.19	β-	5.76	β-	β- 5.64	β-	β-	β-	β-	β-	β-

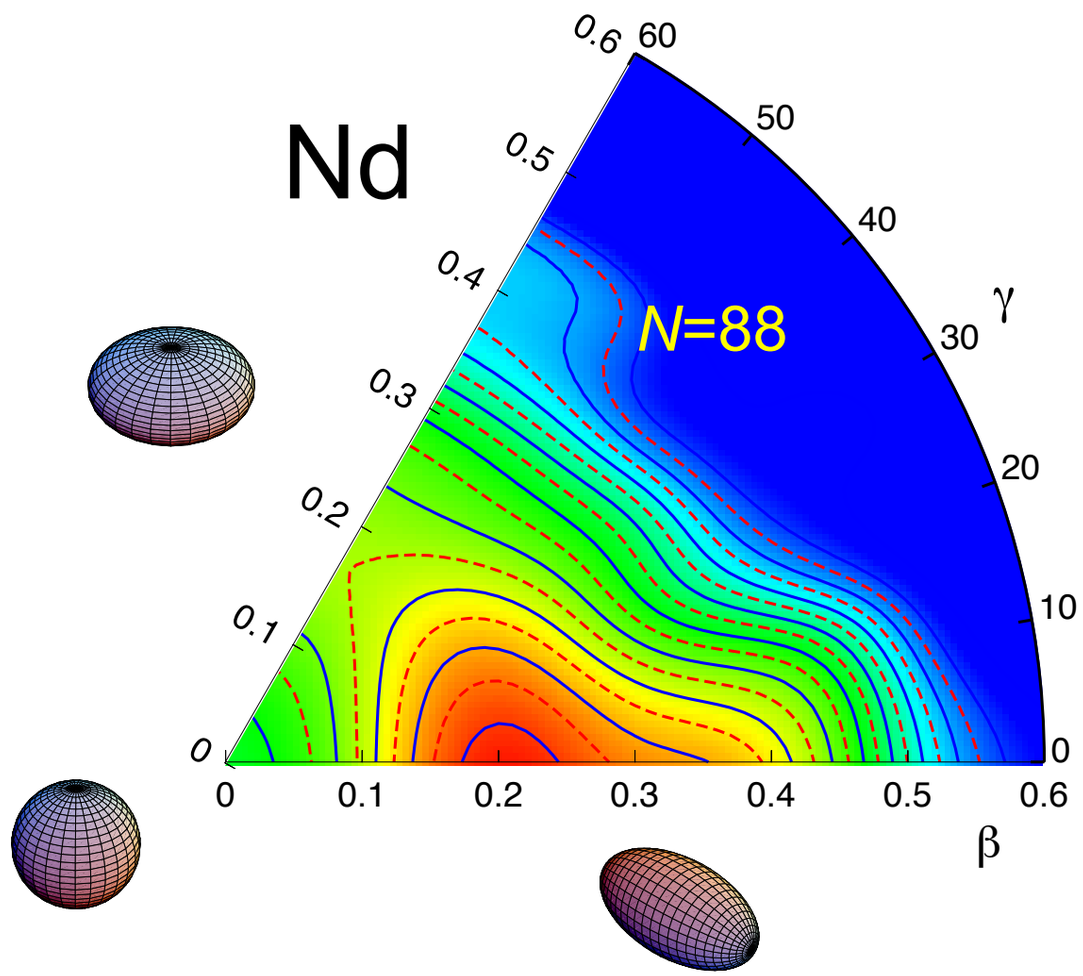

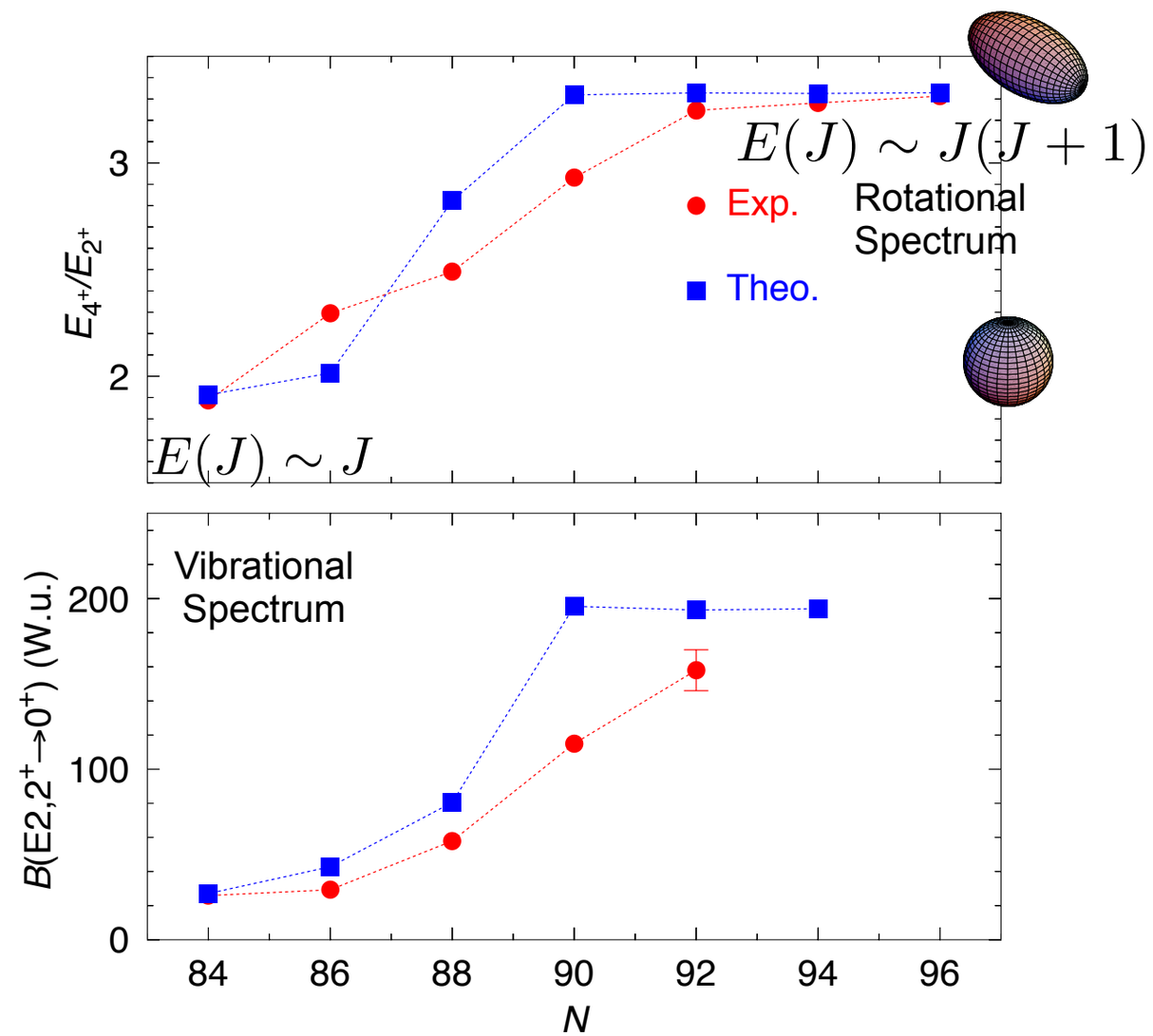

Shape transitions in Nd isotopes

TECHNISCHE UNIVERSITÄT DARMSTADT

T.R.R. and J.L. Egido Phys.Lett. B 663, 49 (2008)

84		86		88		90		92		94		96
Nd144	Nd145	Nd146	Nd147	Nd148	Nd149	Nd150	Nd151	Nd152	Nd153	Nd154	Nd155	Nd156
2.29E+15 y			10.98 d		1.728 h	1.1E19 y	12.44 m	11.4 m	31.6 s	25.9 s	8.9 s	5.47 s
0+	7/2-	0+	5/2-	0+	5/2-	0+	3/2+	0+	(3/2)-	0+		0+
α 23.80	8.30	17.19	β-	5.76	β-	β- 5.64	β-	β-	β-	β-	β-	β-

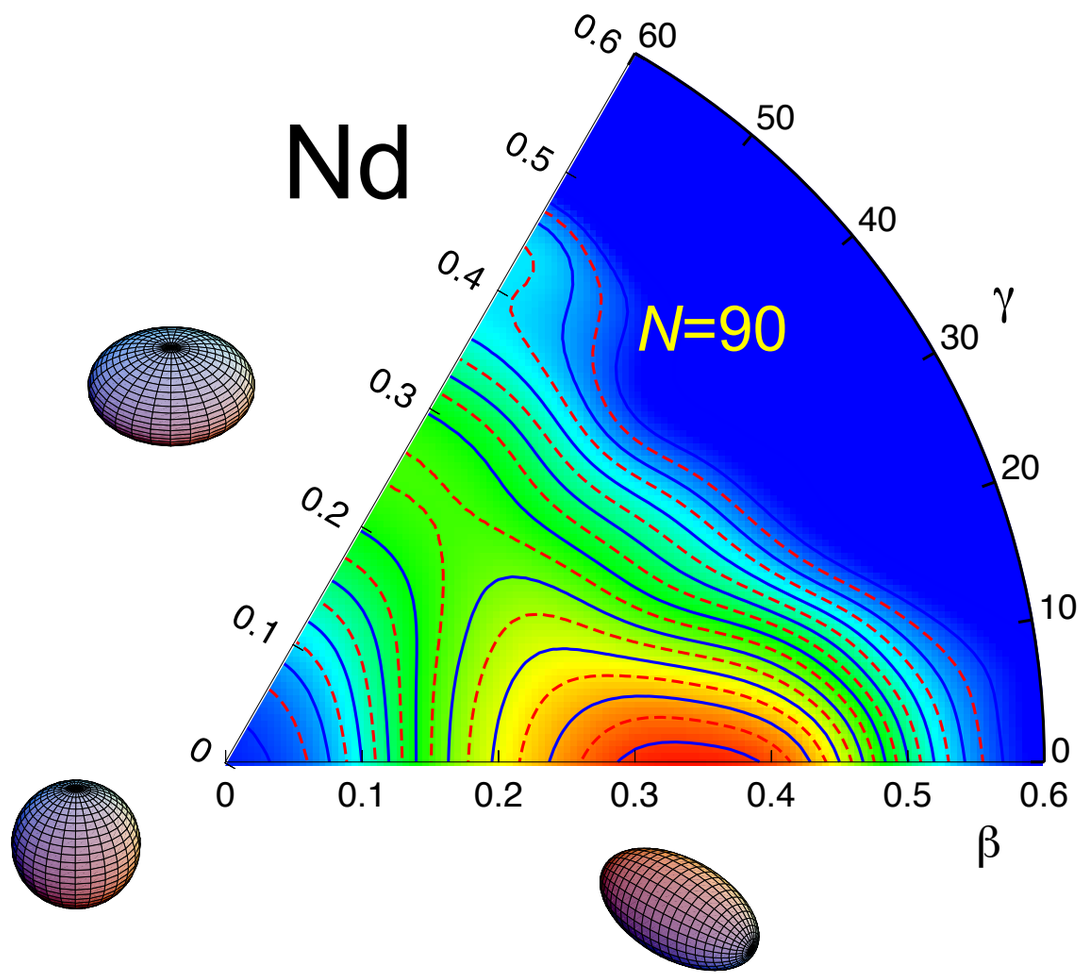

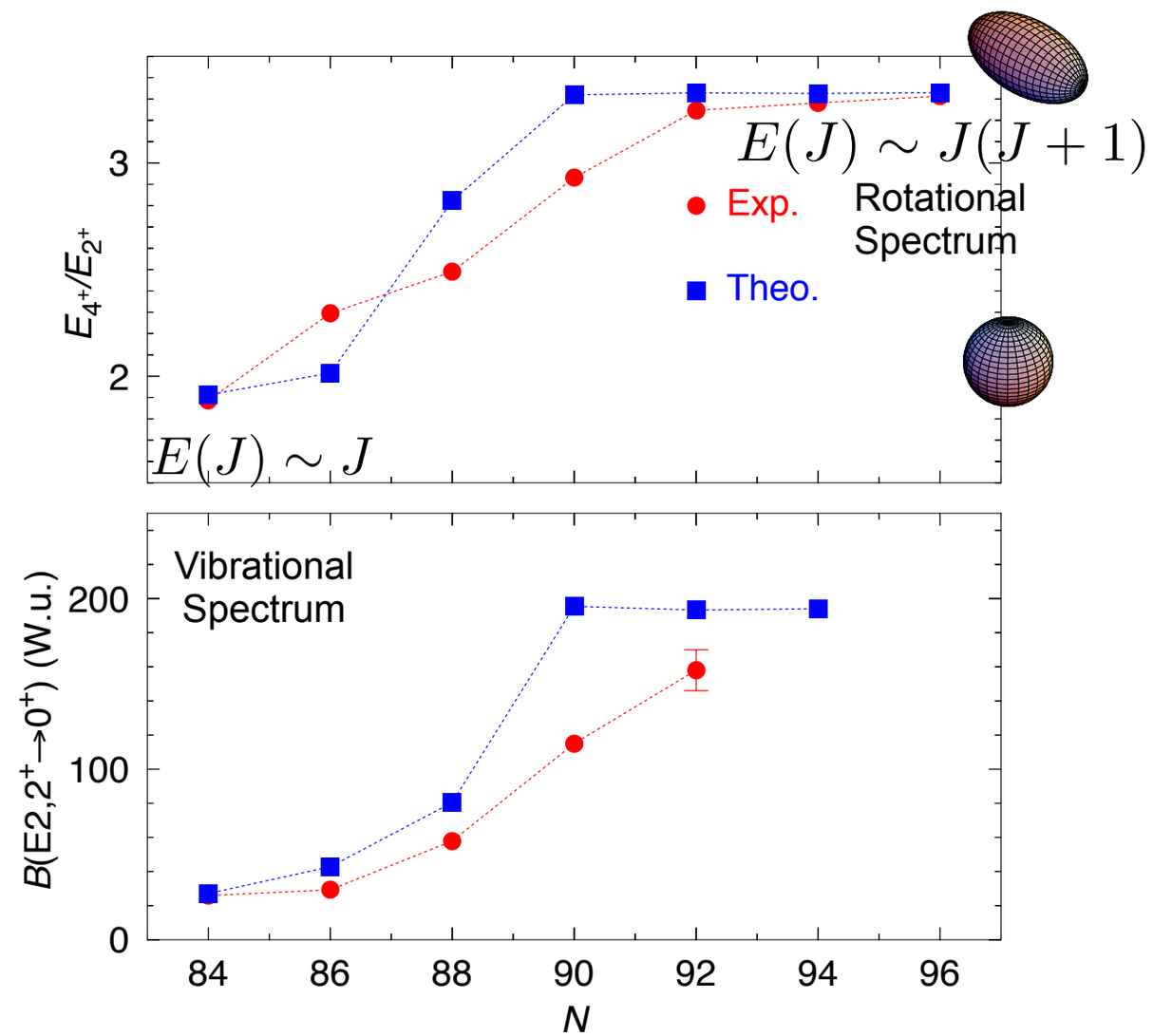

Shape transitions in Nd isotopes

T.R.R. and J.L. Egido Phys.Lett. B 663, 49 (2008)

84		86		88		90		92		94		96
Nd144	Nd145	Nd146	Nd147	Nd148	Nd149	Nd150	Nd151	Nd152	Nd153	Nd154	Nd155	Nd156
2.29E+15 y			10.98 d		1.728 h	1.1E19 y	12.44 m	11.4 m	31.6 s	25.9 s	8.9 s	5.47 s
0+	7/2-	0+	5/2-	0+	5/2-	0+	3/2+	0+	(3/2)-	0+		0+
α 23.80	8.30	17.19	β-	5.76	β-	β- 5.64	β-	β-	β-	β-	β-	β-

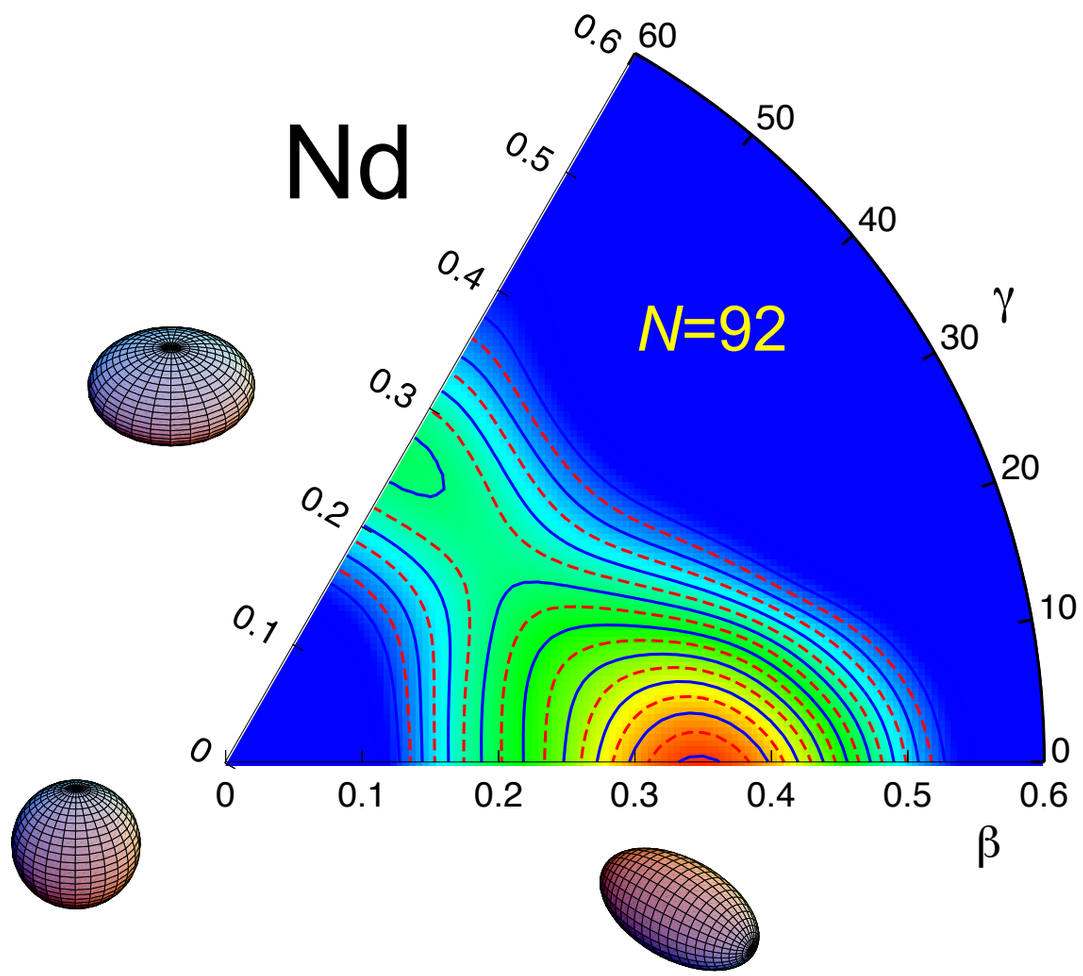

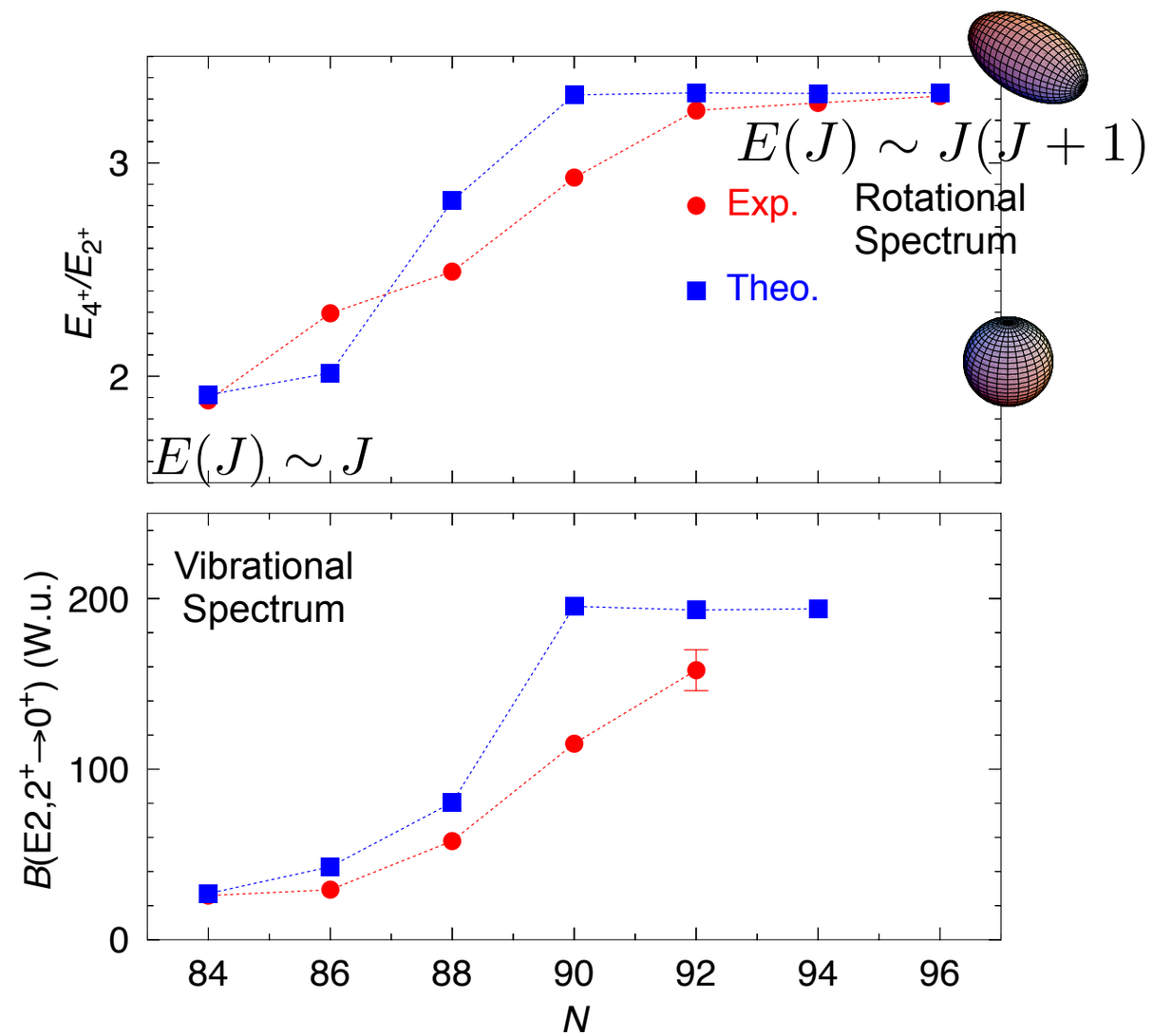

Shape transitions in Nd isotopes

T.R.R. and J.L. Egido Phys.Lett. B 663, 49 (2008)

84		86		88		90		92		94		96
Nd144	Nd145	Nd146	Nd147	Nd148	Nd149	Nd150	Nd151	Nd152	Nd153	Nd154	Nd155	Nd156
2.29E+15 y			10.98 d		1.728 h	1.1E19 y	12.44 m	11.4 m	31.6 s	25.9 s	8.9 s	5.47 s
0+	7/2-	0+	5/2-	0+	5/2-	0+	3/2+	0+	(3/2)-	0+		0+
α 23.80	8.30	17.19	β-	5.76	β-	β- 5.64	β-	β-	β-	β-	β-	β-

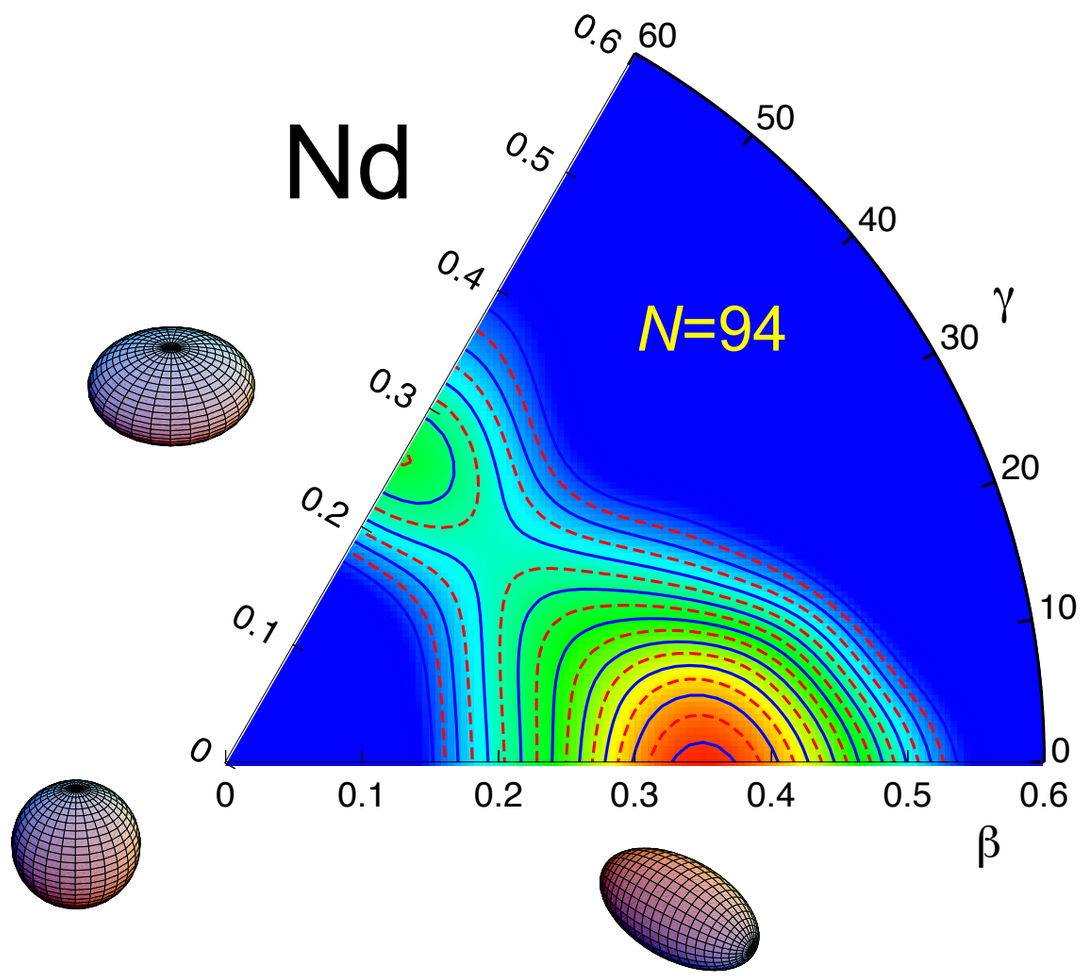

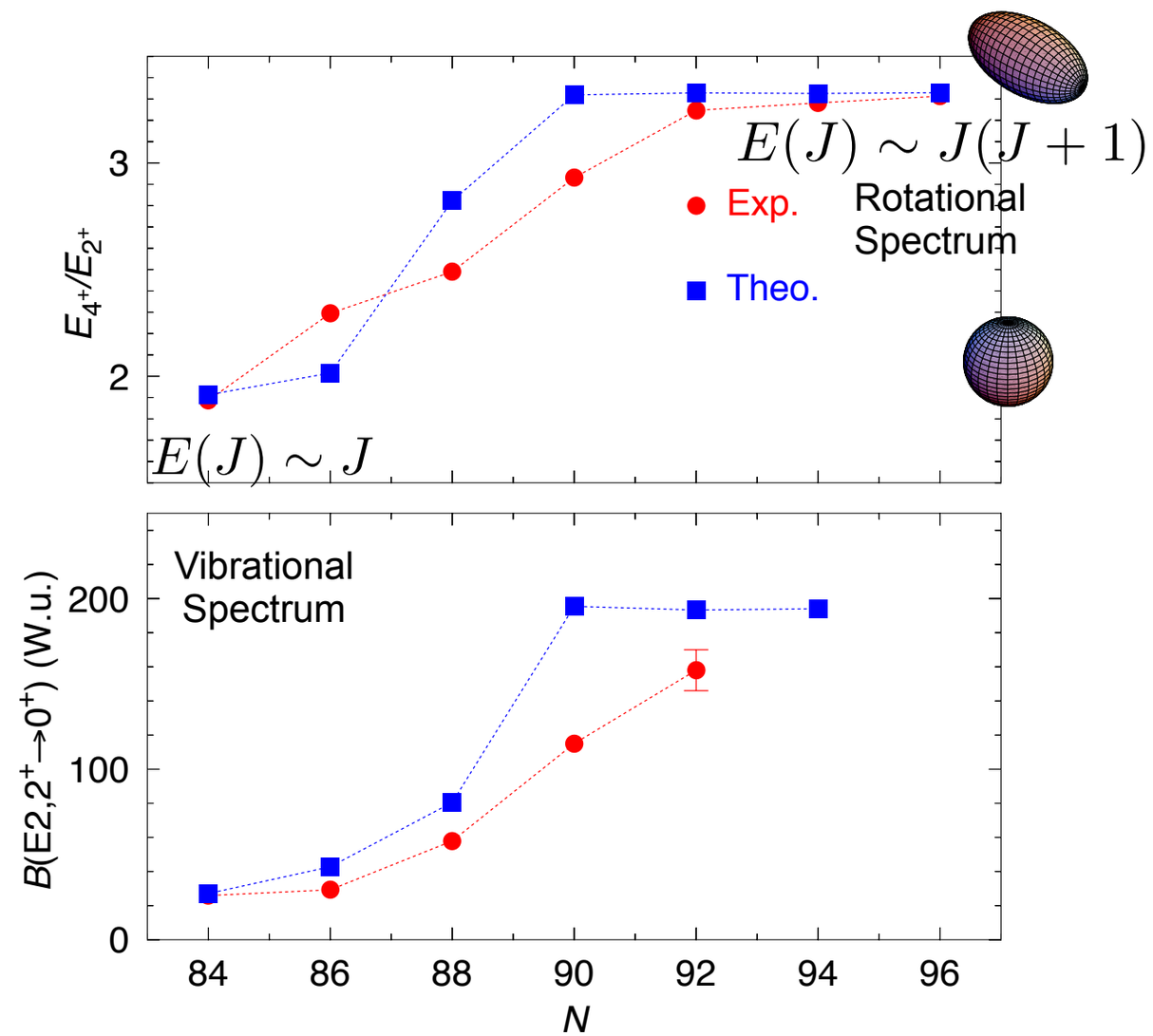

Shape transitions in Nd isotopes

T.R.R. and J.L. Egido Phys.Lett. B 663, 49 (2008)

84		86		88		90		92		94		96
Nd144	Nd145	Nd146	Nd147	Nd148	Nd149	Nd150	Nd151	Nd152	Nd153	Nd154	Nd155	Nd156
2.29E+15 y			10.98 d		1.728 h	1.1E19 y	12.44 m	11.4 m	31.6 s	25.9 s	8.9 s	5.47 s
0+	7/2-	0+	5/2-	0+	5/2-	0+	3/2+	0+	(3/2)-	0+		0+
α 23.80	8.30	17.19	β-	5.76	β-	β- 5.64	β-	β-	β-	β-	β-	β-

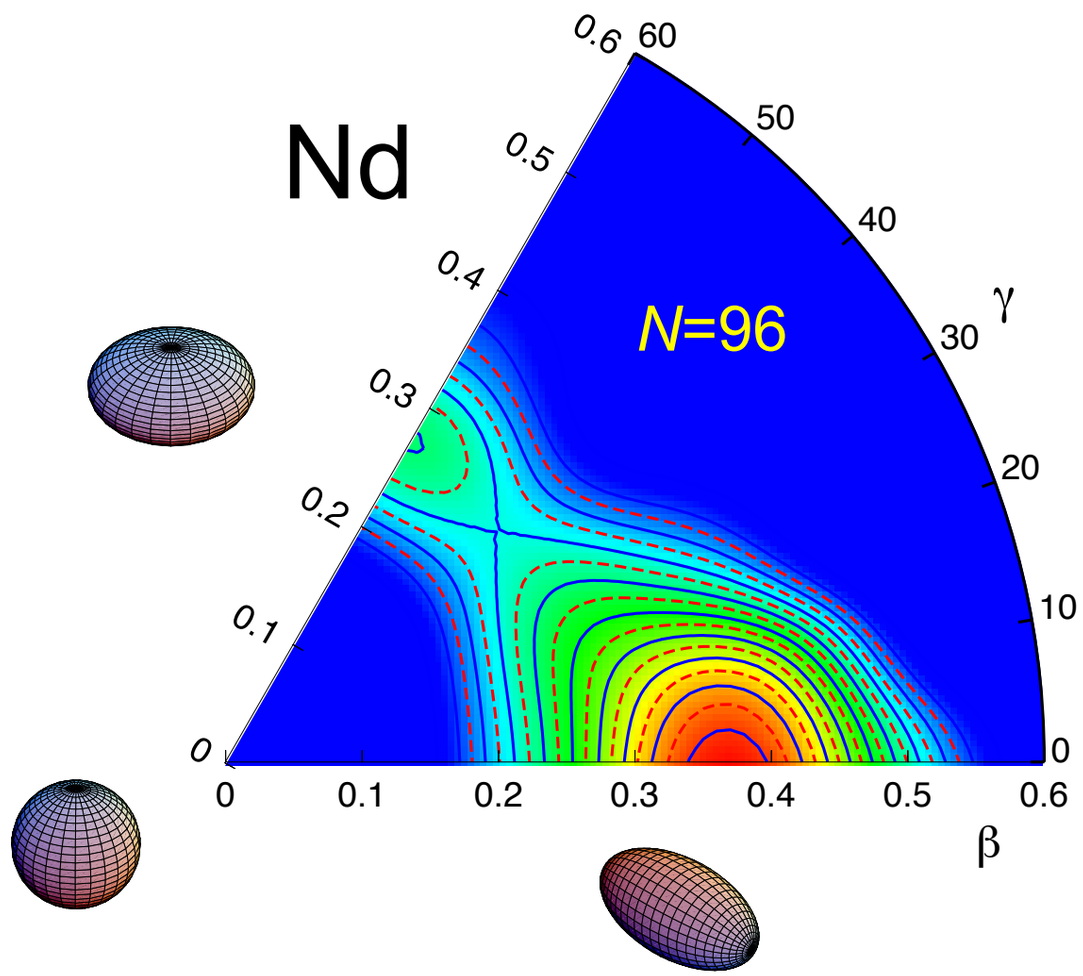

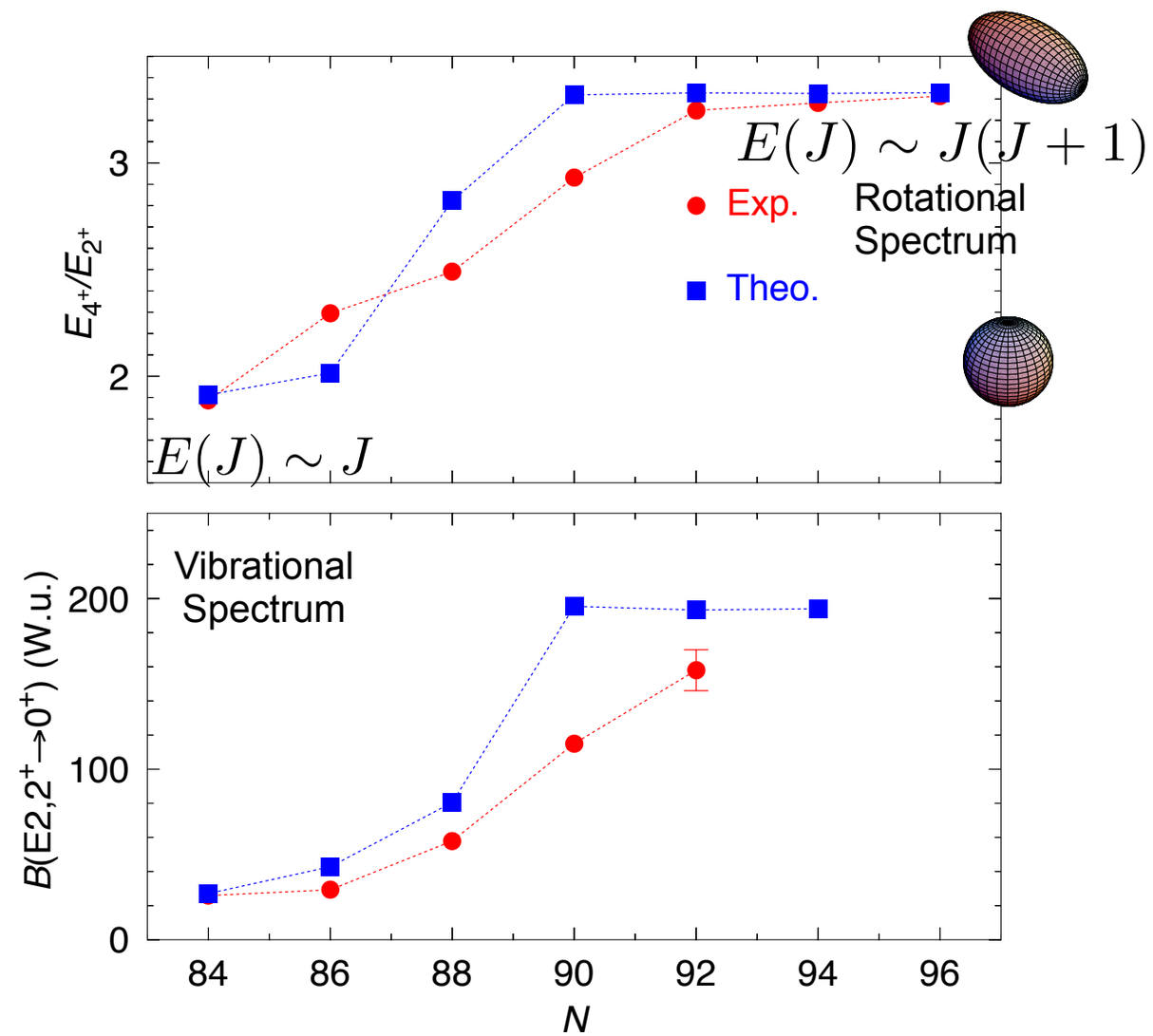

Double beta decay

Process mediated by the weak interaction which occurs in those even-even nuclei where the single beta decay is energetically forbidden.

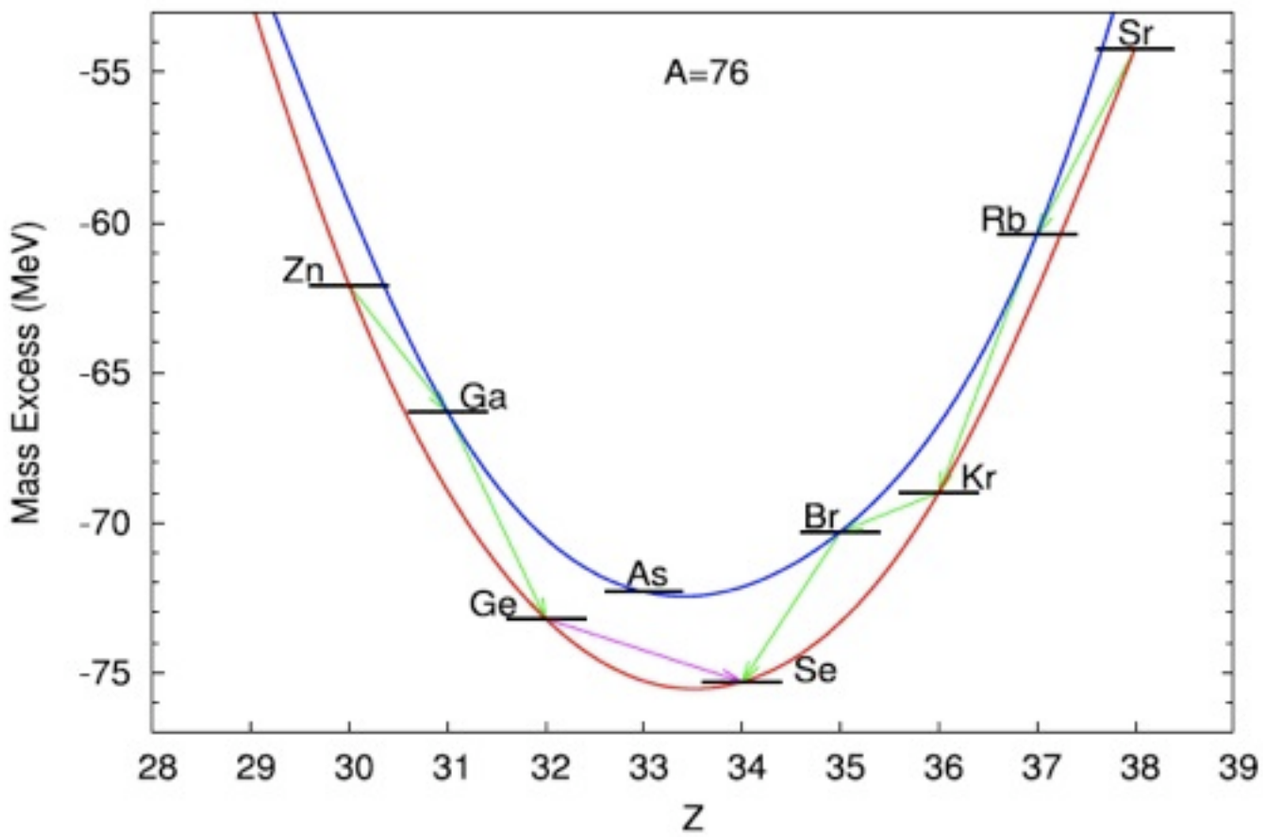

Courtesy J. Menéndez

Double beta decay

Process mediated by the weak interaction which occurs in those even-even nuclei where the single beta decay is energetically forbidden.

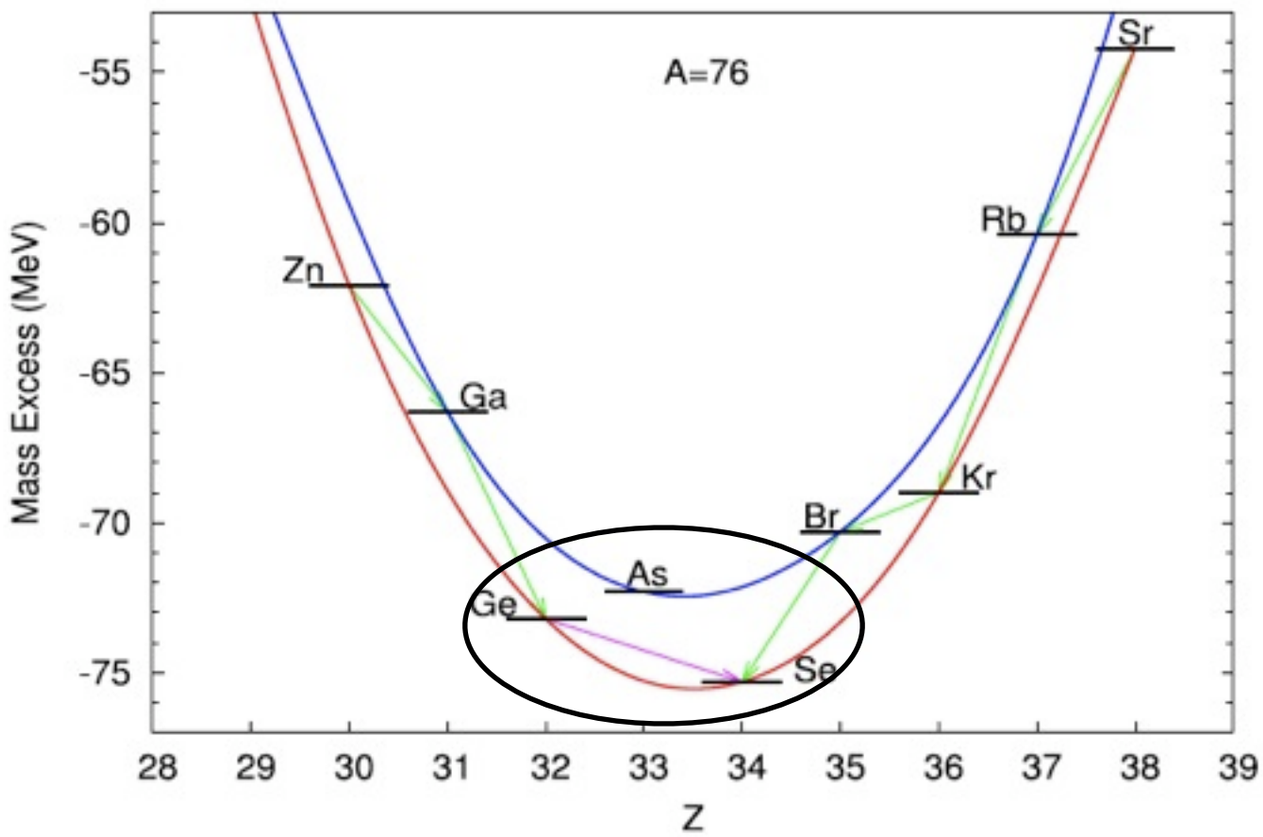

Courtesy J. Menéndez

Double beta decay

Process mediated by the weak interaction which occurs in those even-even nuclei where the single beta decay is energetically forbidden.

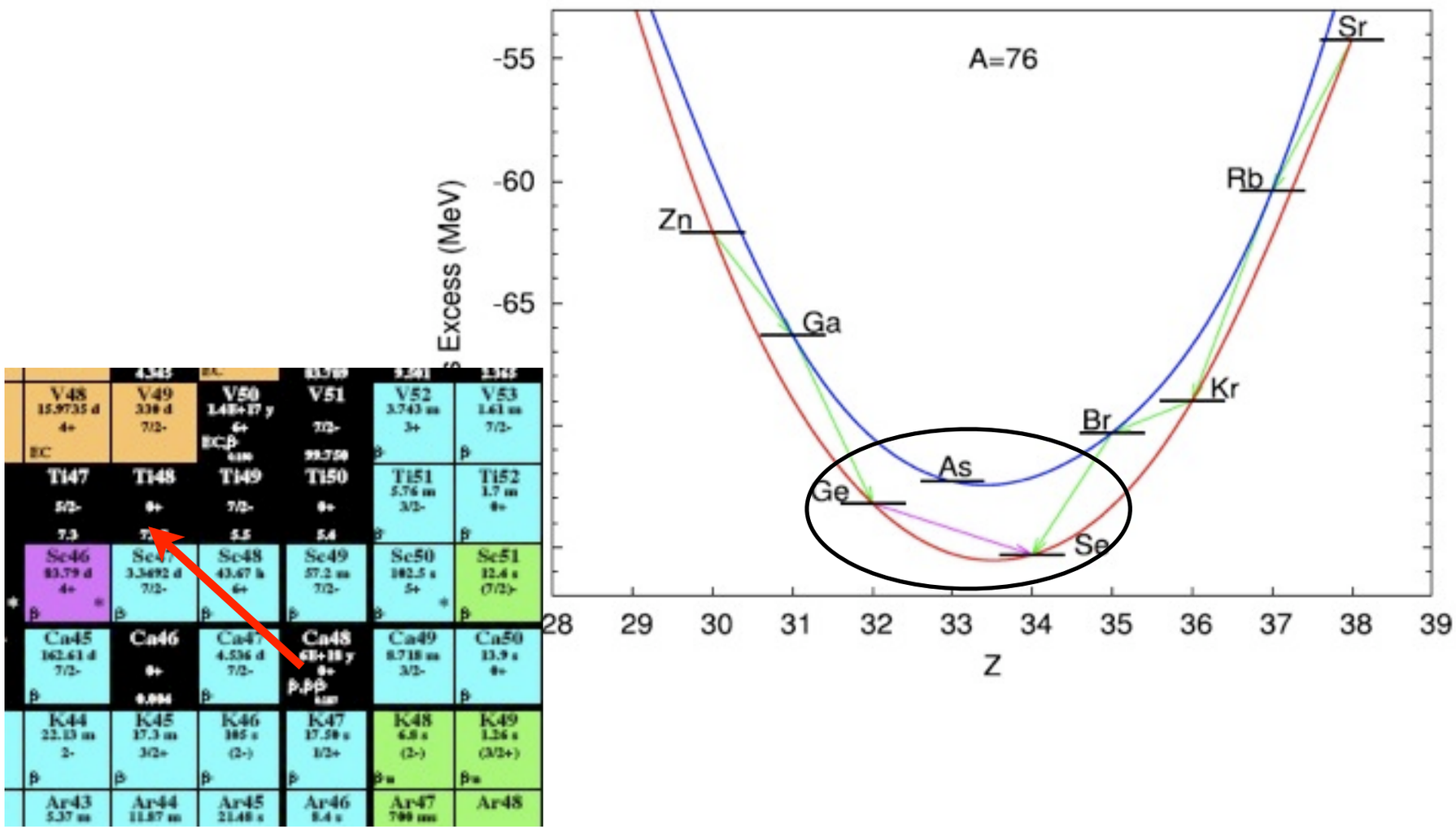

Courtesy J. Menéndez

Double beta decay

Process mediated by the weak interaction which occurs in those even-even nuclei where the single beta decay is energetically forbidden.

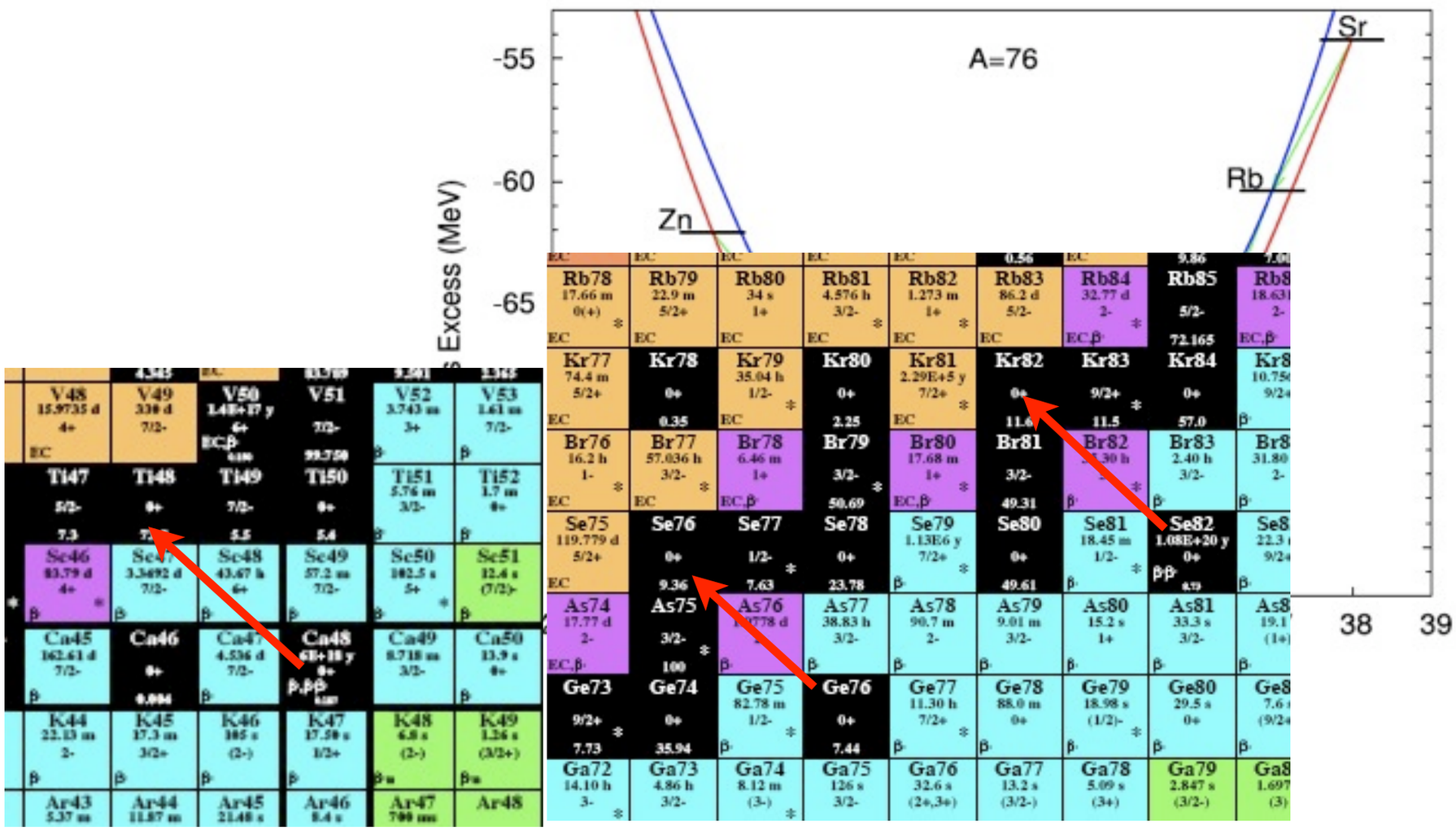

Courtesy J. Menéndez

Double beta decay

Process mediated by the weak interaction which occurs in those even-even nuclei w decay is energetically forbidden.

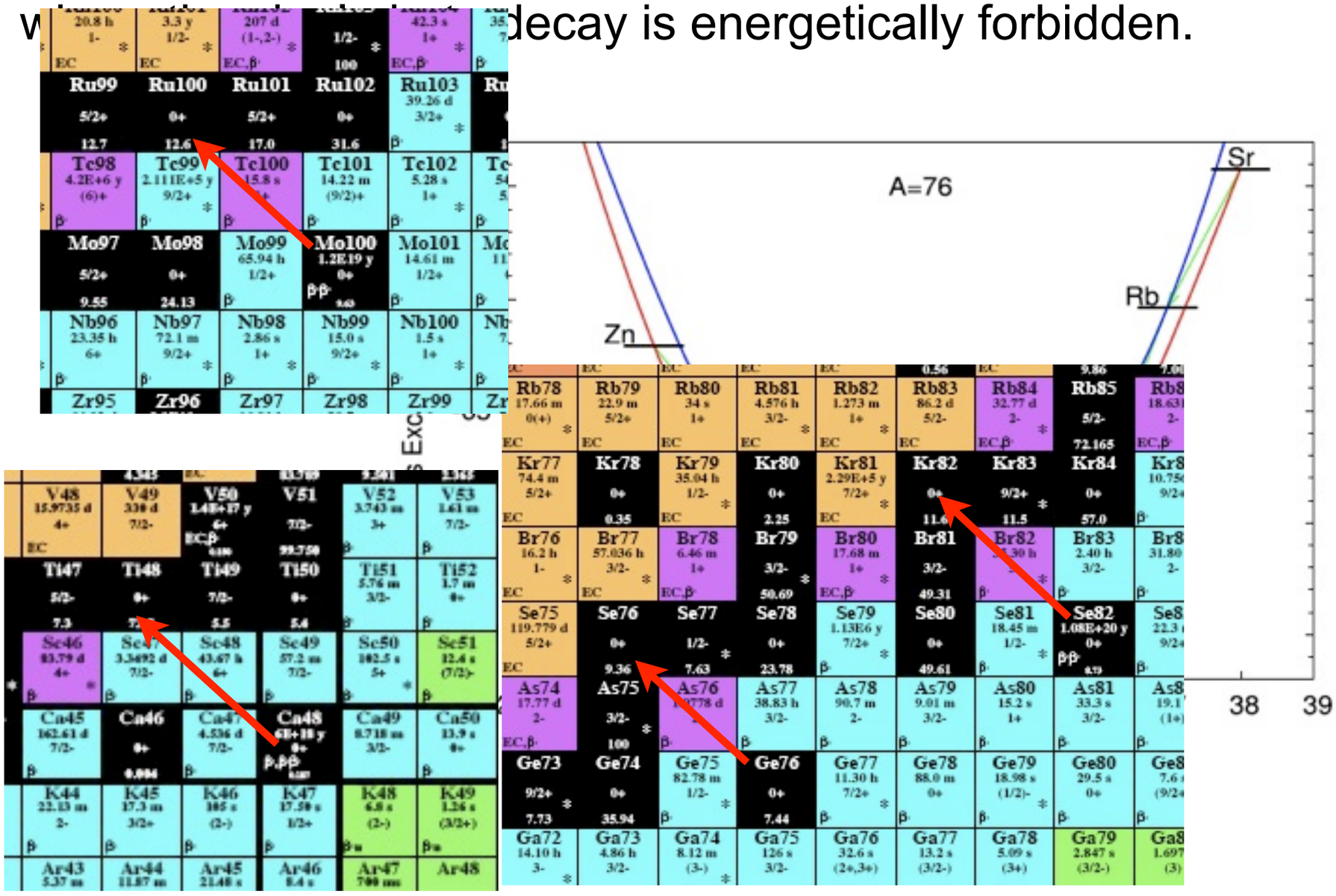

Courtesy J. Menéndez

Double beta decay

Process mediated by the weak interaction which occurs in those even-even nuclei w decay is energetically forbidden.

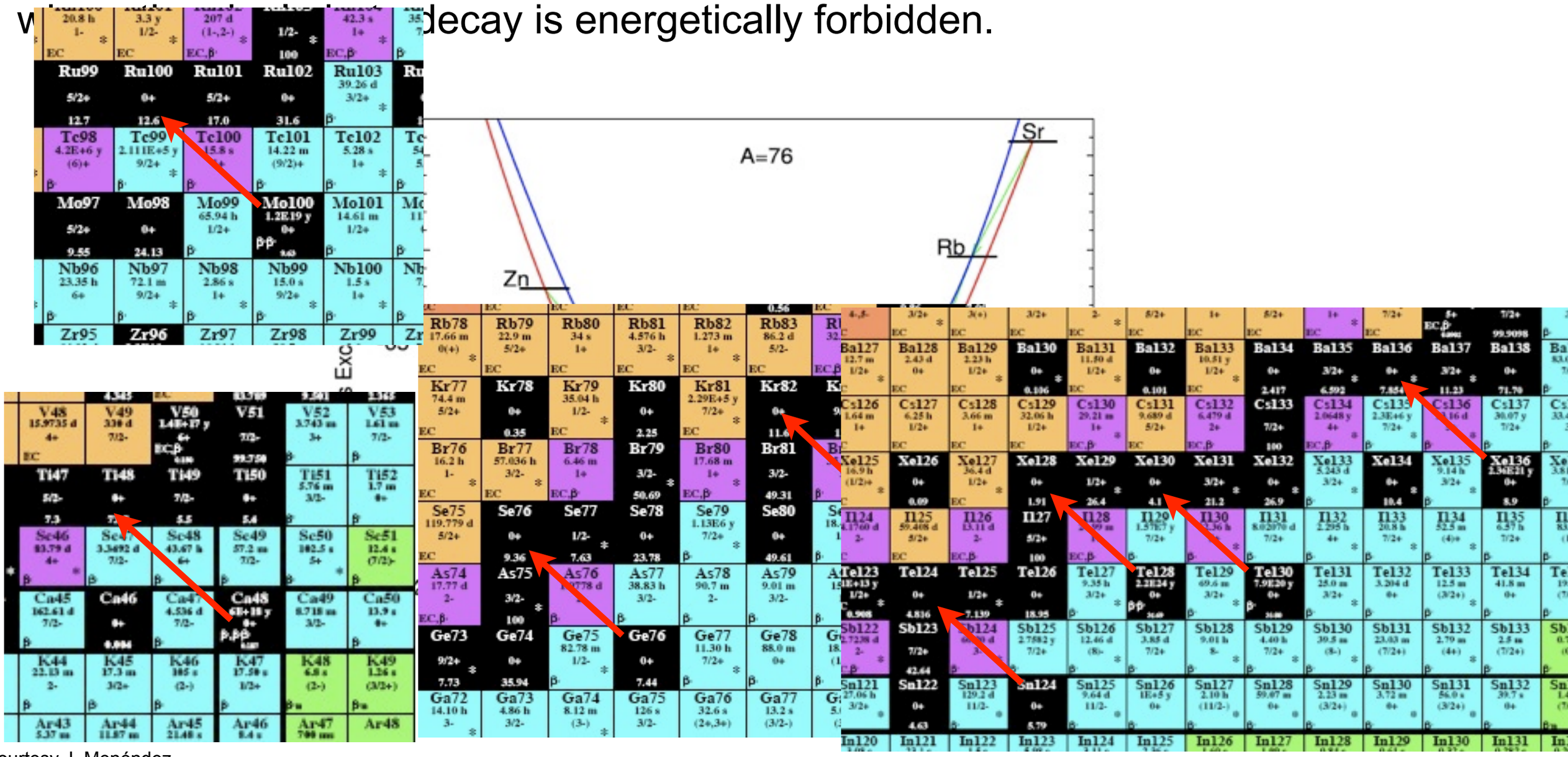

Courtesy J. Menéndez

Double beta decay

Process mediated by the weak interaction which occurs in those even-even nuclei w decay is energetically forb

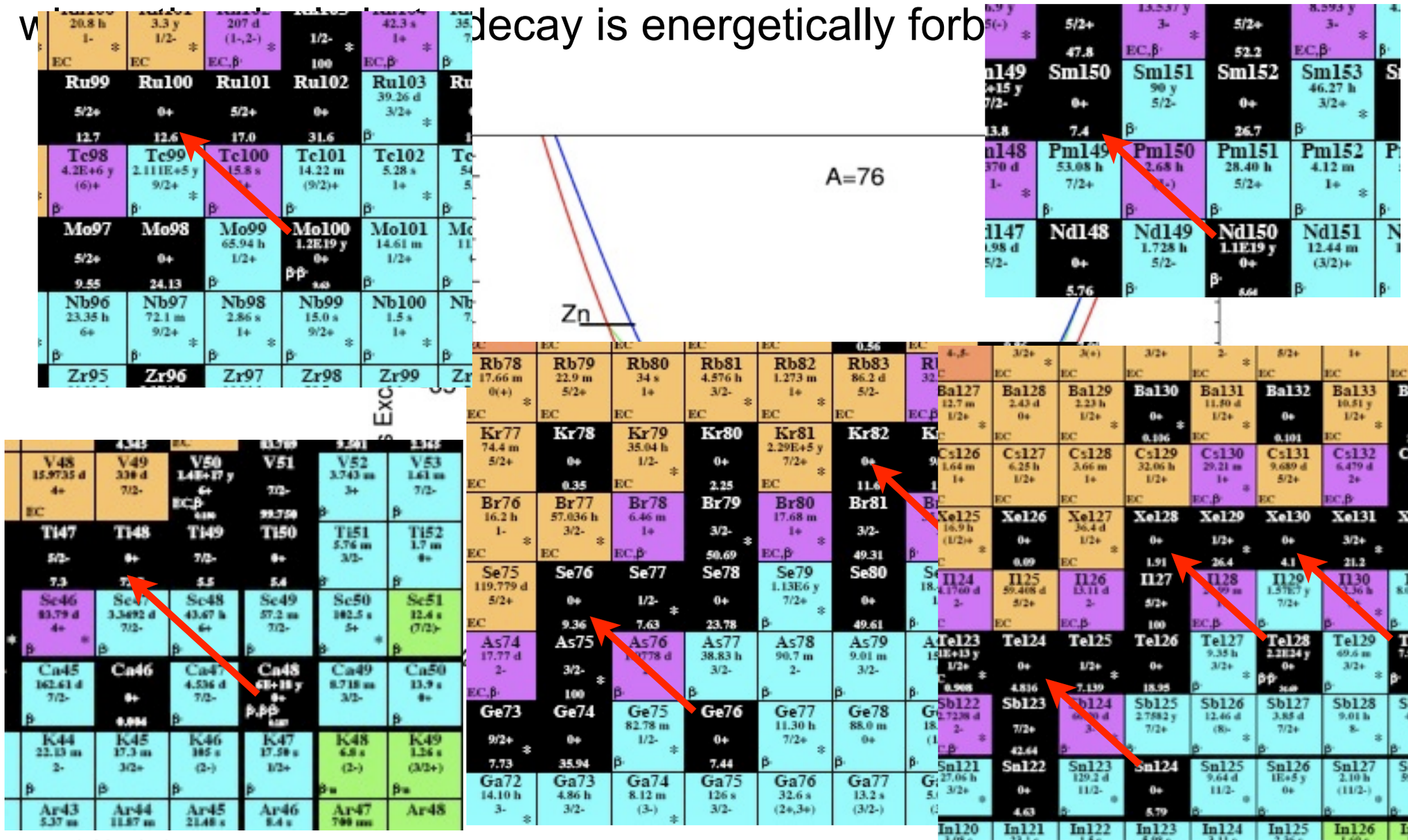

Courtesy J. Menéndez

Neutrinoless double beta decay $0\nu\beta\beta$

$$ {}^{A}_{Z}X_N \Rightarrow {}^{A}_{Z+2}Y_{N-2} + 2e^- $$

- Violates the leptonic number conservation
- Neutrinos are massive Majorana particles
- Mass hierarchy of neutrinos
- Experimentally not observed (yet?) ($T_{1/2}$ >10^{25} y)
- Beyond the Standard Model

$$ \left(T^{0\nu\beta\beta}_{1/2}(0^+ \to 0^+)\right)^{-1} = G_{01}\left|M^{0\nu\beta\beta}\right|^2 \left(\frac{\langle m_\nu \rangle}{m_e}\right)^2 $$

Neutrinoless double beta decay $0\nu\beta\beta$

$$ {}^{A}_{Z}X_N \Rightarrow {}^{A}_{Z+2}Y_{N-2} + 2e^- $$

- Violates the leptonic number conservation
- Neutrinos are massive Majorana particles
- Mass hierarchy of neutrinos
- Experimentally not observed (yet?) ($T_{1/2}$ >10^{25} y)
- Beyond the Standard Model

$$ \left(T^{0\nu\beta\beta}_{1/2}(0^+ \to 0^+)\right)^{-1} = G_{01}\left|M^{0\nu\beta\beta}\right|^2 \left(\frac{\langle m_\nu \rangle}{m_e}\right)^2 $$

NME

$$ M^{0\nu\beta\beta}_{\xi} = \langle 0^+_f | \hat{O}^{0\nu\beta\beta}_{\xi} | 0^+_i \rangle $$

NME: deformation and mixing

$$\frac{\langle 0; N_f Z_f; q_f | \hat{O}^{0\nu\beta\beta}_{\xi} | 0; N_i Z_i; q_i \rangle}{\sqrt{\langle 0; N_f Z_f; q_f | 0; N_f Z_f; q_f \rangle \langle 0; N_i Z_i; q_i | 0; N_i Z_i; q_i \rangle}}$$

A=150

T.R.R., Martínez-Pinedo, PRL 105, 252503 (2010)

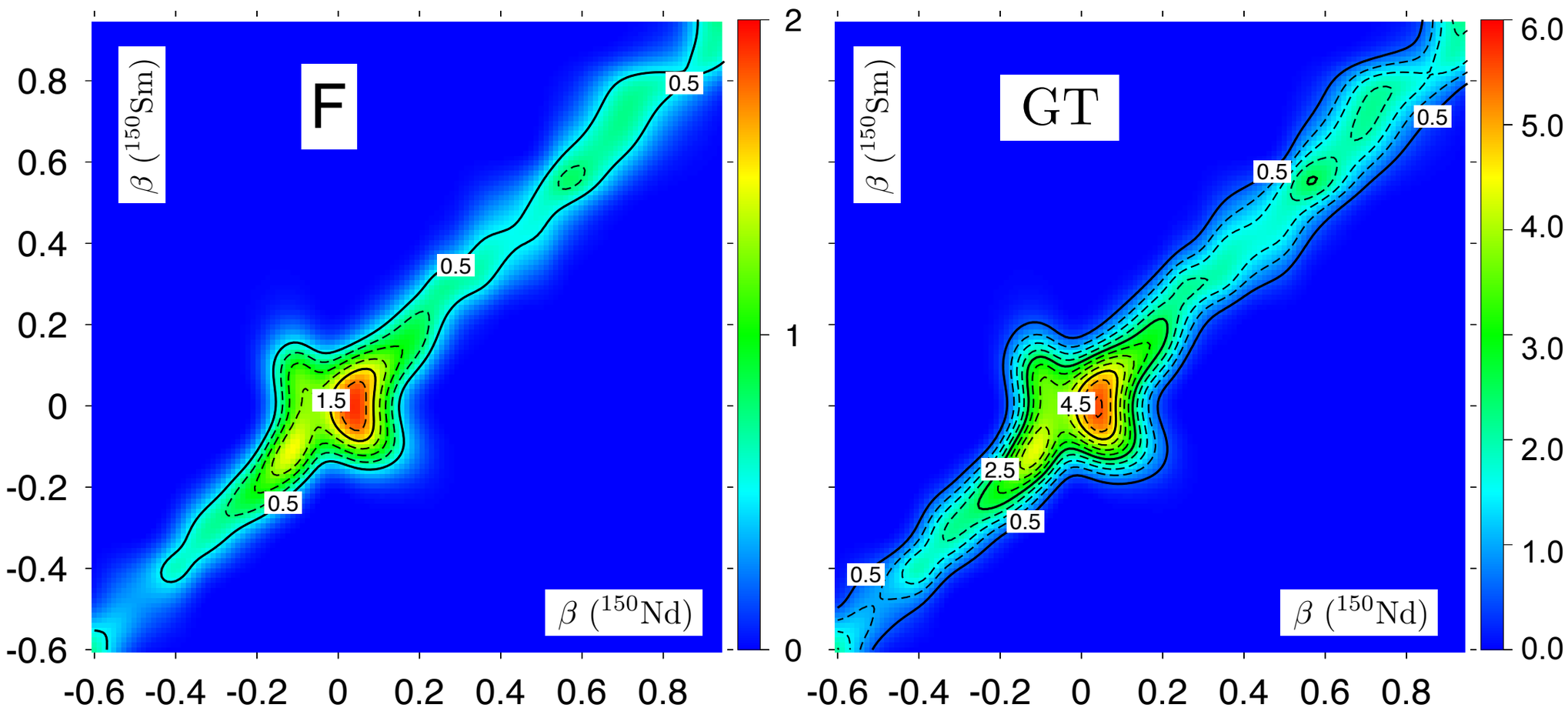

- GT strength greater than Fermi.
- Similar deformation between mother and granddaughter is favored by the transition operators
- Maxima are found close to sphericity although some other local maxima are found

NME: deformation and mixing

$$\frac{\langle 0; N_f Z_f; q_f | \hat{O}^{0\nu\beta\beta}_{\xi} | 0; N_i Z_i; q_i \rangle}{\sqrt{\langle 0; N_f Z_f; q_f | 0; N_f Z_f; q_f \rangle \langle 0; N_i Z_i; q_i | 0; N_i Z_i; q_i \rangle}}$$

A=150

T.R.R., Martínez-Pinedo, PRL 105, 252503 (2010)

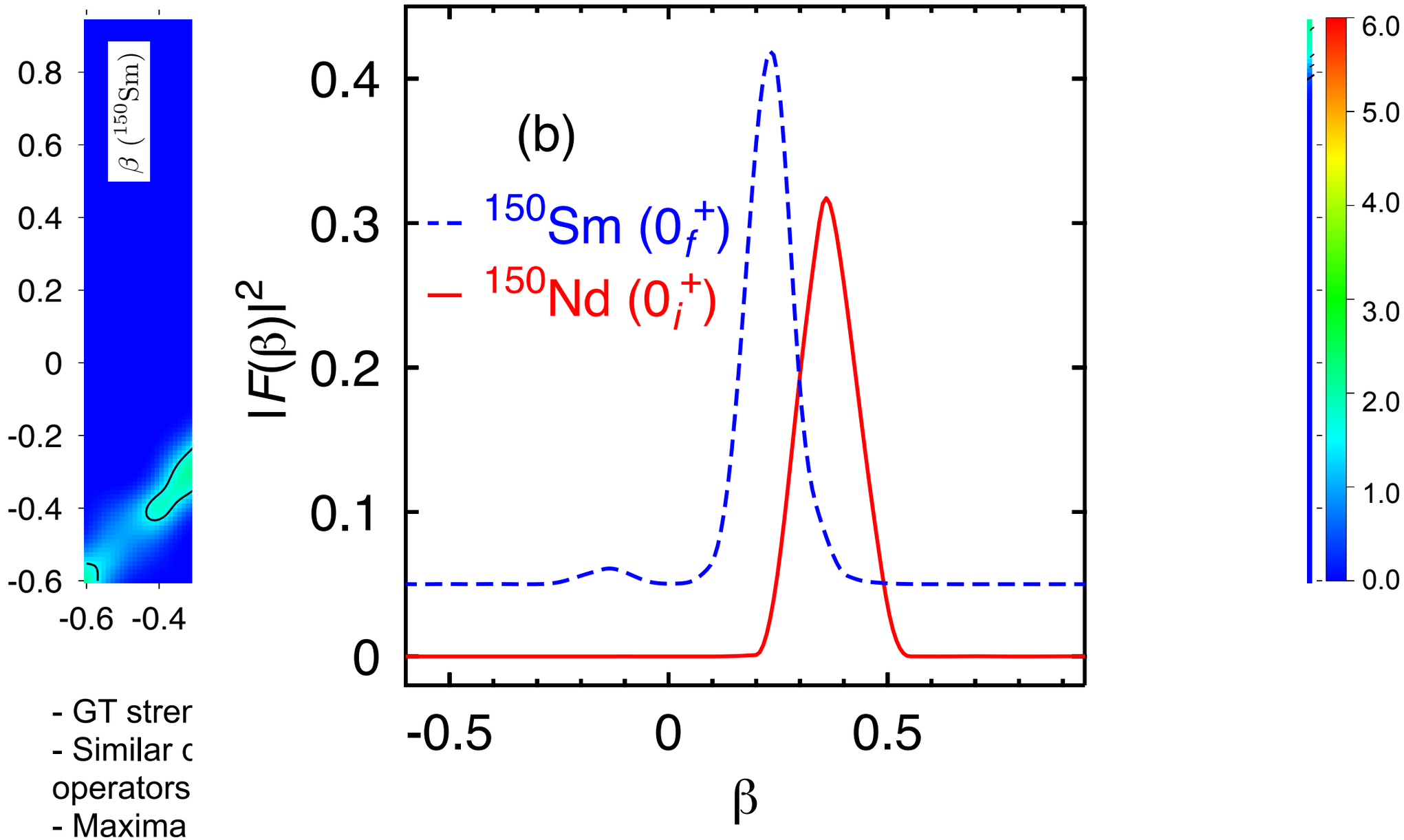

- GT strer
- Similar c
operators
- Maxima

NME: deformation and mixing

$$\frac{\langle 0; N_f Z_f; q_f | \hat{O}_{\xi}^{0\nu\beta\beta} | 0; N_i Z_i; q_i \rangle}{\sqrt{\langle 0; N_f Z_f; q_f | 0; N_f Z_f; q_f \rangle \langle 0; N_i Z_i; q_i | 0; N_i Z_i; q_i \rangle}}$$

A=150

T.R.R., Martínez-Pinedo, PRL 105, 252503 (2010)

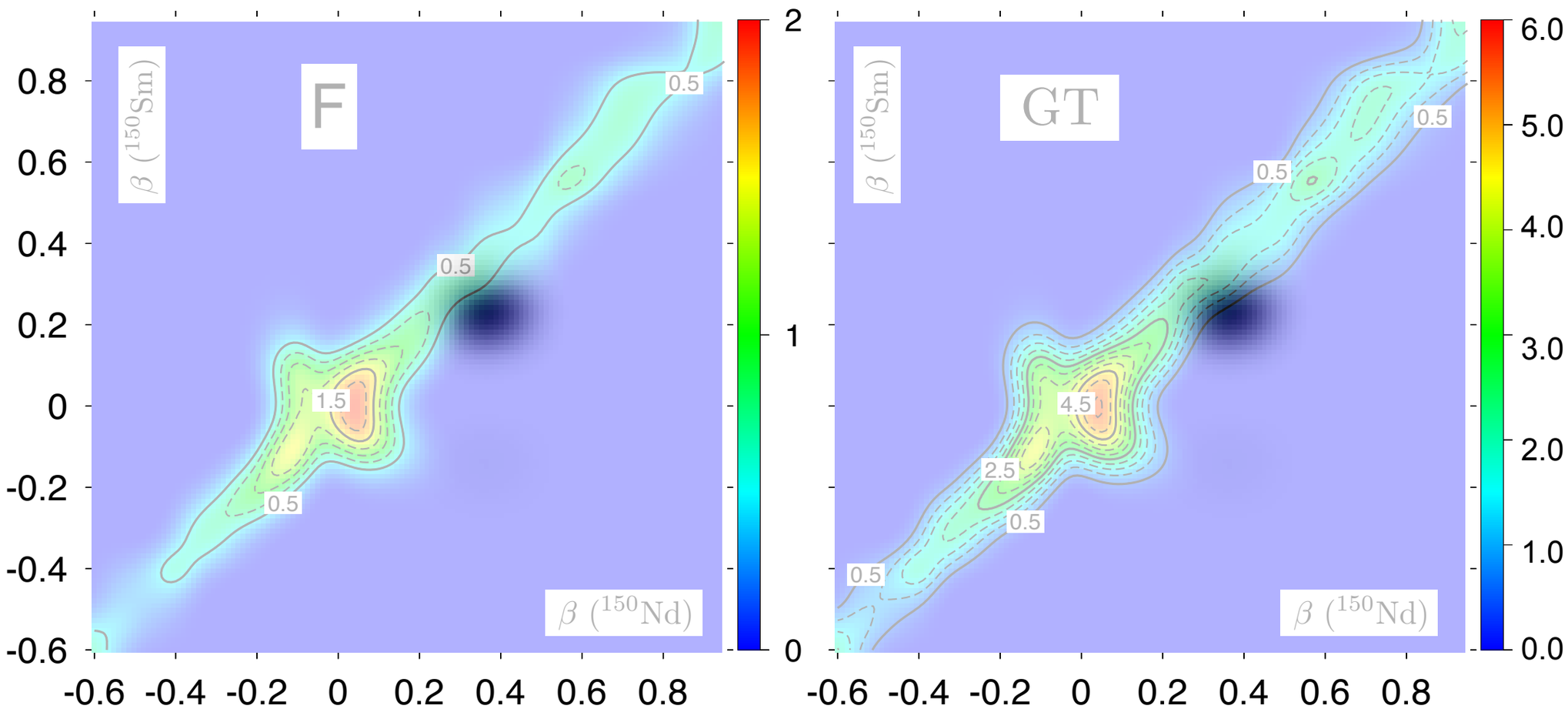

- GT strength greater than Fermi.
- Similar deformation between mother and granddaughter is favored by the transition operators
- Maxima are found close to sphericity although some other local maxima are found

NME: deformation and mixing

$$\frac{\langle 0; N_f Z_f; q_f | \hat{O}_{\xi}^{0\nu\beta\beta} | 0; N_i Z_i; q_i \rangle}{\sqrt{\langle 0; N_f Z_f; q_f | 0; N_f Z_f; q_f \rangle \langle 0; N_i Z_i; q_i | 0; N_i Z_i; q_i \rangle}}$$

A=150

T.R.R., Martínez-Pinedo, PRL 105, 252503 (2010)

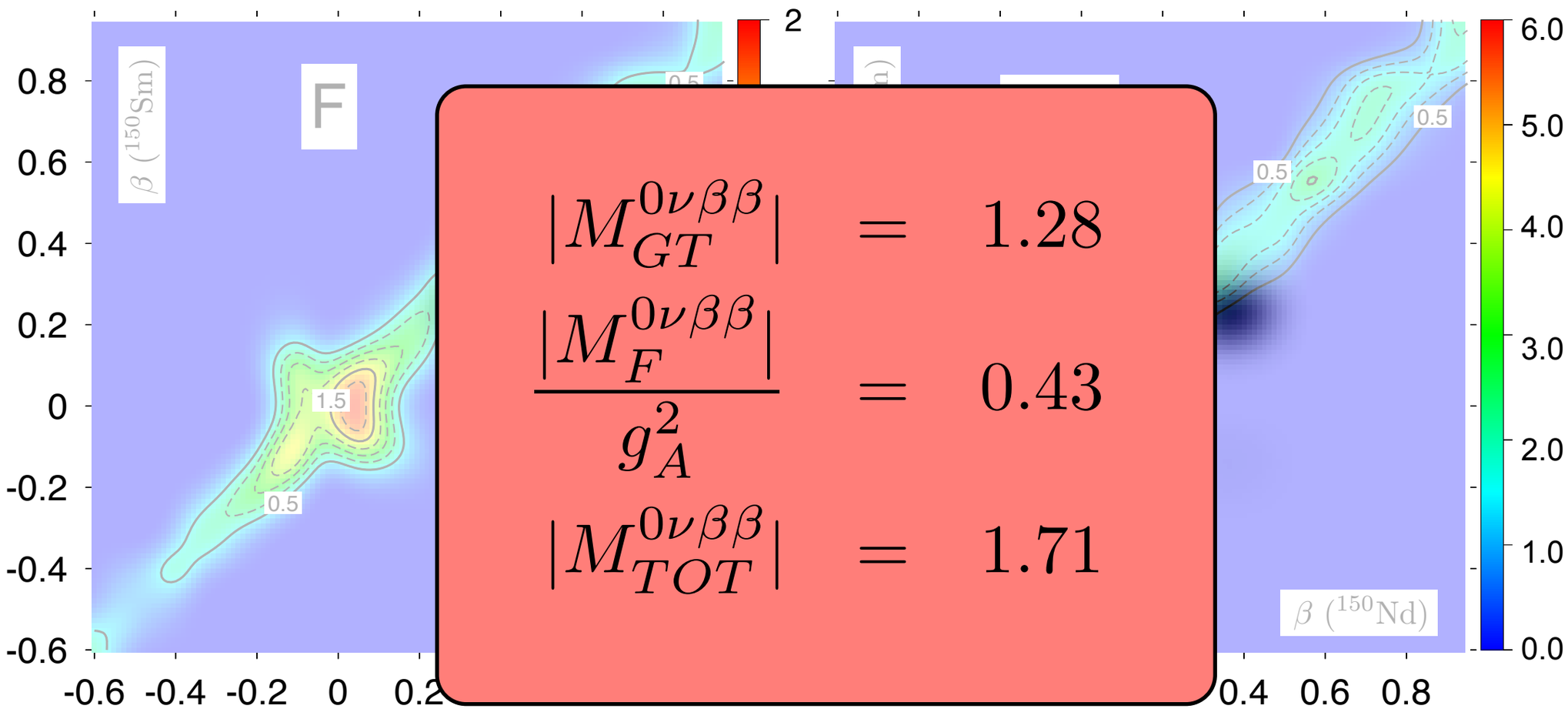

$$|M_{GT}^{0\nu\beta\beta}| = 1.28$$

$$\frac{|M_{F}^{0\nu\beta\beta}|}{g_A^2} = 0.43$$

$$|M_{TOT}^{0\nu\beta\beta}| = 1.71$$

- GT strength greater than Fermi.
- Similar deformation between mother and granddaughter is favored by the transition operators
- Maxima are found close to sphericity although some other local maxima are found

NME: Summary of the results

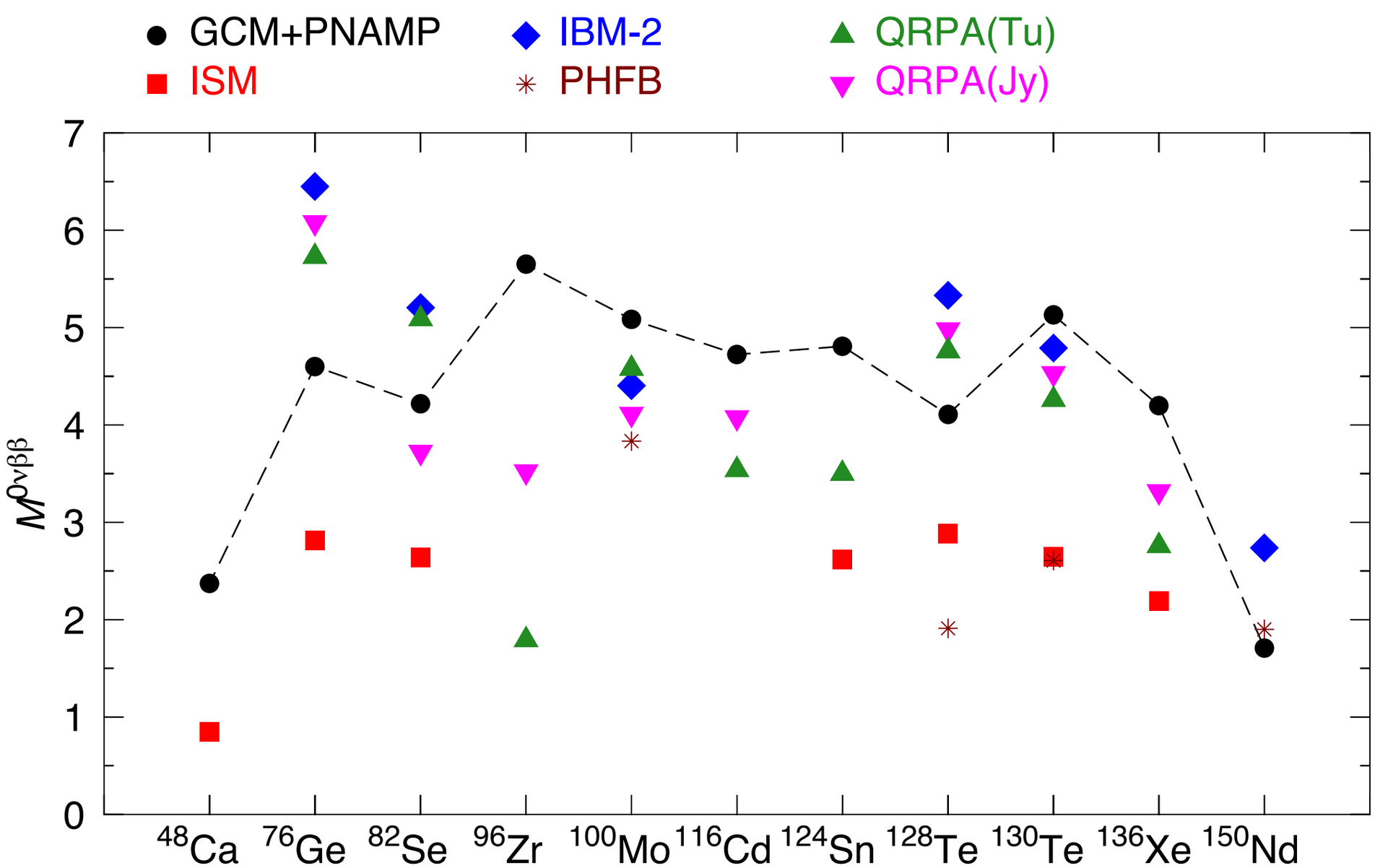

QRPA (Jy):)M. Kortelainen, J. Suhonen, PRC 75, 051303(R) (2007) and PRC 76, 024315 (2007)

QRPA(Tu): F. Simkovic et al., PRC 77, 045503 (2008)

ISM: J. Menendez et al., PRL 100, 52503 (2008)

IBM-2:J. Barea, F. Iachello, PRC 77, 045503 (2008)

PHFB: K. Chaturvedi et al. PRC 78, 054302 (2008)

T.R.R., Martínez-Pinedo, PRL 105, 252503 (2010)

NME: Summary of the results

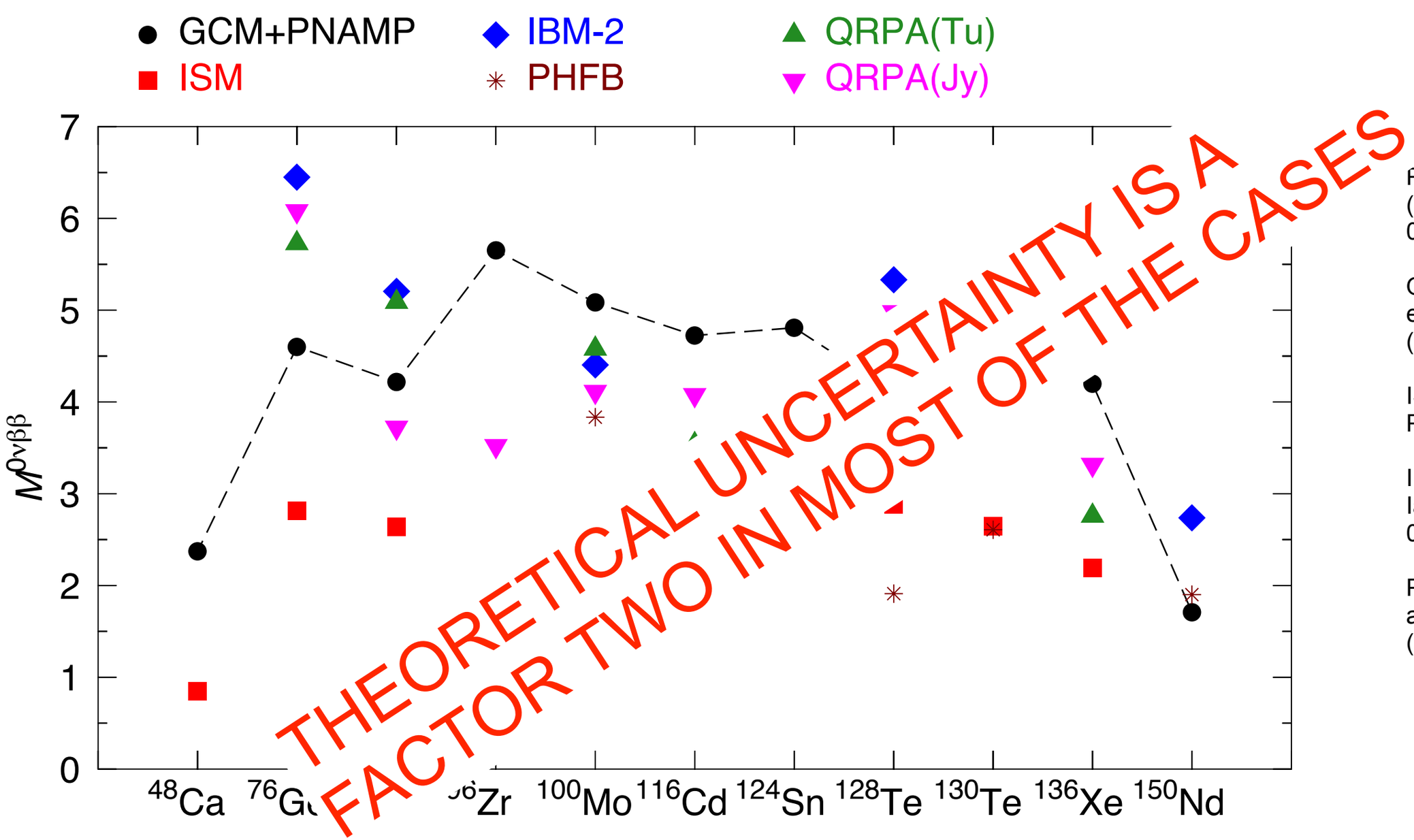

RPA (Jy):)M. ,itelainen, J. Suhonen, PRC 75, 051303(R) (2007) and PRC 76, 024315 (2007)

QRPA(Tu): F. Simkovic et al., PRC 77, 045503 (2008)

ISM: J. Menendez et al., PRL 100, 52503 (2008)

IBM-2:J. Barea, F. Iachello, PRC 77, 045503 (2008)

PHFB: K. Chaturvedi et al. PRC 78, 054302 (2008)

T.R.R., Martínez-Pinedo, PRL 105, 252503 (2010)

Hartree-Fock-Bogoliubov (HFB)

Variational space: $\{|\Phi(\vec{q})\rangle\}$ set of **product-type** wave functions which fulfill:

- Quasiparticle vacua: $$\alpha_k(\vec{q})|\Phi(\vec{q})\rangle = 0$$
- Most general linear combination of the arbitrary single particle basis: $$\alpha_k^\dagger(\vec{q}) = \sum_l U_{lk}(\vec{q})c_l^\dagger + V_{lk}(\vec{q})c_l$$
- Fermionic operators: $$\{\alpha_k^\dagger(\vec{q}), \alpha_{k'}(\vec{q})\} = \delta_{kk'}; \{\alpha_k^\dagger(\vec{q}), \alpha_{k'}^\dagger(\vec{q})\} = \{\alpha_k(\vec{q}), \alpha_{k'}(\vec{q})\} = 0$$

Hartree-Fock-Bogoliubov (HFB)

Variational space: $\{|\Phi(\vec{q})\rangle\}$ set of **product-type** wave functions which fulfill:

- Quasiparticle vacua: $$\alpha_k(\vec{q})|\Phi(\vec{q})\rangle = 0$$
- Most general linear combination of the arbitrary single particle basis: $$\alpha_k^\dagger(\vec{q}) = \sum_l U_{lk}(\vec{q})c_l^\dagger + V_{lk}(\vec{q})c_l$$
- Fermionic operators: $$\{\alpha_k^\dagger(\vec{q}), \alpha_{k'}(\vec{q})\} = \delta_{kk'}; \{\alpha_k^\dagger(\vec{q}), \alpha_{k'}^\dagger(\vec{q})\} = \{\alpha_k(\vec{q}), \alpha_{k'}(\vec{q})\} = 0$$

Variational principle: $$\delta\left[E'^{\mathrm{HFB}}(\vec{q}) = \langle\Phi(\vec{q})|\hat{H} - \lambda_N\hat{N} - \lambda_Z\hat{Z} - \vec{\lambda}_{\vec{q}}\hat{\vec{Q}}|\Phi(\vec{q})\rangle\right]_{|\Phi(\vec{q})\rangle=|\mathrm{HFB}(\vec{q})\rangle} = 0$$

$\lambda_N(\vec{q}) \rightarrow \langle\Phi(\vec{q})|\hat{N}|\Phi(\vec{q})\rangle = N$

$\lambda_Z(\vec{q}) \rightarrow \langle\Phi(\vec{q})|\hat{Z}|\Phi(\vec{q})\rangle = Z$

$\lambda_{\vec{q}}(\vec{q}) \rightarrow \langle\Phi(\vec{q})|\hat{\vec{Q}}|\Phi(\vec{q})\rangle = \vec{q}$

Hartree-Fock-Bogoliubov (HFB)

Variational space: $\{|\Phi(\vec{q})\rangle\}$ set of **product-type** wave functions which fulfill:

- Quasiparticle vacua: $$\alpha_k(\vec{q})|\Phi(\vec{q})\rangle = 0$$
- Most general linear combination of the arbitrary single particle basis: $$\alpha_k^\dagger(\vec{q}) = \sum_l U_{lk}(\vec{q})c_l^\dagger + V_{lk}(\vec{q})c_l$$
- Fermionic operators: $$\{\alpha_k^\dagger(\vec{q}), \alpha_{k'}(\vec{q})\} = \delta_{kk'}; \{\alpha_k^\dagger(\vec{q}), \alpha_{k'}^\dagger(\vec{q})\} = \{\alpha_k(\vec{q}), \alpha_{k'}(\vec{q})\} = 0$$

Variational principle: $$\delta\left[E'^{\mathrm{HFB}}(\vec{q}) = \langle\Phi(\vec{q})|\hat{H} - \lambda_N\hat{N} - \lambda_Z\hat{Z} - \vec{\lambda}_{\vec{q}}\hat{\vec{Q}}|\Phi(\vec{q})\rangle\right]_{|\Phi(\vec{q})\rangle=|\mathrm{HFB}(\vec{q})\rangle} = 0$$

$\lambda_N(\vec{q}) \rightarrow \langle\Phi(\vec{q})|\hat{N}|\Phi(\vec{q})\rangle = N$

$\lambda_Z(\vec{q}) \rightarrow \langle\Phi(\vec{q})|\hat{Z}|\Phi(\vec{q})\rangle = Z$

$\lambda_{\vec{q}}(\vec{q}) \rightarrow \langle\Phi(\vec{q})|\hat{\vec{Q}}|\Phi(\vec{q})\rangle = \vec{q}$

$$E^{\mathrm{HFB}}(\vec{q}) = \langle\Phi(\vec{q})|\hat{H}|\Phi(\vec{q})\rangle$$

$|\mathrm{HFB}(\vec{q})\rangle$ **Product Type**

Hartree-Fock-Bogoliubov (HFB)

Variational space: $\{|\Phi(\vec{q})\rangle\}$ set of **product-type** wave functions which fulfill:

- Quasiparticle vacua: $$\alpha_k(\vec{q})|\Phi(\vec{q})\rangle = 0$$
- Most general linear combination of the arbitrary single particle basis: $$\alpha_k^\dagger(\vec{q}) = \sum_l U_{lk}(\vec{q})c_l^\dagger + V_{lk}(\vec{q})c_l$$
- Fermionic operators: $$\{\alpha_k^\dagger(\vec{q}), \alpha_{k'}(\vec{q})\} = \delta_{kk'}; \{\alpha_k^\dagger(\vec{q}), \alpha_{k'}^\dagger(\vec{q})\} = \{\alpha_k(\vec{q}), \alpha_{k'}(\vec{q})\} = 0$$

1. finite basis!! convergence?

Variational principle: $$\delta\left[E'^{\mathrm{HFB}}(\vec{q}) = \langle\Phi(\vec{q})|\hat{H} - \lambda_N\hat{N} - \lambda_Z\hat{Z} - \vec{\lambda}_{\vec{q}}\hat{\vec{Q}}|\Phi(\vec{q})\rangle\right]_{|\Phi(\vec{q})\rangle=|\mathrm{HFB}(\vec{q})\rangle} = 0$$

$\lambda_N(\vec{q}) \to \langle\Phi(\vec{q})|\hat{N}|\Phi(\vec{q})\rangle = N$

$\lambda_Z(\vec{q}) \to \langle\Phi(\vec{q})|\hat{Z}|\Phi(\vec{q})\rangle = Z$

$\lambda_{\vec{q}}(\vec{q}) \to \langle\Phi(\vec{q})|\hat{\vec{Q}}|\Phi(\vec{q})\rangle = \vec{q}$

$$E^{\mathrm{HFB}}(\vec{q}) = \langle\Phi(\vec{q})|\hat{H}|\Phi(\vec{q})\rangle$$

$|\mathrm{HFB}(\vec{q})\rangle$ **Product Type**

Hartree-Fock-Bogoliubov (HFB)

Variational space: $\{|\Phi(\vec{q})\rangle\}$ set of **product-type** wave functions which fulfill:

- Quasiparticle vacua: $$\alpha_k(\vec{q})|\Phi(\vec{q})\rangle = 0$$
- Most general linear combination of the arbitrary single particle basis: $$\alpha_k^\dagger(\vec{q}) = \sum_l U_{lk}(\vec{q})c_l^\dagger + V_{lk}(\vec{q})c_l$$
- Fermionic operators: $$\{\alpha_k^\dagger(\vec{q}), \alpha_{k'}(\vec{q})\} = \delta_{kk'}; \{\alpha_k^\dagger(\vec{q}), \alpha_{k'}^\dagger(\vec{q})\} = \{\alpha_k(\vec{q}), \alpha_{k'}(\vec{q})\} = 0$$

1. finite basis!! convergence?

2. Breaks the symmetries!!

Variational principle: $$\delta\left[E'^{\mathrm{HFB}}(\vec{q}) = \langle\Phi(\vec{q})|\hat{H} - \lambda_N\hat{N} - \lambda_Z\hat{Z} - \vec{\lambda}_{\vec{q}}\hat{\vec{Q}}|\Phi(\vec{q})\rangle\right]_{|\Phi(\vec{q})\rangle=|\mathrm{HFB}(\vec{q})\rangle} = 0$$

$\lambda_N(\vec{q}) \to \langle\Phi(\vec{q})|\hat{N}|\Phi(\vec{q})\rangle = N$

$\lambda_Z(\vec{q}) \to \langle\Phi(\vec{q})|\hat{Z}|\Phi(\vec{q})\rangle = Z$

$\lambda_{\vec{q}}(\vec{q}) \to \langle\Phi(\vec{q})|\hat{\vec{Q}}|\Phi(\vec{q})\rangle = \vec{q}$

$$E^{\mathrm{HFB}}(\vec{q}) = \langle\Phi(\vec{q})|\hat{H}|\Phi(\vec{q})\rangle$$

$|\mathrm{HFB}(\vec{q})\rangle$ **Product Type**

Some formal aspects

TECHNISCHE UNIVERSITÄT DARMSTADT

Hartree-Fock-Bogoliubov (HFB)

$$\alpha_k^\dagger(\vec{q}) = \sum_l U_{lk}(\vec{q})c_l^\dagger + V_{lk}(\vec{q})c_l$$

- **Most of the calculations are performed in a *finite* harmonic oscillator basis.**
- **Results must not depend on the choice of the arbitrary single particle basis if it is complete.**

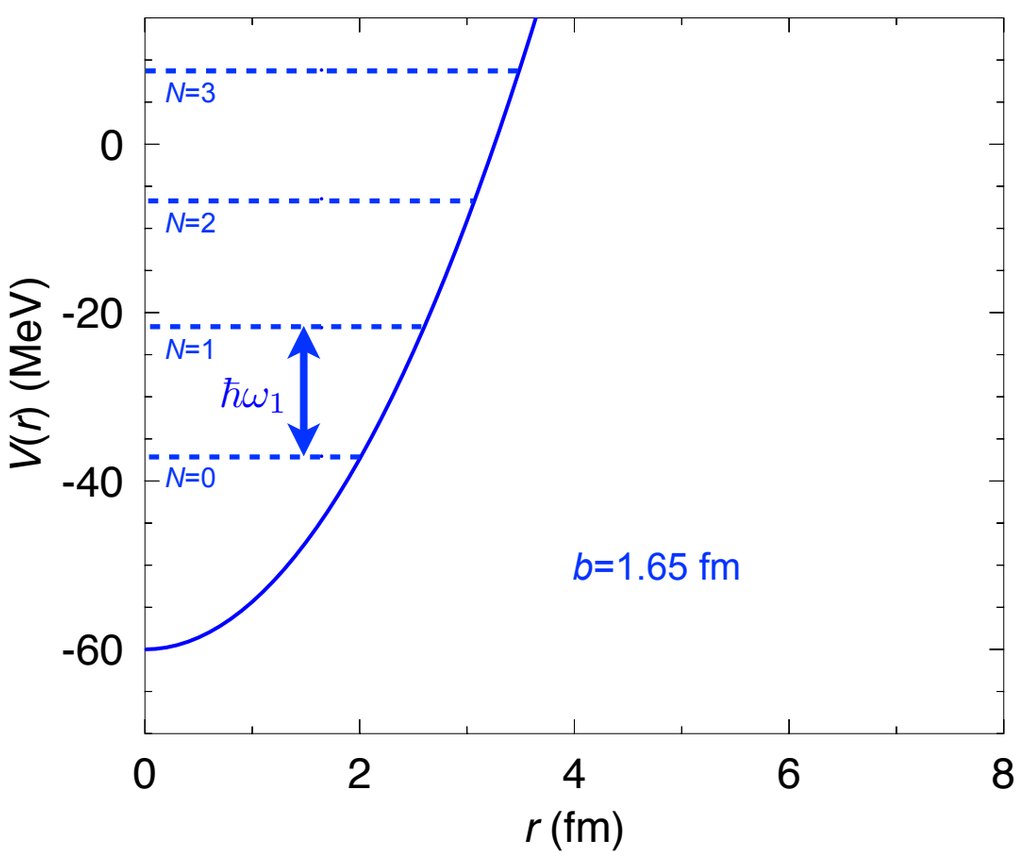

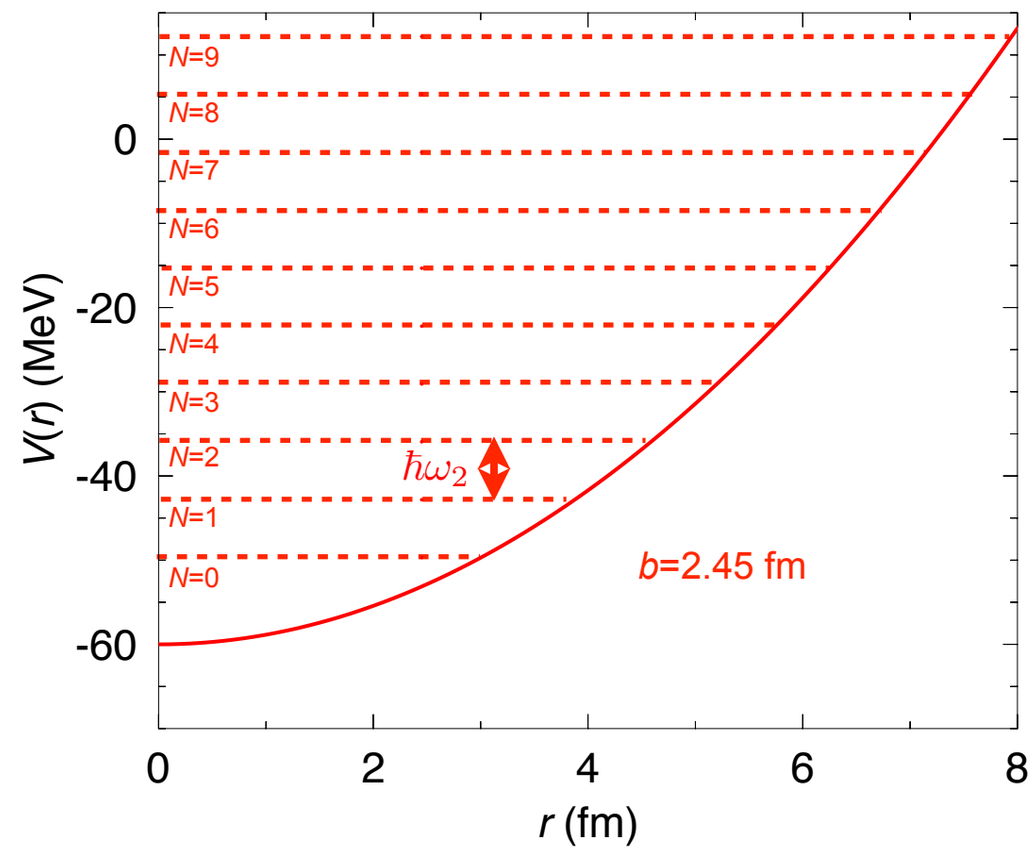

Some formal aspects

TECHNISCHE UNIVERSITÄT DARMSTADT

Hartree-Fock-Bogoliubov (HFB)

$$\alpha_k^\dagger(\vec{q}) = \sum_l U_{lk}(\vec{q})c_l^\dagger + V_{lk}(\vec{q})c_l$$

- **Most of the calculations are performed in a *finite* harmonic oscillator basis.**
- **Results must not depend on the choice of the arbitrary single particle basis if it is complete.**

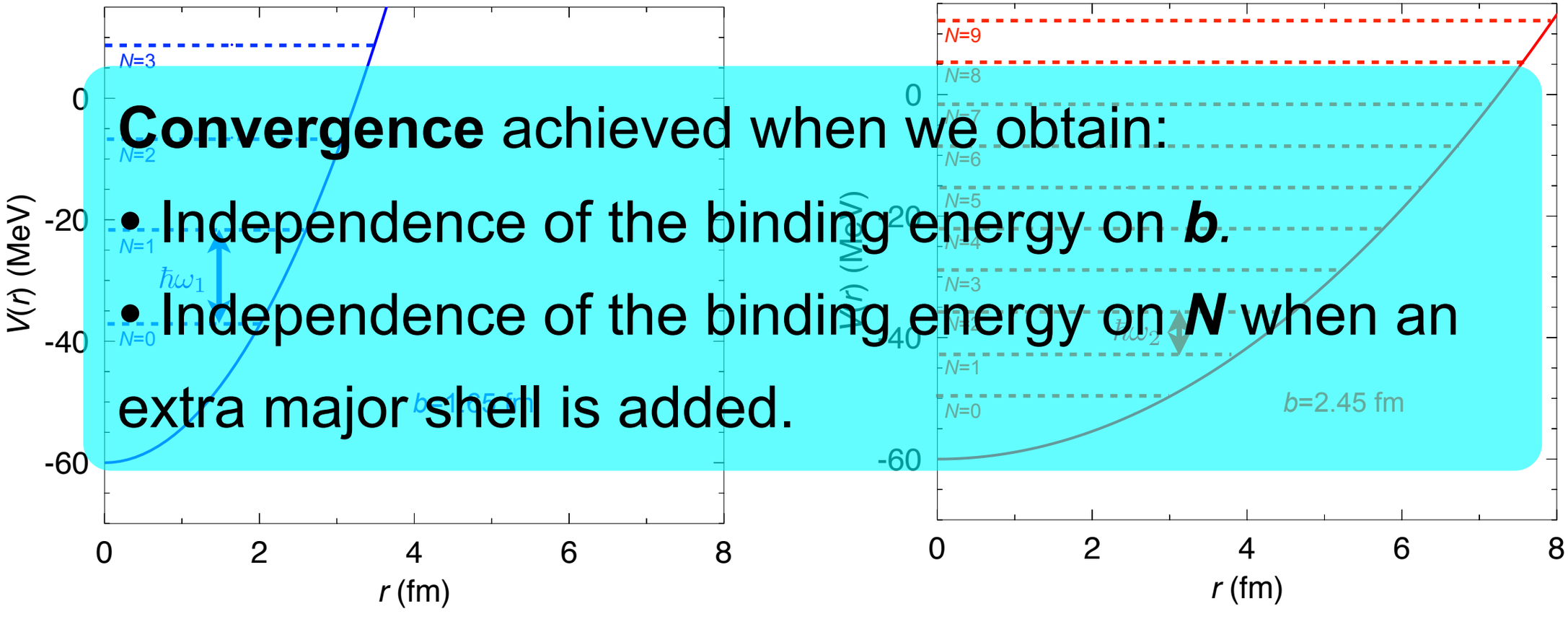

Convergence achieved when we obtain:

- Independence of the binding energy on ***b***.
- Independence of the binding energy on ***N*** when an extra major shell is added.

Examples in *ab-initio* calculations

P. Maris et *al.*, Phys. Rev C 79 (2009)

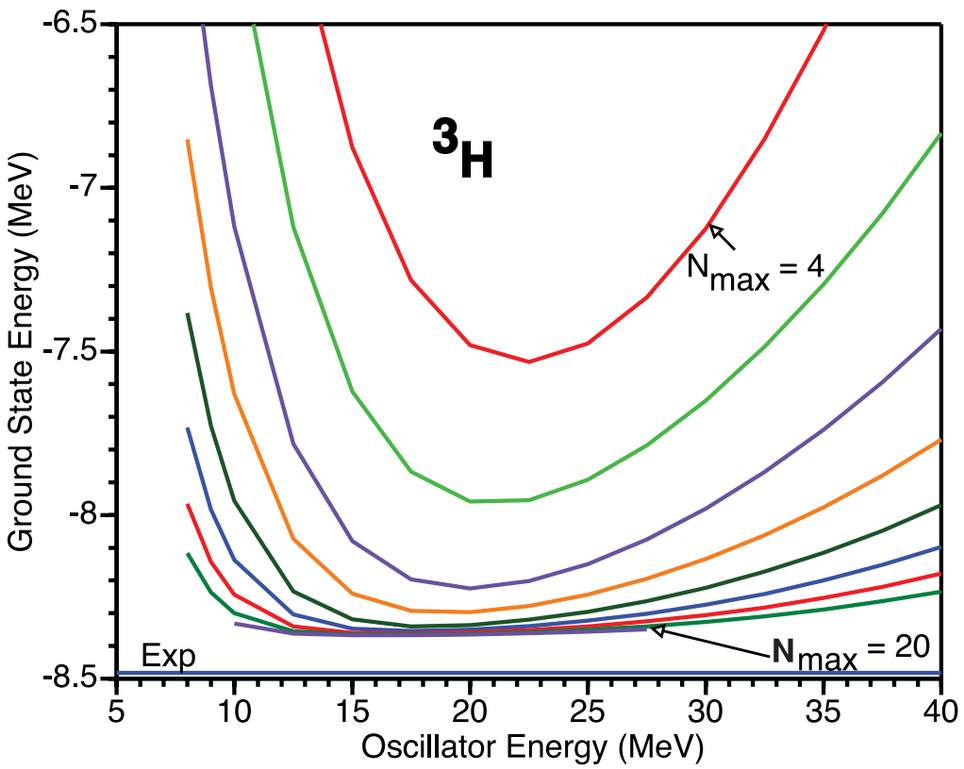

FIG. 10. (Color online) Calculated ground-state energy of ^{3}H as a function of the oscillator energy, $\hbar\Omega$, for selected values of N_{max}. The curve closest to experiment corresponds to the value $N_{max} = 20$ and successively higher curves are obtained with N_{max} decreased by two units for each curve.

R. Roth, Phys. Rev C 79 (2009)

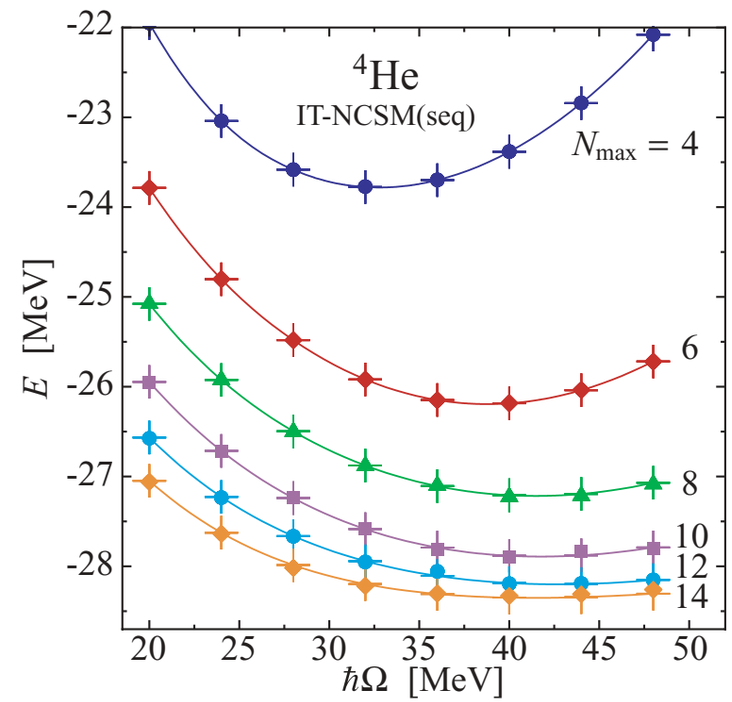

FIG. 7. (Color online) Ground-state energies of ^{4}He obtained for the V_{UCOM} interaction as function of the oscillator frequency $\hbar\Omega$ for different $N_{max}\hbar\Omega$ model spaces. Results of IT-NCSM(seq) calculations (solid symbols) are compared with full NCSM calculations (crosses).

Effects of deformation on the convergence

Example:

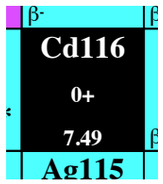

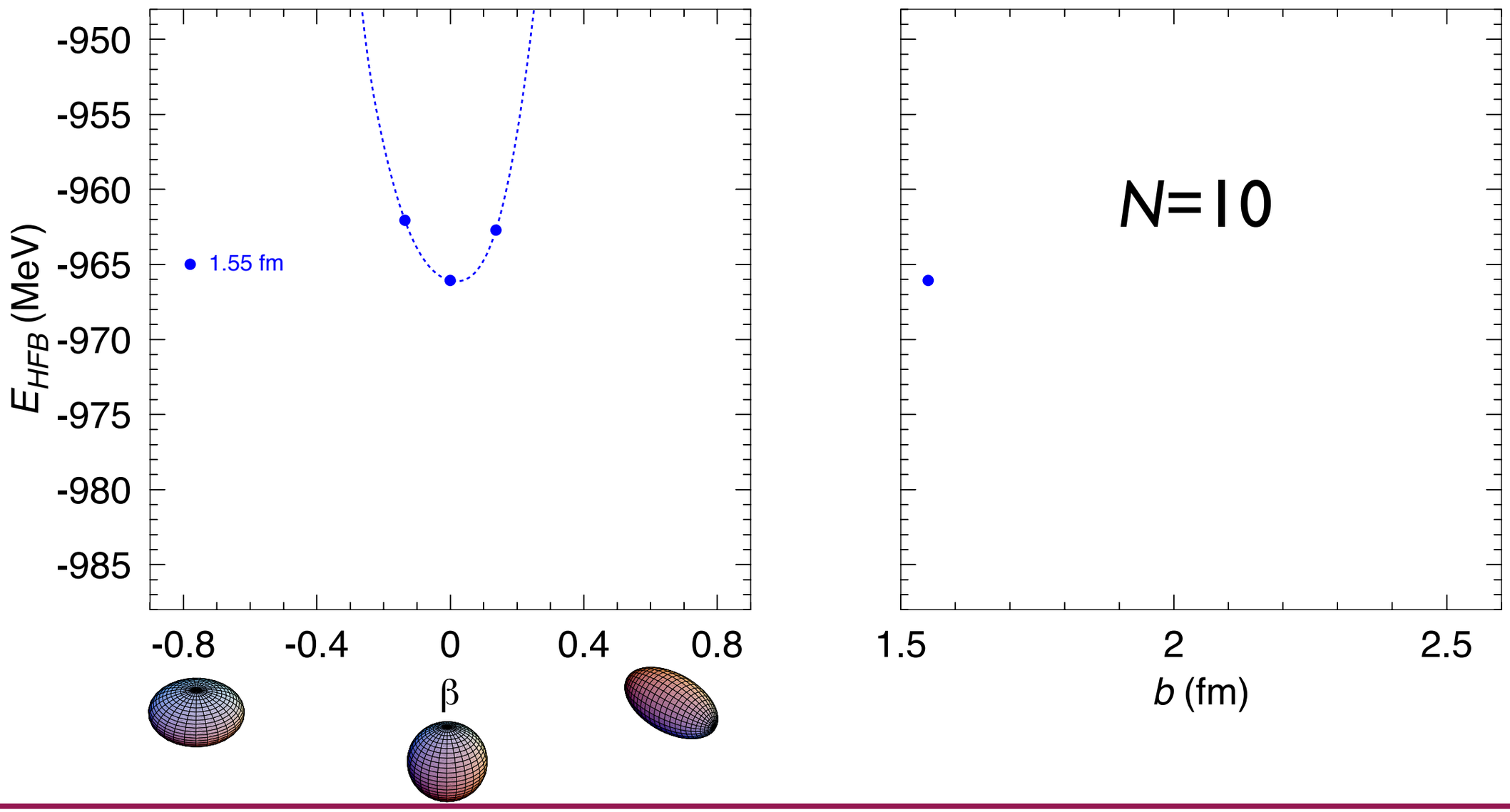

Effects of deformation on the convergence

Example:

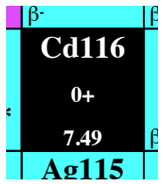

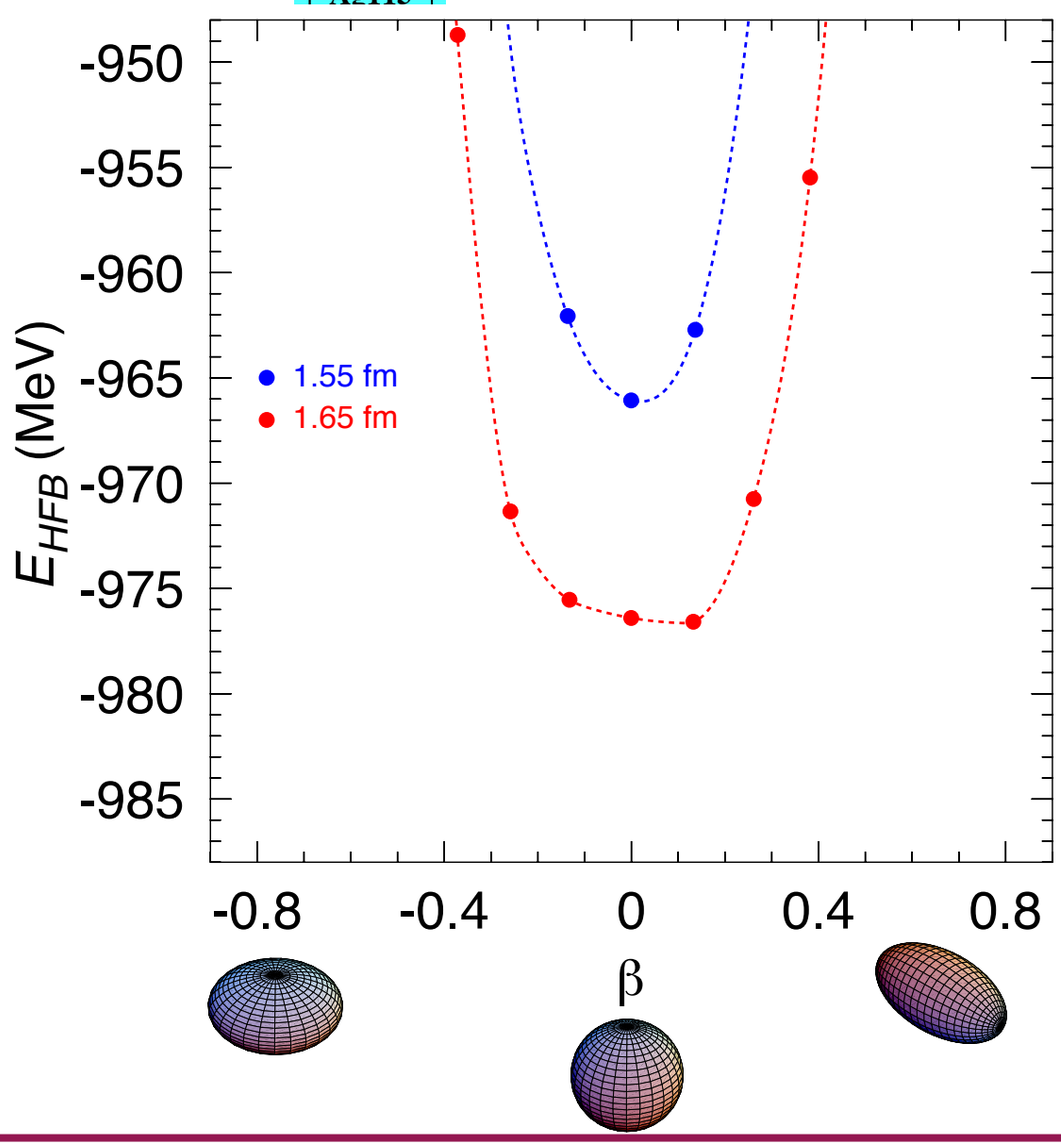

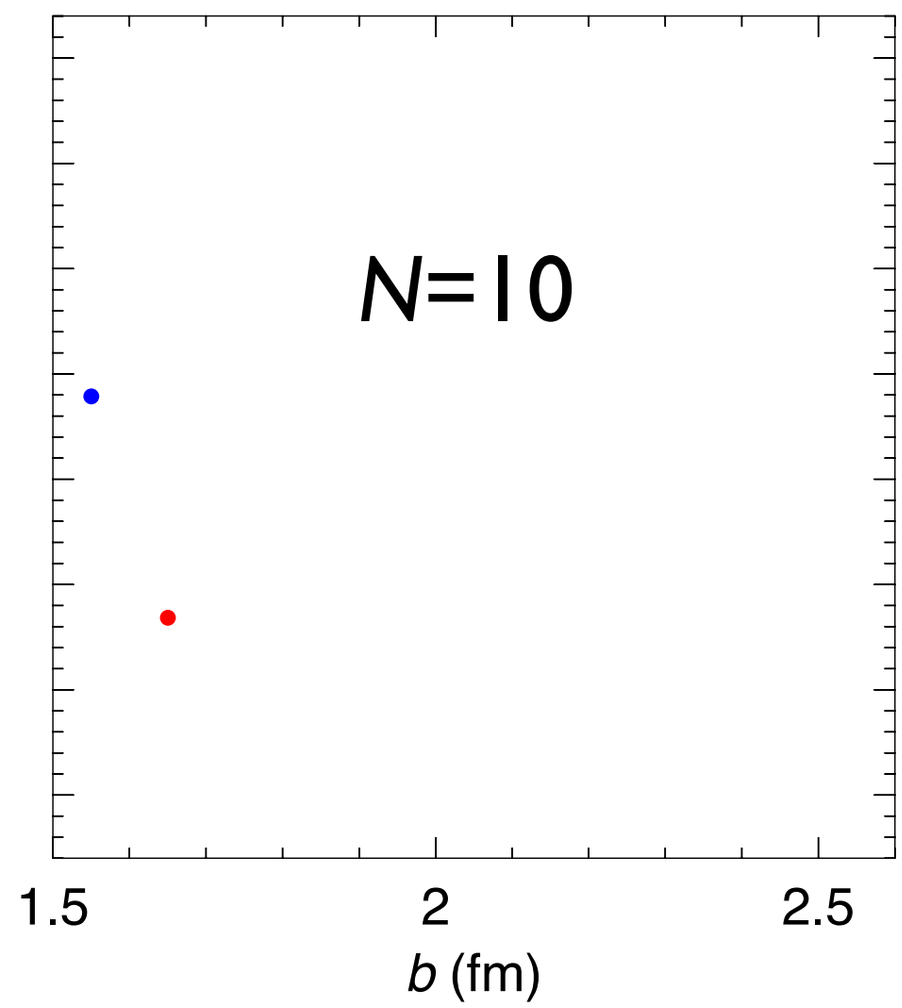

Effects of deformation on the convergence

Example:

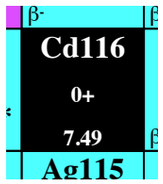

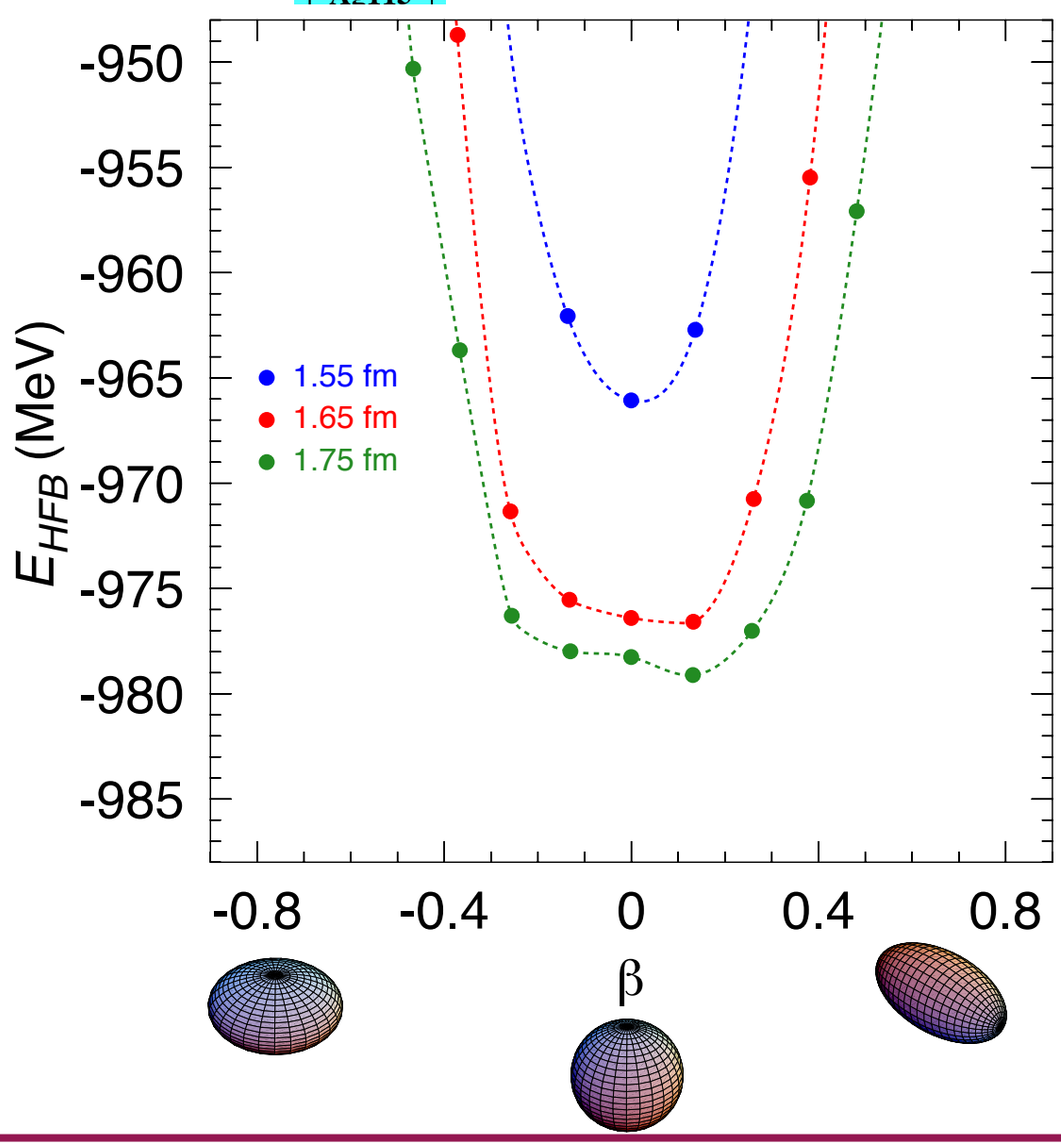

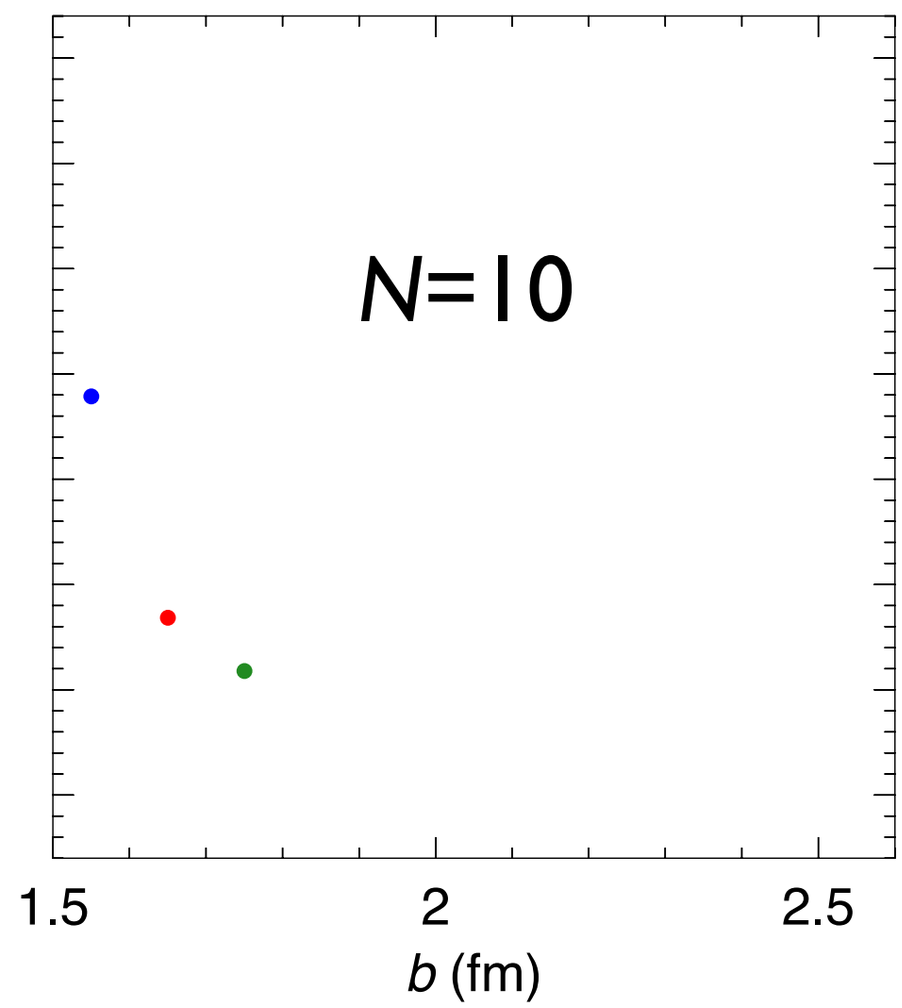

Effects of deformation on the convergence

Example:

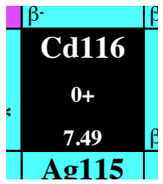

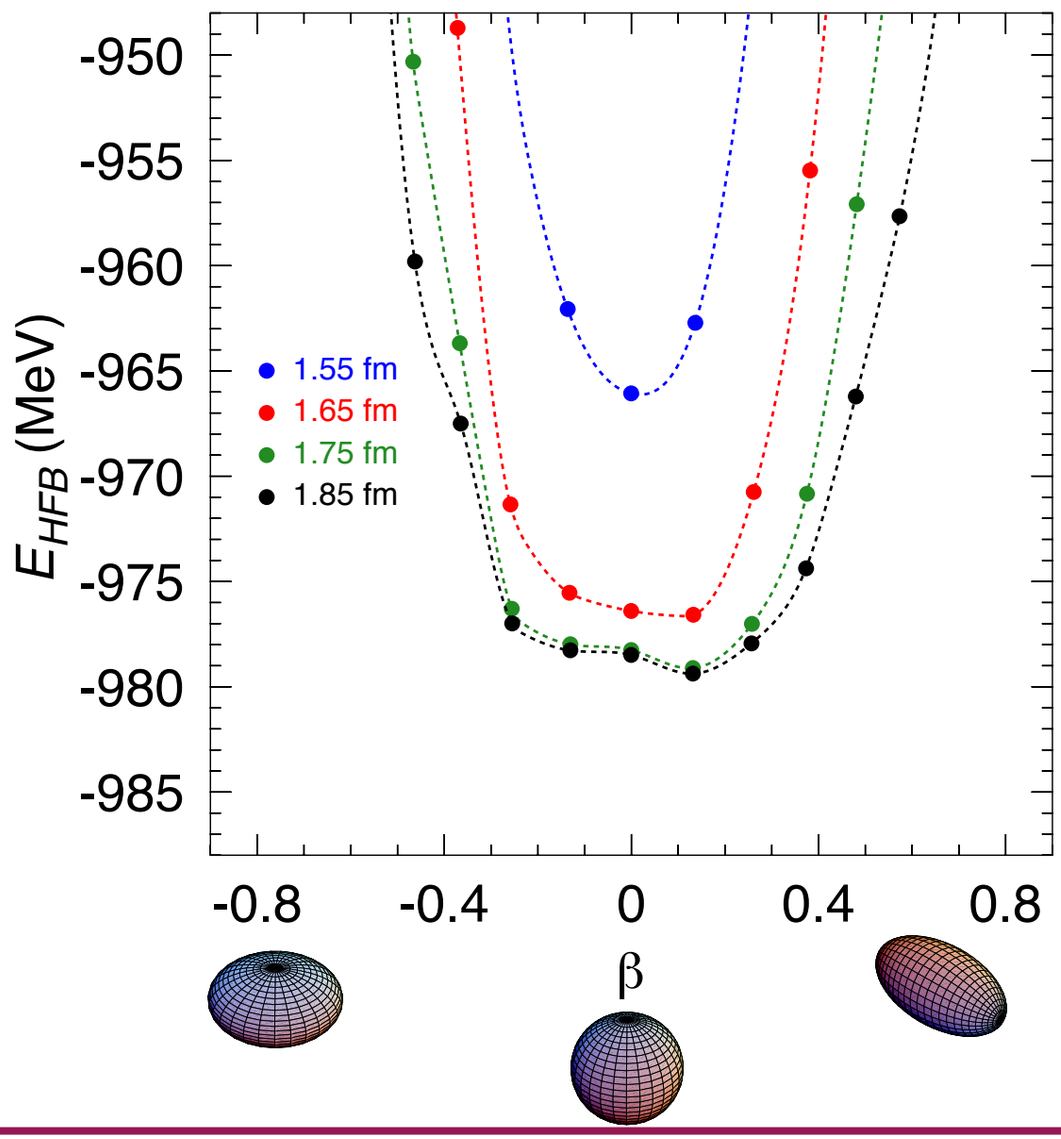

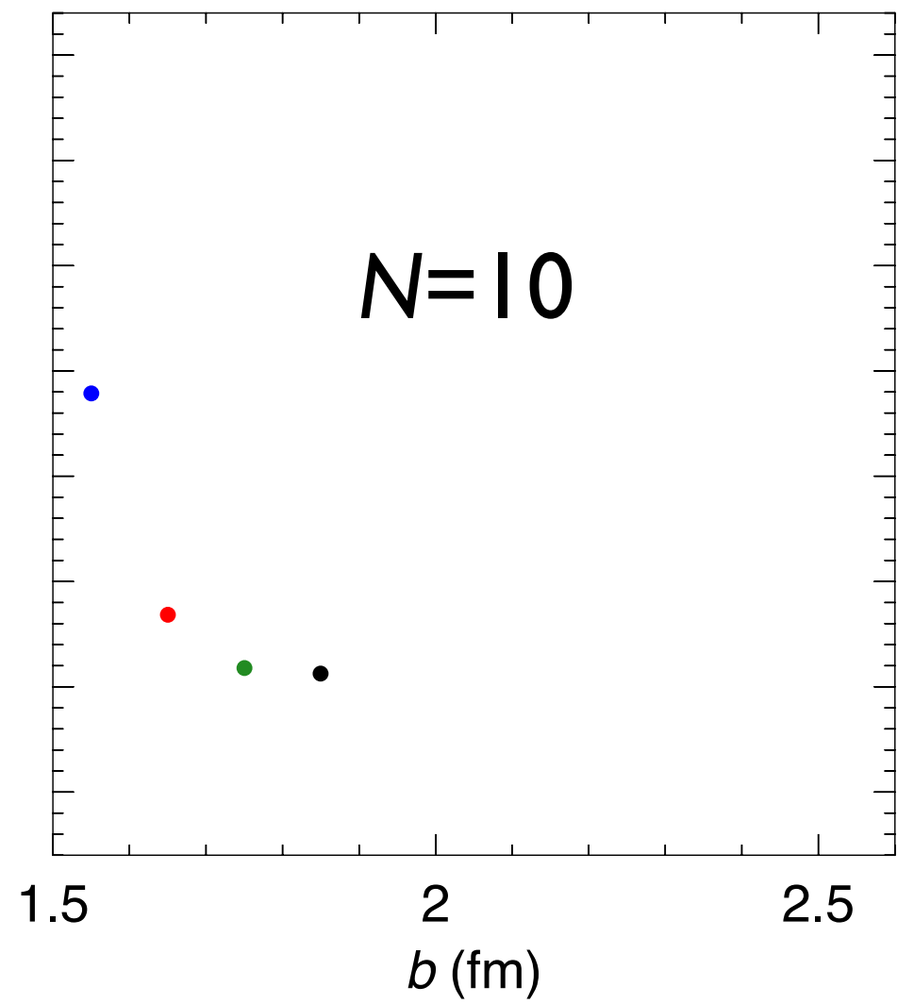

Effects of deformation on the convergence

Example:

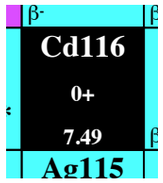

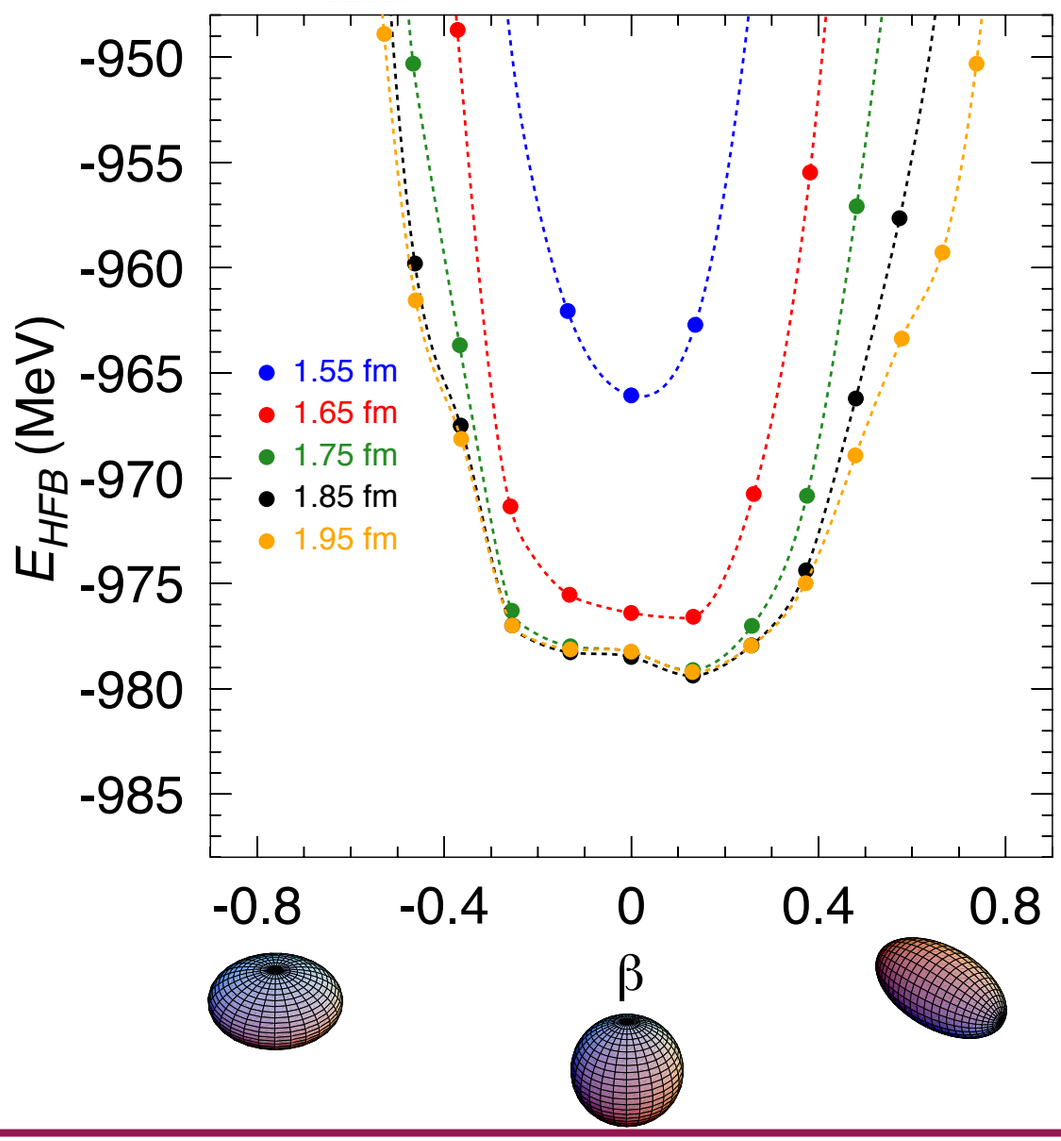

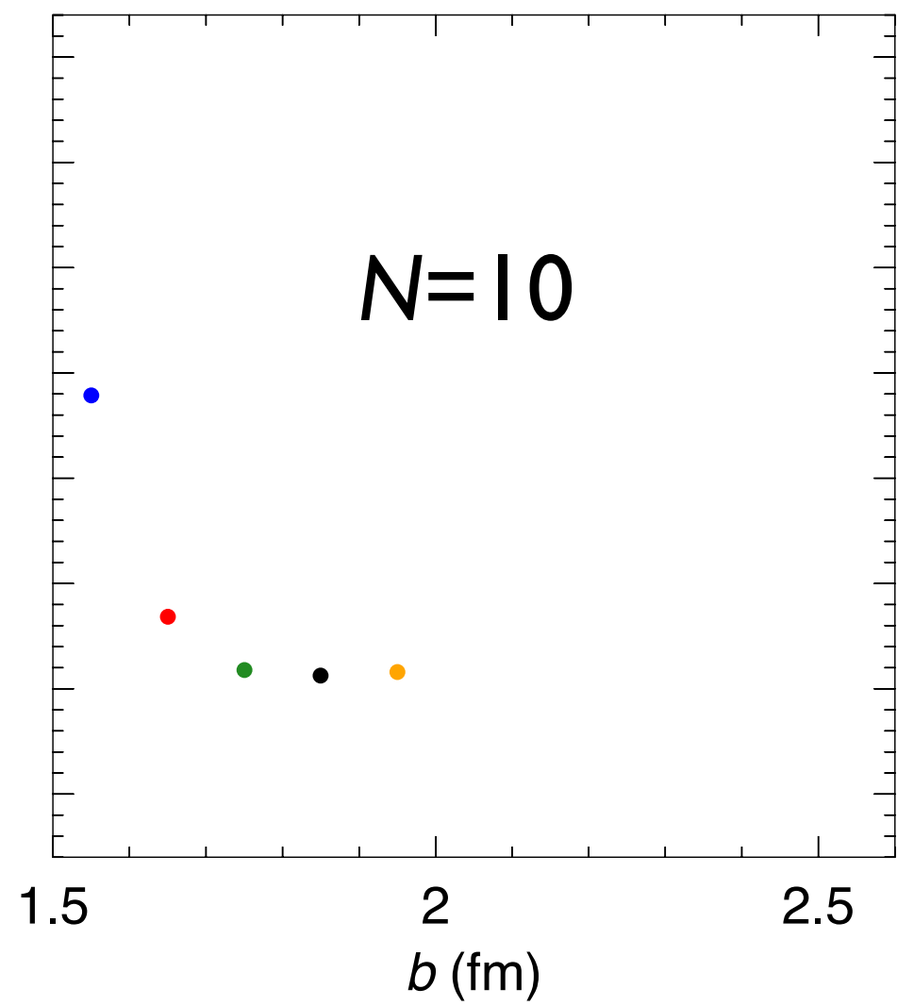

Effects of deformation on the convergence

Example:

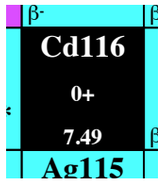

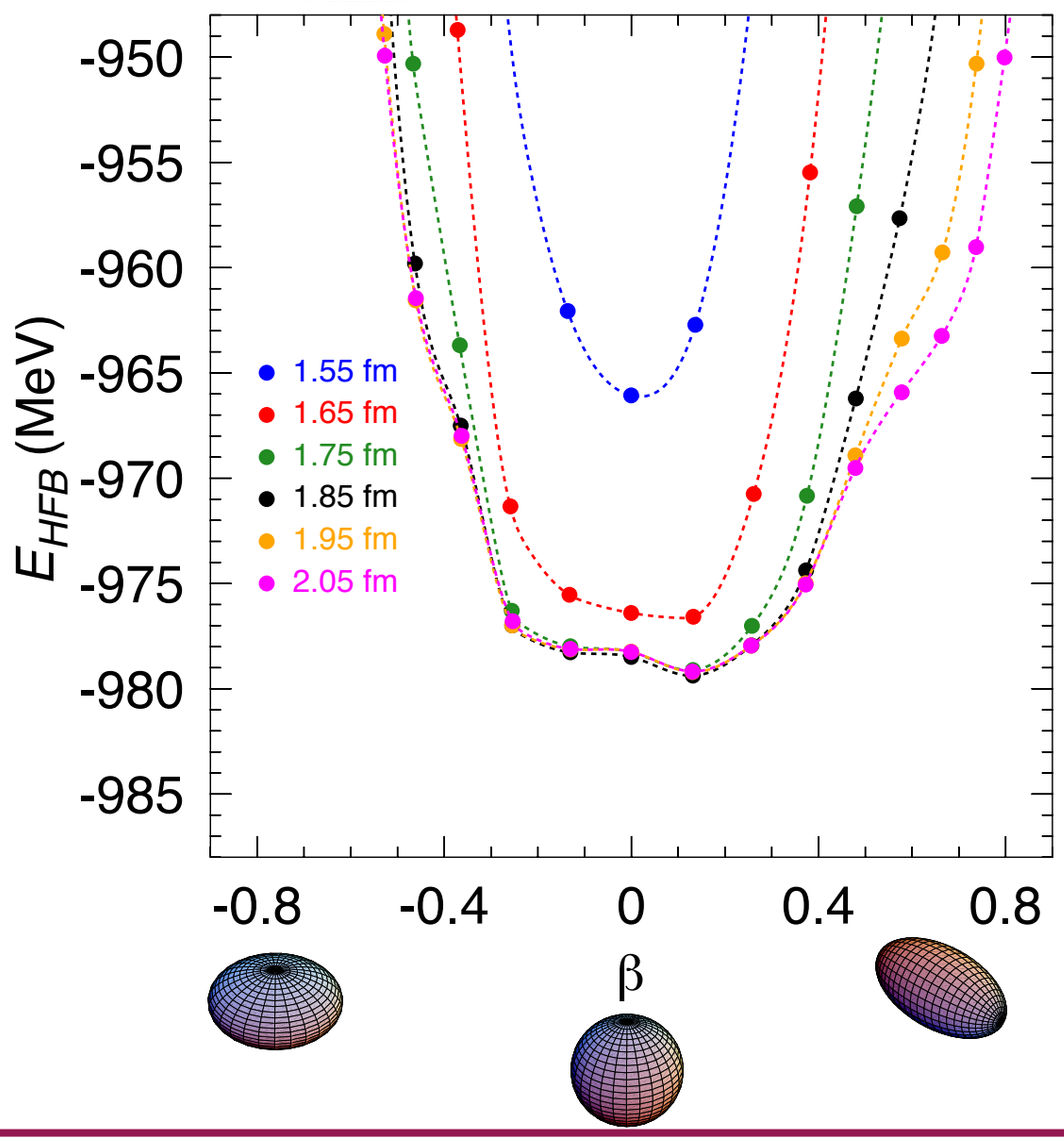

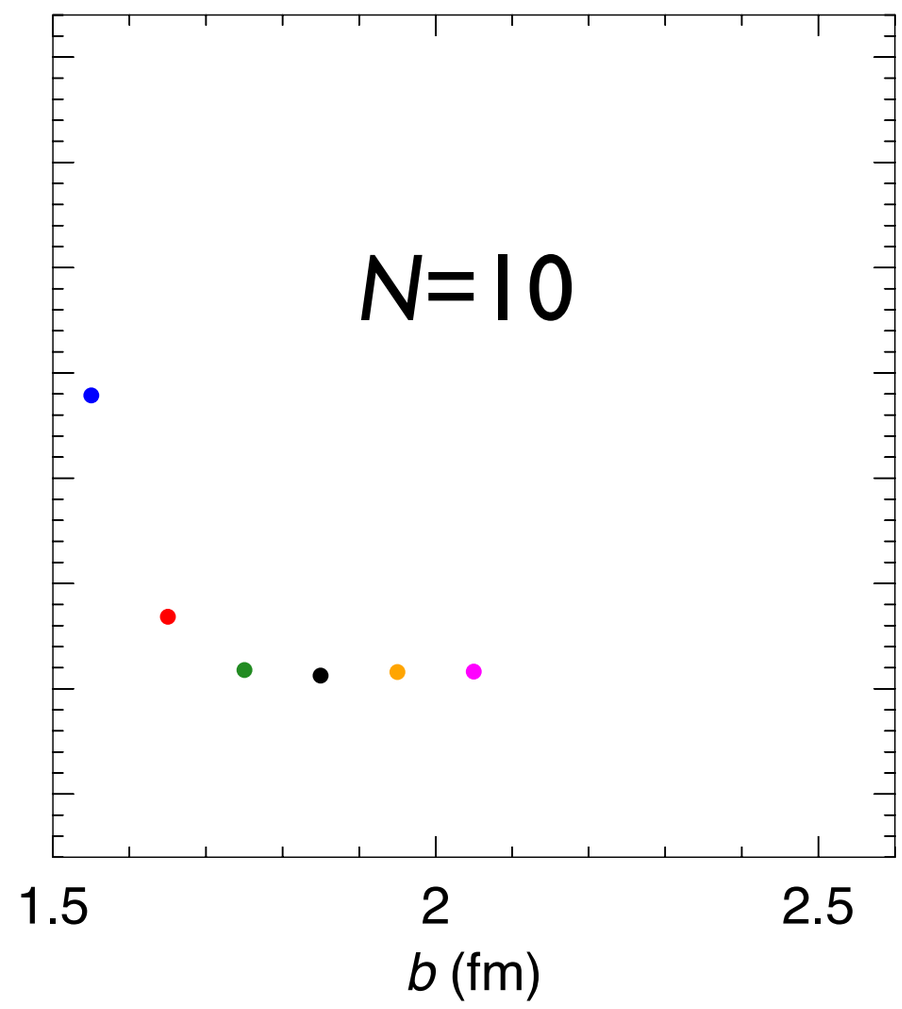

Effects of deformation on the convergence

Example:

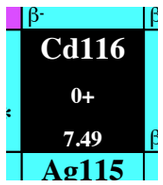

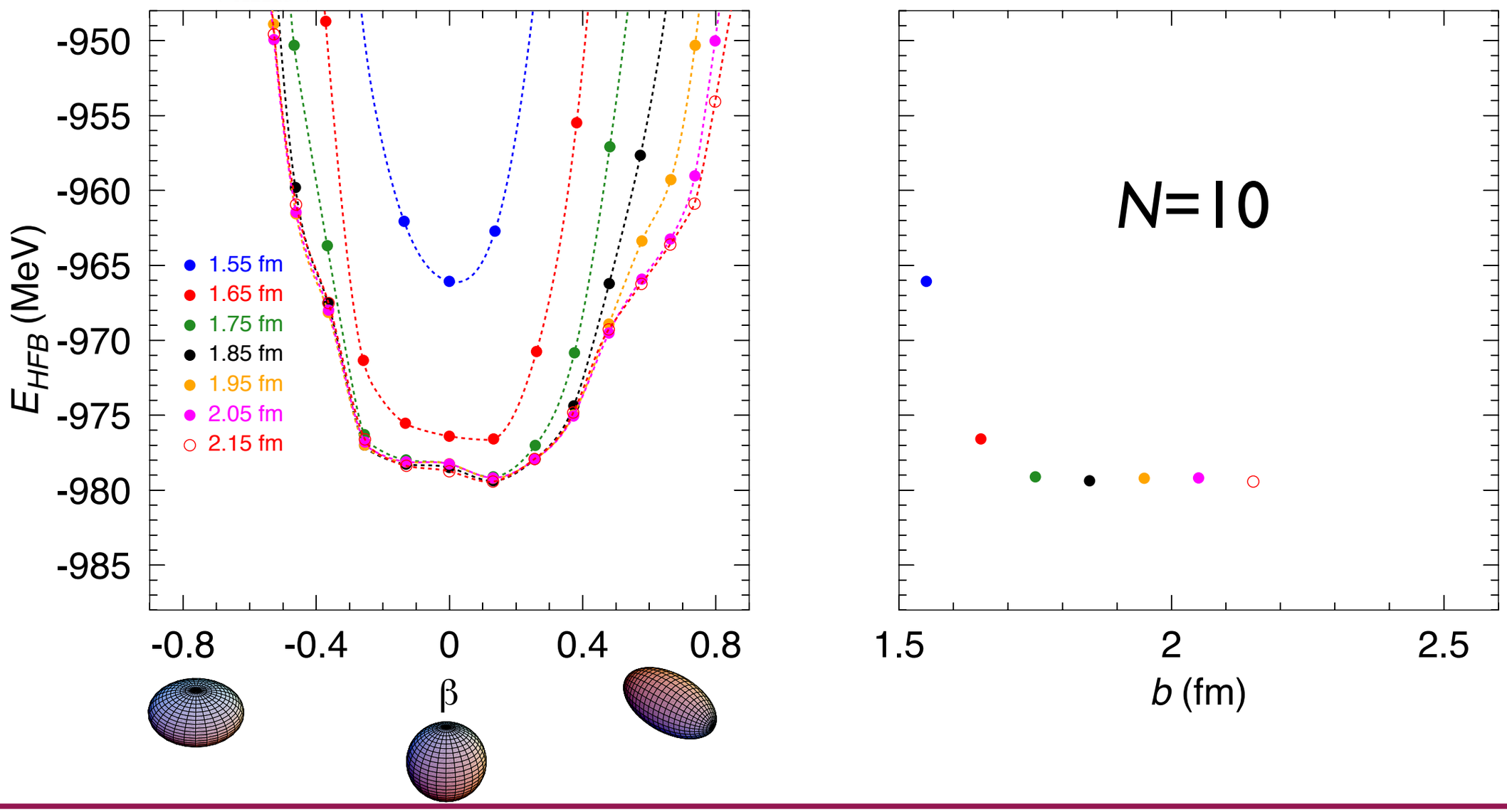

Effects of deformation on the convergence

Example:

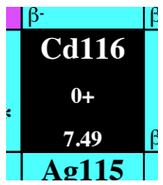

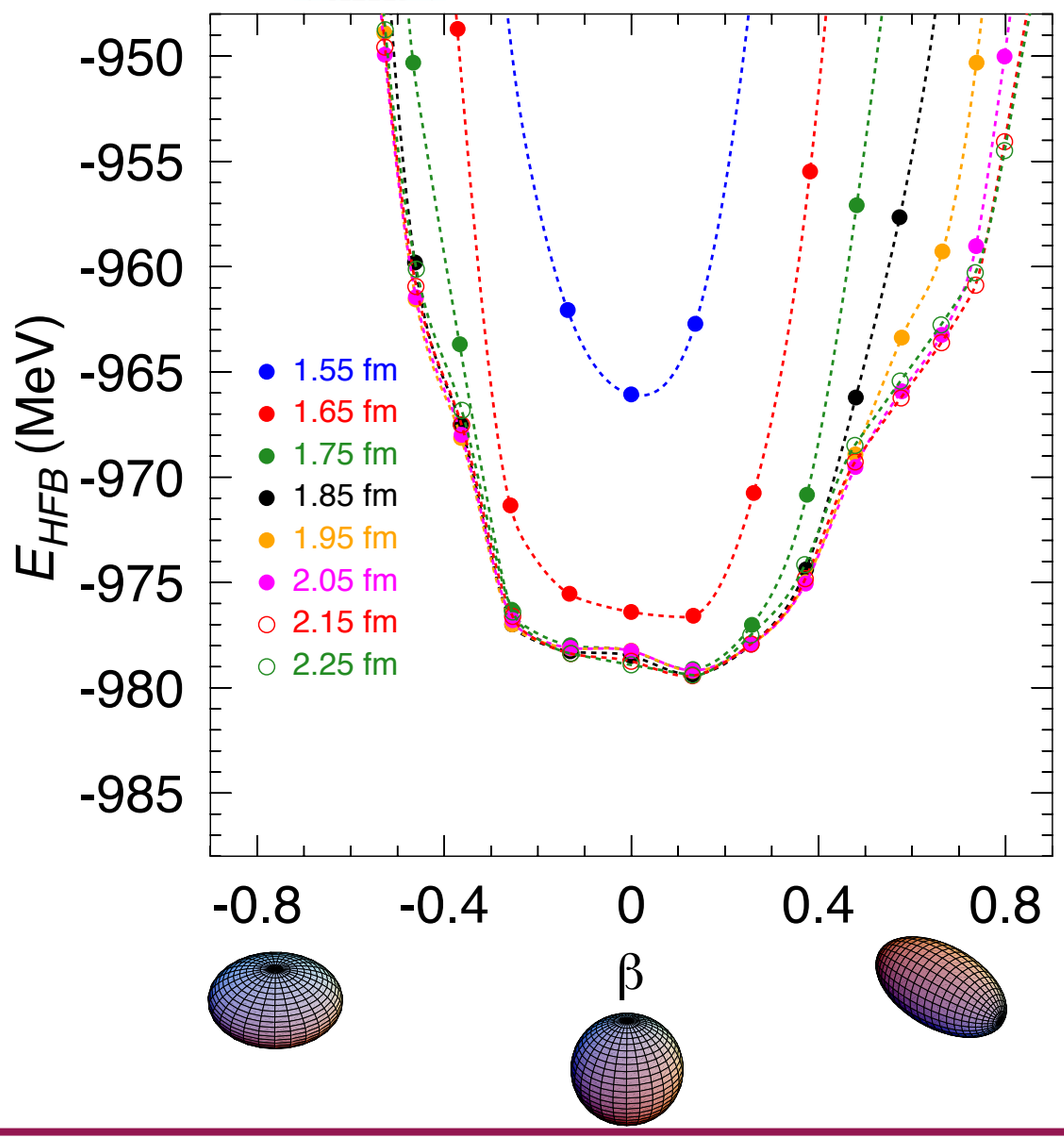

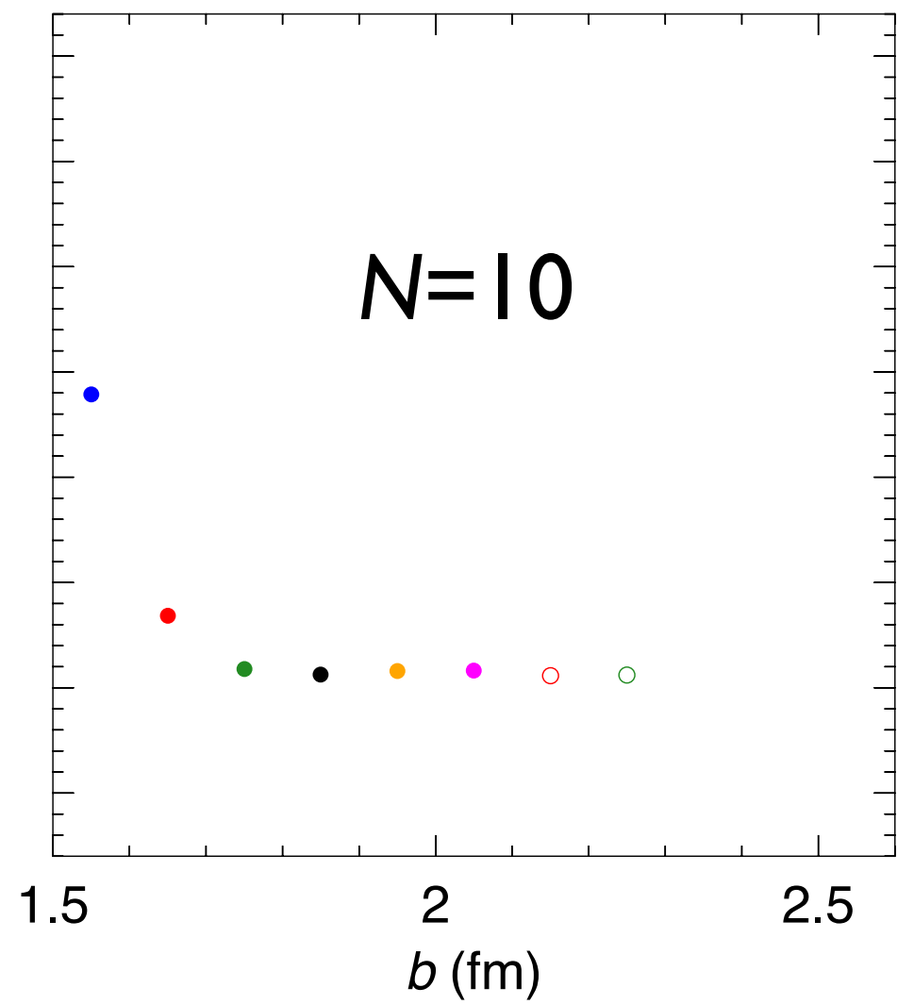

Effects of deformation on the convergence

Example:

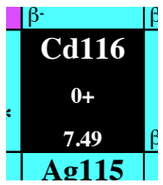

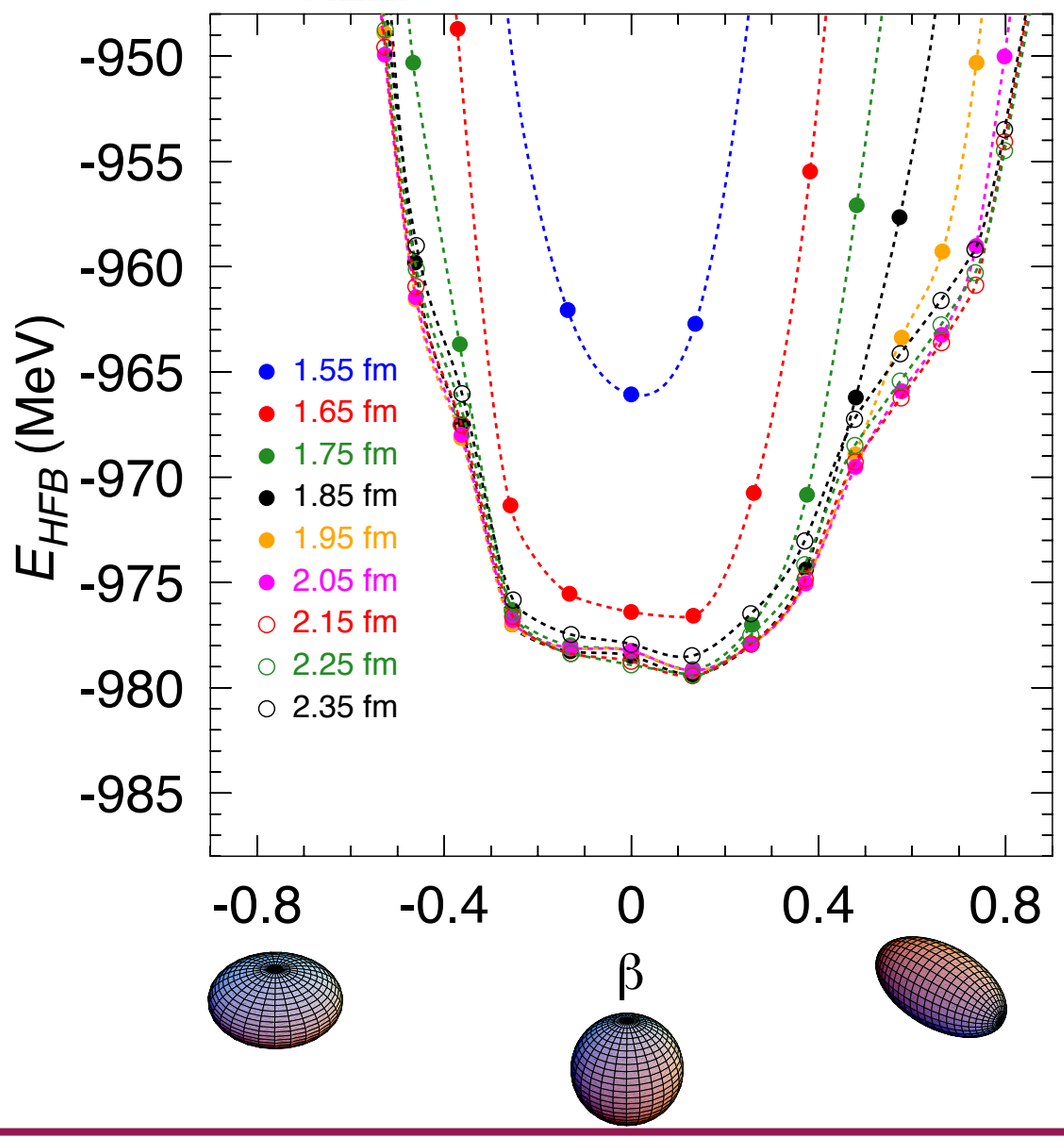

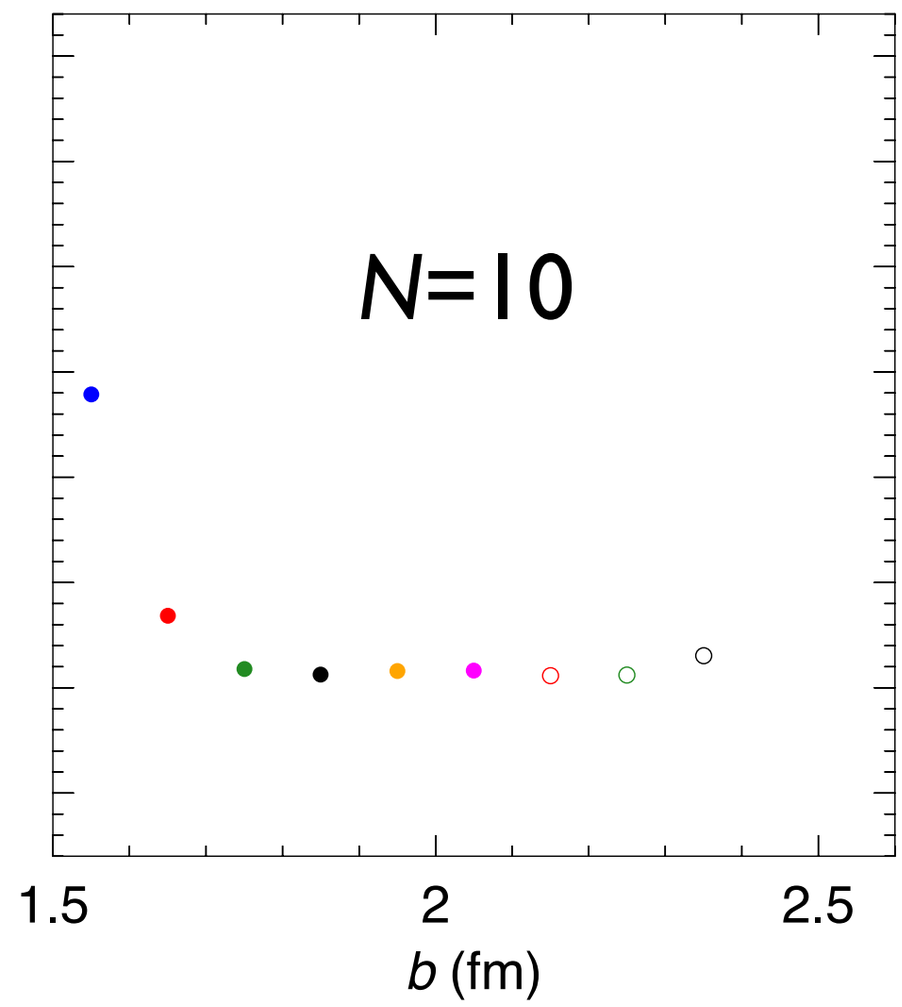

Effects of deformation on the convergence

Example:

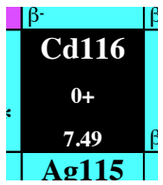

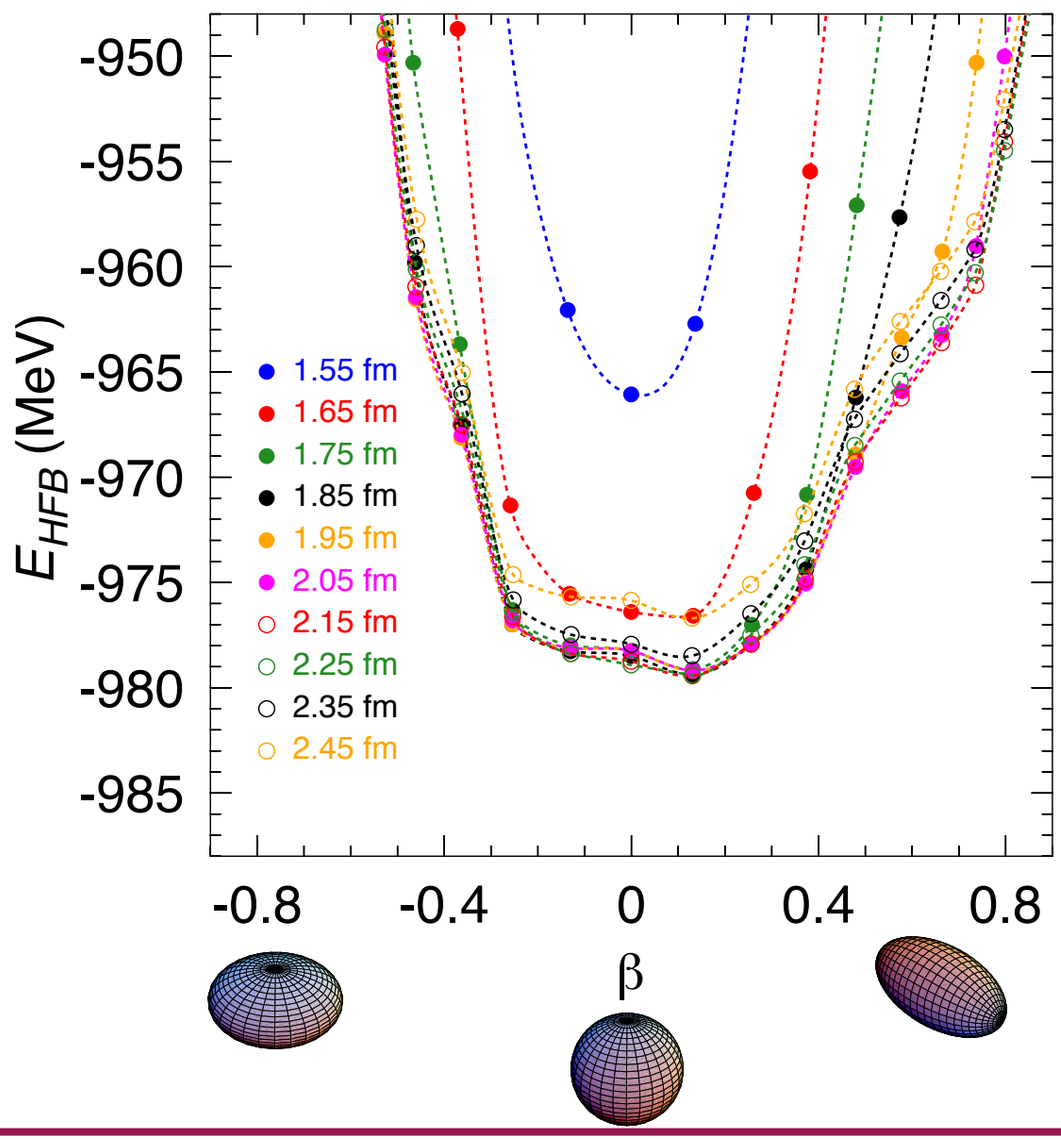

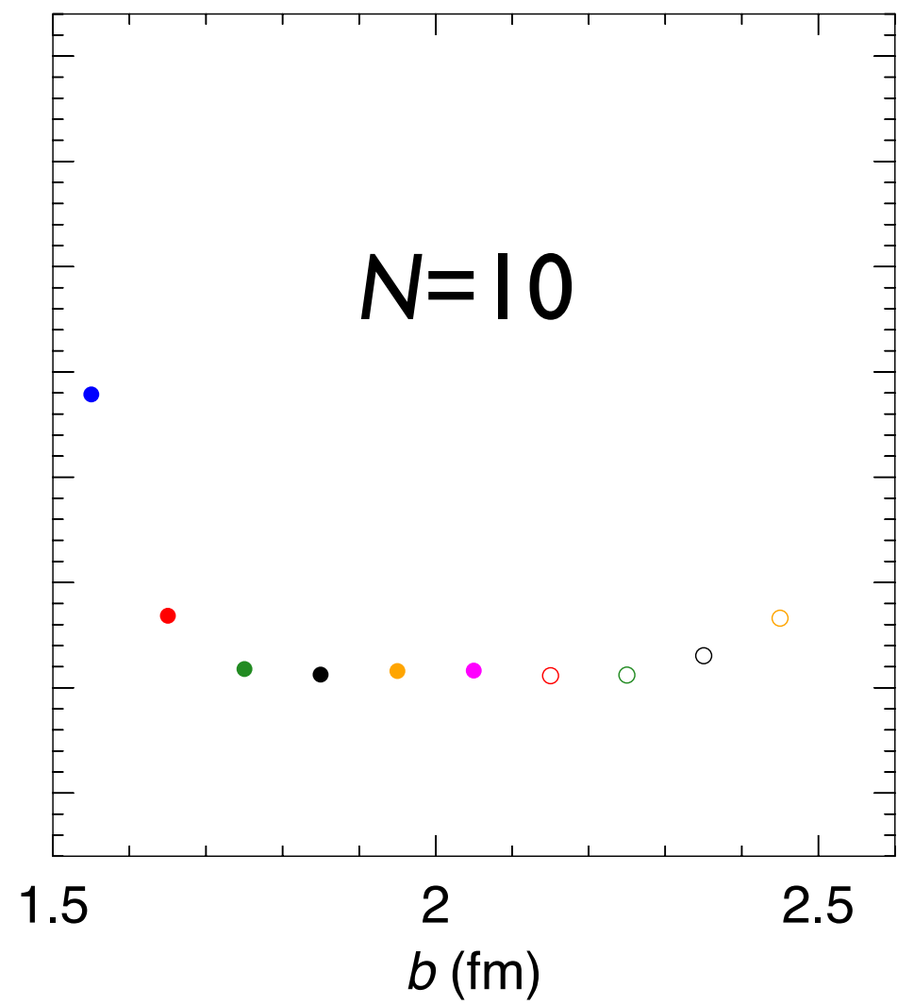

Effects of deformation on the convergence

Example:

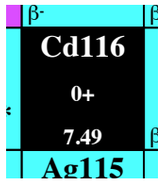

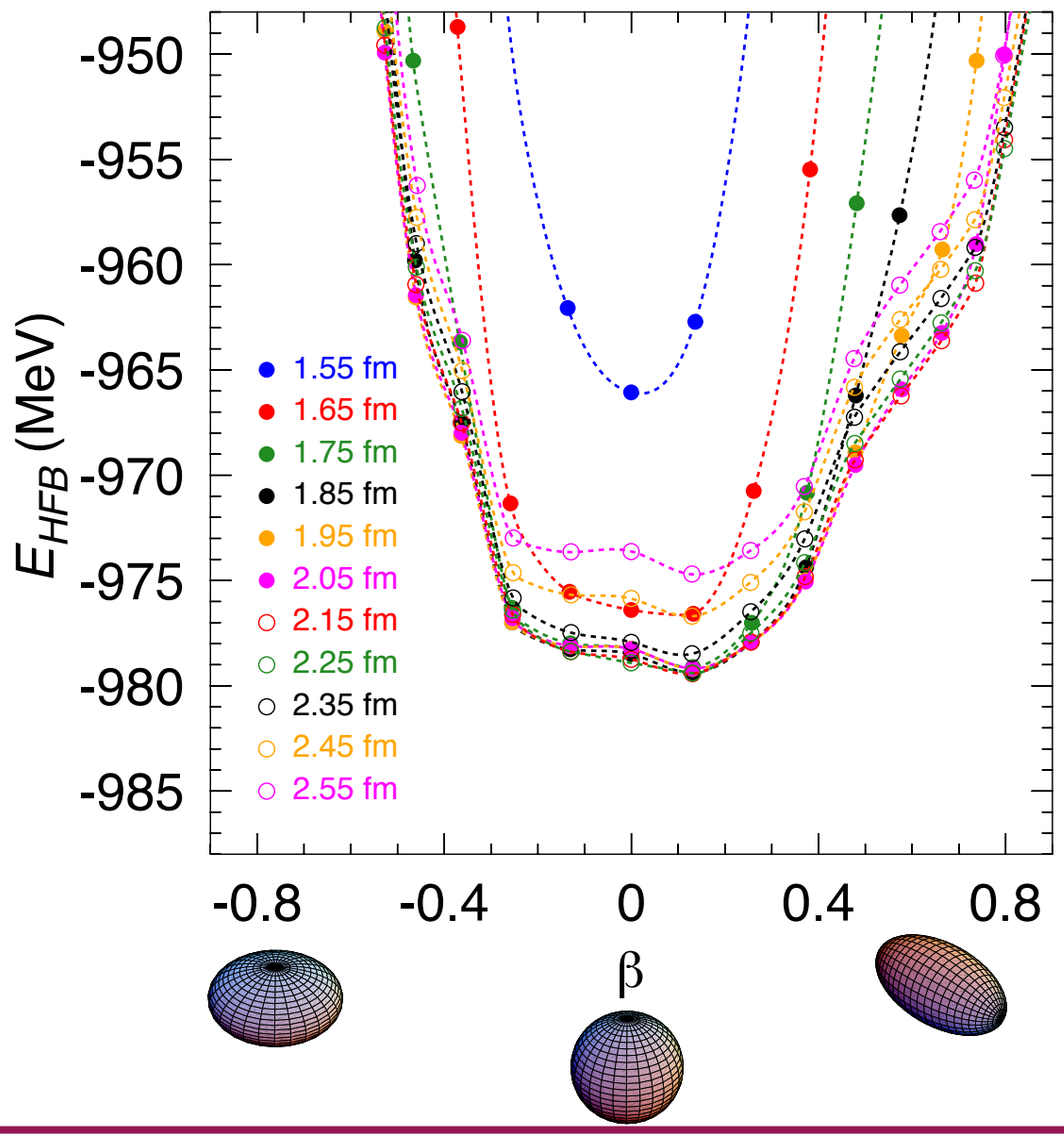

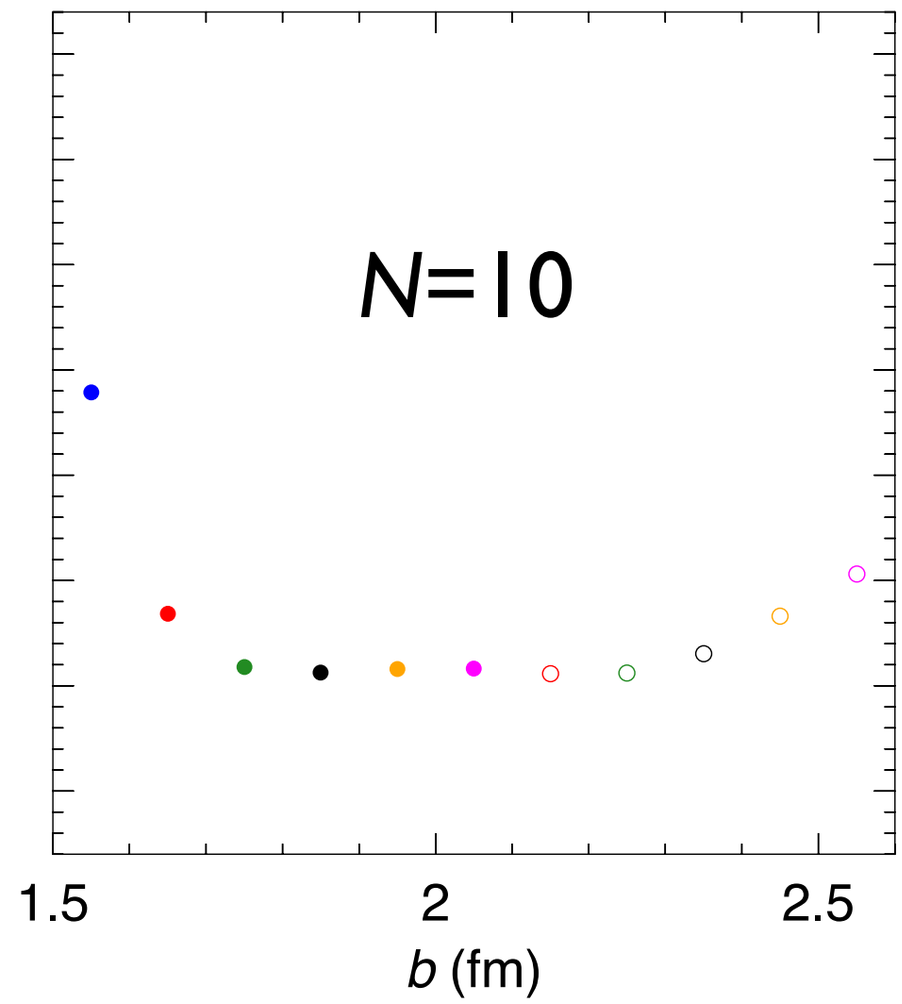

Effects of deformation on the convergence

Example:

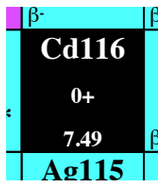

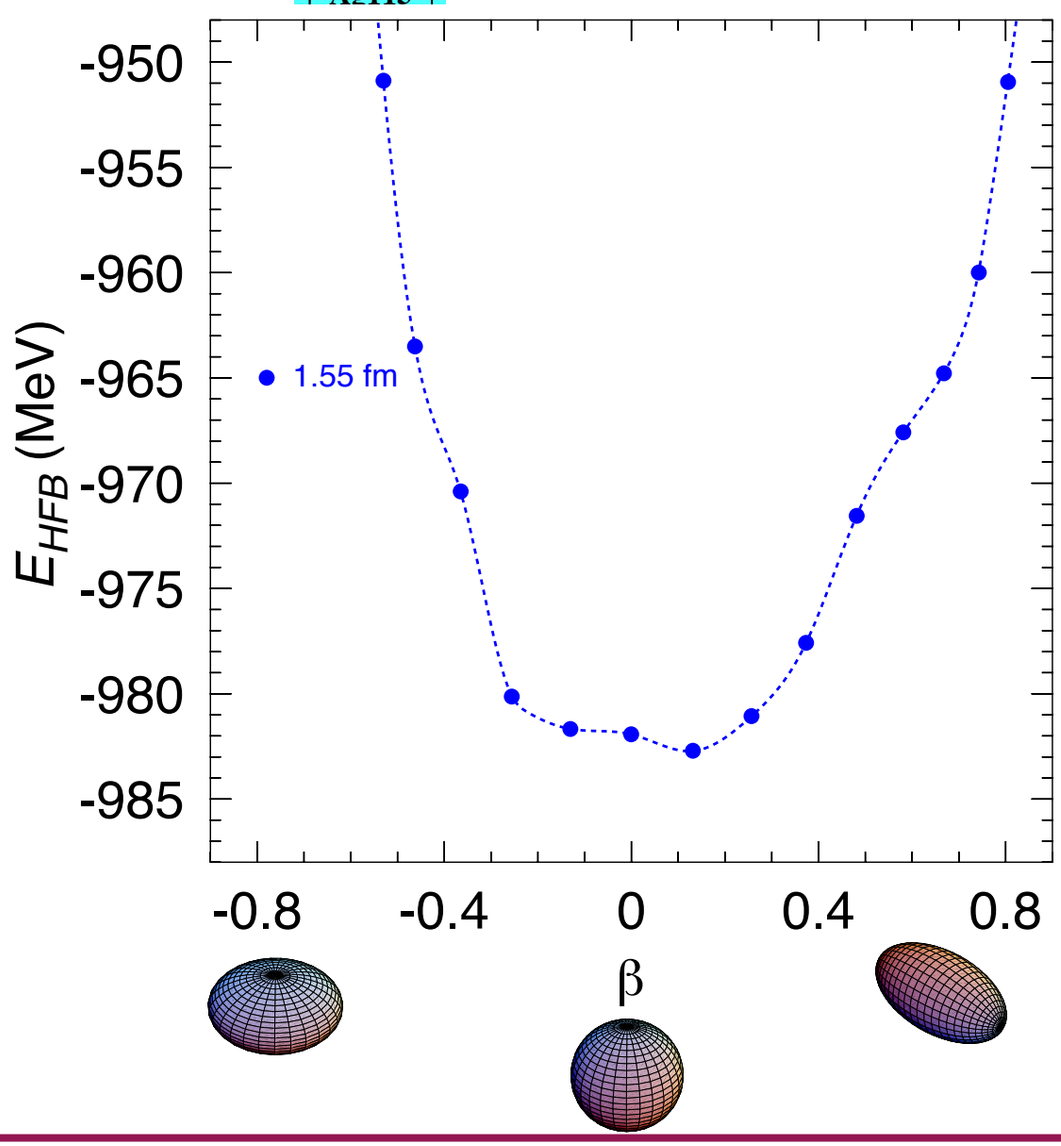

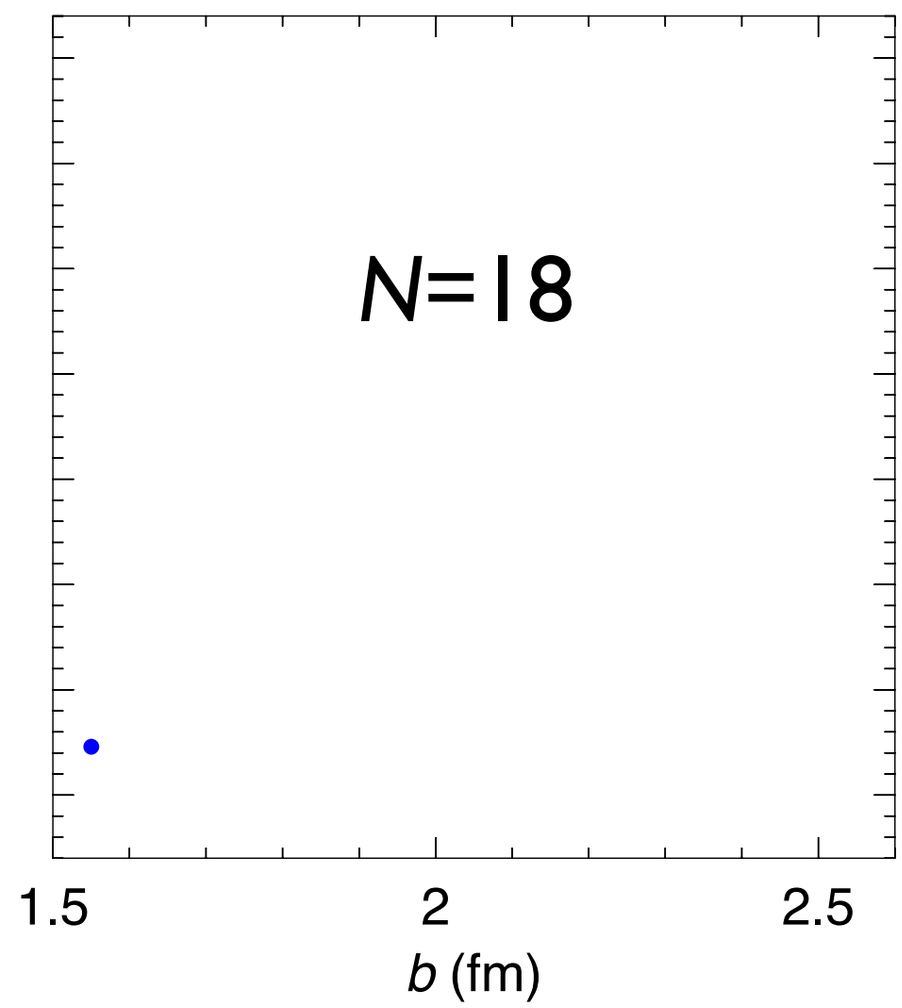

Effects of deformation on the convergence

Example: 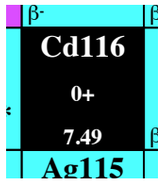

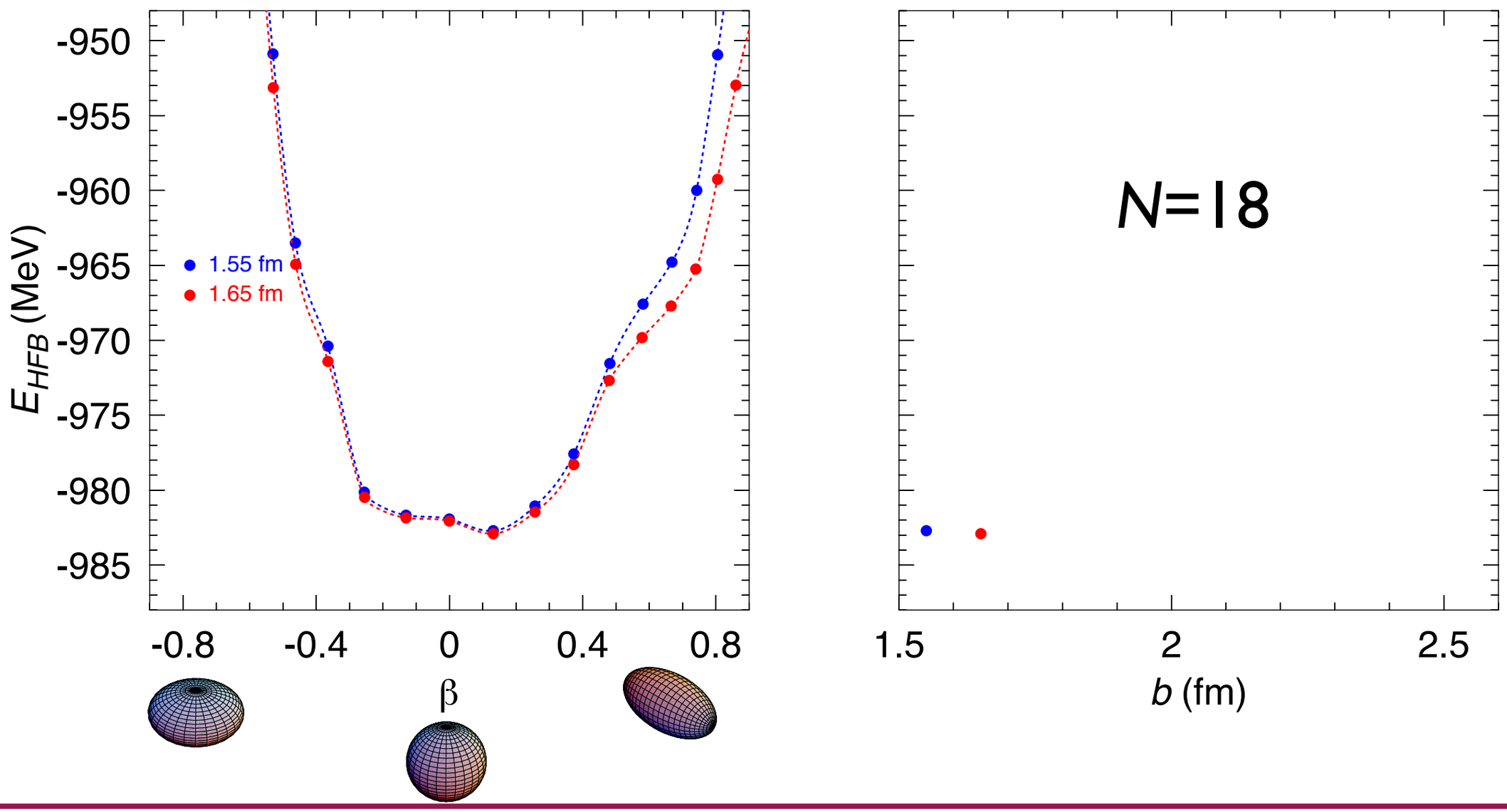

Effects of deformation on the convergence

Example: 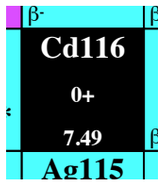

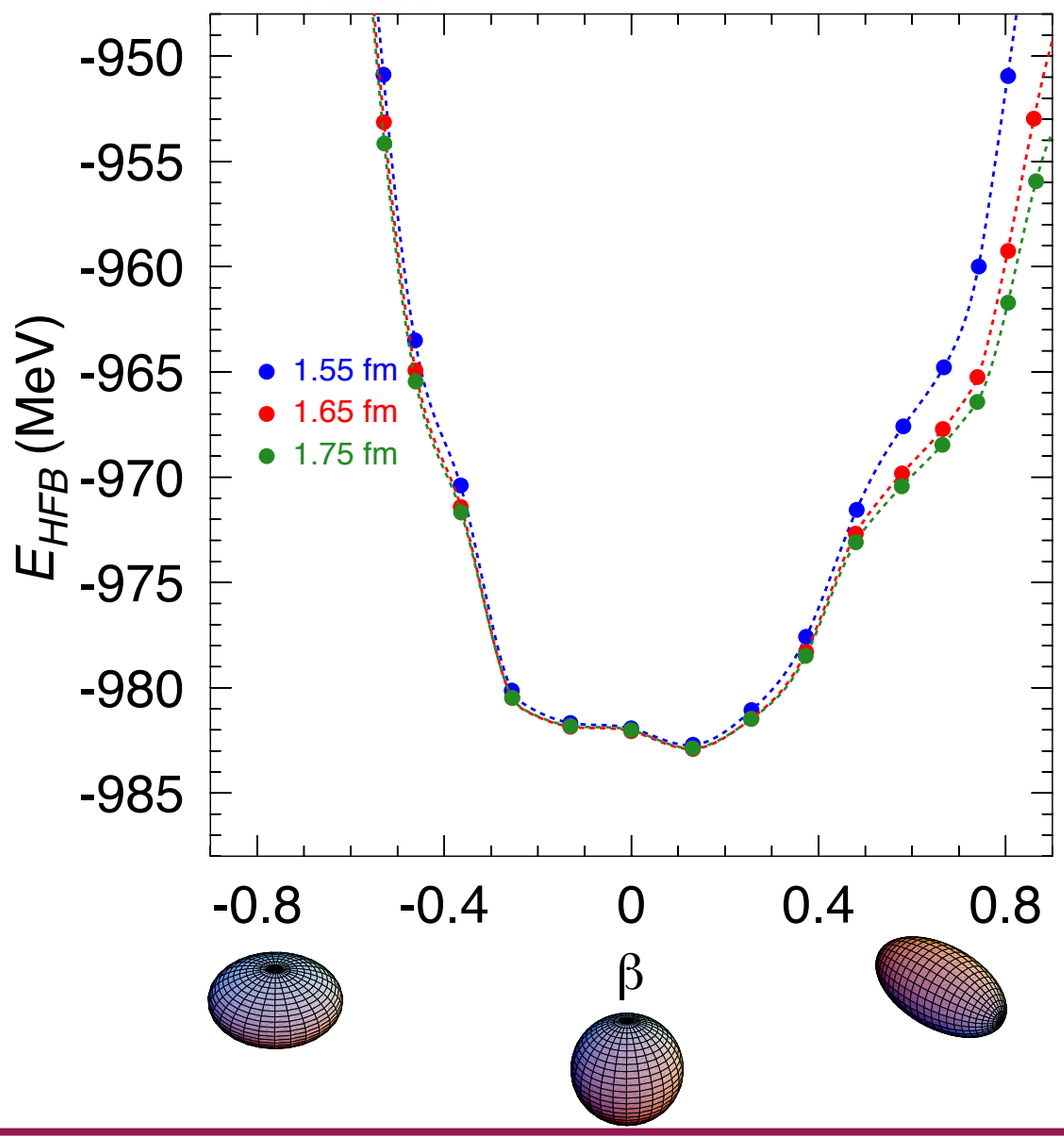

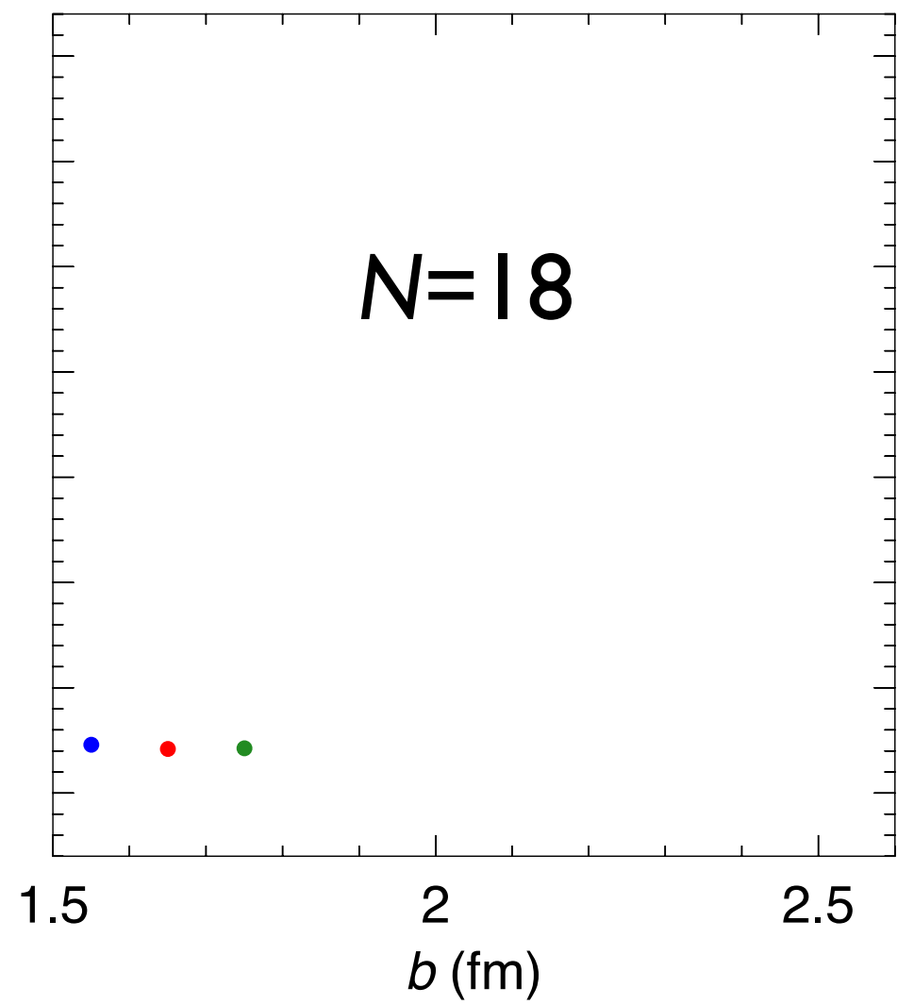

Effects of deformation on the convergence

Example:

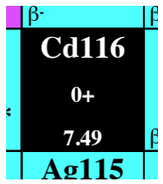

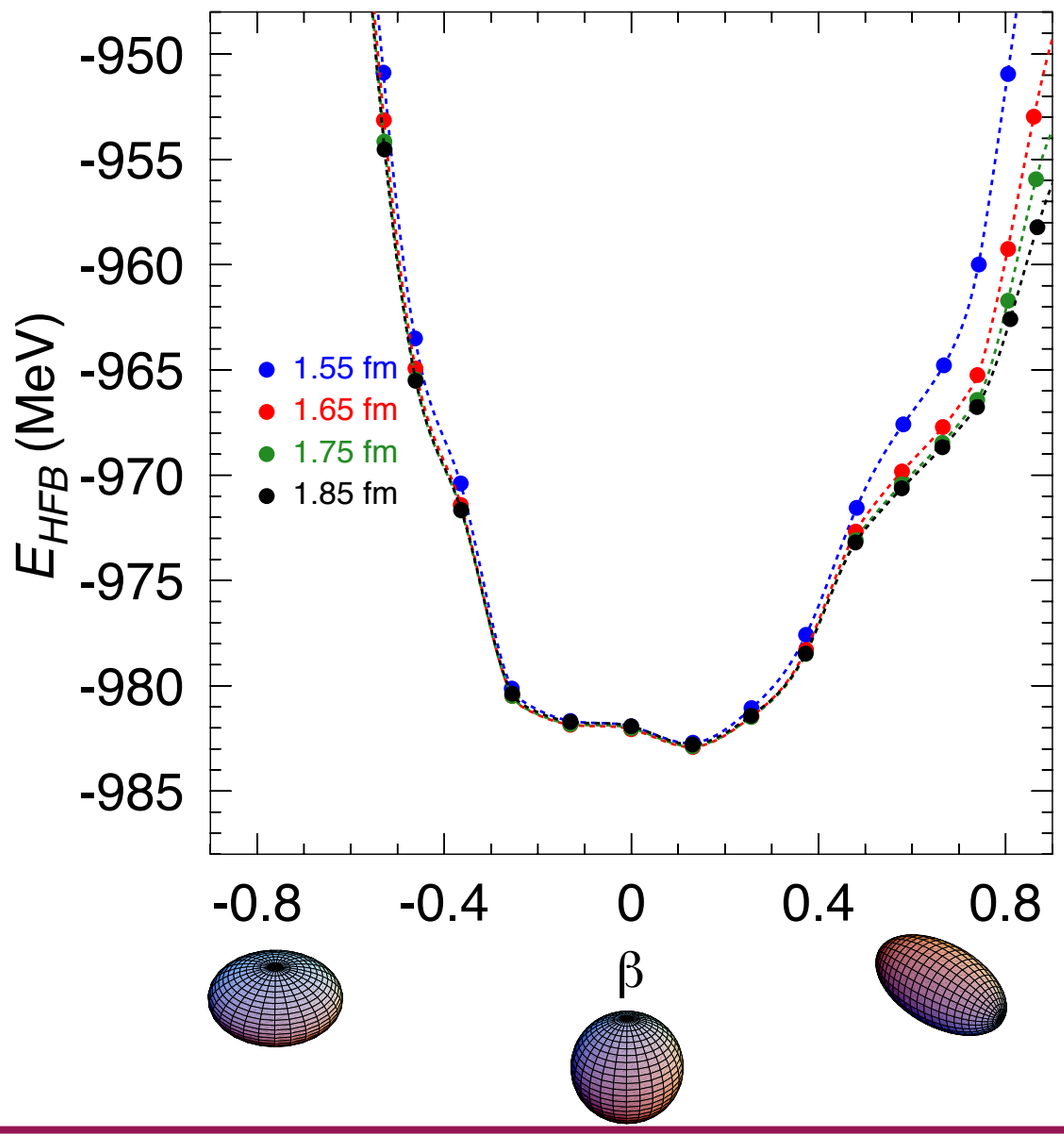

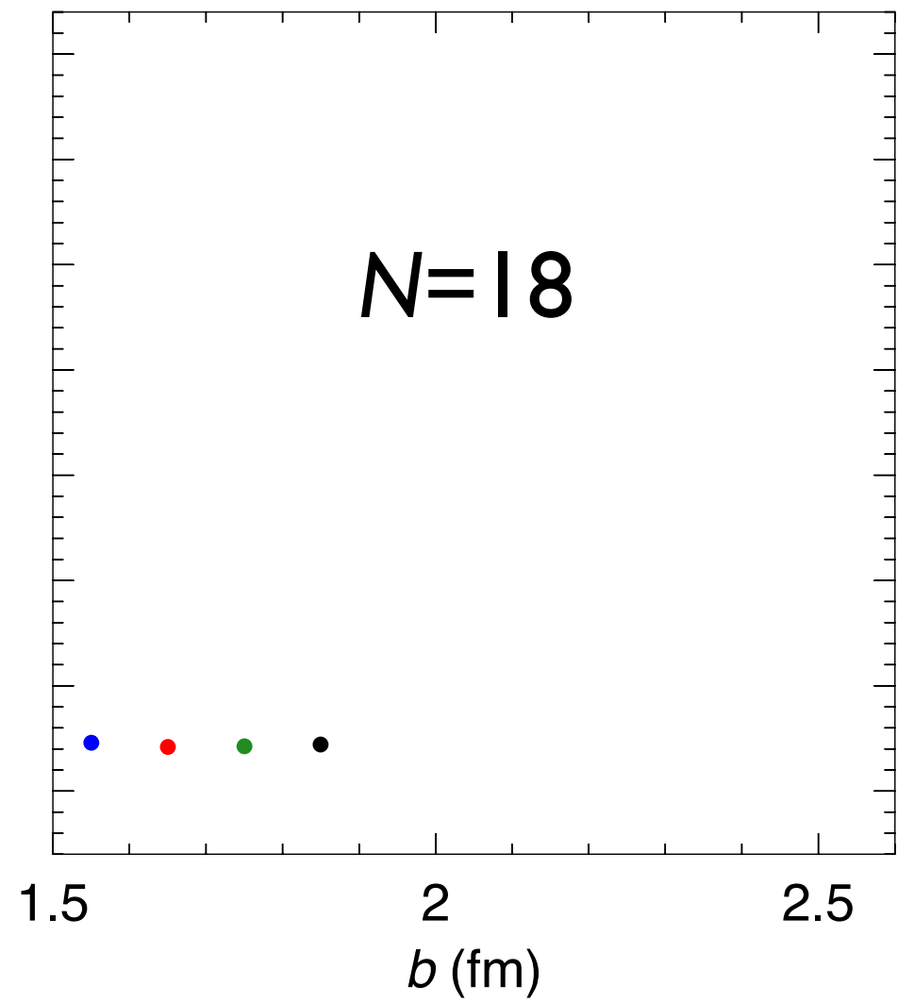

Effects of deformation on the convergence

Example:

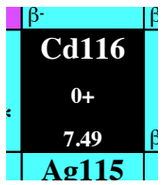

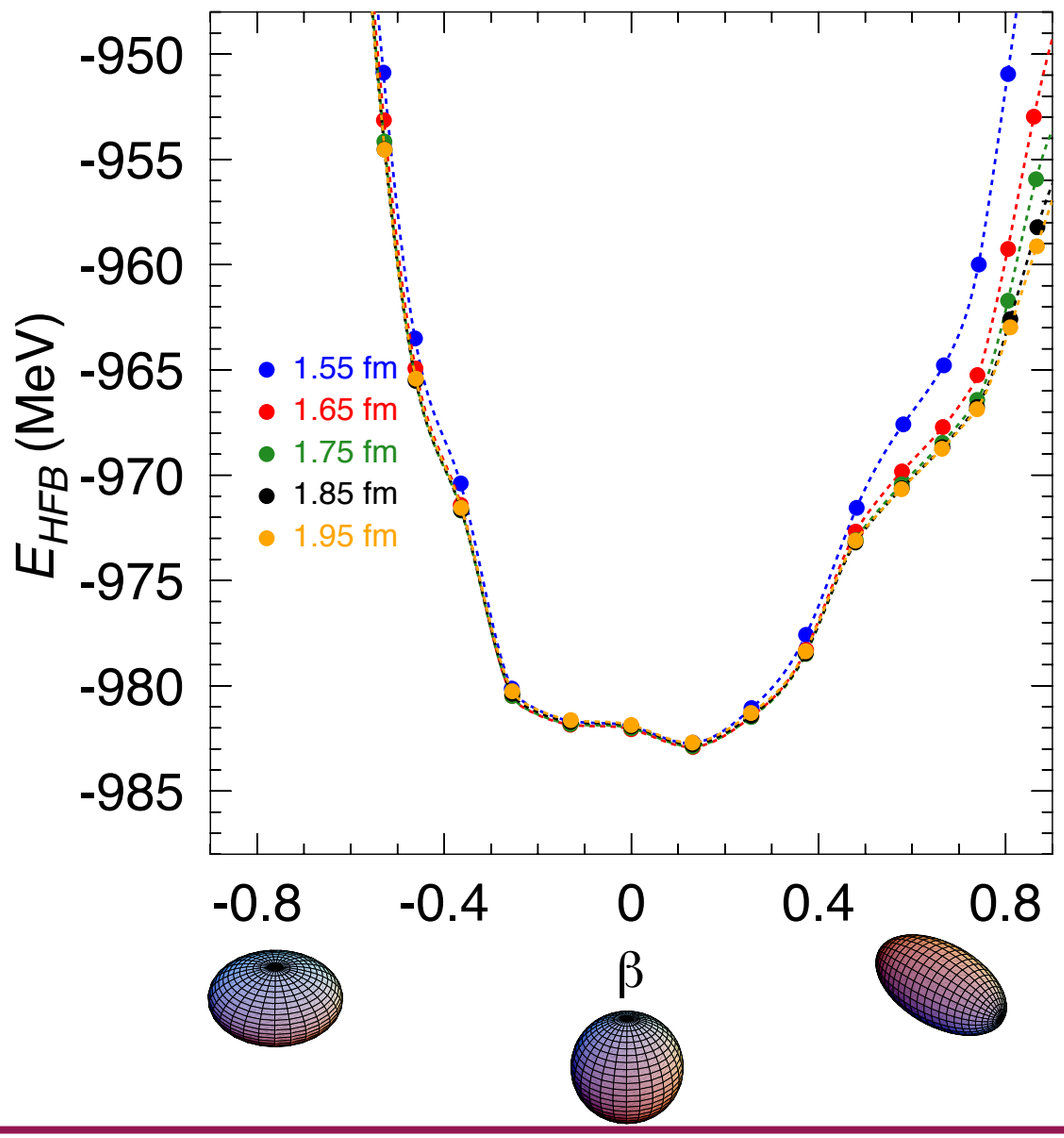

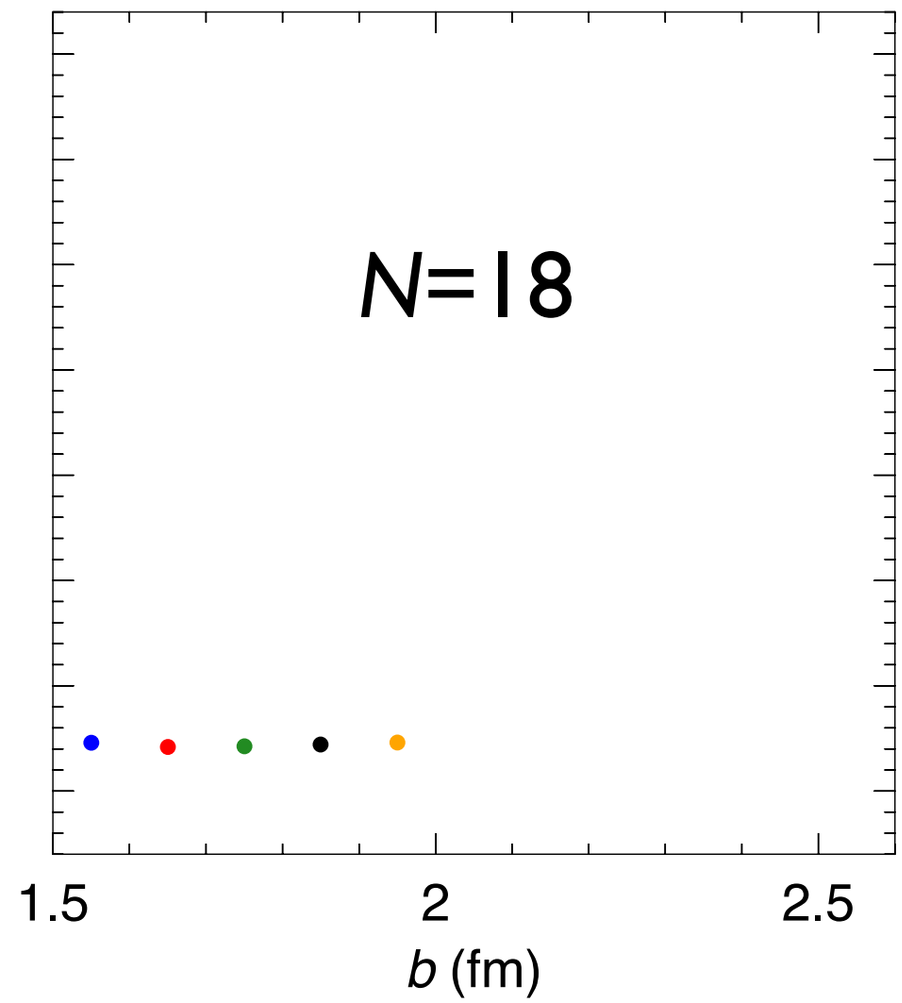

Effects of deformation on the convergence

Example:

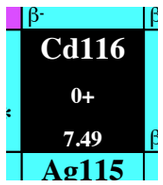

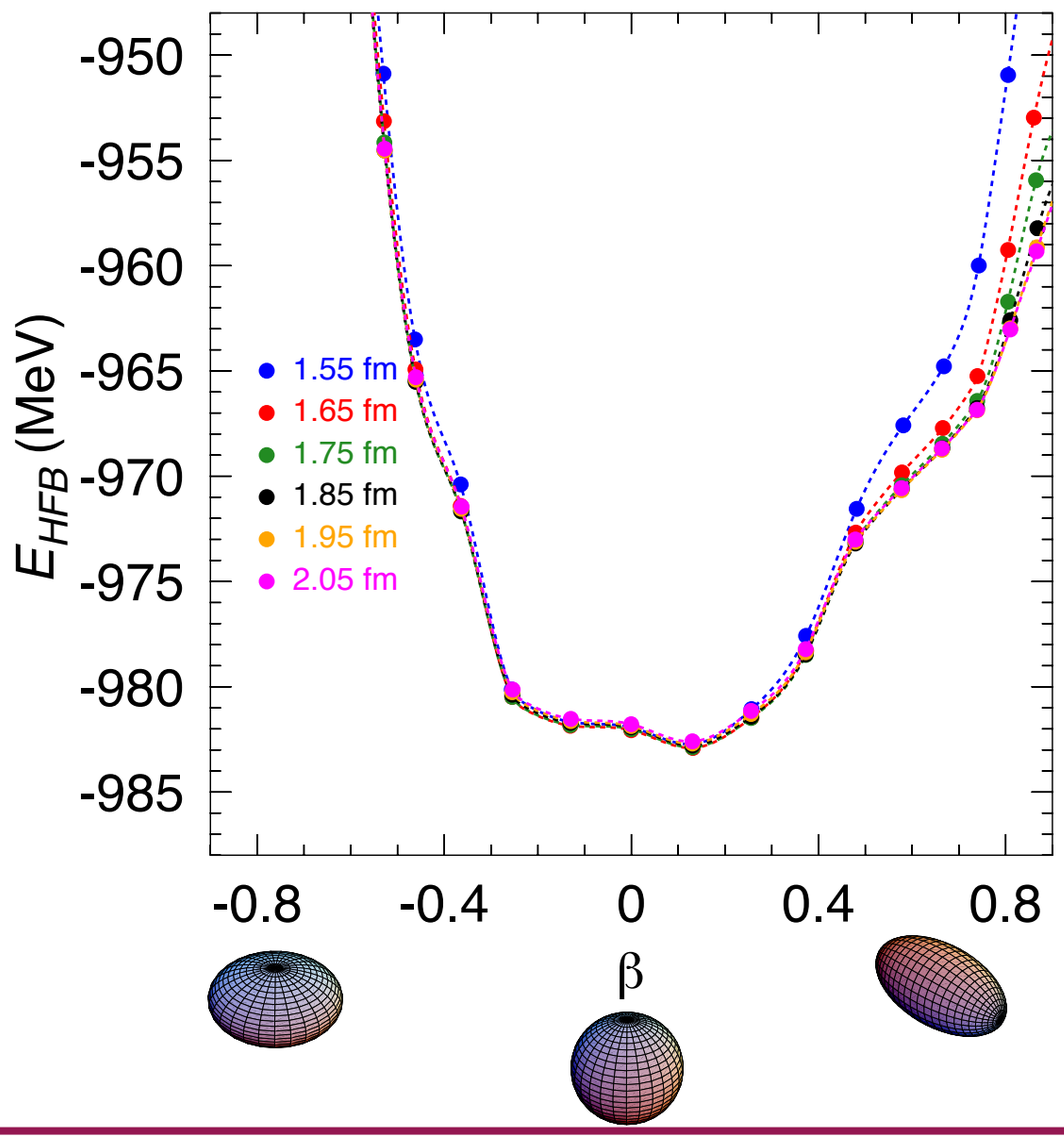

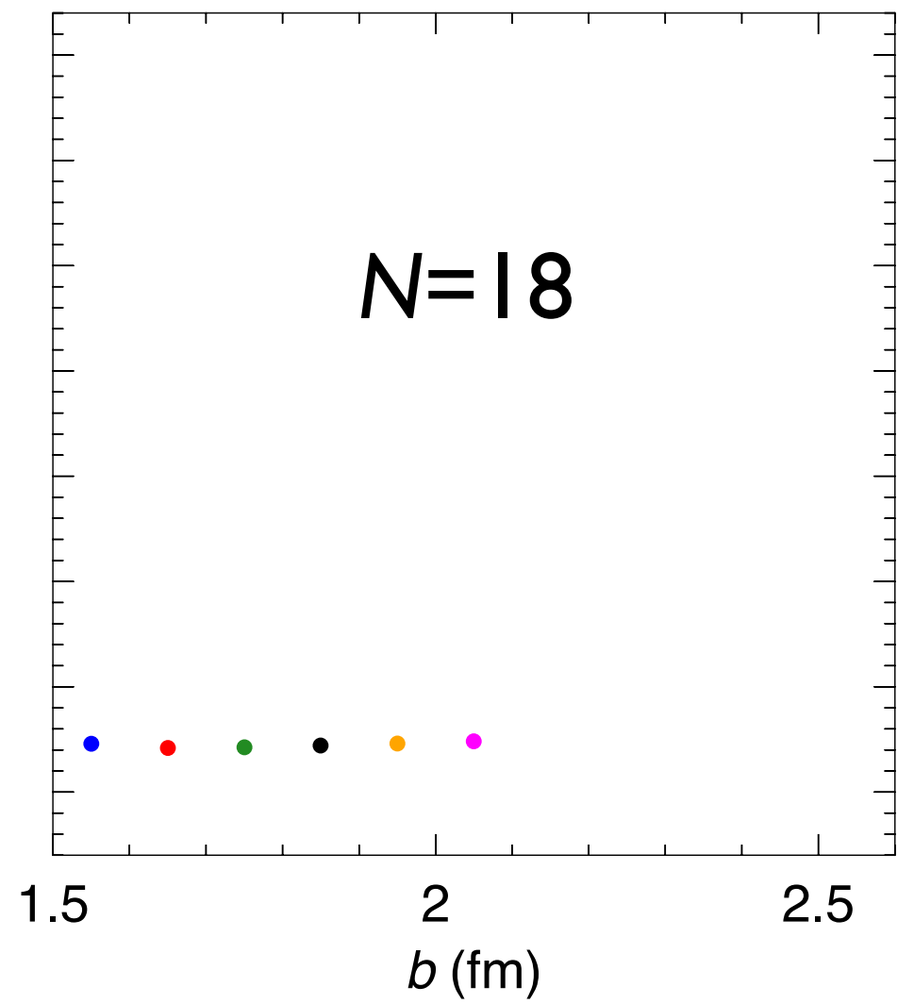

Effects of deformation on the convergence

Example:

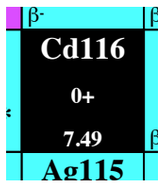

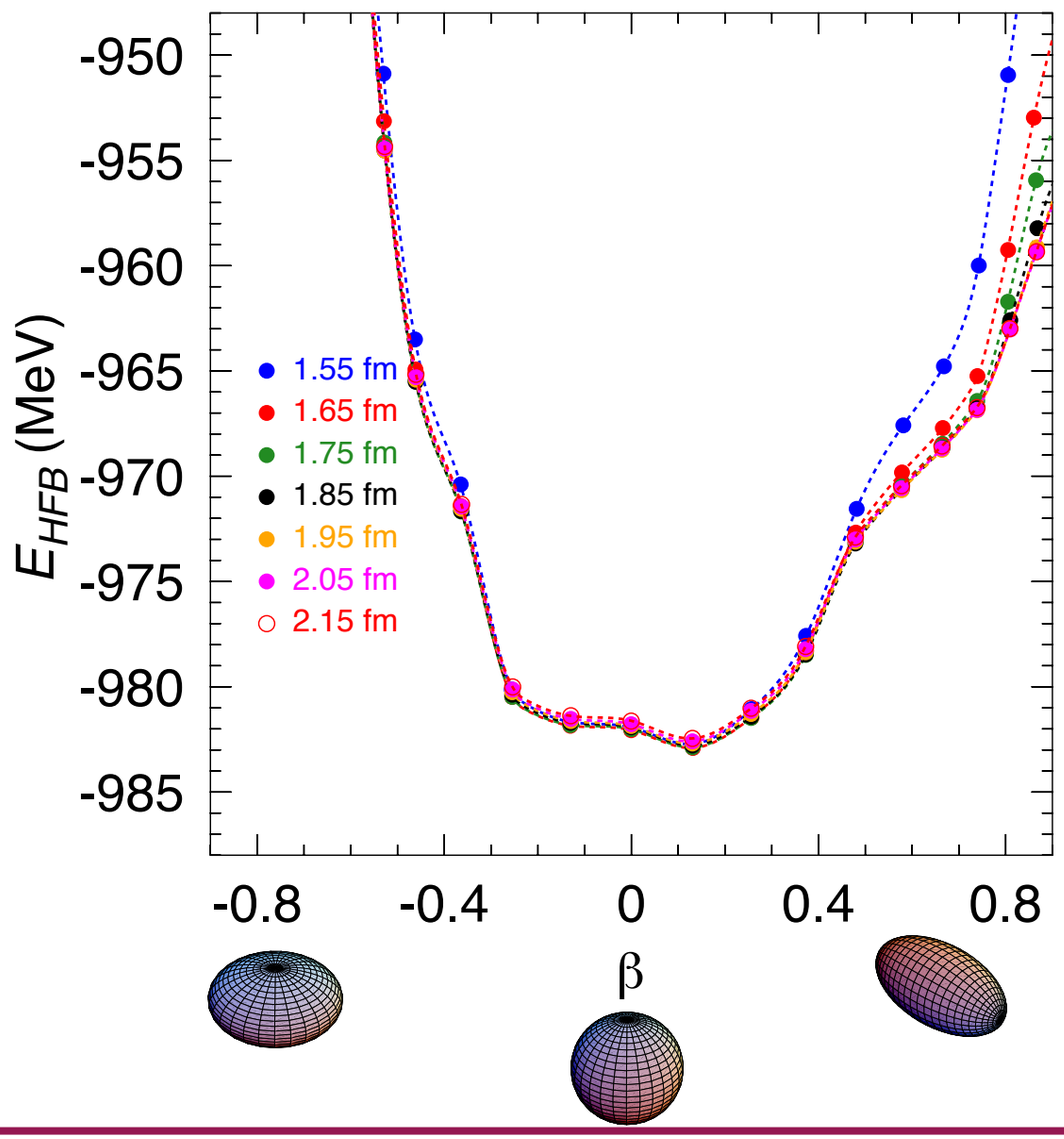

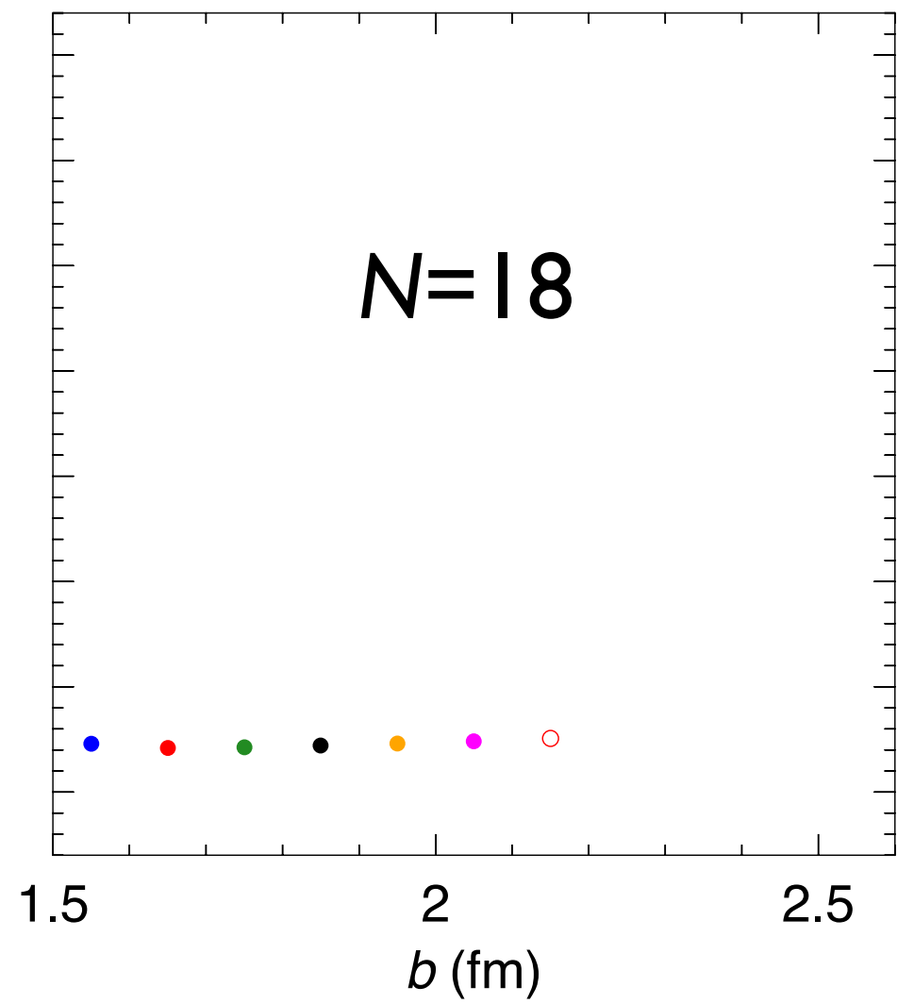

Effects of deformation on the convergence

Example:

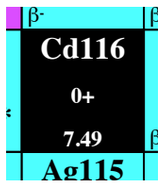

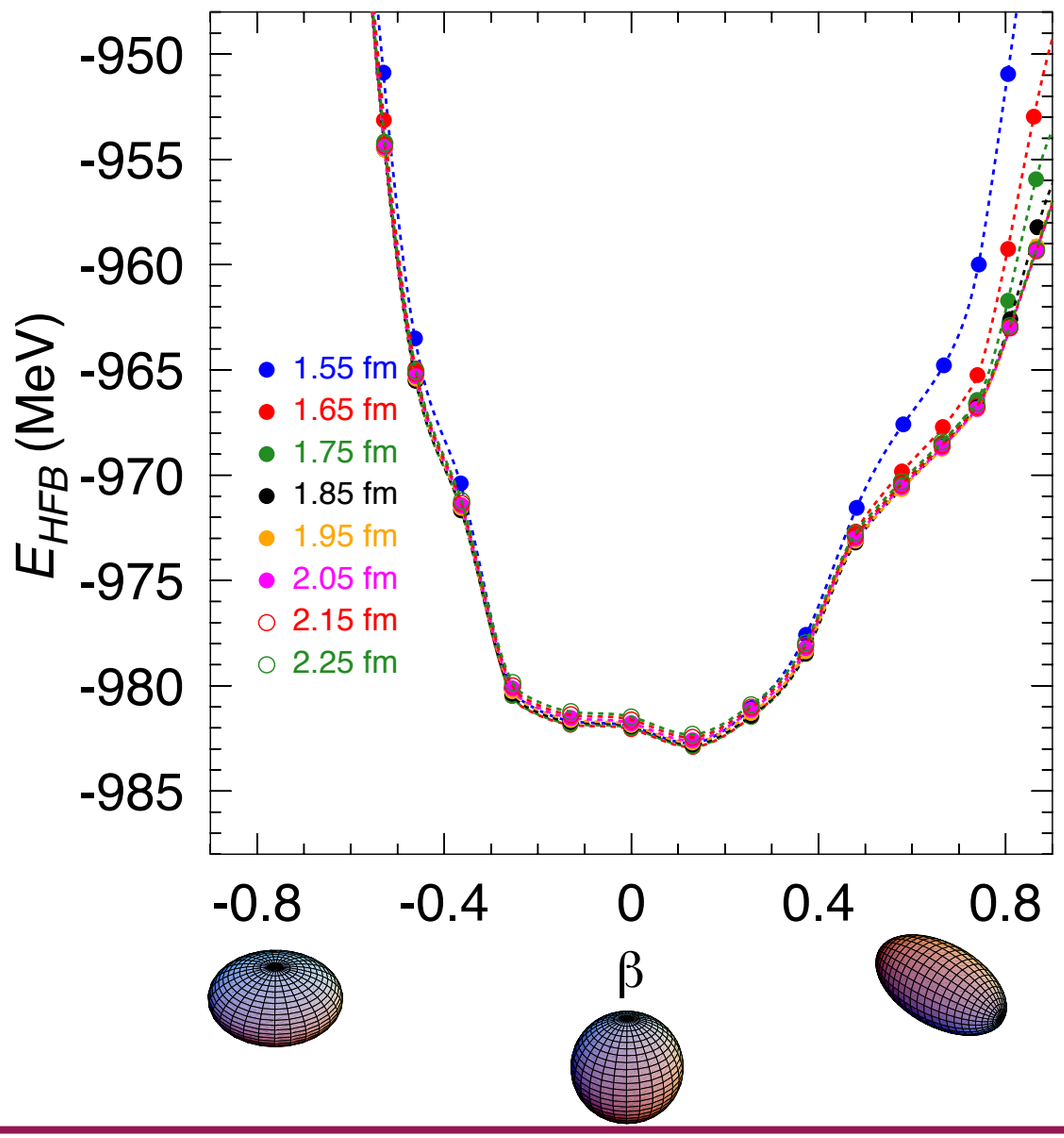

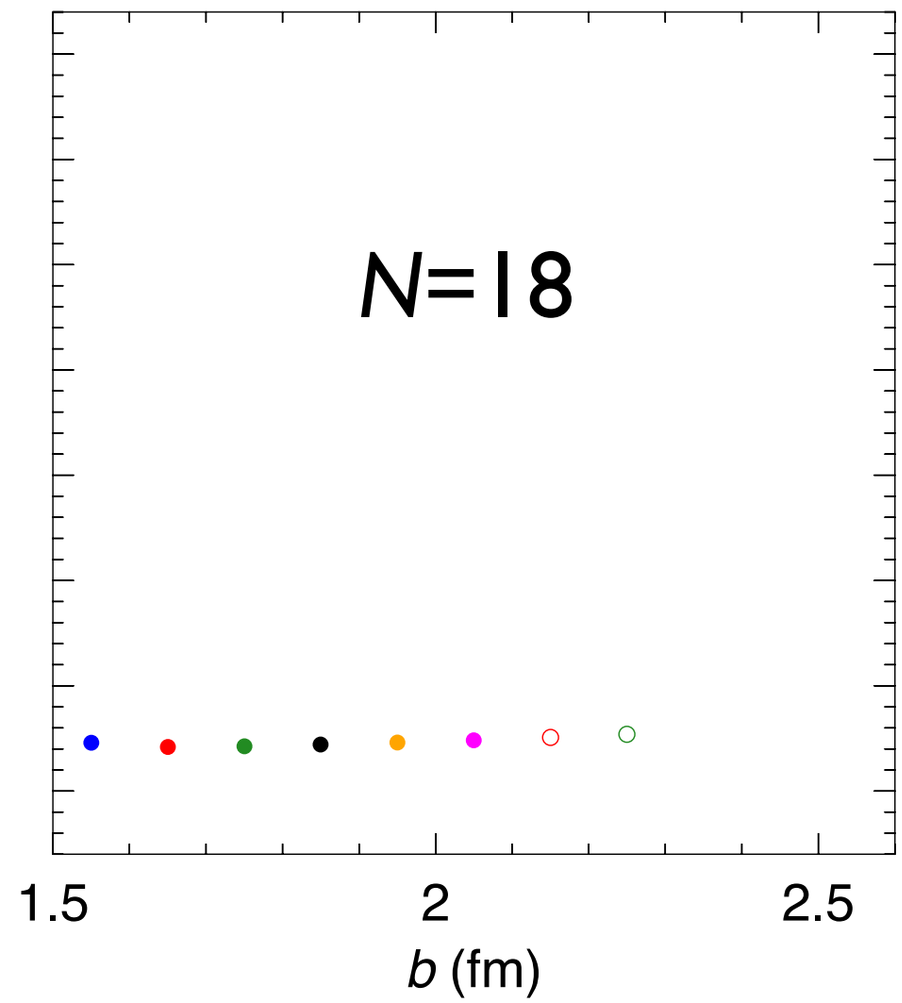

Effects of deformation on the convergence

Example:

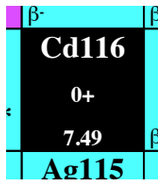

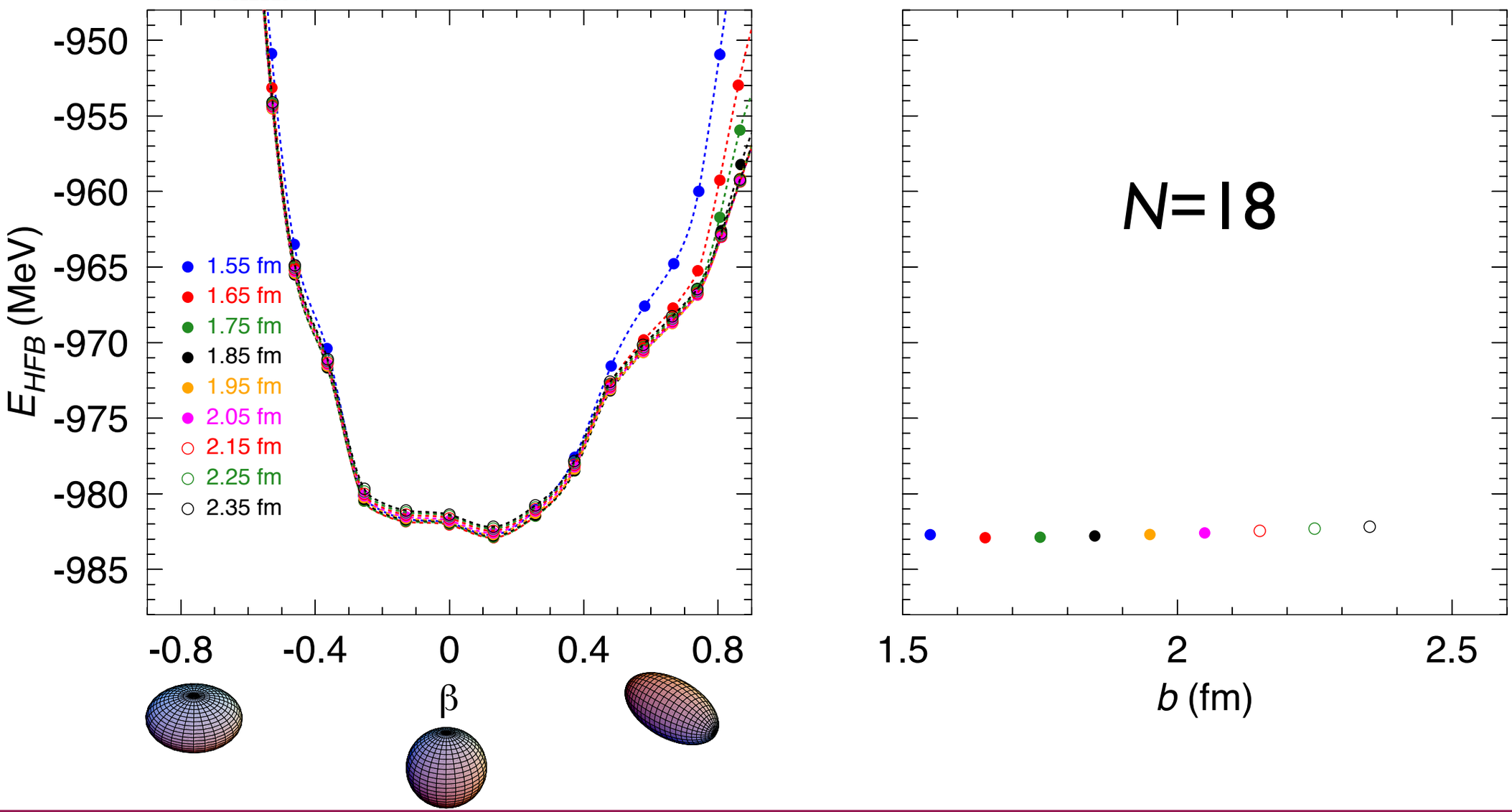

Effects of deformation on the convergence

Example:

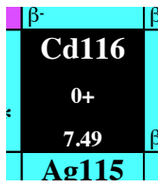

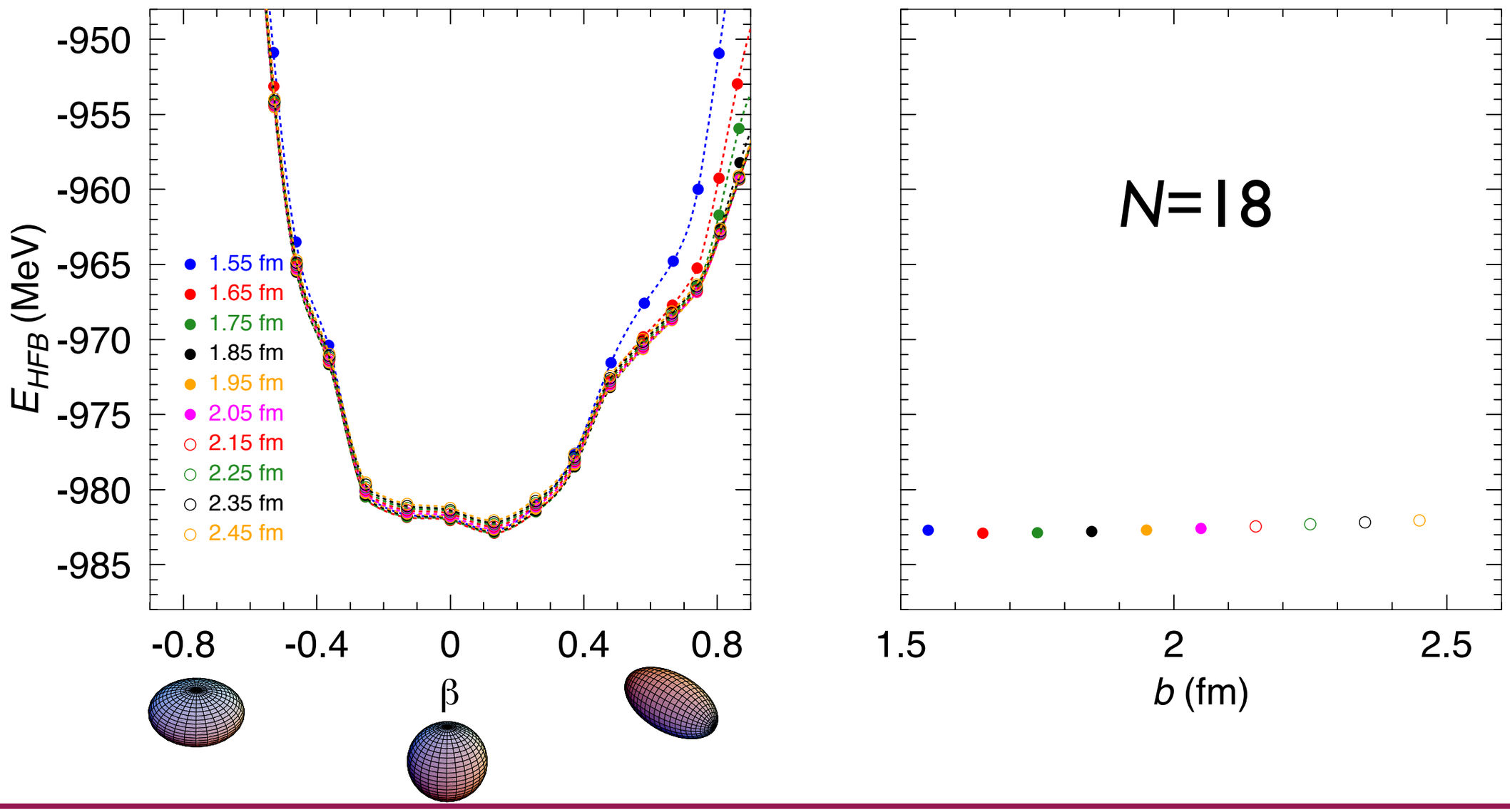

Effects of deformation on the convergence

Example:

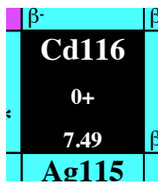

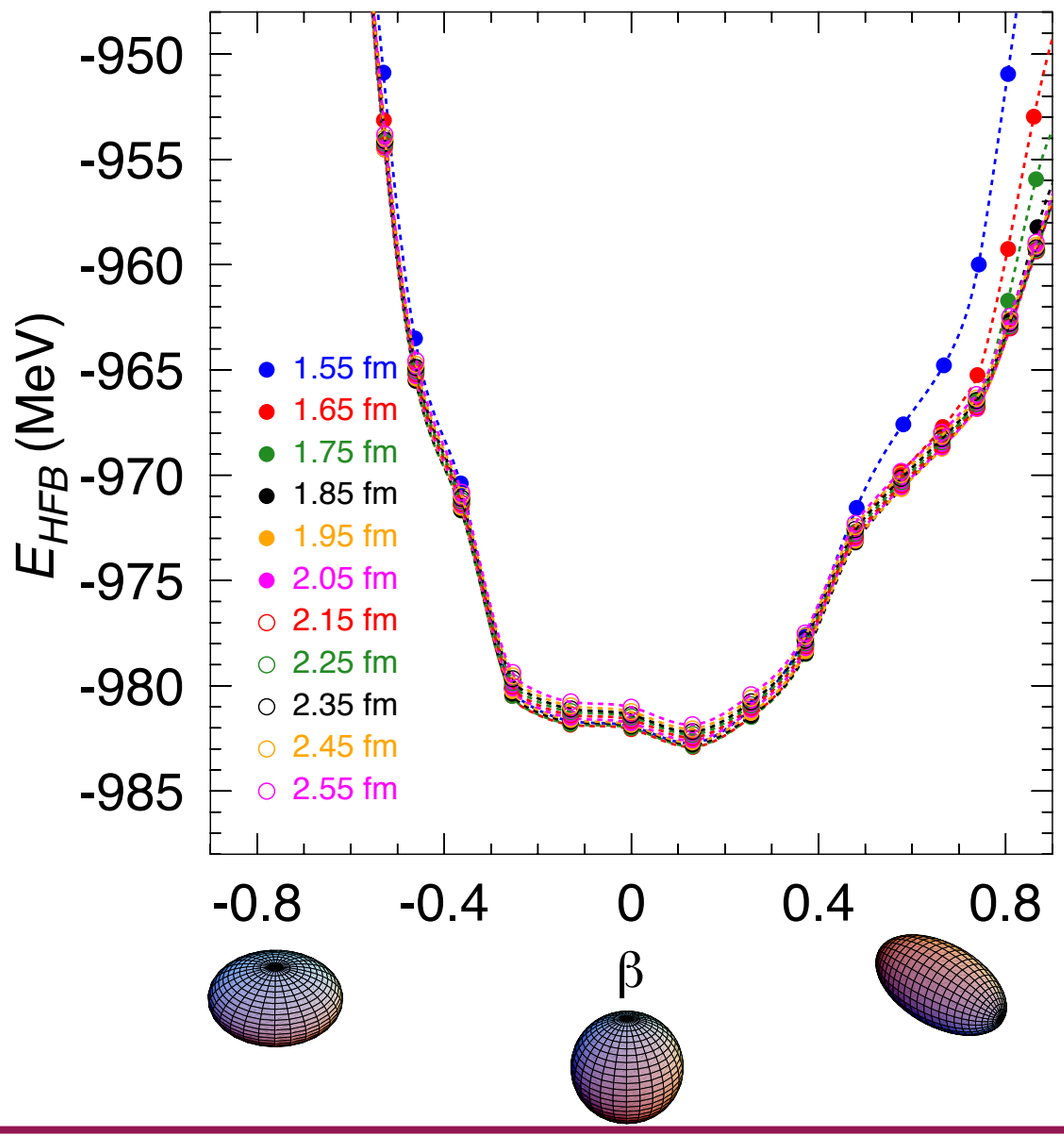

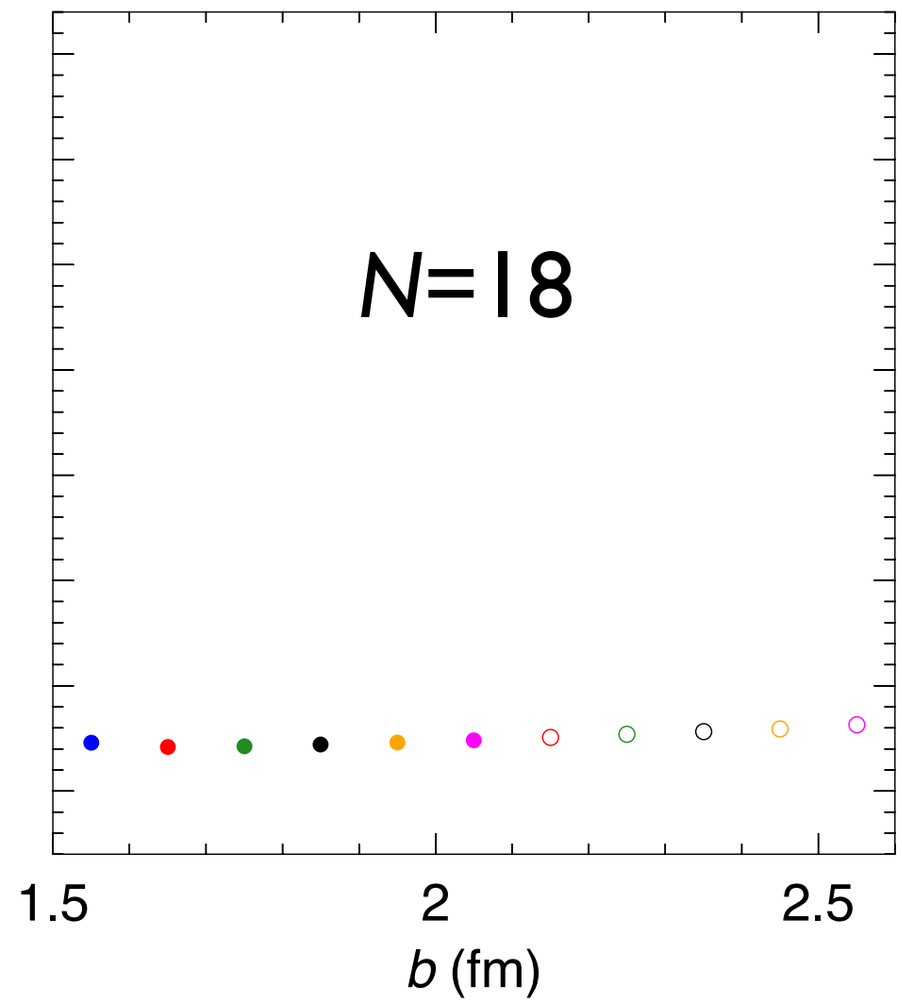

Final convergence

Example:

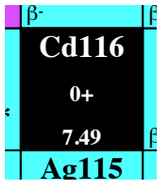

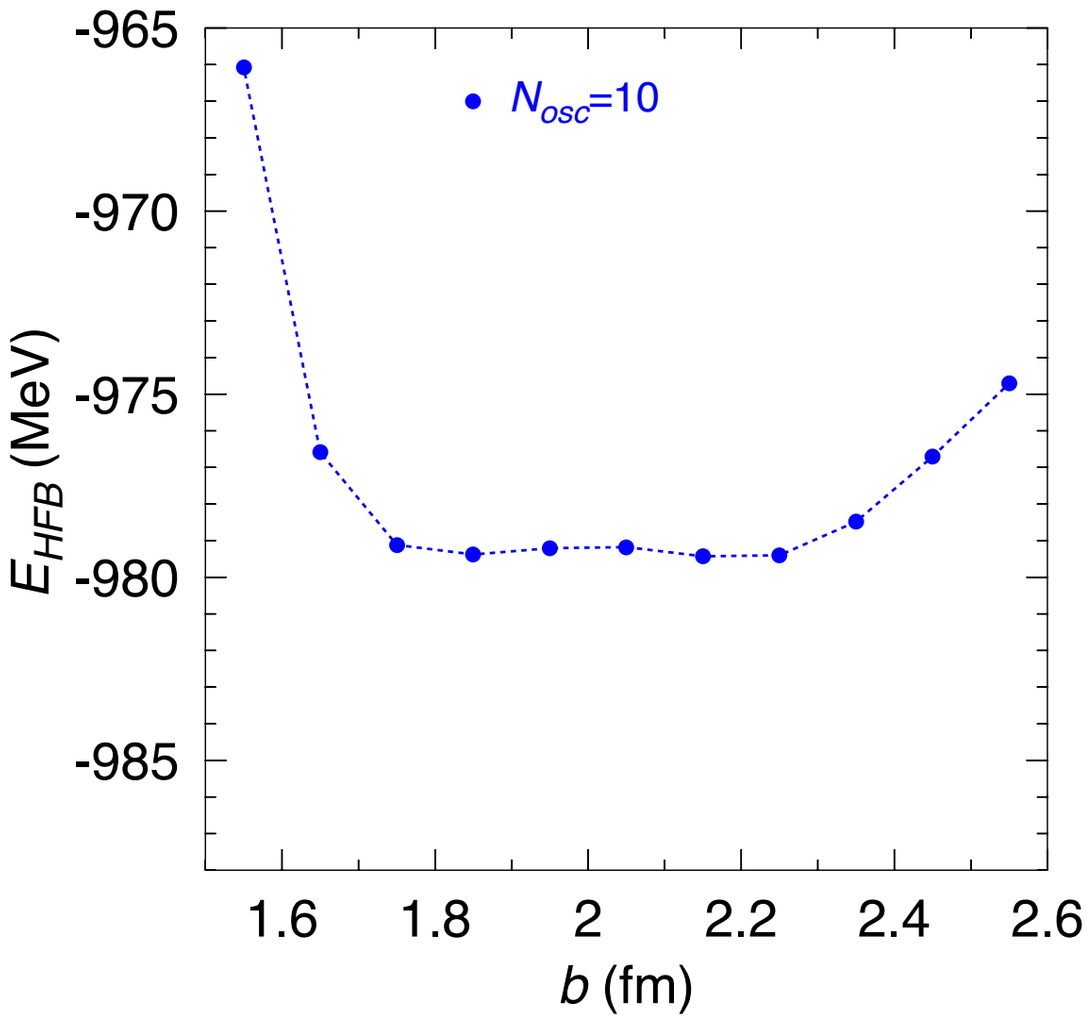

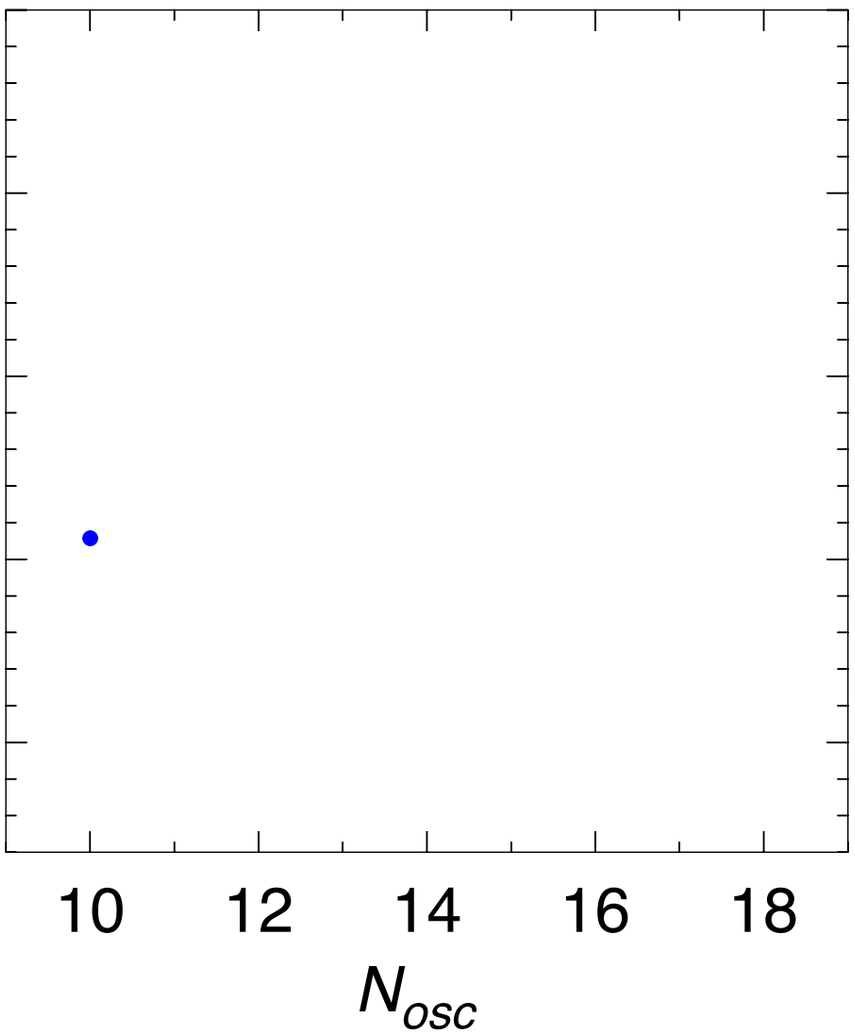

Final convergence

Example:

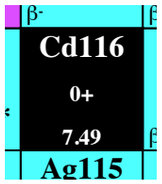

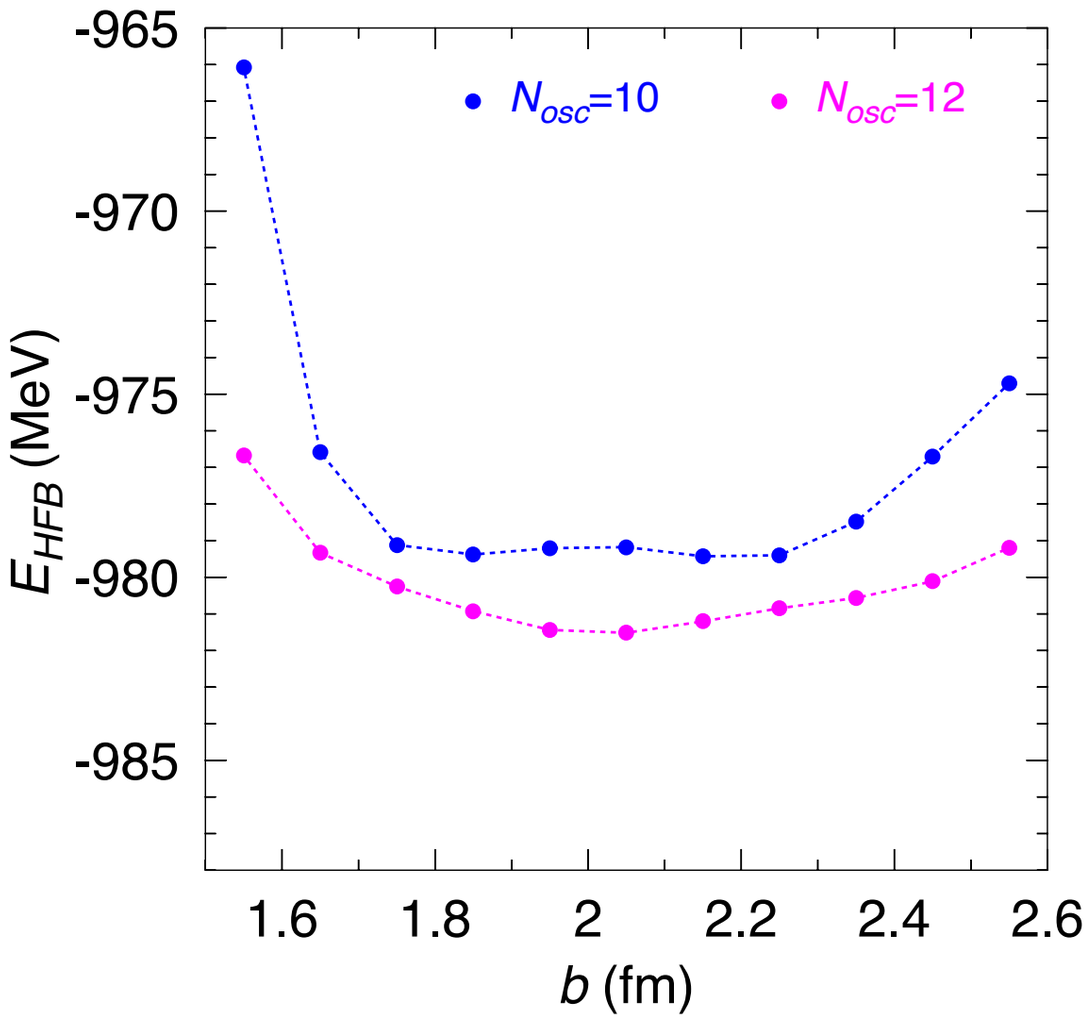

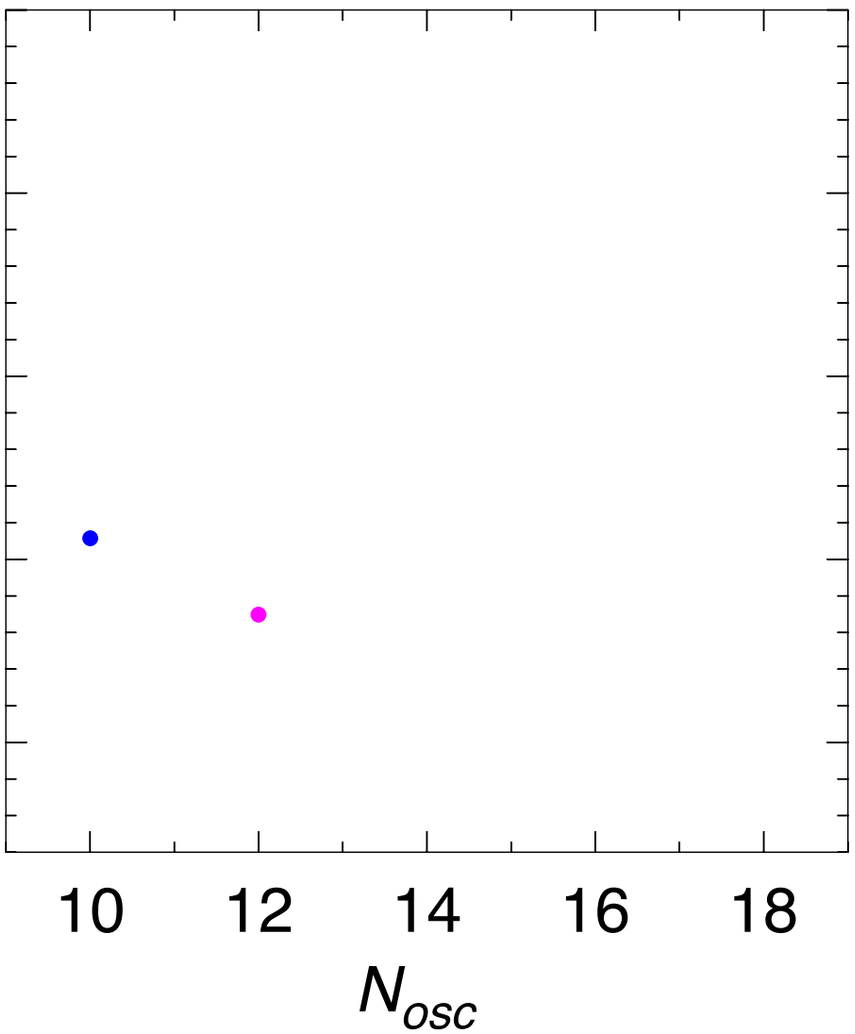

Final convergence

Example:

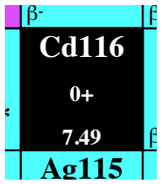

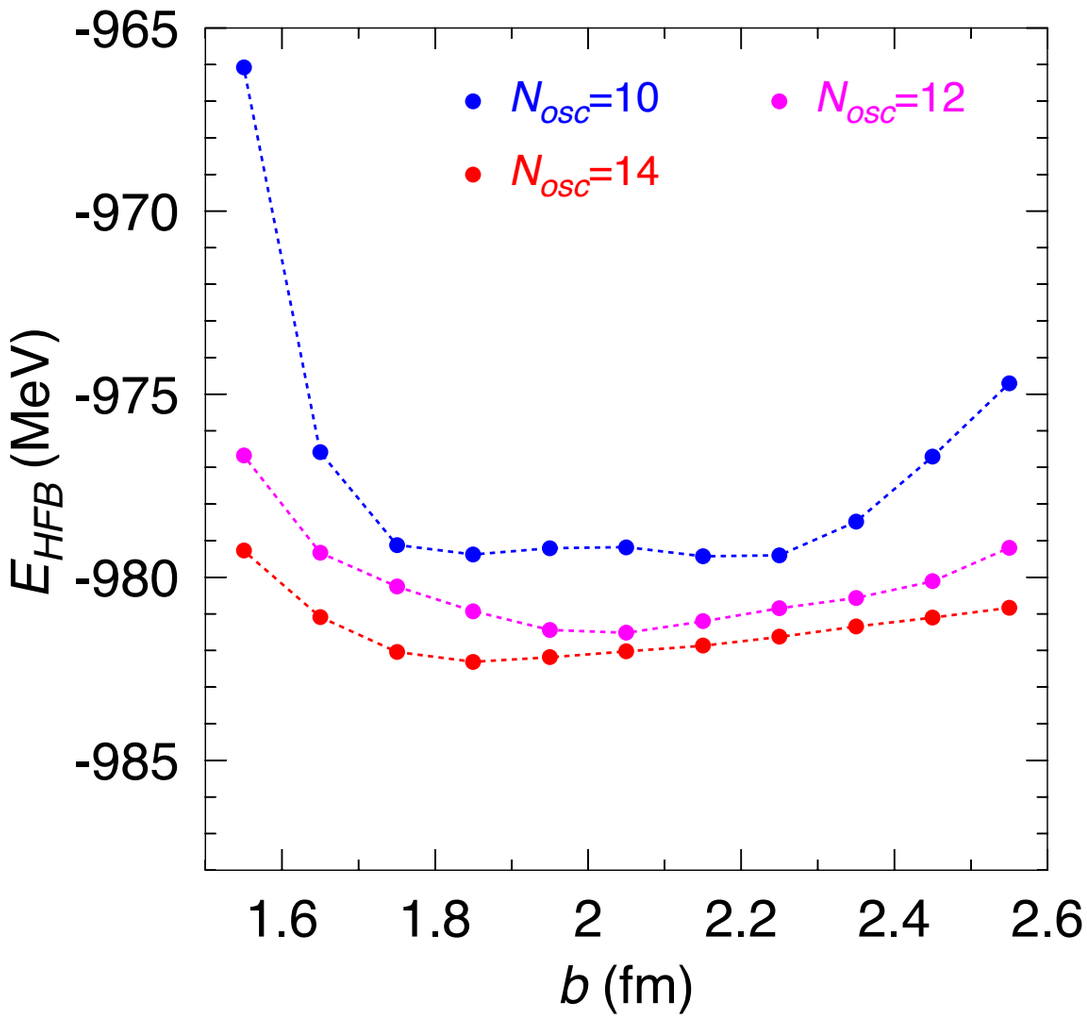

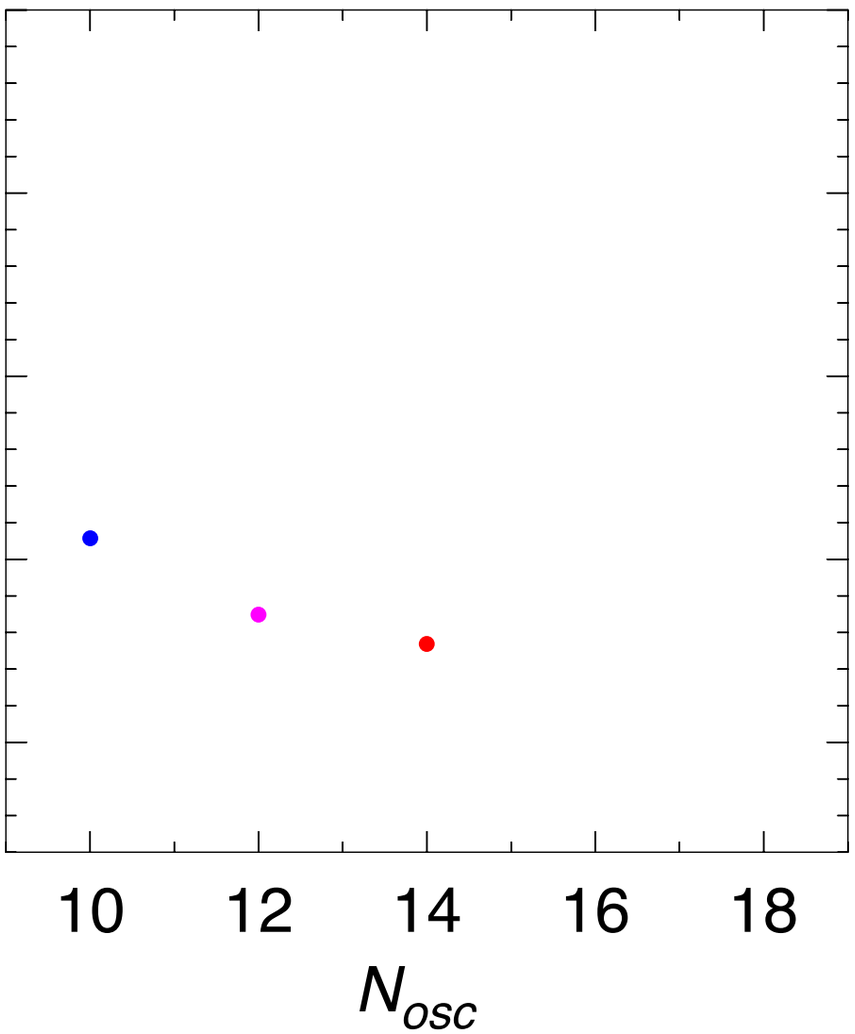

Final convergence

Example:

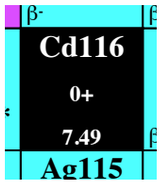

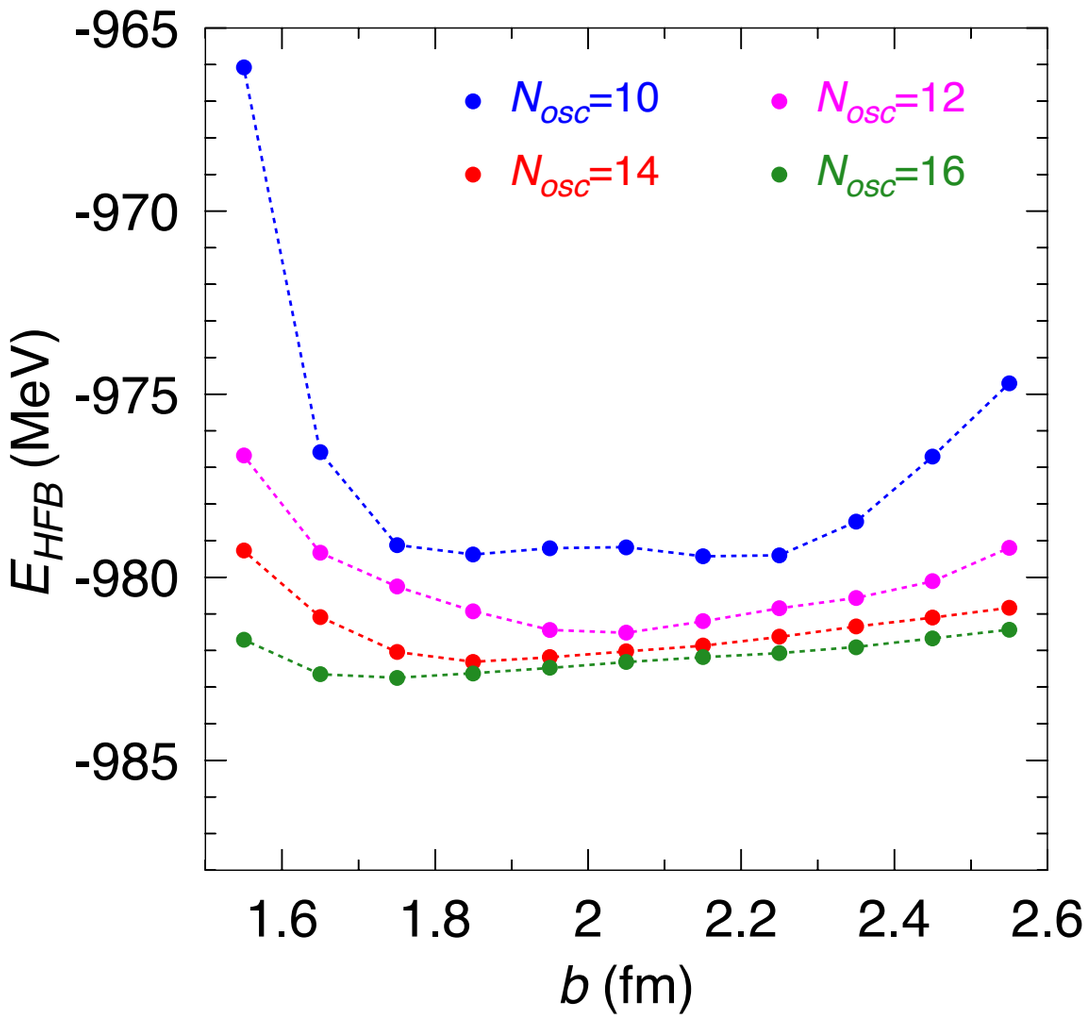

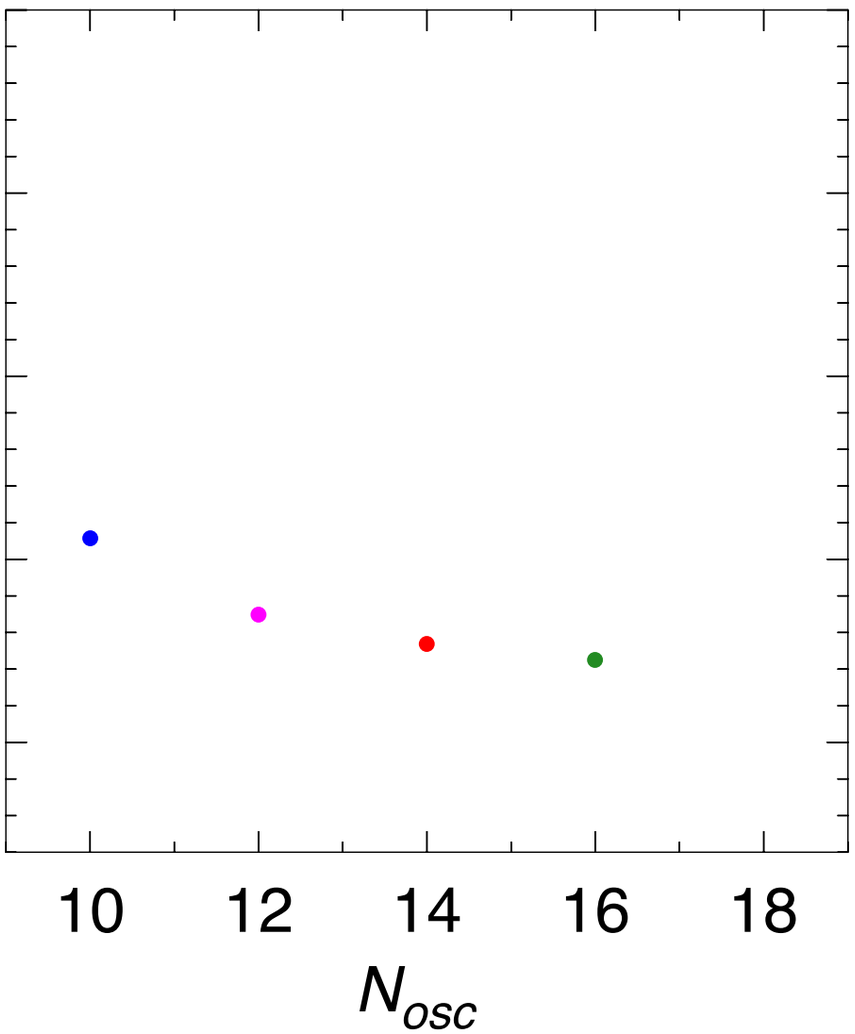

Final convergence

Example:

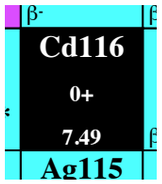

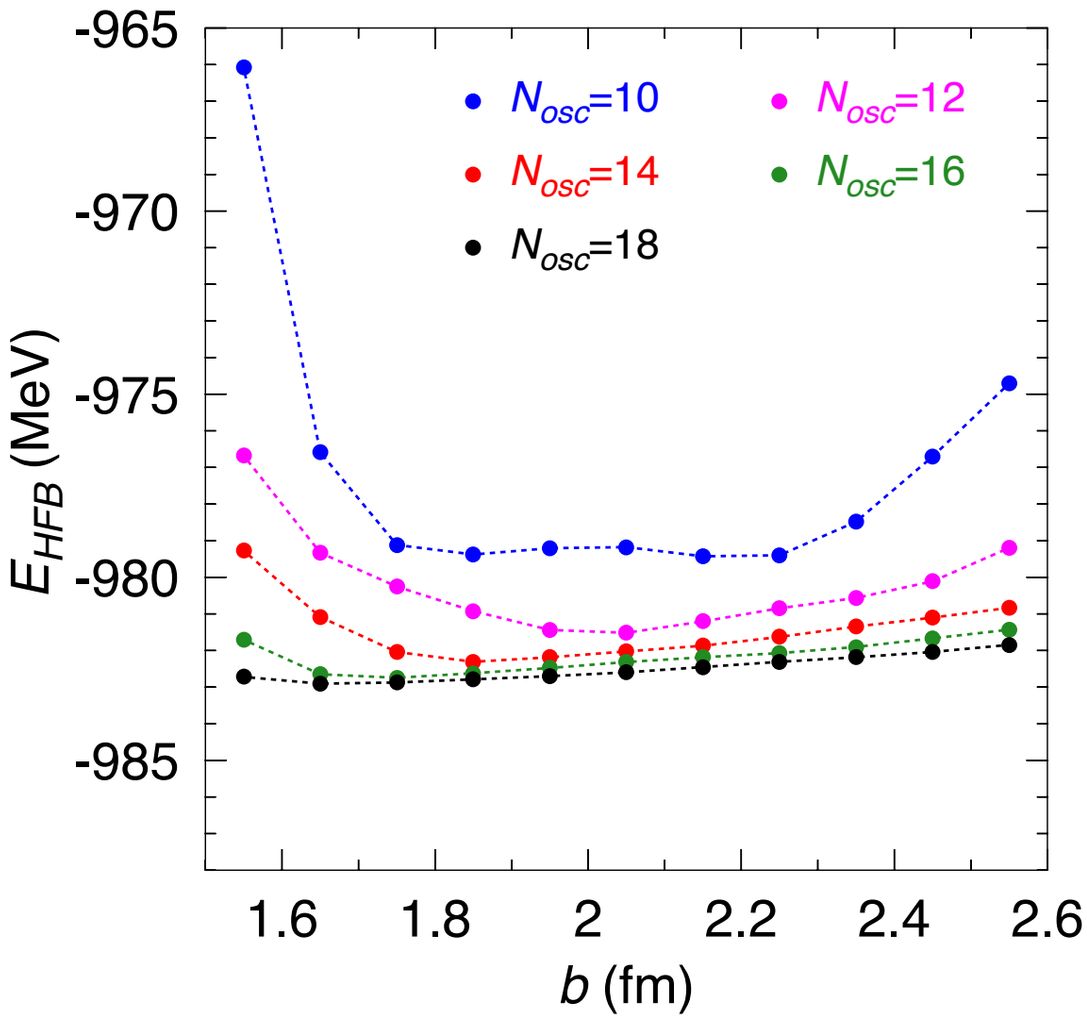

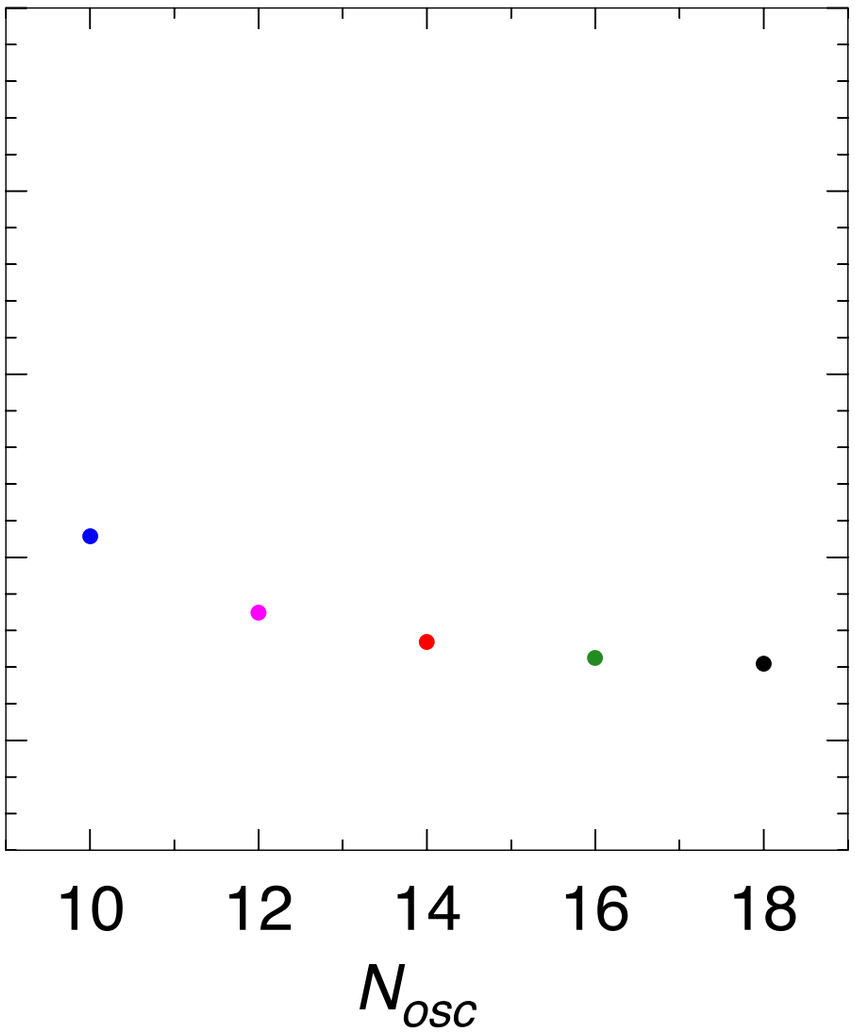

Convergence

- Published tables could contain some lack of convergence in the total binding energy.
- Two neutron separation energies are better converged.
- Artificial ‘jumps’ or ‘noise’ could appear in the S_{2n} due to lack of convergence.

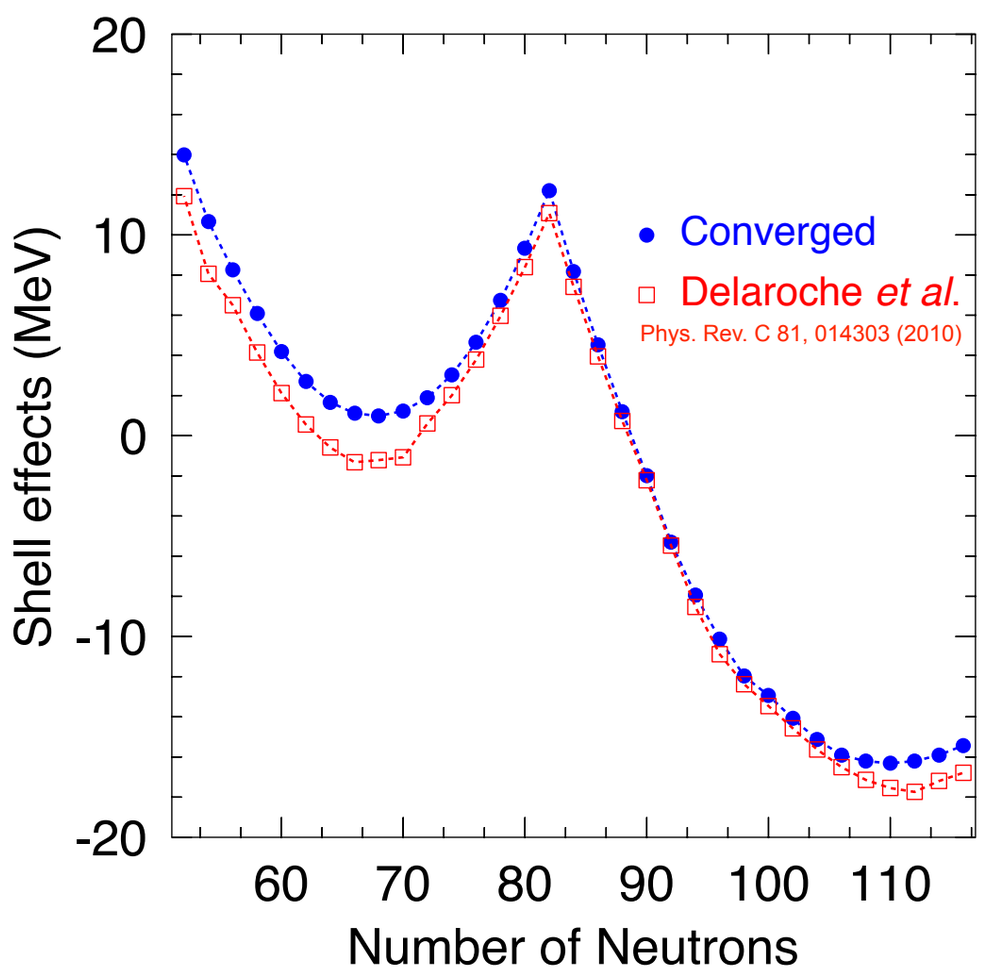

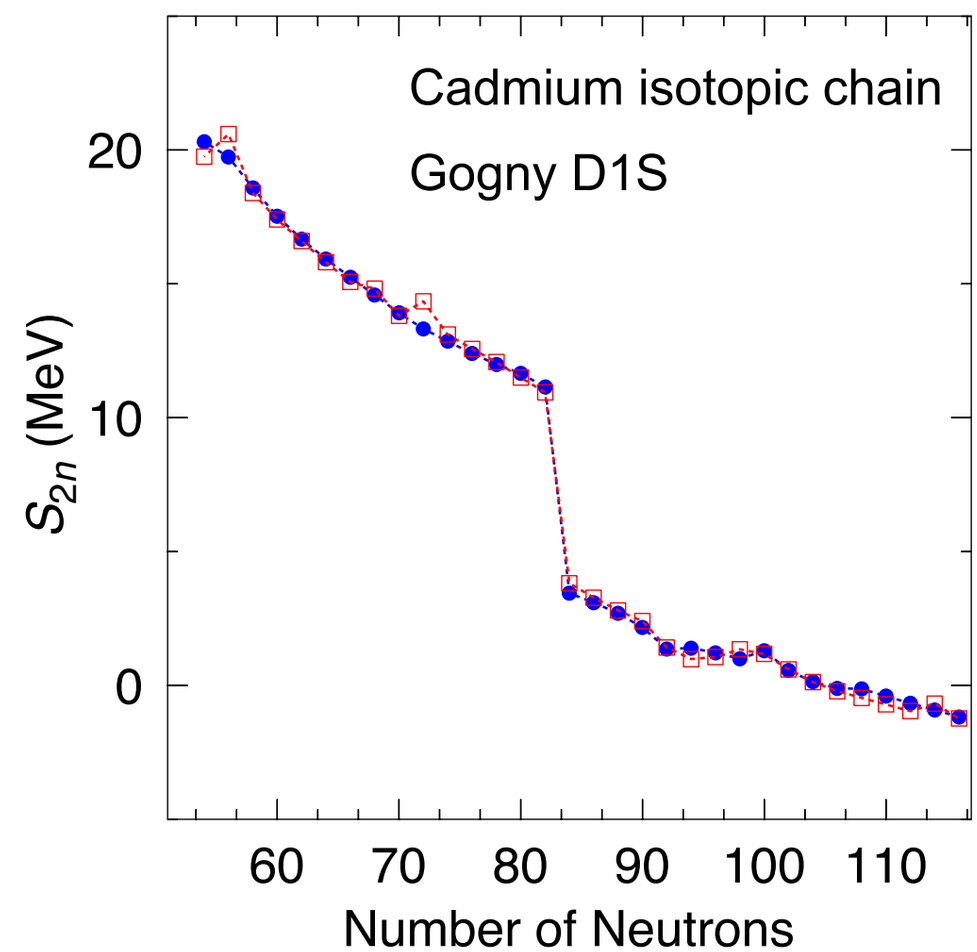

Convergence

- Published tables could contain some lack of convergence in the total binding energy.
- Two neutron separation energies are better converged.
- Artificial 'jumps' or 'noise' could appear in the S_{2n} due to lack of convergence.

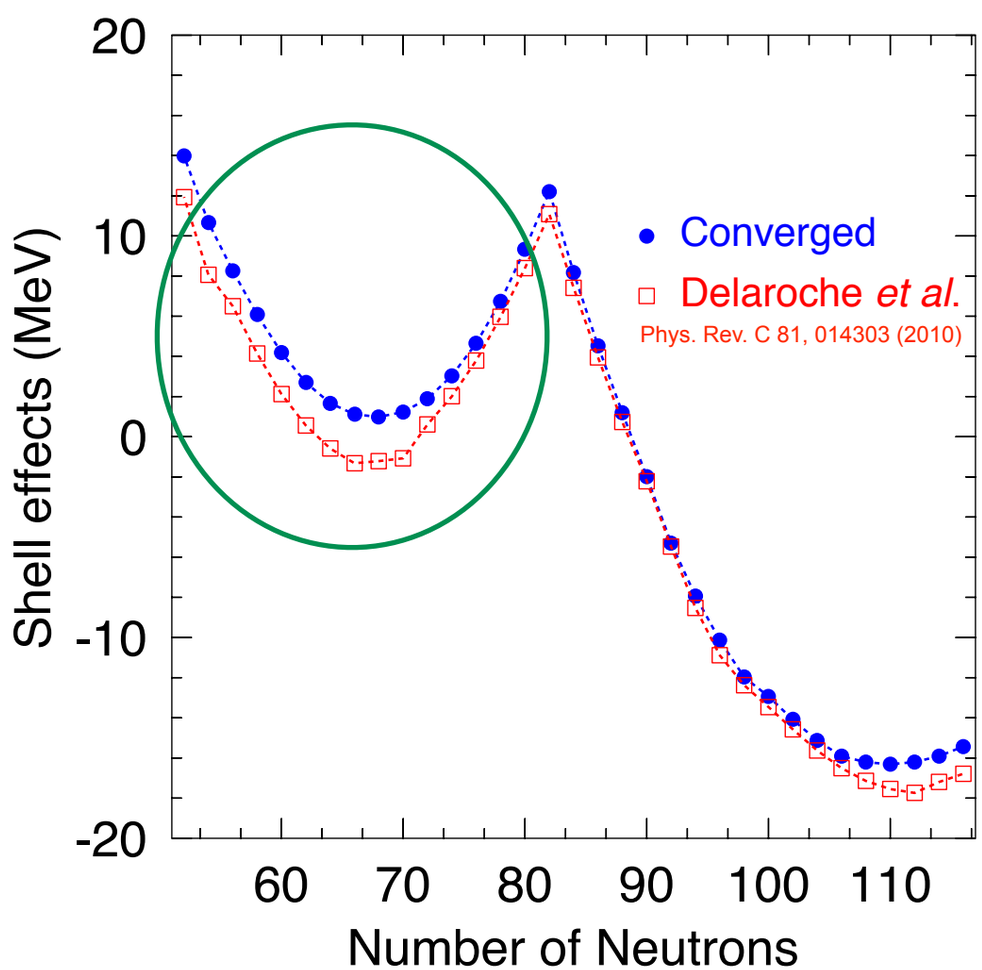

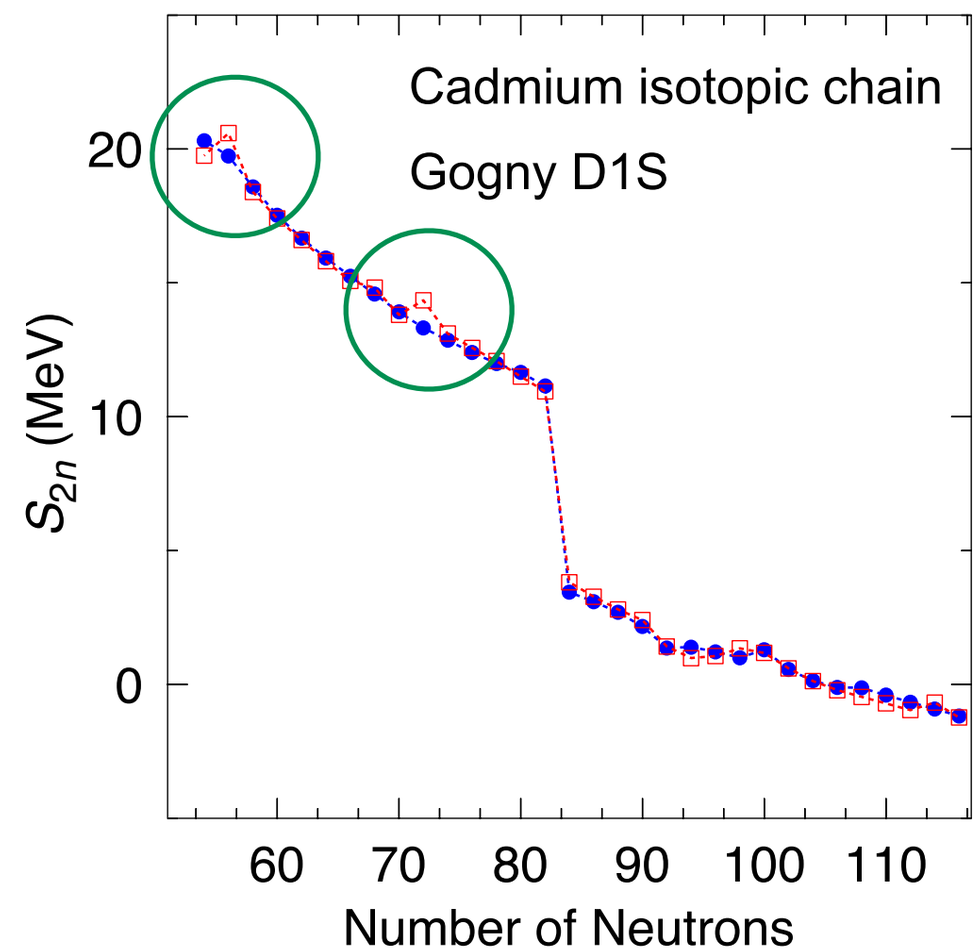

‘Contaminations’

Example: ^{18}O

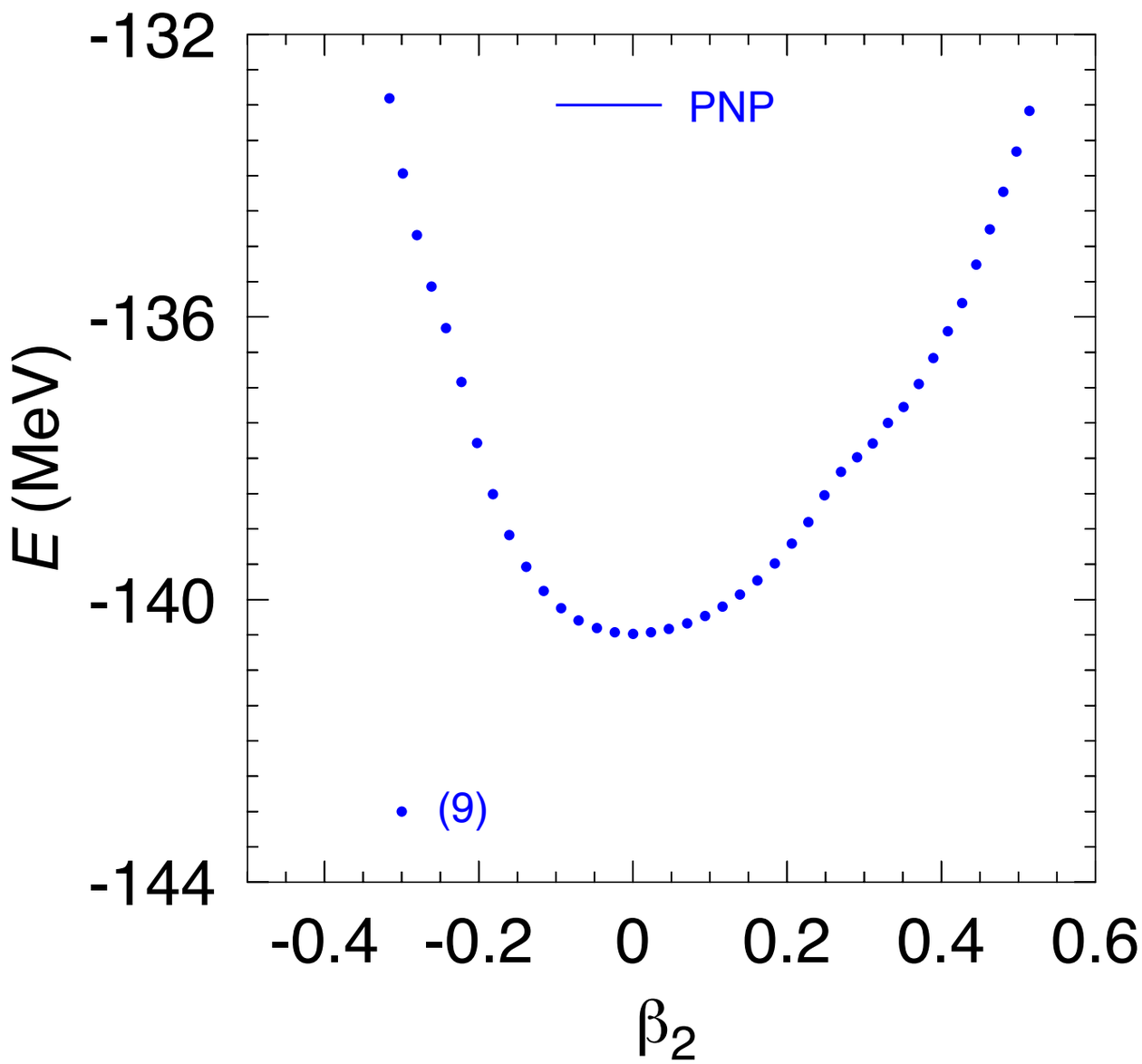

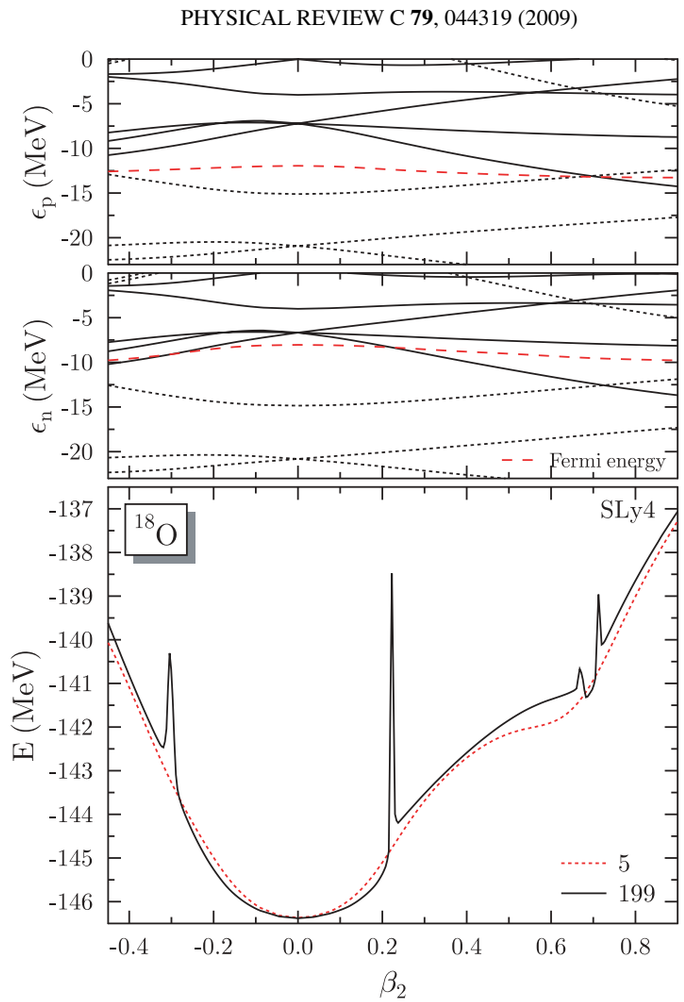

FIG. 1. (Color online) Particle-number-restored deformation energy surface of ^{18}O calculated with SLy4 and a density-dependent pairing interaction and the corresponding single-particle spectra of protons and neutrons as a function of the axial quadrupole deformation for $L = 5$ and 199 discretization points of the integral over the gauge angle (lowest panel). There are clear anomalies that appear when either a proton or neutron single-particle level crosses the Fermi energy. The dimensionless quadrupole deformation β_2 is defined in Eq. (66).

‘Contaminations’

Example: ^{18}O

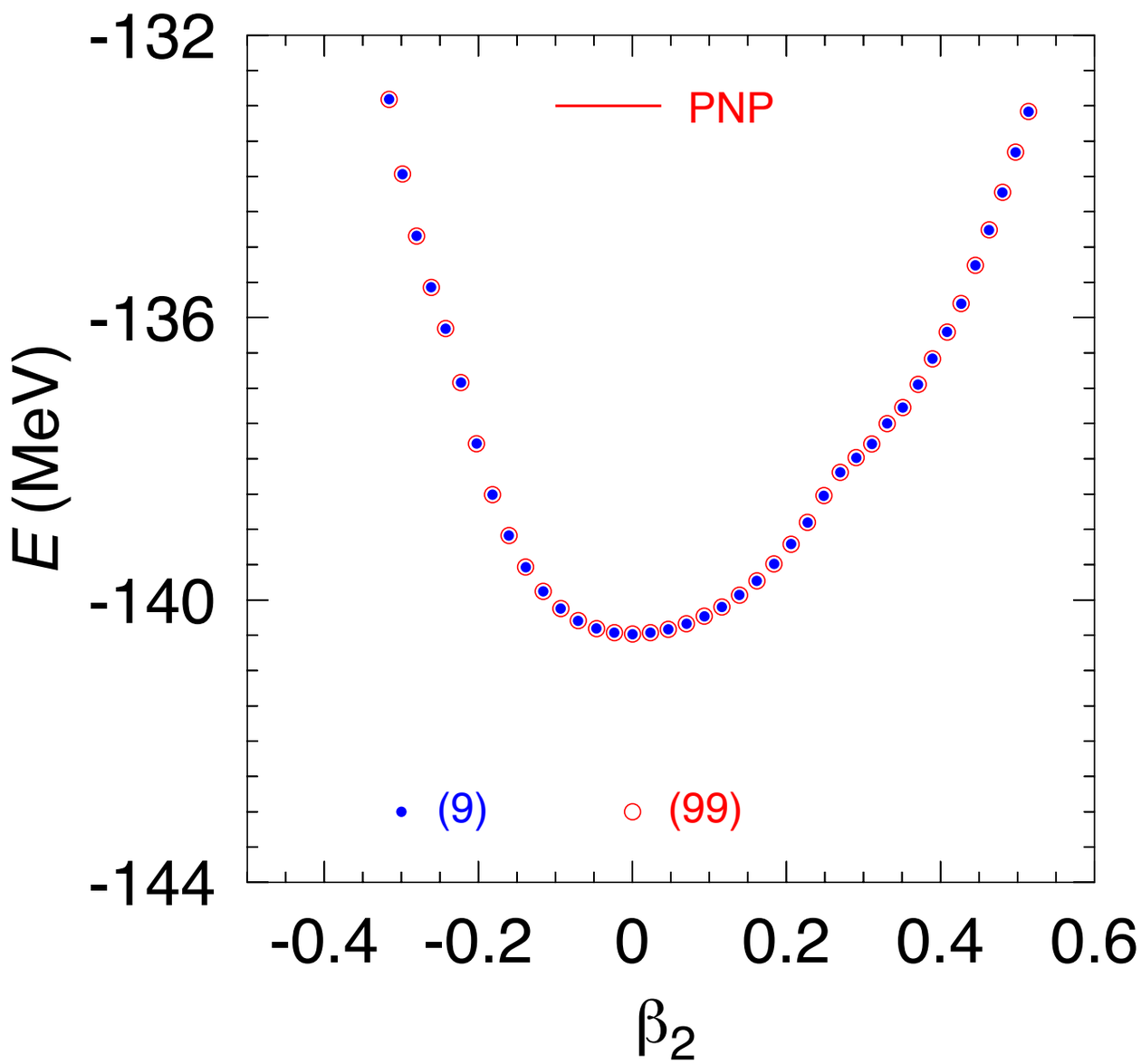

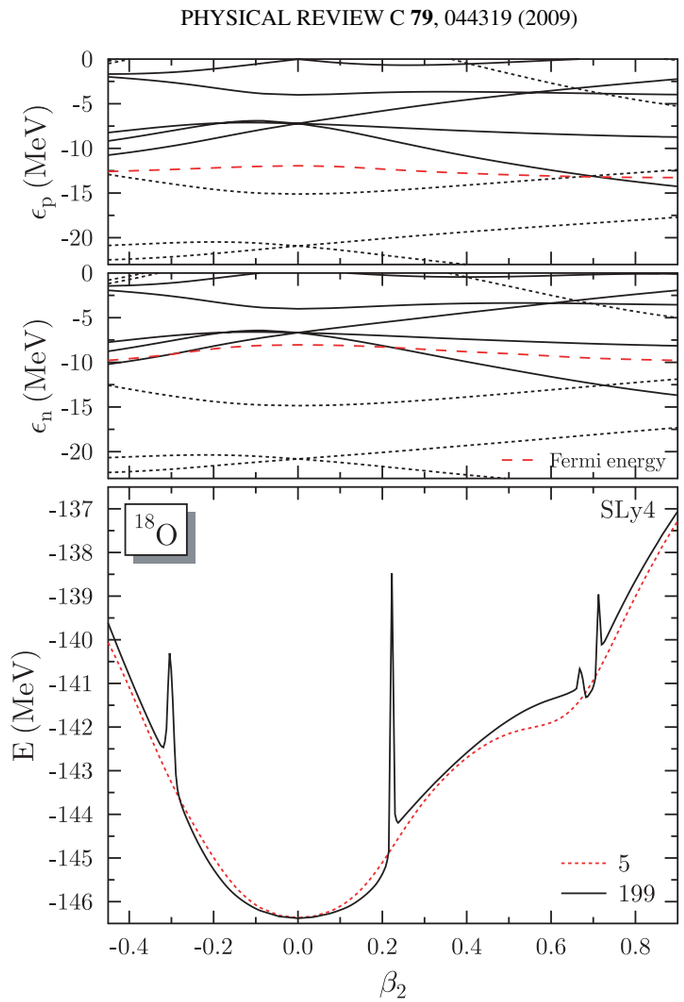

FIG. 1. (Color online) Particle-number-restored deformation energy surface of ^{18}O calculated with SLy4 and a density-dependent pairing interaction and the corresponding single-particle spectra of protons and neutrons as a function of the axial quadrupole deformation for $L = 5$ and 199 discretization points of the integral over the gauge angle (lowest panel). There are clear anomalies that appear when either a proton or neutron single-particle level crosses the Fermi energy. The dimensionless quadrupole deformation β_2 is defined in Eq. (66).

‘Contaminations’

Example: ^{18}O

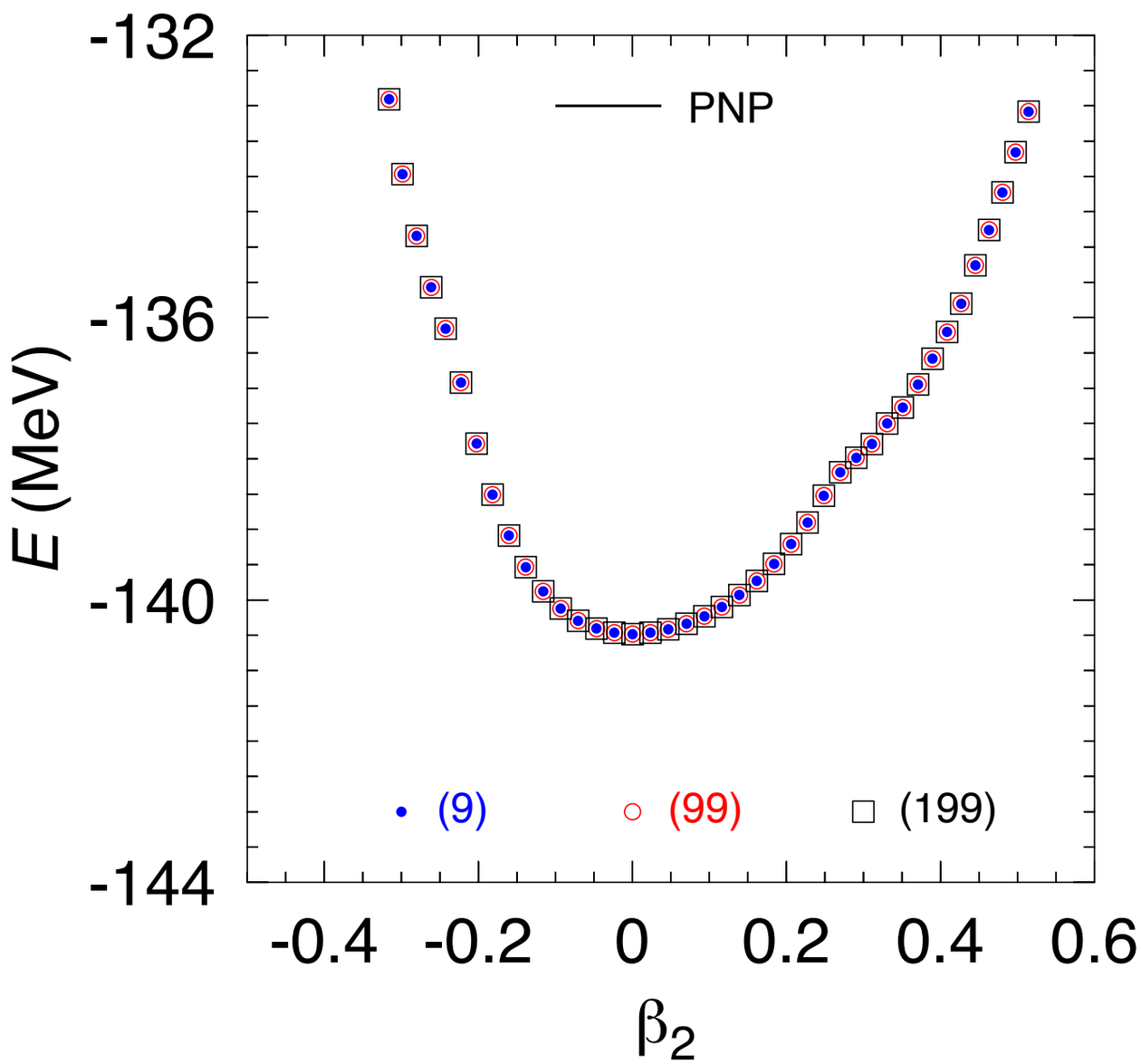

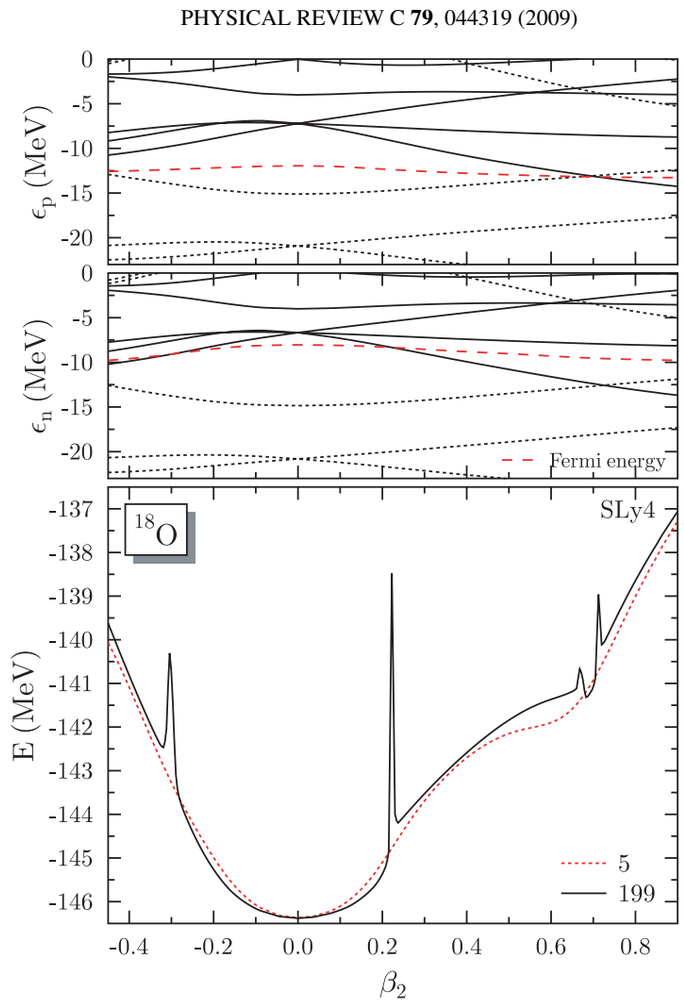

FIG. 1. (Color online) Particle-number-restored deformation energy surface of ^{18}O calculated with SLy4 and a density-dependent pairing interaction and the corresponding single-particle spectra of protons and neutrons as a function of the axial quadrupole deformation for $L = 5$ and 199 discretization points of the integral over the gauge angle (lowest panel). There are clear anomalies that appear when either a proton or neutron single-particle level crosses the Fermi energy. The dimensionless quadrupole deformation β_2 is defined in Eq. (66).

‘Contaminations’

Example: ^{18}O

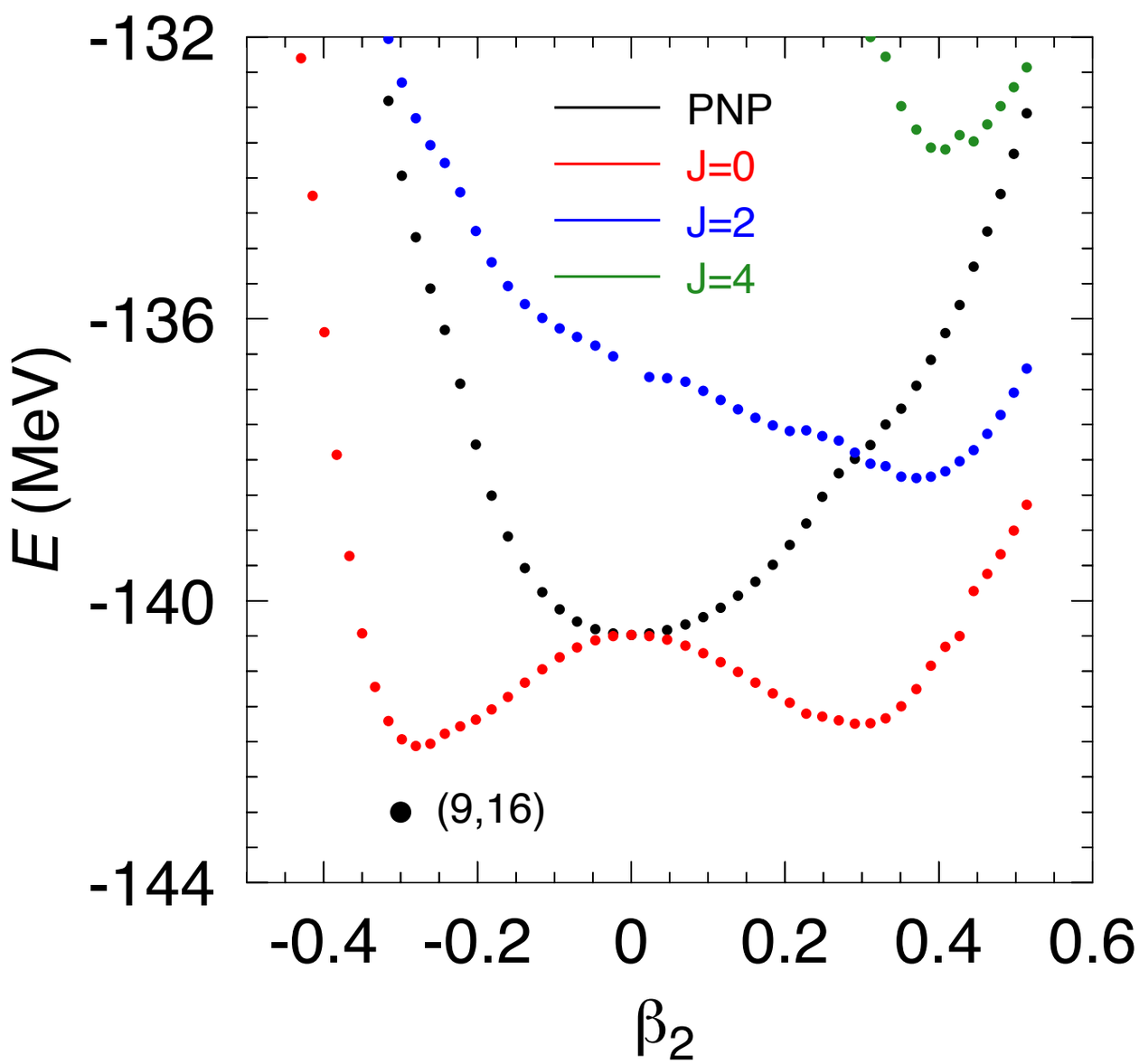

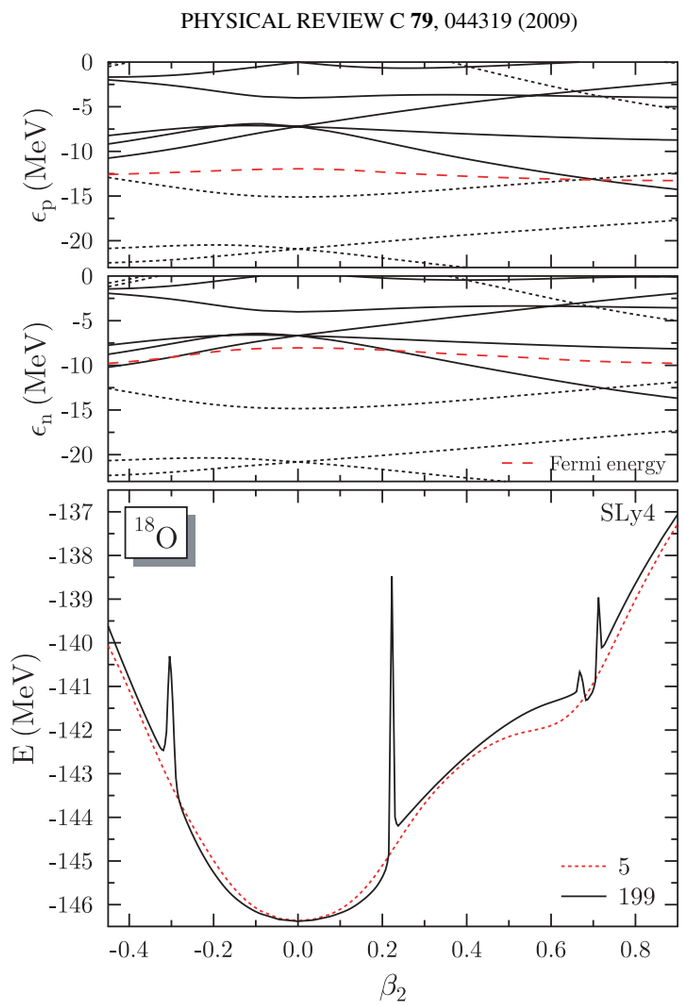

FIG. 1. (Color online) Particle-number-restored deformation energy surface of ^{18}O calculated with SLy4 and a density-dependent pairing interaction and the corresponding single-particle spectra of protons and neutrons as a function of the axial quadrupole deformation for $L = 5$ and 199 discretization points of the integral over the gauge angle (lowest panel). There are clear anomalies that appear when either a proton or neutron single-particle level crosses the Fermi energy. The dimensionless quadrupole deformation β_2 is defined in Eq. (66).

‘Contaminations’

Example: ^{18}O

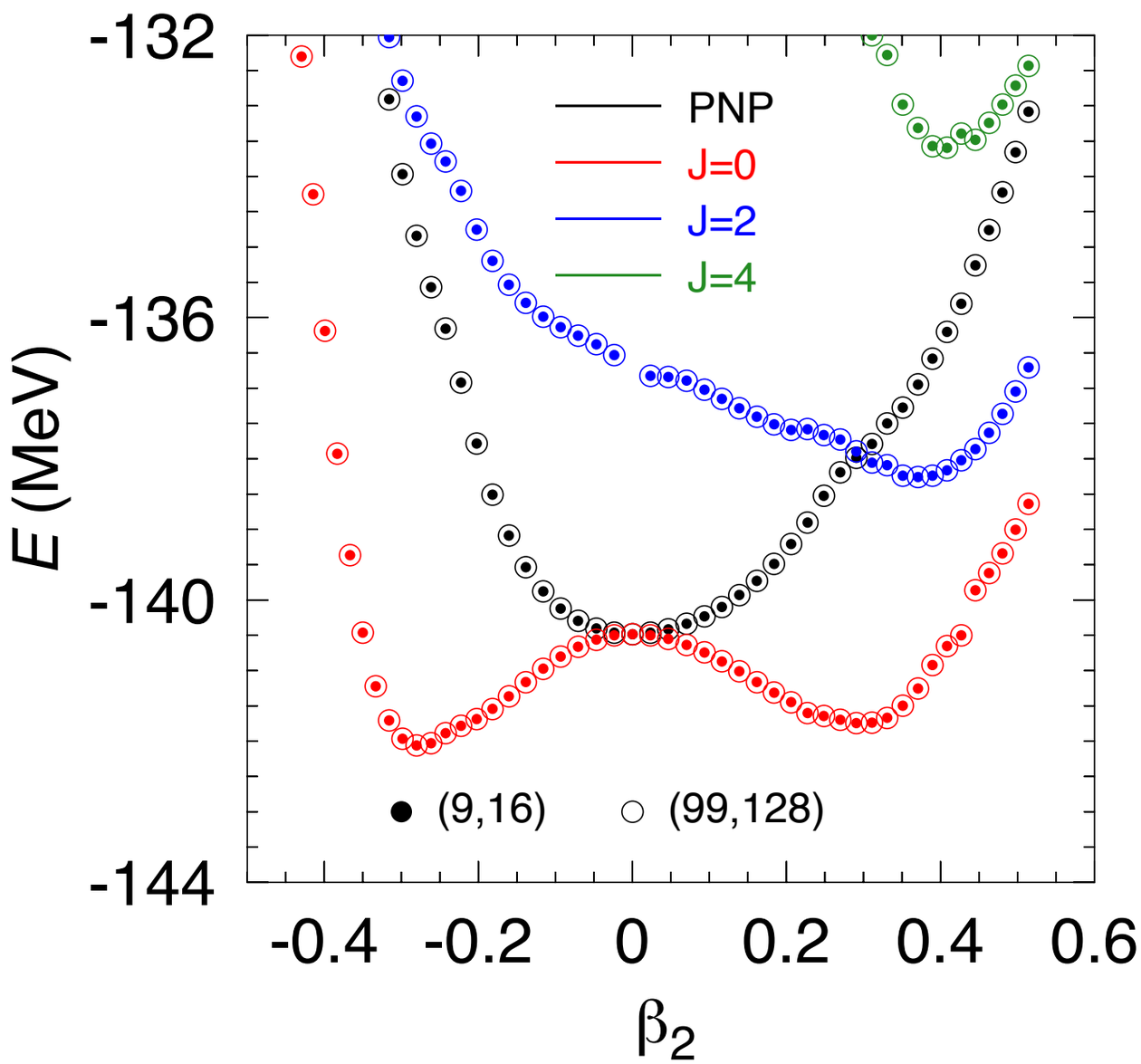

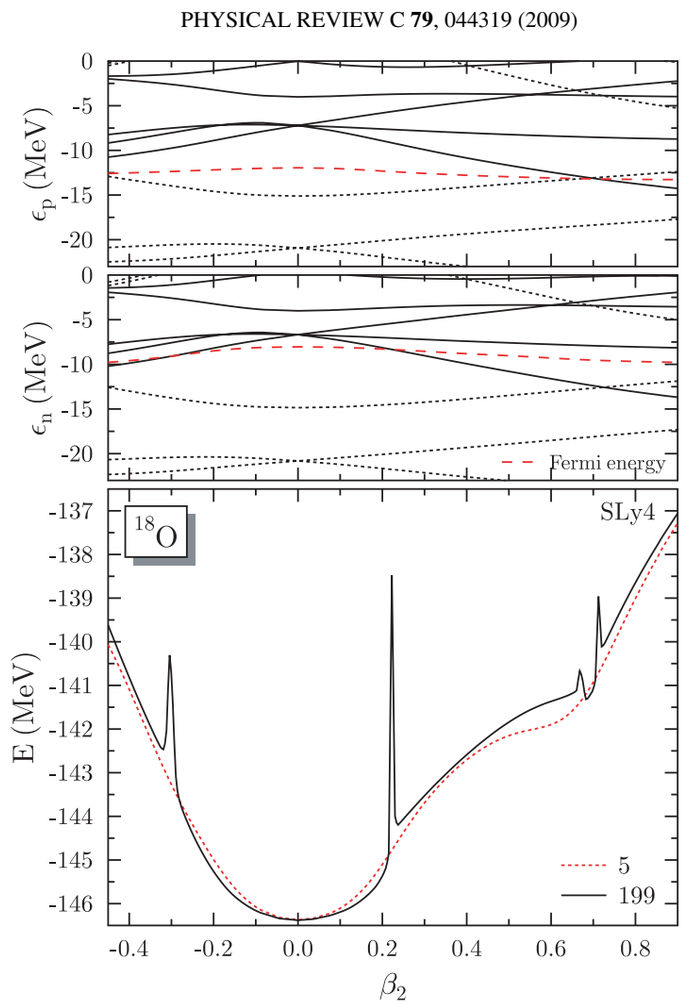

FIG. 1. (Color online) Particle-number-restored deformation energy surface of ^{18}O calculated with SLy4 and a density-dependent pairing interaction and the corresponding single-particle spectra of protons and neutrons as a function of the axial quadrupole deformation for $L = 5$ and 199 discretization points of the integral over the gauge angle (lowest panel). There are clear anomalies that appear when either a proton or neutron single-particle level crosses the Fermi energy. The dimensionless quadrupole deformation β_2 is defined in Eq. (66).

Summary and outlook

- **Energy density functional methods provide a reliable description of nuclear structure observables, nuclear astrophysics input for nucleosynthesis simulations and NMEs in lepton number violating processes.**

- Close connections with other models (Shell Model, IBM, ...)

- Other degrees of freedom will be also explored.

- **Need of energy density functionals adjusted to beyond mean field results.**

- **Description of odd nuclei at the same level. Beta decays!!**

Acknowledgments

J. L. Egido (UAM Madrid)
G. Martínez-Pinedo (TUD-Darmstadt)

C. Bauer (TUD Darmstadt)
K. Blaum (U-Heidelberg)
C. Domingo-Pardo (IFIC-CSIC Valencia)
T. Duguet (CEA-Saclay)
A. Jungclaus (IEMM-CSIC Madrid)
K. Langanke (GSI Darmstadt)
N. López Vaquero (UAM Madrid)
J. Menéndez (TU Darmstadt)
V. Modamio (INFN-Legnaro)
F. Nowacki (CNRS-Strasbourg)
A. Poves (UAM Madrid)
L. Robledo (UAM Madrid)
C. Smorra (U-Heidelberg)
K. Sieja (CNRS-Strasbourg)

Some back up slides...

Nuclear Matrix Elements

$$M^{0\nu\beta\beta} = -\left(\frac{g_V(0)}{g_A(0)}\right)^2 M_F^{0\nu\beta\beta} + M_{GT}^{0\nu\beta\beta} - M_T^{0\nu\beta\beta}$$

- Each term can be written as the expectation value of a transition operator acting on the initial al final states:

$$M_\xi^{0\nu\beta\beta} = \langle 0_f^+ | \hat{O}_\xi^{0\nu\beta\beta} | 0_i^+ \rangle$$

- Nuclear structure methods for calculating these NME:
  - Quasiparticle Random Phase Approximation in different versions: QRPA, RQRPA, SRQRPA. (Tübingen group, Jyüvaskylä group)
  - Interacting Shell Model -ISM- (Strasbourg-Madrid collaboration, Michigan)
  - Interacting Boson Model -IBM- (Yale group)
  - Projected Hartree-Fock-Bogoliubov -PHFB- (Lucknow-UNAM group)
  - Energy Density Functional

Nuclear Matrix Elements

$$M^{0\nu\beta\beta} = -\left(\frac{g_V(0)}{g_A(0)}\right)^2 M_F^{0\nu\beta\beta} + M_{GT}^{0\nu\beta\beta} - M_T^{0\nu\beta\beta}$$

- Each term can be written as the expectation value of a transition operator acting on the initial al final states:

$$M_\xi^{0\nu\beta\beta} = \langle 0_f^+ | \hat{O}_\xi^{0\nu\beta\beta} | 0_i^+ \rangle$$

- Nuclear structure methods for calculating these NME:

Different ways to deal with:
- Finding the best initial and final ground states.
- Handling the transition operator (inclusion of most relevant terms, corrections, approximations, etc.).

Some remarks about these methods:
- Calculations with limited single particle bases.
- Interactions fitted to the specific region (ISM) or to each nucleus individually (rest).
- Difficulties to include collective degrees of freedom.
- Problems with particle number conservation.

Neutrino potentials

Starting from the weak lagrangian that describes the process some approximations are made:

1. Non-relativistic approach in the hadronic part.
2. Closure approximation in the virtual intermediate state
3. Nucleon form factors taken in the dipolar approximation.
4. Tensor contribution is neglected.
5. High order currents are included (HOC).
6. Short range correlations are included with an UCOM correlator.

- Find the initial and final 0^+ states within the GCM+PNAMP method (axial calculations)
- Evaluate the transition operators between these states

Nuclear Matrix Elements

- Neglect the tensor term.
- Closure approximation (10% error at most)

$$M^{0\nu\beta\beta} = -\left(\frac{g_V(0)}{g_A(0)}\right)^2 M_F^{0\nu\beta\beta} + M_{GT}^{0\nu\beta\beta} - \cancel{M_T^{0\nu\beta\beta}}$$

$$\begin{aligned} M_F^{0\nu\beta\beta} &= \left(\frac{g_A(0)}{g_V(0)}\right)^2 \langle 0_f^+ | \hat{V}_F(1,2) \hat{\tau}_-^{(1)} \hat{\tau}_-^{(2)} | 0_i^+ \rangle \\ M_{GT}^{0\nu\beta\beta} &= \langle 0_f^+ | \hat{V}_{GT}(1,2) \hat{\tau}_-^{(1)} \hat{\tau}_-^{(2)} | 0_i^+ \rangle \end{aligned}$$

$$\begin{aligned} \langle \vec{r}_1 \vec{r}_2 | \hat{V}_F(1,2) | \vec{r}\,'_1 \vec{r}\,'_2 \rangle &= v_F(|\vec{r}_1 - \vec{r}_2|) \delta(\vec{r}_1 - \vec{r}\,'_1) \delta(\vec{r}_2 - \vec{r}\,'_2) \\ \langle \vec{r}_1 \vec{r}_2 | \hat{V}_{GT}(1,2) | \vec{r}\,'_1 \vec{r}\,'_2 \rangle &= v_{GT}(|\vec{r}_1 - \vec{r}_2|) \delta(\vec{r}_1 - \vec{r}\,'_1) \delta(\vec{r}_2 - \vec{r}\,'_2) \hat{\vec{\sigma}}^{(1)} \cdot \hat{\vec{\sigma}}^{(2)} \end{aligned}$$

Nuclear Matrix Elements

- Neglect the tensor term.
- Closure approximation (10% error at most)

$$M^{0\nu\beta\beta} = -\left(\frac{g_V(0)}{g_A(0)}\right)^2 M_F^{0\nu\beta\beta} + M_{GT}^{0\nu\beta\beta} - \cancel{M_T^{0\nu\beta\beta}}$$

$$\begin{aligned} M_F^{0\nu\beta\beta} &= \left(\frac{g_A(0)}{g_V(0)}\right)^2 \langle 0_f^+ | \hat{V}_F(1,2) \hat{\tau}_-^{(1)} \hat{\tau}_-^{(2)} | 0_i^+ \rangle \\ M_{GT}^{0\nu\beta\beta} &= \langle 0_f^+ | \hat{V}_{GT}(1,2) \hat{\tau}_-^{(1)} \hat{\tau}_-^{(2)} | 0_i^+ \rangle \end{aligned}$$

$$\begin{aligned} \langle \vec{r}_1 \vec{r}_2 | \hat{V}_F(1,2) | \vec{r}\,'_1 \vec{r}\,'_2 \rangle &= v_F(|\vec{r}_1 - \vec{r}_2|) \delta(\vec{r}_1 - \vec{r}\,'_1) \delta(\vec{r}_2 - \vec{r}\,'_2) \\ \langle \vec{r}_1 \vec{r}_2 | \hat{V}_{GT}(1,2) | \vec{r}\,'_1 \vec{r}\,'_2 \rangle &= v_{GT}(|\vec{r}_1 - \vec{r}_2|) \delta(\vec{r}_1 - \vec{r}\,'_1) \delta(\vec{r}_2 - \vec{r}\,'_2) \hat{\vec{\sigma}}^{(1)} \cdot \hat{\vec{\sigma}}^{(2)} \end{aligned}$$

Neutrino potentials

Transitions

1. Axial states $K = 0$
2. Angular momentum $I = 0$
3. Quadrupole deformations $q = q_{20}$

$\longrightarrow$

$$|0; N_i Z_i; \sigma\rangle = \sum_{\Lambda_i} G^{0;N_i Z_i;\sigma}_{\Lambda_i} |\Lambda_i^{0;N_i Z_i}\rangle$$

$$|0; N_f Z_f; \sigma\rangle = \sum_{\Lambda_f} G^{0;N_f Z_f;\sigma}_{\Lambda_f} |\Lambda_f^{0;N_f Z_f}\rangle$$

Transitions

1. Axial states $K = 0$
2. Angular momentum $I = 0$
3. Quadrupole deformations $q = q_{20}$

$\longrightarrow$

$$|0; N_i Z_i; \sigma\rangle = \sum_{\Lambda_i} G^{0;N_i Z_i;\sigma}_{\Lambda_i} |\Lambda_i^{0;N_i Z_i}\rangle$$

$$|0; N_f Z_f; \sigma\rangle = \sum_{\Lambda_f} G^{0;N_f Z_f;\sigma}_{\Lambda_f} |\Lambda_f^{0;N_f Z_f}\rangle$$

TRANSITIONS:

$$M_\xi^{0\nu\beta\beta} = \langle 0_f^+ | \hat{O}_\xi^{0\nu\beta\beta} | 0_i^+ \rangle = \langle 0; N_f Z_f | \hat{O}_\xi^{0\nu\beta\beta} | 0; N_i Z_i \rangle =$$

$$\sum_{\Lambda_f \Lambda_i} \left(G^{0;N_f Z_f}_{\Lambda_f} \right)^* \langle \Lambda_f^{0;N_f Z_f} | \hat{O}_\xi^{0\nu\beta\beta} | \Lambda_i^{0;N_i Z_i} \rangle G^{0;N_i Z_i}_{\Lambda_i} = \sum_{q_i q_f; \Lambda_f \Lambda_i}$$

$$\left(\frac{u^{0;N_f Z_f}_{q_f,\Lambda_f}}{\sqrt{n^{0;N_f Z_f}_{\Lambda_f}}} \right)^* \left(G^{0;N_f Z_f}_{\Lambda_f} \right)^* \langle 0; N_f Z_f; q_f | \hat{O}_\xi^{0\nu\beta\beta} | 0; N_i Z_i; q_i \rangle \left(G^{0;N_i Z_i}_{\Lambda_i} \right) \left(\frac{u^{0;N_i Z_i}_{q_i,\Lambda_i}}{\sqrt{n^{0;N_i Z_i}_{\Lambda_i}}} \right)$$

Transitions

1. Axial states $K = 0$
2. Angular momentum $I = 0$
3. Quadrupole deformations $q = q_{20}$

$$\longrightarrow \quad |0; N_i Z_i; \sigma\rangle = \sum_{\Lambda_i} G^{0;N_i Z_i;\sigma}_{\Lambda_i} |\Lambda_i^{0;N_i Z_i}\rangle$$

$$|0; N_f Z_f; \sigma\rangle = \sum_{\Lambda_f} G^{0;N_f Z_f;\sigma}_{\Lambda_f} |\Lambda_f^{0;N_f Z_f}\rangle$$

TRANSITIONS:

$$M_\xi^{0\nu\beta\beta} = \langle 0_f^+ | \hat{O}_\xi^{0\nu\beta\beta} | 0_i^+\rangle = \langle 0; N_f Z_f | \hat{O}_\xi^{0\nu\beta\beta} | 0; N_i Z_i\rangle =$$

$$\sum_{\Lambda_f \Lambda_i} \left(G^{0;N_f Z_f}_{\Lambda_f}\right)^* \langle \Lambda_f^{0;N_f Z_f} | \hat{O}_\xi^{0\nu\beta\beta} | \Lambda_i^{0;N_i Z_i}\rangle G^{0;N_i Z_i}_{\Lambda_i} = \sum_{q_i q_f; \Lambda_f \Lambda_i}$$

$$\left(\frac{u^{0;N_f Z_f}_{q_f,\Lambda_f}}{\sqrt{n^{0;N_f Z_f}_{\Lambda_f}}}\right)^* \left(G^{0;N_f Z_f}_{\Lambda_f}\right)^* \langle 0; N_f Z_f; q_f | \hat{O}_\xi^{0\nu\beta\beta} | 0; N_i Z_i; q_i\rangle \left(G^{0;N_i Z_i}_{\Lambda_i}\right) \left(\frac{u^{0;N_i Z_i}_{q_i,\Lambda_i}}{\sqrt{n^{0;N_i Z_i}_{\Lambda_i}}}\right)$$

Matrix elements of the double beta transition operators between particle number and angular momentum projected states

NME: deformation and mixing

$$\frac{\langle 0; N_f Z_f; q_f | \hat{O}^{0\nu\beta\beta}_{\xi} | 0; N_i Z_i; q_i \rangle}{\sqrt{\langle 0; N_f Z_f; q_f | 0; N_f Z_f; q_f \rangle \langle 0; N_i Z_i; q_i | 0; N_i Z_i; q_i \rangle}}$$

A=76

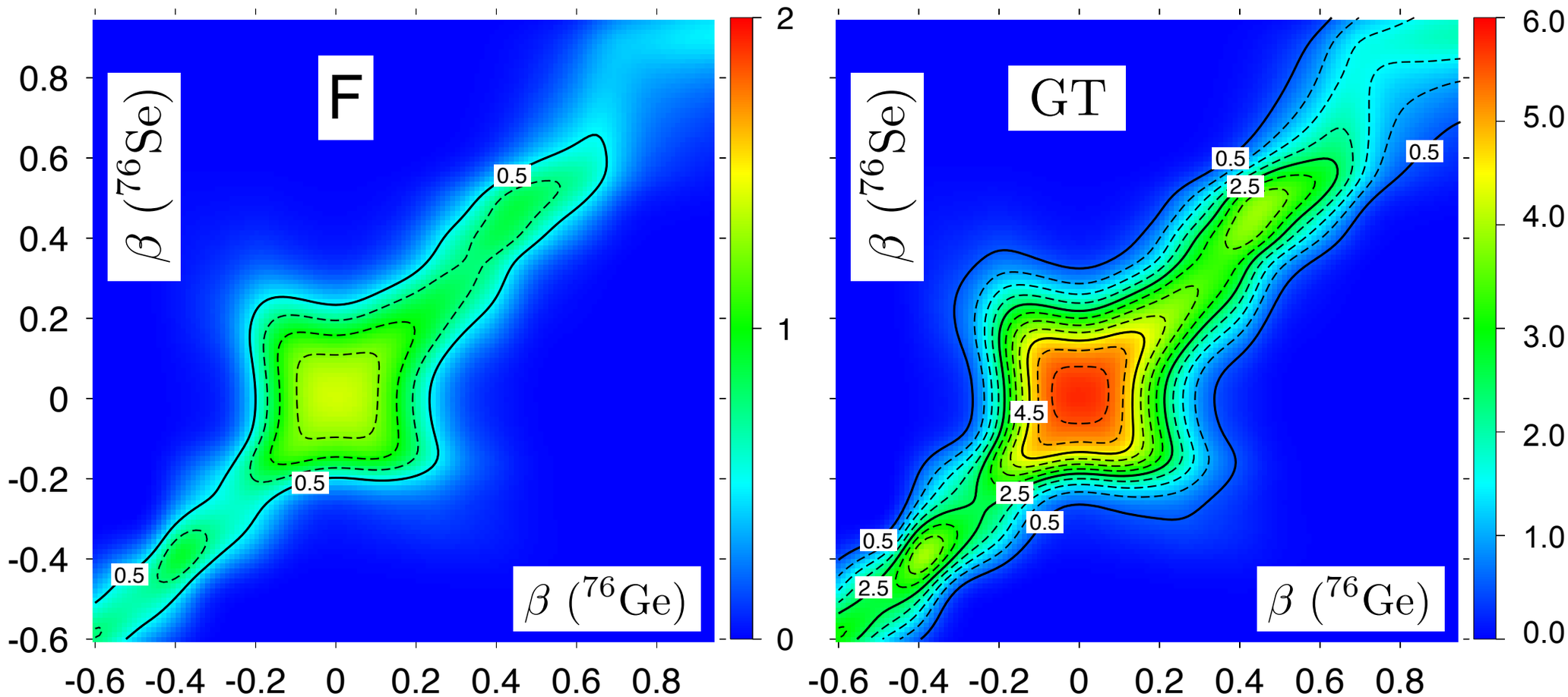

- GT strength greater than Fermi.
- Similar deformation between mother and granddaughter is favored by the transition operators
- Maxima are found close to sphericity although some other local maxima are found

NME: deformation and mixing

$$\frac{\langle 0; N_f Z_f; q_f | \hat{O}_\xi^{0\nu\beta\beta} | 0; N_i Z_i; q_i \rangle}{\sqrt{\langle 0; N_f Z_f; q_f | 0; N_f Z_f; q_f \rangle \langle 0; N_i Z_i; q_i | 0; N_i Z_i; q_i \rangle}}$$

A=76

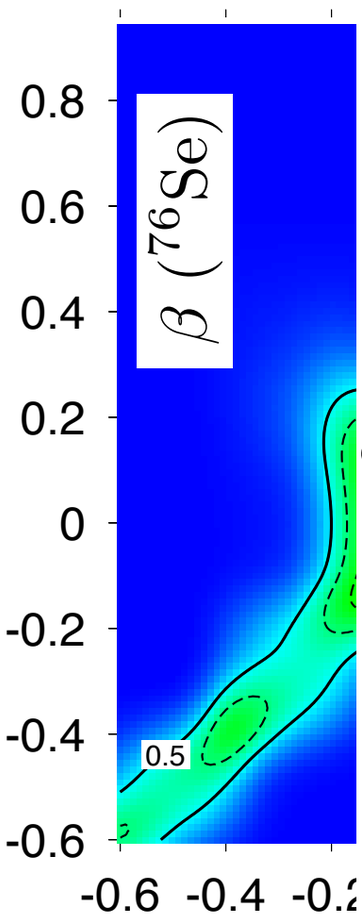

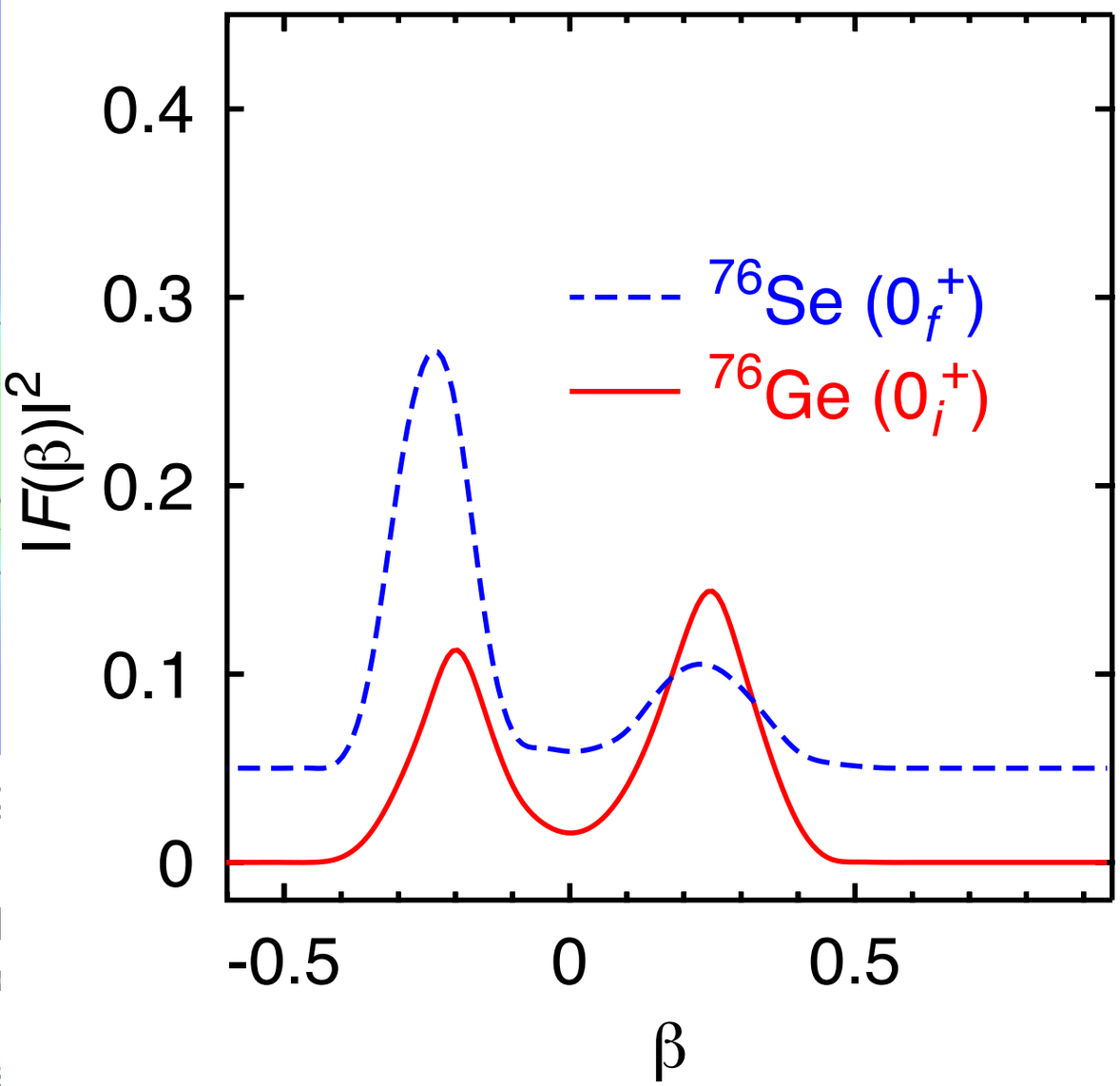

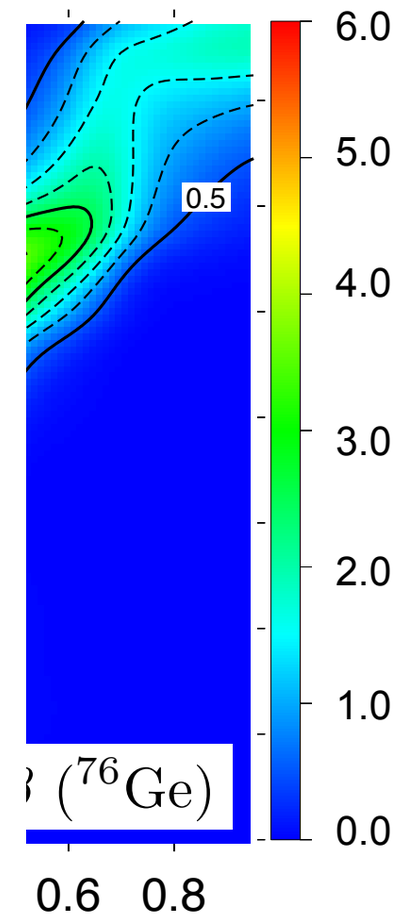

- GT strengtl
- Similar def
operators
- Maxima ar
- Final result
collective sta

transition

initial and final
e found

NME: deformation and mixing

$$\frac{\langle 0; N_f Z_f; q_f | \hat{O}_{\xi}^{0\nu\beta\beta} | 0; N_i Z_i; q_i \rangle}{\sqrt{\langle 0; N_f Z_f; q_f | 0; N_f Z_f; q_f \rangle \langle 0; N_i Z_i; q_i | 0; N_i Z_i; q_i \rangle}}$$

A=76

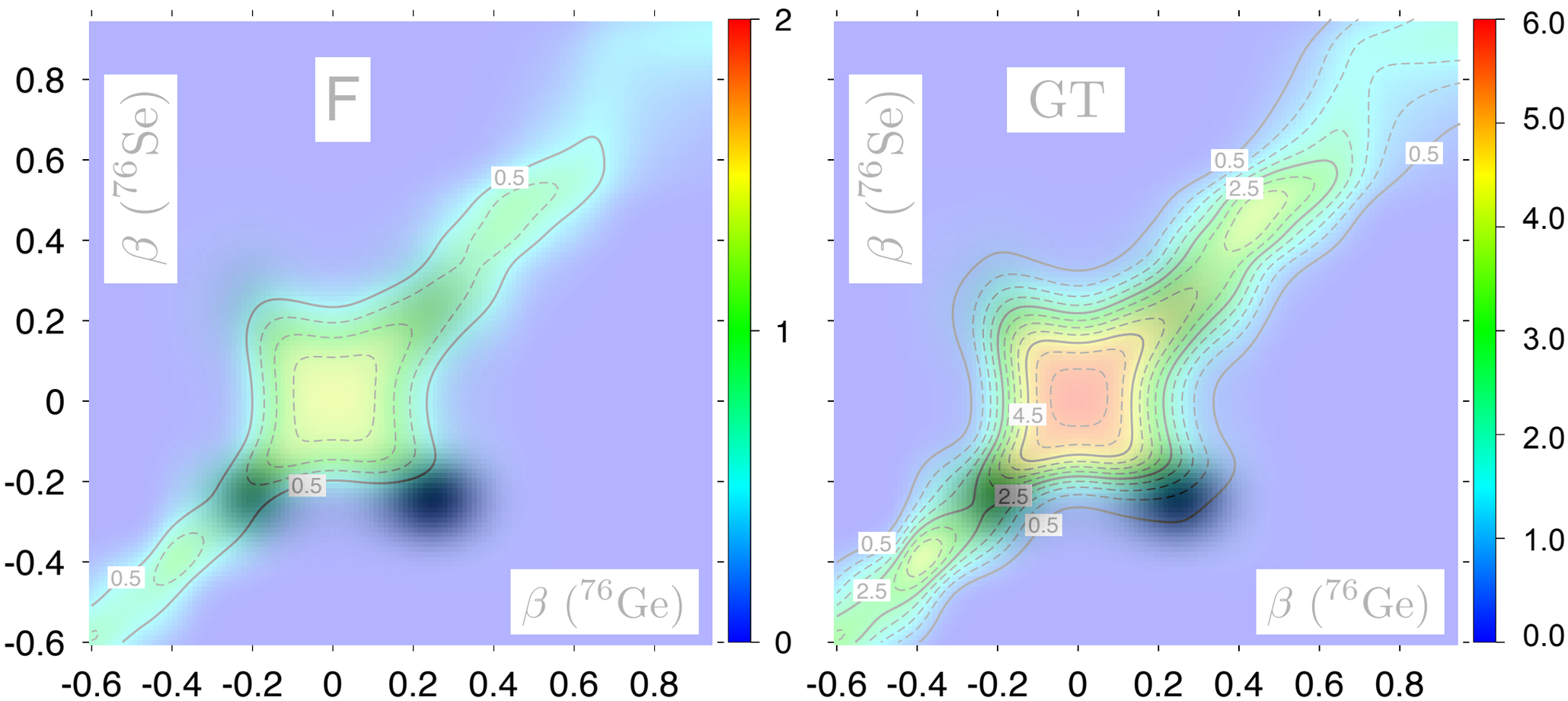

- GT strength greater than Fermi.
- Similar deformation between mother and granddaughter is favored by the transition operators
- Maxima are found close to sphericity although some other local maxima are found

- Final result depends on the distribution of probability of the corresponding initial and final collective states within this plot

NME: deformation and mixing

$$\frac{\langle 0; N_f Z_f; q_f | \hat{O}^{0\nu\beta\beta}_{\xi} | 0; N_i Z_i; q_i \rangle}{\sqrt{\langle 0; N_f Z_f; q_f | 0; N_f Z_f; q_f \rangle \langle 0; N_i Z_i; q_i | 0; N_i Z_i; q_i \rangle}}$$

A=76

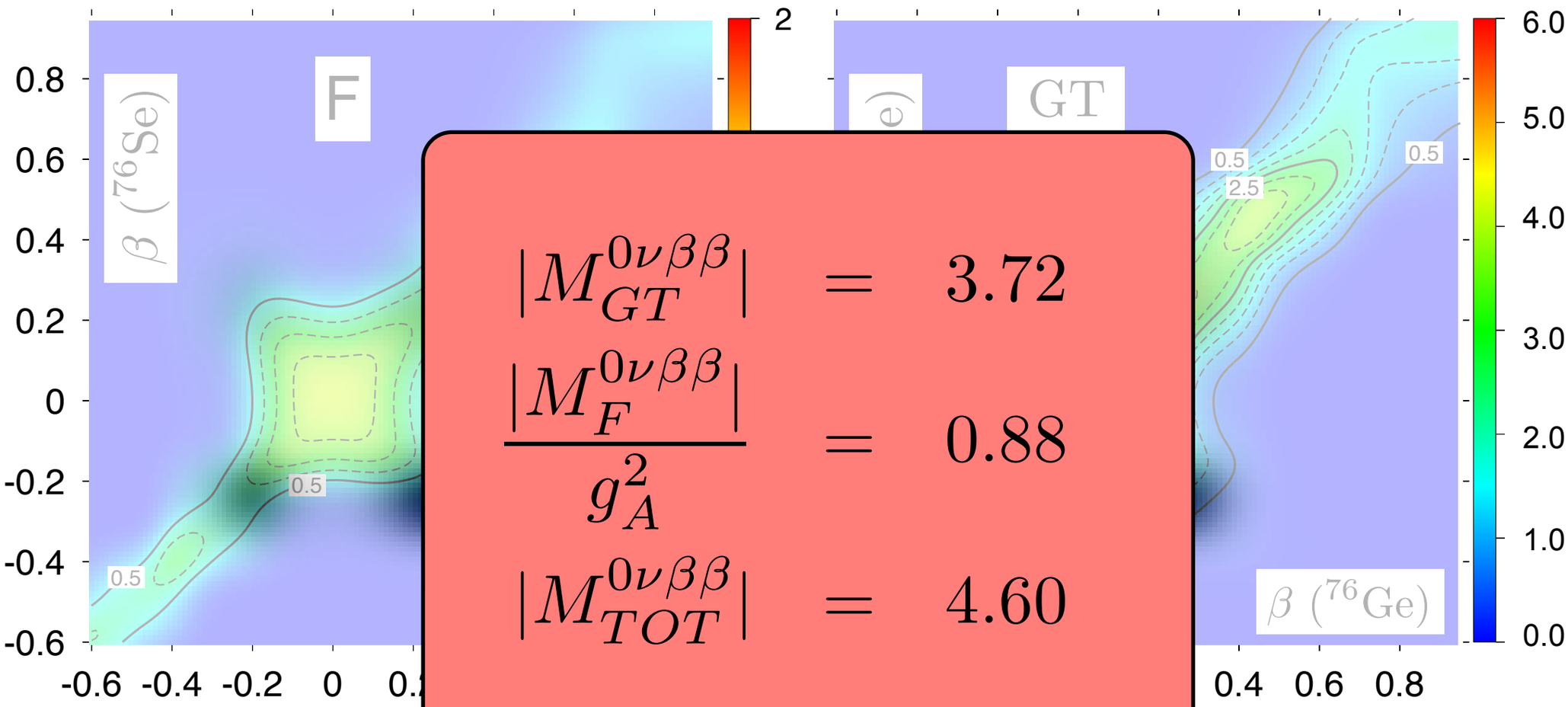

$$|M^{0\nu\beta\beta}_{GT}| = 3.72$$

$$\frac{|M^{0\nu\beta\beta}_{F}|}{g_A^2} = 0.88$$

$$|M^{0\nu\beta\beta}_{TOT}| = 4.60$$

- GT strength greater than Fermi.
- Similar deformation between mother and granddaughter is favored by the transition operators
- Maxima are found close to sphericity although some other local maxima are found

- Final result depends on the distribution of probability of the corresponding initial and final collective states within this plot

NME: Summary of the results

Gogny D1S parametrization

A	48	76	82	96	100	116	124	128	130	136	150	152	164	180
$M^{0\nu}$	2.37	4.60	4.22	5.65	5.08	4.72	4.81	4.11	5.13	4.20	1.71	1.07	0.64	0.58
$T_{1/2}$ (y)	28.5 $\times10^{23}$	76.9 $\times10^{23}$	20.8 $\times10^{23}$	5.48 $\times10^{23}$	8.64 $\times10^{23}$	9.24 $\times10^{23}$	16.2 $\times10^{23}$	343.1 $\times10^{23}$	8.84 $\times10^{23}$	12.7 $\times10^{23}$	16.5 $\times10^{23}$	4.2 $\times10^{31}$	1.3 $\times10^{36}$	1.6 $\times10^{34}$

Gogny D1M parametrization

A	48	76	82	96	100	116	124	128	130	136	150	152	164	180
$M^{0\nu}$	2.43	4.64	4.28	5.70	5.19	4.83	4.71	3.98	5.07	4.29	1.36	0.89	0.50	0.38
$T_{1/2}$ (y)	27.1 $\times10^{23}$	75.6 $\times10^{23}$	20.2 $\times10^{23}$	5.38 $\times10^{23}$	8.28 $\times10^{23}$	8.82 $\times10^{23}$	16.9 $\times10^{23}$	365.8 $\times10^{23}$	9.05 $\times10^{23}$	12.2 $\times10^{23}$	26.1 $\times10^{23}$	6.2 $\times10^{31}$	2.1 $\times10^{36}$	3.8 $\times10^{34}$

double beta decay

double electron capture

NME: deformation and mixing

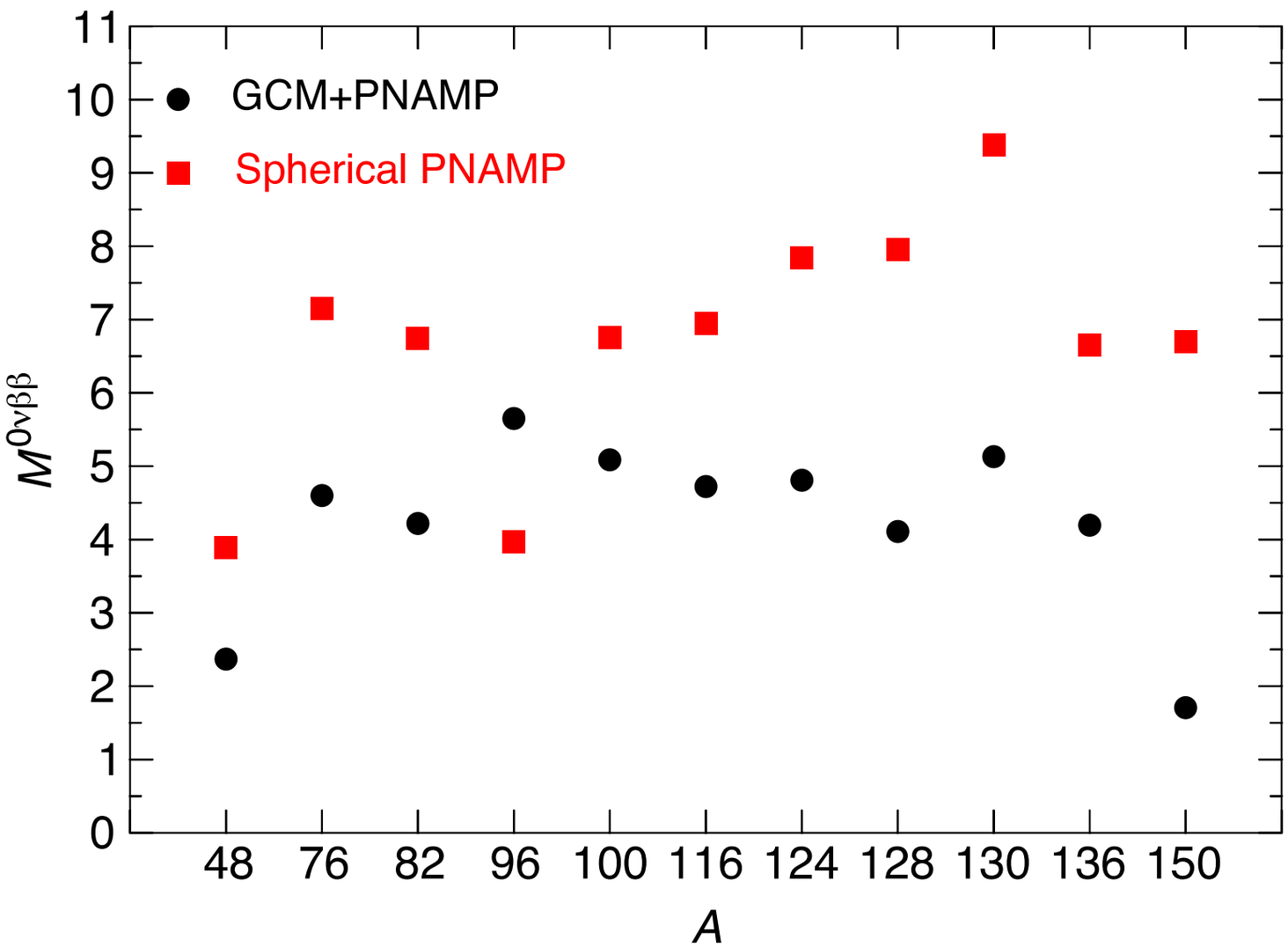

Noticeable difference in the NME if only intrinsic spherical configurations are considered without configuration mixing.

T.R.R., Martínez-Pinedo, PPNP 66, 436 (2011)

Shape evolution

Shape evolution in the Cadmium isotopic chain

- ✓ Shape evolves from *N*=50 to *N*=82 magic number through prolate axially symmetric structures
- ✓ Highest deformation is found in mid-shell nuclei (**β**~0.2)
- ✓ Rest of calculations will assume axial symmetry

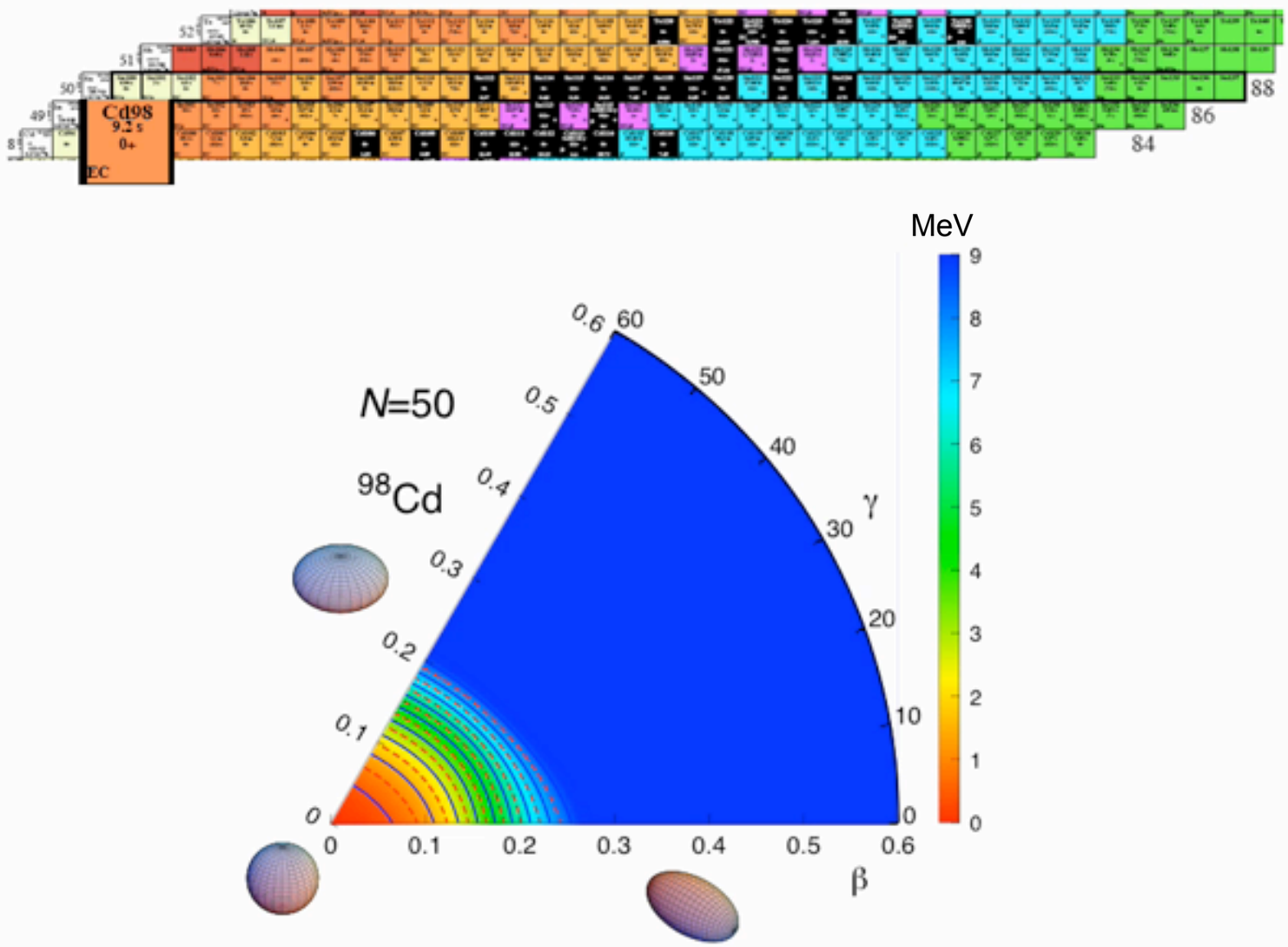

T.R.R, J.L. Egido, A. Jungclaus, Phys. Lett. B 668, 410 (2008)

Summary and outlook

- **Energy density functional methods provide a reliable description of nuclear structure observables, nuclear astrophysics input for nucleosynthesis simulations and NMEs in lepton number violating processes.**

- Close connections with other models (Shell Model, IBM, ...)

- Other degrees of freedom will be also explored.

- **Need of energy density functionals adjusted to beyond mean field results.**

- **Description of odd nuclei at the same level. Beta decays!!**

Theoretical framework

In order to give a proper description of the nuclear system we need:

➡ A good **interaction** or energy density functional (EDF) that describes the dynamics of the constituent nucleons.

➡ A good **method** -adapted to the corresponding interaction/EDF- for solving the quantum many body problem.

Theoretical framework

In order to give a proper description of the nuclear system we need:

➡ A good **interaction** or energy density functional (EDF) that describes the dynamics of the constituent nucleons.

➡ A good **method** -adapted to the corresponding interaction/EDF- for solving the quantum many body problem.

Theoretical framework

In order to give a proper description of the nuclear system we need:

➡ A good **interaction** or energy density functional (EDF) that describes the dynamics of the constituent nucleons.

➡ A good **method** -adapted to the corresponding interaction/EDF- for solving the quantum many body problem.

Some considerations:

see also Duguet, Papenbrock, Lesinski talks

- Both mean field (SR-EDF) and beyond mean field (MR-EDF) methods use intrinsic many-body auxiliary wave functions.

Theoretical framework

In order to give a proper description of the nuclear system we need:

➡ A good **interaction** or energy density functional (EDF) that describes the dynamics of the constituent nucleons.

➡ A good **method** -adapted to the corresponding interaction/EDF- for solving the quantum many body problem.

Some considerations:

see also Duguet, Papenbrock, Lesinski talks

- Both mean field (SR-EDF) and beyond mean field (MR-EDF) methods use intrinsic many-body auxiliary wave functions.
- Density matrices (normal and abnormal) and spatial densities are written in terms of these auxiliary wave functions.

Theoretical framework

In order to give a proper description of the nuclear system we need:

➡ A good **interaction** or energy density functional (EDF) that describes the dynamics of the constituent nucleons.

➡ A good **method** -adapted to the corresponding interaction/EDF- for solving the quantum many body problem.

Some considerations:

see also Duguet, Papenbrock, Lesinski talks

- Both mean field (SR-EDF) and beyond mean field (MR-EDF) methods use intrinsic many-body auxiliary wave functions.
- Density matrices (normal and abnormal) and spatial densities are written in terms of these auxiliary wave functions.
- All the observables and variational procedures in EDF methods are expressed in terms of density matrices and spatial densities.

Theoretical framework

In order to give a proper description of the nuclear system we need:

➡ A good **interaction** or energy density functional (EDF) that describes the dynamics of the constituent nucleons.

➡ A good **method** -adapted to the corresponding interaction/EDF- for solving the quantum many body problem.

Some considerations:

see also Duguet, Papenbrock, Lesinski talks

- Both mean field (SR-EDF) and beyond mean field (MR-EDF) methods use intrinsic many-body auxiliary wave functions.
- Density matrices (normal and abnormal) and spatial densities are written in terms of these auxiliary wave functions.
- All the observables and variational procedures in EDF methods are expressed in terms of density matrices and spatial densities.
- The usual EDF methods consist in determining the “best” auxiliary many body wave functions

Convergence

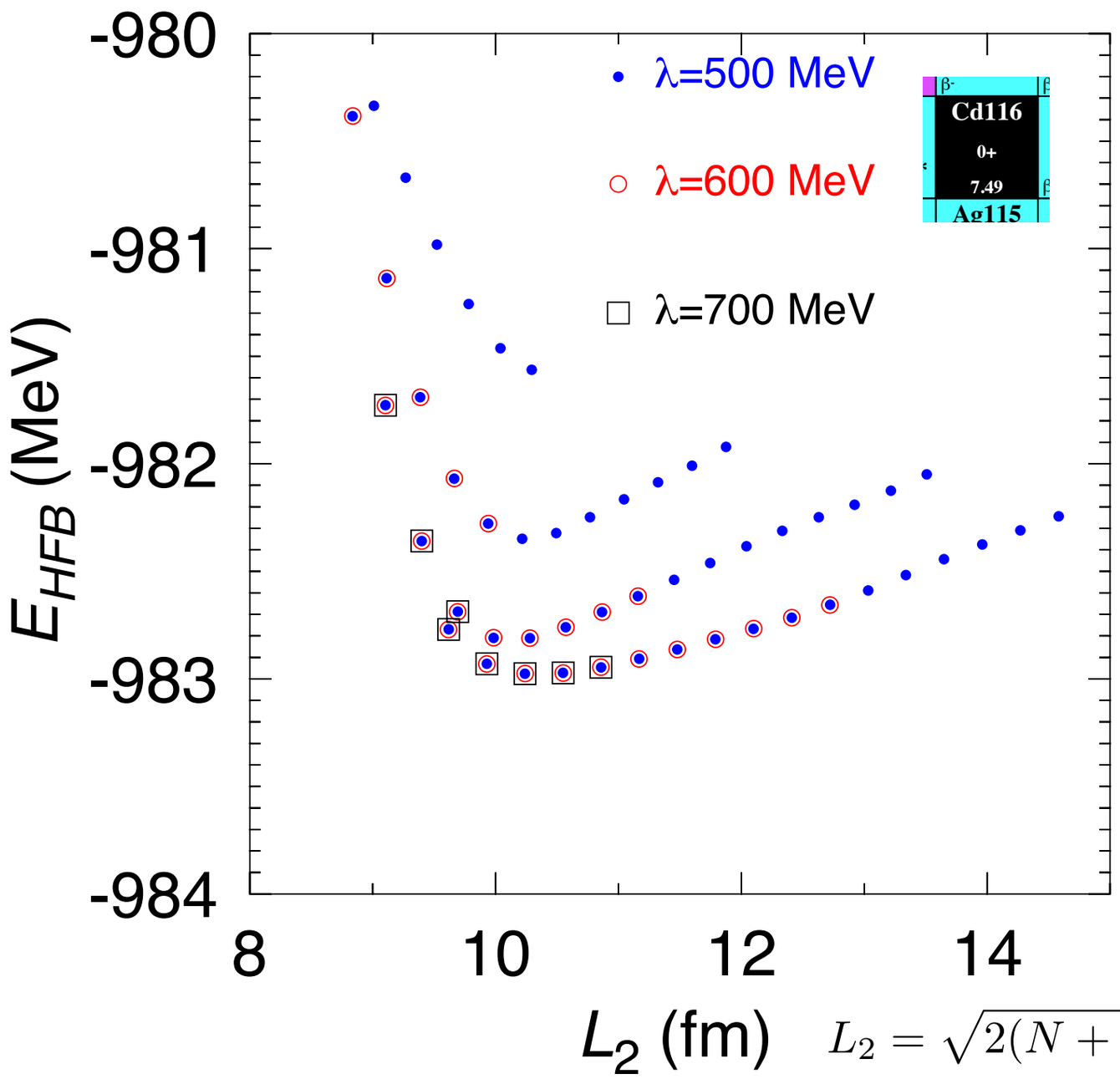

$L_2 = \sqrt{2(N+3/2+2)}b$

$r_0 A^{1/3} < \sqrt{2(N+3/2)}b$ • IR convergence

$\lambda < \sqrt{2(N+3/2)}\hbar/b$ • UV convergence

PHYSICAL REVIEW C **86**, 031301(R) (2012)

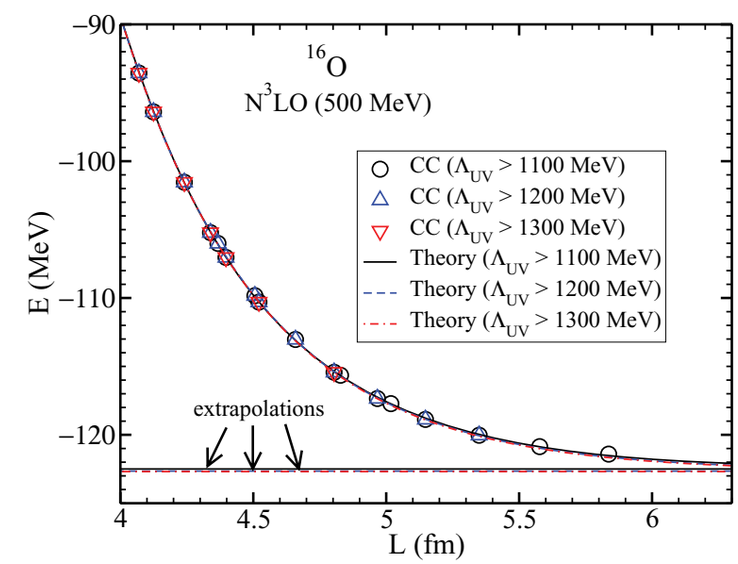

FIG. 2. (Color online) Open symbols: Ground-state energy of ^{16}O as a function of L. Lines: Fits to Eq. (11) yield $E_\infty \approx -122.6$ MeV and $k_\infty \approx 0.95\ \mathrm{fm}^{-1}$. Λ_{UV} from Eq. (1).